

UNIVERSITY OF STRATHCLYDE
FACULTY OF ENGINEERING
DEPARTMENT OF BIOMEDICAL ENGINEERING

DEVELOPMENT OF A CARDIAC PATCH
FOR THE REGENERATION OF
INFARCTED HEARTS

By
ANNA GALLUZZO

A thesis presented in fulfilment for the requirements of the

Degree of Doctor of Philosophy

2019

Declaration of Authenticity

This thesis is the result of the author's original research. It has been composed by the author and has not been previously submitted for examination which has led to the award of a degree.

The copyright of this thesis belongs to the author under the terms of the United Kingdom Copyright Acts as qualified by University of Strathclyde Regulation 3.50. Due acknowledgement must always be made of the use of any material contained in, or derived from, this thesis.

Signed:

Date:// 2019

Abstract

The inflammation that occurs after cardiac ischemia/reperfusion leads to high levels of oxidative stress, which produces deleterious effects that ultimately limit regeneration of the myocardium. This stress response can be prolonged, thereby affecting various stages of cardiac repair remodelling. Efforts to control such remodelling and stimulate cardiac tissue regeneration have therefore included the use of antioxidant or anti-inflammatory drug strategies. To date, such approaches have involved delivery of the drugs orally or by injection. The use of a scaffold that can be placed onto the heart immediately following surgery would allow sustained delivery of high concentrations of drug *in situ*, directly targeting the affected area. Moreover, implantation of such a material has the potential to encourage cell infiltration into the matrix, thereby promoting regeneration. The ultimate aim of this project was to develop a cardiac scaffold loaded with a drug with antioxidant and anti-inflammatory activity.

Pyruvate is a well characterised anti-inflammatory and antioxidant drug. It has been added to cardioplegia by some surgical groups for its potential cardioprotective effects, although the therapeutic value of sustained delivery of this drug into the myocardium following cardiac surgery has not been investigated. Ethyl Pyruvate (EP) is a more stable form of this drug and was therefore the drug selected for investigation in the present study. Various alginate scaffolds were developed as drug delivery vehicles, with EP release characterised *in vitro*.

Alginate gels prepared with (1-2%) low viscosity high guluronate alginate and cross-linked with 1:1 (0.6-1%) calcium chloride solution provided sustained release of about 2,000 – 3,000 μM of EP over 28-days period, characterised by an initial burst of about 85% of EP released in the first week, and the remaining EP was released over the following weeks.

Since it is likely that an optimal scaffold for cardiac regeneration will have a porous structure with interconnected pores to allow cell infiltration and proliferation, a series of macro-porous alginate scaffolds were developed. Different methods were used to prepare the scaffolds and thus different EP release profiles were obtained. Overall, the

scaffolds prepared with 1% low viscosity high guluronate alginate and double cross-linked with 1:1 (0.4-1%) calcium gluconate solution and 0.2 M calcium chloride bath and prepared with one cycle of free-drying (method 6) released about 5,000- 5,500 μg over 28 days (with 88-98% drug loading efficiency), the highest compared to the other formulations.

The potential therapeutic benefits of such EP release were then investigated *in vitro*. When primary rat cardiac fibroblast cells were exposed to hydrogen peroxide (150 μM) in the presence of EP (1,000 – 20,000 μM), EP improved cell viability as measured by alamarBlue assay. Moreover, at (1,000 - 10,000 μM), EP significantly increased cell viability compared to the control. In contrast, EP had no protective effect on the cells that had been previously exposed to H_2O_2 (150 μM) for 24 hours.

Alginate macro-porous scaffolds (prepared using method 6), which showed high porosity, the best EP release profiles and the highest EP loading efficiency, were then tested in a cardiac fibroblasts culture and cell viability was measured by Neutral Red assay after 5 days. In order to improve cell attachment in the scaffolds prepared in this study, Arginine-Glycine-Aspartic acid modified RGD alginate was also used to prepared the scaffolds for the cardiac fibroblast study. Cells seeded onto the RGD- Alginate + EP scaffolds presented higher cell viability compared to the scaffolds without EP, demonstrating that the cells benefit from the structure of the scaffold, as well as from the presence of EP.

This study has demonstrated for the first time that alginate represents a suitable delivery system for providing sustained release of EP. The protective effective of this drug on cardiac fibroblasts shown here, combined with the promising cell viability observed within the delivery scaffold, mean that this approach has significant potential for future development towards clinical evaluation.

Acknowledgements

First and foremost, I am thankful to my beloved family. I am and always will be grateful to my parents for their unconditional love and support.

I would like to express my gratitude to my supervisors Prof. Terry Gourlay and Dr. Chris McCormick for their guidance and constant support over the years of my PhD.

I would like to thank Prof. Helen Grant, Valerie Carlaw and Katie Henderson for unfailing support and assistance. Furthermore, I would like to thank the University of Strathclyde Scholarship for funding my PhD research.

Table of Contents

Declaration of Authenticity	II
Abstract	III
Acknowledgements	V
List of figures	XII
List of tables	XXXI
List of abbreviations	XXXII
1 CHAPTER ONE	1
1.1 Introduction	1
1.2 Clinical needs for cardiac regeneration	1
1.2.1 Myocardial Ischemia and left ventricular remodelling	1
1.2.2 Oxidative stress and inflammation in injured hearts	4
1.2.3 Current treatments for damaged myocardium	7
1.3 Novel strategies to alleviate cardiac injury	8
1.3.1 Cell therapy for cardiac regeneration	8
1.3.2 Summary of current limitations in cell therapy	11
1.3.3 Gene therapy	12
1.3.4 Protein delivery	12
1.3.5 Novel Pharmacological Therapies	14
1.4 Pyruvate	18
1.5 Ethyl Pyruvate	19
1.5.1 <i>In vitro</i> effects of Ethyl Pyruvate	19
1.5.2 <i>In vivo</i> effects of Ethyl Pyruvate	21
1.6 Hydrogels for cardiac repair and regeneration	22
1.6.1 Introduction	22
1.6.2 Collagen	24
1.6.3 Chitosan	25

1.7	Alginate as tissue engineering scaffold	26
1.7.1	Introduction	26
1.7.2	Alginate hydrogel formation	26
1.7.3	Biocompatibility.....	28
1.7.4	Biodegradability of alginate hydrogels	29
1.7.5	Porous alginate scaffolds.....	29
1.7.6	Alginate hydrogels for protein/small drug delivery	30
1.8	Summary of study rationale.....	32
1.9	OBJECTIVES.....	34
2	CHAPTER TWO	35
	MATERIALS AND GENERAL METHODS	35
2.1	<i>In-vitro</i> cell culture studies.....	35
2.1.1	Materials.....	35
2.1.2	3T3 cell culture	35
2.1.3	Cardiac fibroblasts cell culture.....	36
2.1.4	Cell assays	37
2.1.5	Live/dead staining and confocal imaging	42
2.2	Alginate hydrogel for EP delivery.....	42
2.2.1	Alginate hydrogel production	42
2.2.2	Alginate Hydrogel stability in PBS.....	44
2.3	Alginate scaffolds for EP delivery	44
	Materials.....	44
2.3.1	Calcium gluconate alginate scaffolds preparation	47
2.3.2	Calcium chloride alginate scaffolds preparation.....	47
2.3.3	Double cross-linked alginate scaffolds preparation	47
2.3.4	Degradation study of alginate scaffolds.....	48
2.4	EP release studies	48
2.4.1	Sample preparation.....	48

2.4.2	Sample collection.....	48
2.5	Measurement of EP	49
2.5.1	Direct measurement of EP	49
2.5.2	Indirect measurement of EP.....	54
2.6	EP stability study.....	56
2.7	Morphological analysis	56
2.7.1	Porosity	56
2.7.2	SEM analysis.....	57
3	CHAPTER THREE.....	58
3.1	Introduction	58
3.1.1	Aim and objectives.....	59
3.2	Methods.....	60
3.3	Results	60
3.3.1	Pyruvate assay.....	60
3.3.2	DPPH antioxidant assay.....	62
3.3.3	ABTS antioxidant assay.....	66
3.4	Measurement of EP using UV spectroscopy.....	68
3.4.1	UV/Vis spectrophotometer.....	68
3.4.2	Nano-spectrometer	70
3.4.3	HPLC.....	71
3.5	EP stability <i>in vitro</i>	76
3.5.1	Introduction.....	76
3.5.2	Methodology	77
3.5.3	Results.....	77
3.6	Discussion.....	80
3.6.1	Introduction.....	80
3.6.2	EP measurement <i>in vitro</i>	80
3.6.3	EP stability study.....	84

3.7	Limitations.....	85
3.8	Future work	85
3.9	Summary conclusions.....	86
4	CHAPTER FOUR.....	87
4.1	Introduction	87
4.1.1	Aim and objectives.....	90
4.2	Alginate gel preparation	91
4.2.1	High mannuronate content sodium alginate (preliminary study).....	91
4.2.2	High guluronate content sodium alginate (preliminary study)	95
4.3	Stability study of alginate hydrogels <i>in vitro</i>	96
4.4	SEM imaging of ethyl pyruvate loaded alginate gels.....	100
4.5	<i>In-vitro</i> ethyl pyruvate release study from alginate gels	101
4.5.1	1% alginate hydrogels	102
4.5.2	2% alginate hydrogels	104
4.6	Drug loading efficiency	106
4.7	Discussion.....	107
4.7.1	Introduction.....	107
4.7.1	Alginate hydrogels preparation	107
4.7.2	Stability study of alginate hydrogels.....	109
4.7.3	EP delivery study	109
4.8	Limitations.....	111
4.9	Summary conclusions.....	112
5	CHAPTER FIVE.....	113
5.1	Introduction	113
5.2	Aims	114
5.3	Methodology.....	115
5.3.1	Preliminary study - Calcium gluconate alginate scaffolds	115
5.4	Alginate scaffolds preparation.....	115
5.4.1	Introduction.....	115
5.4.2	Single cross-linked scaffold production.....	117

5.4.3	Double cross-linked scaffold production	120
5.5	Stability of alginate scaffolds <i>in vitro</i>	121
5.5.1	Methodology	121
5.5.2	Results	122
5.6	<i>In vitro</i> ethyl pyruvate release study from alginate sponges	142
5.6.1	Alginate scaffolds cross-linked with CaCl ₂	143
5.6.2	Alginate scaffolds with double cross-linking.....	154
5.7	Drug Loading Efficiency	161
	Methods.....	161
	Results	162
5.8	Characterisation of alginate scaffolds	163
5.8.1	Introduction	163
5.8.2	Porosity	163
5.8.3	SEM analysis.....	167
5.9	Discussion.....	172
5.9.1	Introduction	172
5.9.2	Stability study.....	173
5.9.3	EP release study	175
5.9.4	Characterisation of alginate scaffolds	177
5.10	Limitations	179
5.11	Summary conclusions	179
6	CHAPTER SIX	181
6.1	Introduction	181
6.2	<i>In vitro</i> effects of EP on cardiac fibroblasts	183
6.2.1	Preliminary cell viability study - neutral red and MTT assay.....	183
6.2.2	Cell viability – alamarBlue™ assay.....	185
6.2.3	Cell proliferation – BrdU assay.....	188
6.2.4	Live/dead staining and confocal imaging	189

6.3	Effect of EP on cardiac fibroblasts treated with hydrogen peroxide.....	190
6.4	Preliminary study of alginate scaffold biocompatibility using 3T3 cells..	193
6.4.1	LDH activity.....	193
6.4.2	Live/dead staining and confocal imaging	194
6.5	Effect of double cross-linked alginate scaffold on cardiac fibroblasts.....	197
6.5.1	Cell viability – Neutral Red assay.....	197
6.5.2	LDH assay	199
6.5.3	Live/dead staining and confocal imaging	200
6.6	Discussion.....	203
6.6.1	Introduction	203
6.6.2	EP effects on cardiac fibroblast cell viability and proliferation.....	203
6.6.3	Anti-oxidant effects of EP in cardiac fibroblasts	204
6.6.4	<i>In vitro</i> investigation of alginate-EP patches in cell culture	205
6.6.5	Limitations	206
6.6.6	Future work	207
6.6.7	Summary conclusions	207
7	CHAPTER SEVEN.....	208
7.1	Summary.....	208
7.2	Summary of Contribution.....	218
7.3	Summary of Limitations.....	219
7.4	Future Research Directions	220
7.5	Summary Conclusions.....	221
9	Bibliography.....	223

List of figures

Figure 1.1 Schematic representation of the ROS and NO involvement of the initiation of the inflammation state at the cellular level and consequent development of cardiac diseases. Adapted from (Elahi, et al., 2009).....	5
Figure 1.2 Schematic Mechanism of ROS scavenging by Pyruvate.....	19
Figure 1.3 Metabolism of Ethyl Pyruvate. EP can be hydrolysed by Esterase enzymes or ROS. Adapted from (Keshari & Wilson, 2014).....	20
Figure 1.4 Alginate homopolymeric blocks of mannuronate (M) and guluronate (G) residues. Adapted from (Pereira, et al., 2013).....	26
Figure 1.5 Schematic representation of a) sodium alginate cross-linked with Calcium ions; b) molecular structure of sodium alginate, with the alginate blocks (G=guluronate residues, M=mannuronate residues) and the cross-linked junction between the positively charged calcium ions and the negatively charged G blocks (egg-box structure).....	27
Figure 2.1 Schematic representation of the Lactate Dehydrogenase (LDH) reaction.	41
Figure 2.2 Schematic representation of alginate gel preparation steps.....	43
Figure 2.3 Freeze-drying method used to prepare macro-porous alginate scaffolds. a) Micro Modulyo Freeze Drier 1.5L (Thermo Savant); b) Frozen samples were placed in the freeze-drier and freeze-dried at -50 °C. c) Alginate scaffolds were then ready after 24h of freeze-drying.....	45
Figure 2.4. Schematic representation of the sample collection for EP release study. Alginate hydrogels and alginate scaffolds were placed in a 1:1 PBS solution and stored in an incubator at 37 °C at a constant gentle agitation. At different time points (1 hour, 1 day, 3 days, 7 days, 14 days, 21 days, 28 days) half of PBS	

solution was collected and stored in an Eppendorf -20 °C for future measurement. In order to maintain the volume of the release solution constant, the same volume of solution removed was replaced by an equal amount of fresh PBS solution and the vial returned to the incubator. 49

Figure 2.5 UV 2401 PC UV/VIS Recording Spectrophotometer used to measure EP in PBS solution..... 50

Figure 2.6 Example of linear calibration curve..... 52

Figure 2.7 Scanning Electron Microscope (SEM) (HITACHI TM-1000 Tabletop Microscope) used to investigate the morphology of the alginate structures..... 57

Figure 3.1 Calibration curve of Ethyl pyruvate and pyruvate using the Pyruvate assay. Pyruvate standards and ethyl pyruvate standards in the range of 40-400 µM were prepared and used to plot the calibration curve. a) Calibration curve of pyruvate and ethyl pyruvate; b) Calibration curve of pyruvate and ethyl pyruvate excluding the highest concentration value. All standards were run in duplicate and the data presented represent the mean of these measurements..... 61

Figure 3.2 Calibration curve of a) AGI-1067 and b) Ethyl pyruvate using the DPPH assay. AGI-1067 and ethyl pyruvate were determined by measuring their ability to scavenge DPPH. AGI-1067, was used as a positive control and DPPH without antioxidants as a negative control. The absorbance values correspond to the reduction in DPPH in presence of one of the antioxidants. Standards were prepared in PBS in the range of 6 - 400 µM for AGI-1067, 6 µM - 12.8 mM for EP. All standards were run in triplicates, with the data presented representing the mean of these samples ± Stdev 63

Figure 3.3 Calibration curve of a) AGI-1067 and b) Ethyl pyruvate using the DPPH assay. Ethyl pyruvate was determined by measuring their ability to scavenge DPPH. In presence of an antioxidant agent DPPH is reduced and the colour changes from violet to colourless (Garcia, et al., 2012). The change in colour was measured by a spectrophotometer plate reader at 517 nm after 100 minutes of

incubation. The standards were prepared in PBS in the range of 25-6,400 μM and used to plot the calibration curve. All standards were run in triplicate..... 65

Figure 3.4 Calibration curve of a) Trolox and b) Ethyl pyruvate using the ABTS assay. ABTS can be oxidised, producing a green colour and the absorbance can be measured at 405 nm with a colorimeter. Trolox is an antioxidant and it was used as a positive control. EP standards were prepared in PBS in the range of 0.5-3.2 mM and used to plot the calibration curve. c) EP calibration curve narrowing the concentration range of the graph in b) to 200-1,600 μM . All standards were run in duplicate and the data presented represent the mean of these measurements. 67

Figure 3.5 UV/Vis spectrophotometric measurement of ethyl pyruvate in PBS. a) Ethyl pyruvate absorption spectra (190 -300 nm). EP standards were prepared in PBS in the range of 40-20,000 μM and PBS was used as a blank. b) EP calibration curve obtained by plotting the value of the peaks against the concentration for each EP standard. EP calibration curves were prepared by narrowing the concentration range of the graph in a) to 40-5,000 μM , due to saturation at higher concentration. Note that this is preliminary data and that more validation is required. 69

Figure 3.6 Calibration curve of Ethyl pyruvate using the Nanospec. Calibration curve of Ethyl pyruvate prepared with the absorbance values measured at the wavelength of 198 nm. EP standards were prepared in PBS in the range of 78-20,000 μM and used to plot the calibration curve. PBS was used as a blank and the standards were measured at two wavelengths, the peak wavelength at 198 nm and the zero wavelength at 300 nm. The values obtained were normalised by subtracting the zero absorbance from the absorbance at 198 nm before plotting the calibration curve..... 71

Figure 3.7 HPLC graphs of EP measurement in PBS at different EP concentrations. Milli absorbance unit (mAU) versus retention time. HPLC was used to measure EP standards in the range of 70 – 50,000 μM in PBS, although here are shown the graphs of some of the standards measured (from top to bottom, 98, 782, 1563,

12,5000 and 50,000 μM EP). The flow rate used was 0.3mL/min for 10 minutes. The absorbance was measured at the wavelength of 203 nm. 73

Figure 3.8 HPLC graphs of ethyl pyruvate measurement in methanol at different EP concentrations. Milli absorbance unit (mAU) versus retention time. HPLC was used to measure EP standards in the range of 70 – 50,000 μM in methanol, although here are shown the graphs of some of the standards measured (from top to bottom, 98, 782, 1563, 12,5000 and 50,000 μM EP). The flow rate used was 0.3mL/min for 10 minutes. The absorbance was measured at the wavelength of 205 nm..... 74

Figure 3.9 Calibration curve of ethyl pyruvate in methanol (HPLC). HPLC was used to measure EP standards in the range of 70 – 50,000 μM in methanol. The absorbance was measured at the wavelength of 205 nm. a) EP calibration curve obtained by plotting the value of the peaks against the concentration for each EP standard in the range of 70 – 50,000 μM in methanol. b) EP calibration curve prepared by narrowing the concentration range of the graph in a) to 70-12,500 μM , due to saturation at higher concentration. Note that this is preliminary data and that more validation is required..... 75

Figure 3.10 Calibration curve of ethyl pyruvate in methanol (UV/Vis spec). UV/Vis spec was used to measure EP standards in the range of 78 – 2,500 μM in PBS. The absorbance was measured at the wavelength of 205 nm. Data represent the mean \pm st dev of three consecutive measurements. 76

Figure 3.11 Stability study of ethyl pyruvate in PBS a) after freezing/thawing; b) at 37°C over time (UV/Vis spec). EP standards in PBS were prepared in the concentration range of 0.078 to 2.5 mM. The standards were then split into 2 batches which were then stored at 2 different temperatures. The reference standards were stored at -20°C, while the others were stored in the incubator at 37°C. The absorbance was measured with the UV/Vis spec at 205nm at different time points, at 1, 3, 7 and 14 days. Day 0 curve is the reference curve. Note that this is preliminary data and that more validation is required. 78

Figure 3.12 Stability study of ethyl pyruvate in PBS a) after freezing/thawing; b) at 37°C over time (Nanospec). EP standards in PBS were prepared in the concentration range of 0.078-2.5 mM. The standards were then split into 2 batches which were then stored at 2 different temperatures. The reference standards were stored at -20°C, while the others were stored in the incubator at 37C. The absorbance was measured with the Nanospec at 198 nm and the wavelengths 300 was used as the zero point. The measurement was performed at different time points, at 1, 3, 7 and 14 days. Note that this is preliminary data and that more validation is required..... 79

Figure 4.1 Alginate gels prepared with 1% LV alginate solution (Sigma) and different CaCl₂ concentrations n=3..... 94

Figure 4.2 Examples of Alginate hydrogels prepared high G content. Left panel shows an alginate hydrogel prepared with 1:1 1% alginate (LVG Novamatrix) solution and 0.6%, CaCl₂ solution. The right panel shows alginate hydrogels prepared with 1:1 1%-2% alginate (LVG Novamatrix) solution and 0.6%, 1%, 1.5% CaCl₂ solution..... 96

Figure 4.3 EP (10mM) loaded alginate hydrogels stability in PBS over 28 days. Alginate gels were placed in PBS and incubated at 37°C at constant agitation. Alginate gels were prepared with a) 1%alginate and b)2% alginate solution using different CaCl₂ concentrations (0.6%, 1%, and 1.5%). The change in weight of the gels was measured at different time point (1 hour, 1 day, 3 days, 5 days, 7 days, 14 days 21 days, 28 days). The weight change (%) is shown in figure as a measurement of hydrogel stability. Data represent the mean ± st dev from three samples. The weight change at the beginning of the experiment (1 hour) was compared to the one at the end of the experiment (28 days) (*p<0.05)..... 98

Figure 4.4. Comparison of the stability of EP loaded alginate hydrogels prepared with 1%alginate and 2% alginate in PBS at 28 days. Alginate gels were placed in PBS and incubated at 37°C at constant agitation. Alginate gels were prepared with either 1%alginate or 2% alginate solution using different CaCl₂ concentrations (0.6%, 1%, and 1.5%). The change in weight of the gels was measured at different

time point (1 hour, 1 day, 3 days, 5 days, 7 days, 14 days, 21 days, 28 days). The weight change (%) is shown in figure as a measurement of hydrogel stability. Data represent the mean \pm st dev from three samples(*p<0.05)..... 99

Figure 4.5 SEM imaging of alginate hydrogels. a) SEM images of the surface and the cross-section of alginate hydrogel without EP; b) SEM images of the surface and the cross-section of alginate hydrogel with (10mM) EP. The hydrogels were prepared with 2% alginate and cross-linked with 1.5% CaCl₂ 101

Figure 4.6 Cumulative EP released from 1% alginate hydrogels over 28 days. a) Cumulative EP release from the gels over time; b) Percentage of EP release over time. The gels were immersed in PBS and incubated at 37 °C at a constant level of agitation. At different time points (1 hour, 1 day, 3 days, 7 days, 14 days, 21 days, 28 days) the samples were collected and stored in the freezer at -20°C. The EP contained in the samples was measured with the Nanospec at 198 nm wavelength. The percentage was calculated using the total amount of EP released by the hydrogel as the total EP present in the hydrogel. 103

Figure 4.7 EP released from 2% alginate hydrogels over 28 days. a) Cumulative EP release from the gels over time; b) Percentage of EP release over time. The gels were immersed in PBS and incubated at 37 °C at a constant level of agitation. At different time points (1 hour, 1 day, 3 days, 7 days, 14 days, 21 days, 28 days) the samples were collected and stored in the freezer at -20°C. The EP contained in the samples was measured with the Nanospec at 198 nm wavelength. The percentage was calculated using the total amount of EP released by the hydrogel as the total EP present in the hydrogel. Data represent the mean \pm st dev from three samples..... 104

Figure 4.8. Comparison of total EP released from 1%alginate hydrogels and 2% alginate hydrogels at 28 days. The gels were immersed in PBS and incubated at 37 °C at a constant level of agitation. At different time points (1 hour, 1 day, 3 days, 7 days, 14 days, 21 days, 28 days) the samples were collected and stored in the freezer at -20°C. The EP contained in the samples was measured with the

Nanospec at 198 nm wavelength. Data represent the mean \pm st dev from three samples. No Significant differences were observed between the datasets..... 105

Figure 5.1 Schematic representation of the experimental design used to investigate the impact of various factors on final gel characteristics. In the methods 1 to 4, a single cross-linker (Calcium chloride) was used to create the bonds within the alginate structure. On the other hand, in the methods 5 and 6 double cross-linking was used to produce the scaffolds (calcium gluconate followed by calcium chloride). 5 replicates were prepared for every formulation..... 116

Figure 5.2 Schematic representation of method 1..... 118

Figure 5.3 Schematic representation of method 2..... 118

Figure 5.4 Schematic representation of method 3..... 119

Figure 5.5 Schematic representation of method 4..... 119

Figure 5.6 Schematic representation of method 5..... 120

Figure 5.7 Schematic representation of method 6..... 121

Figure 5.8 Macro-porous alginate scaffolds stability in PBS over 28 days. A) Alginate scaffolds without EP and b) EP loaded Alginate scaffolds were prepared at either -20 °C (NOEP -20) or -80°C (NOEP -80) using method 1, placed in 1.5 mL PBS and incubated at 37°C at constant agitation. Alginate gels were prepared with 0.5 mL 2% alginate solution and cross-linked in a 1mL 0.2M CaCl₂ bath. The swelling ratio was measured at different time point (1 hour, 1 day, 3 days, 7 days, 14 days 21 days, 28 days). The swelling ratio (%) is shown in figure as a measurement of alginate scaffold stability. Data represent the mean \pm st dev from five samples (*p<0.05, compared to zero-day dataset (paired t-test, two tailed). 123

Figure 5.9. Macro-porous alginate scaffolds stability in PBS at day 28. Alginate scaffolds without EP and EP were prepared at either -20 °C or -80°C using method 1, placed in 1.5 mL PBS and incubated at 37°C at constant agitation.

Alginate gels were prepared with 0.5 mL 2% alginate solution and cross-linked in a 1mL 0.2M CaCl₂ bath. The swelling ratio was measured at different time point (1 hour, 1 day, 3 days, 7 days, 14 days 21 days, 28 days) but here it is shown only at day 28. The swelling ratio (%) is shown in figure as a measurement of alginate scaffold stability. Data represent the mean ± st dev from five samples. No significant differences were observed between the datasets. 124

Figure 5.10 Macro-porous alginate scaffolds stability in PBS over 28 days. a) Alginate scaffolds without EP and b) EP loaded alginate scaffolds were prepared at either -20 °C or -80°C using method 2, placed in 1.5 mL PBS and incubated at 37°C at constant agitation. Alginate gels were prepared with 0.5 mL 2% alginate solution and cross-linked in a 1mL 0.2M CaCl₂ bath. The swelling ratio was measured at different time point (1 hour, 1 day, 3 days, 7 days, 14 days 21 days, 28 days). The swelling ratio (%) is showed in figure as a measurement of alginate scaffold stability. Data represent the mean ± st dev from five samples (*p<0.05)..... 126

Figure 5.11. Macro-porous alginate scaffolds stability in PBS at day 28. Alginate scaffolds without EP and EP were prepared at either -20 °C or -80°C using method 2, placed in 1.5 mL PBS and incubated at 37°C at constant agitation. Alginate gels were prepared with 0.5 mL 2% alginate solution and cross-linked in a 1mL 0.2M CaCl₂ bath. The swelling ratio was measured at different time point (1 hour, 1 day, 3 days, 7 days, 14 days 21 days, 28 days) but here it is shown only at day 28. The swelling ratio (%) is shown in figure as a measurement of alginate scaffold stability. Data represent the mean ± st dev from five samples (*p<0.05)..... 127

Figure 5.12 Comparison of method 1 and method 2 macro-porous alginate scaffolds stability in PBS at day 28. In method 1 scaffolds were prepared with two cycles of freeze-drying. Method 2 was then used to prepare scaffolds with one cycle of freeze-drying, Alginate scaffolds without EP and EP were prepared at either -20 °C or -80°C, placed in 1.5 mL PBS and incubated at 37°C at constant agitation. Alginate gels were prepared with 0.5 mL 2% alginate solution and cross-linked in a 1mL 0.2M CaCl₂ bath. The swelling ratio was measured at different time point (1 hour, 1 day, 3 days, 7 days, 14 days 21 days, 28 days) but here it is shown

only at day 28. The swelling ratio (%) is shown in figure as a measurement of alginate scaffold stability. Data represent the mean \pm st dev from five samples (*p<0.05)..... 128

Figure 5.13 Macro-porous alginate scaffolds stability in PBS over 28 days. a) Alginate scaffolds without EP and b) EP loaded alginate scaffolds were prepared at either -20 °C or -80°C using method 3, placed in 1.5 mL PBS and incubated at 37°C at constant agitation. Alginate gels were prepared with 0.5 mL 2% alginate solution and cross-linked in a 1mL 0.2M CaCl₂ bath. The swelling ratio was measured at different time point (1 hour, 1 day, 3 days, 7 days, 14 days 21 days, 28 days). The swelling ratio (%) is showed in figure as a measurement of alginate scaffold stability. Data represent the mean \pm st dev from five samples (*p<0.05)..... 130

Figure 5.14. Comparison of method 1 and method 3 macro-porous alginate scaffolds stability in PBS at day 28. In method 3 was prepared by adding EP to the alginate solution at the early stage of the scaffold preparation, while in method 1 EP was added at the already formed scaffold. Alginate scaffolds without EP and EP were prepared at either -20 °C or -80°C, placed in 1.5 mL PBS and incubated at 37°C at constant agitation. Alginate gels were prepared with 0.5 mL 2% alginate solution and cross-linked in a 1mL 0.2M CaCl₂ bath. The swelling ratio was measured at different time point (1 hour, 1 day, 3 days, 7 days, 14 days 21 days, 28 days) but here it is shown only at day 28. The swelling ratio (%) is shown in figure as a measurement of alginate scaffold stability. Data represent the mean \pm st dev from five samples (*p<0.05). 131

Figure 5.15 Macro-porous alginate scaffolds stability in PBS over 28 days. a) Alginate scaffolds without EP and b) EP loaded alginate scaffolds were prepared at either -20 °C or -80°C using method 4, placed in 1.5 mL PBS and incubated at 37°C at constant agitation. Alginate gels were prepared with 0.5 mL 2% alginate solution and cross-linked in a 1mL 0.2M CaCl₂ bath. The swelling ratio was measured at different time point (1 hour, 1 day, 3 days, 7 days, 14 days 21 days, 28 days). The swelling ratio (%) is showed in figure as a measurement of alginate scaffold stability. Data represent the mean \pm st dev from five samples (*p<0.05)..... 133

Figure 5.16 Stability in PBS of macro-porous alginate scaffolds prepared with Method 4 at day 28. Alginate scaffolds without EP and EP were prepared at either -20 °C or -80°C using method 4, placed in 1.5 mL PBS and incubated at 37°C at constant agitation. Alginate gels were prepared with 0.5 mL 2% alginate solution and cross-linked in a 1mL 0.2M CaCl₂ bath. The swelling ratio was measured at different time point (1 hour, 1 day, 3 days, 7 days, 14 days 21 days, 28 days) but here it is shown the values of the peak (highest swelling ratio which was at day 21 for all the samples except for the ep-80) and the values at day 28. The swelling ratio (%) is shown in figure as a measurement of alginate scaffold stability. Data represent the mean ± st dev from five samples (*p<0.05). 134

Figure 5.17. Stability study in PBS at 28 days of alginate scaffolds prepared with method 4 compared with the scaffolds prepared with method 2 and method 3. In method 3 scaffolds were prepared with two cycles of freeze-drying, while in Method 4 only one cycle of freeze-drying was used. Method 2 and method 4 consist of similar steps, such as 1 cycles of freeze-drying and CaCl₂ cross-linking bath. The main difference between the two methods is that method 4 was prepared by adding EP to the alginate solution at the early stage of the scaffold preparation, while in method 2 EP was added at the already formed scaffold. Alginate scaffolds without EP and EP were prepared at either -20 °C or -80°C, placed in 1.5 mL PBS and incubated at 37°C at constant agitation. Alginate gels were prepared with 0.5 mL 2% alginate solution and cross-linked in a 1mL 0.2M CaCl₂ bath. The swelling ratio was measured at different time point (1 hour, 1 day, 3 days, 7 days, 14 days 21 days, 28 days) but here it is shown only at day 28. The swelling ratio (%) is shown in figure as a measurement of alginate scaffold stability. Data represent the mean ± st dev from five samples. No Significant differences were observed between the datasets. 135

Figure 5.18 Macro-porous alginate scaffolds stability in PBS over 28 days. a) Alginate scaffolds without EP and b) EP loaded alginate scaffolds were prepared at either -20 °C or -80°C using method 5, placed in 3 mL PBS and incubated at 37°C at constant agitation. Alginate gels were prepared with 0.5 mL 2% alginate solution and double- cross-linked with 0.4-1% Calcium gluconate and 0.2M CaCl₂. The

swelling ratio was measured at different time point (1 hour, 1 day, 3 days, 7 days, 14 days 21 days, 28 days). The swelling ratio (%) is showed in figure as a measurement of alginate scaffold stability. Data represent the mean \pm st dev from five samples. No Significant differences were observed between the datasets. 137

Figure 5.19. Macro-porous alginate scaffolds stability in PBS at day 28. Alginate scaffolds without EP and EP were prepared at either -20 °C (-0.4% Caglu;-1% Caglu) or -80°C (-0.4% Caglu;-1% Caglu) using method 5, placed in 3 mL PBS and incubated at 37°C at constant agitation. Alginate gels were prepared with 0.5 mL 2% alginate solution and 0.5mL of either 0.4% or 1% calcium chloride and placed in a 2mL 0.2M CaCl₂ bath. The swelling ratio was measured at different time point (1 hour, 1 day, 3 days, 7 days, 14 days 21 days, 28 days) but here it is shown only at day 28. The swelling ratio (%) is shown in figure as a measurement of alginate scaffold stability. Data represent the mean \pm st dev from five samples (*p<0.05)..... 138

Figure 5.20 Macro-porous alginate scaffolds stability in PBS over 28 days. a) Alginate scaffolds without EP and b) EP loaded alginate scaffolds. Scaffolds were prepared at either -20 °C or -80°C using method 6, placed in 3 mL PBS and incubated at 37°C at constant agitation. Alginate gels were prepared with 0.5 mL 2% alginate solution and double- cross-linked with 0.4-1% Calcium gluconate and 0.2M CaCl₂. The swelling ratio was measured at different time point (1 hour, 1 day, 3 days, 7 days, 14 days 21 days, 28 days). The swelling ratio (%) is showed in figure as a measurement of alginate scaffold stability. Data represent the mean \pm st dev from five samples. No Significant differences were observed between the datasets. 140

Figure 5.21. Macro-porous alginate scaffolds stability in PBS at day 28 prepared with method 6. Alginate scaffolds without EP and EP were prepared at either -20 °C (-0.4% Caglu;-1% Caglu) or -80°C (-0.4% Caglu;-1% Caglu) using method 6, placed in 3 mL PBS and incubated at 37°C at constant agitation. Alginate gels were prepared with 0.5 mL 2% alginate solution and 0.5mL of either 0.4% or 1% calcium chloride and placed in a 2mL 0.2M CaCl₂ bath. The swelling ratio was

measured at different time point (1 hour, 1 day, 3 days, 7 days, 14 days 21 days, 28 days) but here it is shown only at day 28. The swelling ratio (%) is shown in figure as a measurement of alginate scaffold stability. Data represent the mean \pm st dev from five samples. No Significant differences were observed between the datasets. 141

Figure 5.22. Comparison of stability of macro-porous alginate scaffolds at day 28 prepared with method 6 and method 5. In method 5, scaffolds were prepared with two cycles of freeze-drying, while in method 6 one cycle of freeze-drying was used. Alginate scaffolds without EP and EP were prepared at either -20 °C (-0.4% Caglu;-1% Caglu) or -80°C (-0.4% Caglu;-1% Caglu) using method 6, placed in 3 mL PBS and incubated at 37°C at constant agitation. Alginate gels were prepared with 0.5 mL 2% alginate solution and 0.5mL of either 0.4% or 1% calcium chloride and placed in a 2mL 0.2M CaCl₂ bath. The swelling ratio was measured at different time point (1 hour, 1 day, 3 days, 7 days, 14 days 21 days, 28 days) but here it is shown only at day 28. The swelling ratio (%) is shown in figure as a measurement of alginate scaffold stability. Data represent the mean \pm st dev from five samples (*p<0.05). 142

Figure 5.23 EP release study from alginate scaffolds. a) Cumulative EP release profile and b) percentage of EP released from scaffolds produce using method 1 (-20 and -80 values are shown but overlapping). Scaffolds were produced with an initial concentration of 2% alginate with two cycles of freeze-drying. EP was added to the scaffolds after the first freeze-drying cycle, before the CaCl₂ bath. Data represent the mean \pm st dev from five samples No Significant differences were observed between the datasets). 144

Figure 5.24 EP release study from alginate scaffolds. a) Cumulative EP release profile and b) percentage of EP released from scaffolds produce using method 2. Scaffolds were produced with an initial concentration of 2% alginate with one cycle of freeze-drying. EP was added to the scaffolds after the freeze-drying cycle, before the CaCl₂ bath. Data represent the mean \pm st dev from five samples. 146

Figure 5.25. Comparison of total EP release from Alginate scaffolds prepared at either -20 °C or -80°C using method 1 and method 2. In method 1 scaffolds were prepared with two cycles of freeze-drying. Method 2 was then used to prepare scaffolds with one cycle of freeze-drying, Alginate scaffolds without EP and EP were prepared at either -20 °C or -80°C, placed in 1.5 mL PBS and incubated at 37°C at constant agitation. Alginate gels were prepared with 0.5 mL 2% alginate solution and cross-linked in a 1mL 0.2M CaCl₂ bath. EP release was measured at different time point (1 hour, 1 day, 3 days, 7 days, 14 days 21 days, 28 days) but here it is shown the total EP release of the scaffolds. Data represent the mean ± st dev from five samples (*p<0.05). 147

Figure 5.26 EP release study from alginate scaffolds. a) Cumulative EP release profile and b) percentage of EP released from scaffolds produce using method 3. Scaffolds were produced with an initial concentration of 2% alginate with two cycles of freeze-drying. EP was added to the alginate solution before the first freeze-drying cycle. Data represent the mean ± st dev from five samples..... 149

Figure 5.27. Comparison of total EP release from Alginate scaffolds prepared at either -20 °C or -80°C using method 1 and method 3. In method 1 EP was added to the formed scaffolds after the first freeze-drying cycle, while in method 3 EP was added to the alginate solution, at the early stage of alginate scaffold preparation. Alginate scaffolds without EP and EP were prepared at either -20 °C or -80°C, placed in 1.5 mL PBS and incubated at 37°C at constant agitation. Alginate gels were prepared with 0.5 mL 2% alginate solution and cross-linked in a 1mL 0.2M CaCl₂ bath. EP release was measured at different time point (1 hour, 1 day, 3 days, 7 days, 14 days 21 days, 28 days) but here it is shown the total EP release of the scaffolds. Data represent the mean ± st dev from five samples (*p<0.05). 150

Figure 5.28 EP release study from alginate scaffolds. a) Cumulative EP release profile and b) percentage of EP released from scaffolds produce using method 4. Scaffolds were produced with an initial concentration of 2% alginate with one cycle of freeze-drying. EP was added to the alginate solution before the first freeze-drying cycle. Data represent the mean ± st dev from five samples..... 152

Figure 5.29. Comparison of total EP release from Alginate scaffolds prepared at either -20 °C or -80°C using method 4 and method 3. In method 3 scaffolds were prepared with two cycles of freeze-drying. Method 4 was then used to prepare scaffolds with one cycle of freeze-drying. Alginate scaffolds without EP and EP were prepared at either -20 °C or -80°C, placed in 1.5 mL PBS and incubated at 37°C at constant agitation. Alginate scaffolds were prepared with 0.5 mL 2% alginate solution and cross-linked in a 1mL 0.2M CaCl₂ bath. EP release was measured at different time point (1 hour, 1 day, 3 days, 7 days, 14 days 21 days, 28 days) but here it is shown the total EP release of the scaffolds. Data represent the mean ± st dev from five samples (*p<0.05)..... 153

Figure 5.30. Comparison of total EP release from Alginate scaffolds prepared at either -20 °C or -80°C using method 4 and method 2. In method 2 EP was added to the formed scaffolds after the first freeze-drying cycle, while in method 4 EP was added to the alginate solution, at the early stage of alginate scaffold preparation. Alginate scaffolds without EP and EP were prepared at either -20 °C or -80°C, placed in 1.5 mL PBS and incubated at 37°C at constant agitation. Alginate gels were prepared with 0.5 mL 2% alginate solution and cross-linked in a 1mL 0.2M CaCl₂ bath. EP release was measured at different time point (1 hour, 1 day, 3 days, 7 days, 14 days 21 days, 28 days) but here it is shown the total EP release of the scaffolds. Data represent the mean ± st dev from five samples (*p<0.05). 154

Figure 5.31 EP release study from alginate scaffolds. a) Cumulative EP release profile and b) percentage of EP released from scaffolds produce using method 5. Scaffolds were produced with an initial concentration of 2% alginate and cross-linked twice with 0.4% or 1% calcium gluconate and then with 0.2M CaCl₂. The scaffolds were produced with two cycles of freeze-drying. EP was added to the alginate solution before the first freeze-drying cycle. Data represent the mean ± st dev from five samples. 156

Figure 5.32. Comparison of total EP release from alginate scaffolds prepared with method 5. Scaffolds were prepared with an initial concentration of 2% alginate and cross-linked twice with 0.4% or 1% calcium gluconate and then with 0.2M

CaCl₂. The scaffolds were produced with two cycles of freeze-drying. EP was added to the alginate solution before the first freeze-drying cycle. Data represent the mean ± st dev from five samples (*p<0.05)..... 157

Figure 5.33 EP release study from alginate scaffolds. a) Cumulative EP release profile and b) percentage of EP released from scaffolds produce using method 6. Scaffolds were produced with an initial concentration of 2% alginate and cross-linked twice with 0.4% or 1% calcium gluconate and then with 0.2M CaCl₂. The scaffolds were produced with one cycle of freeze-drying. EP was added to the alginate solution before the freeze-drying cycle. Data represent the mean ± st dev from five samples..... 159

Figure 5.34. Comparison of total EP release from alginate scaffolds prepared with method 6. Scaffolds were prepared with an initial concentration of 2% alginate and cross-linked twice with 0.4% or 1% calcium gluconate and then with 0.2M CaCl₂. The scaffolds were produced with two cycles of freeze-drying. EP was added to the alginate solution before the first freeze-drying cycle. Data represent the mean ± st dev from five samples (*p<0.05)..... 160

Figure 5.35. Comparison of total EP release of scaffolds prepared with method 6 and method 5. In method 5, scaffolds were prepared with two cycles of freeze-drying, while in method 6 one cycle of freeze-drying was used. Alginate scaffolds without EP and EP were prepared at either -20 °C (-0.4% Caglu;-1% Caglu) or -80°C (-0.4% Caglu;-1% Caglu) using method 6, placed in 3 mL PBS and incubated at 37°C at constant agitation. Alginate gels were prepared with 0.5 mL 2% alginate solution and 0.5mL of either 0.4% or 1% calcium chloride and placed in a 2mL 0.2M CaCl₂ bath. EP release was measured at different time point (1 hour, 1 day, 3 days, 7 days, 14 days 21 days, 28 days) but here it is shown the total EP release. Data represent the mean ± st dev from five samples (*p<0.05). 161

Figure 5.36 Porosity measurement of the alginate scaffolds prepared with single crosslinking. The scaffolds were prepared with methods 1-4. Data represent the mean ± st dev from five samples (*p<0.05)..... 164

- Figure 5.37 Porosity measurement of the alginate scaffolds prepared with single crosslinking. The scaffolds were prepared with methods 1-5. Data represent the mean \pm st dev from five samples (*p<0.05)..... 166
- Figure 5.38 Representative SEM images of alginate scaffolds surface prepared with method 6. Scaffolds were prepared a) at -20°C without EP; b) at -20°C with EP; c) at -80°C without EP and d) at -80°C with EP. The images were obtained from dry scaffolds at different magnification (x150 and x300)..... 169
- Figure 5.39 Representative SEM images of alginate scaffolds cross-section prepared with method 6. Scaffolds were prepared a) at -20°C without EP; b) at -20°C with EP; c) at -80°C without EP and d) at -80°C with EP. The images were obtained from dry scaffolds at x150 magnification. 171
- Figure 6.1 Assessment of EP toxicity on cardiac fibroblasts. a) Cell viability measured with Neutral red assay after 5 days of EP exposure in culture. b) Metabolic activity of cardiac fibroblasts measured with MTT assay after 5 days of EP exposure in culture. Cells were seeded at a cell density of 3.5×10^4 cells/ml (700 cells /well). Cells with no EP treatment were used as a Control. Data represent the mean \pm standard deviation from three technical replicates from a single culture *p<0.05..... 184
- Figure 6.2 Effect of EP on AB reduction. EP standards in 20% serum media and in serum free media were prepared in a sterile environment. 200 μ L of each standard was placed in a 24 well plate. 10% AB was added to each well and incubated at 37°C for 4 hours. 20% serum media and serum free media were used as Control respectively. Data represent the mean \pm standard deviation from three replicate measurements from a single experiment. No Significant differences were observed between the serum-free and 20% serum media. 186
- Figure 6.3 Cell viability measurement of cardiac fibroblasts treated with EP (1,000 – 20,000 μ M) for 5 days. Cell viability was measured with alamarBlue assay after 1 day, 3 days and 5 days of EP exposure in culture. Cells were seeded at a cell density of 3.5×10^4 cells/ml (700 cells /well). Cells with no EP treatment

in 20% serum media were used as a negative control, cells with no EP treatment in serum-free media were used as a positive control. Data represent the mean +/- standard deviation from three replicate measurements from three experiments. No Significant differences were observed between the datasets. 187

Figure 6.4 Cell proliferation measurement of cardiac fibroblasts treated with EP (1,000 – 20,000 μ M). Cell proliferation was measured with BrdU assay after 1 day and 5 days of EP exposure in culture. Cells were seeded at a cell density of 3.5×10^4 cells/ml (700 cells /well). Cells with no EP treatment in 20% serum media were used as a negative Control, cells with no EP treatment in serum free media were used as a positive Control. Data represent the mean +/- standard deviation from three replicate measurements from three experiments * $p < 0.05$ 188

Figure 6.5 Representative images of Live/dead staining of cardiac fibroblasts treated with EP for 5 days. a) cardiac fibroblasts with no EP treatment in serum media (Control); b) cardiac fibroblasts treated with 3,000 μ M EP; c) Cardiac fibroblasts treated with 10,000 μ M EP. Cells were seeded at a cell density of 3.5×10^4 cells/ml in 35 mm culture Petri dishes (20 μ m)..... 189

Figure 6.6 Preliminary study of the EP effect on cardiac fibroblasts exposed to 100 μ M H₂O₂ for 24 hours. EP was administered after H₂O₂ exposure (blue) or in combination with H₂O₂ (orange). Cell viability was determined with alamarBlue assay. Cells were seeded at a cell density of 3.5×10^4 cells/ml (700 cells /well). Cells in serum media without hydrogen peroxide and EP treatment were used as a negative Control and cells treated with 100 μ M H₂O₂ without EP were used as a positive control. Data represent the mean +/- standard deviation from three replicate measurements from one experiment. No Significant differences were observed between the datasets. 191

Figure 6.7 Preliminary study of EP effect on cardiac fibroblasts exposed to 150 μ M H₂O₂ for 24 hours. EP was administered after H₂O₂ exposure (dark grey) or in combination with H₂O₂ (light grey). Cell viability was determined with alamarBlue assay. Cells were seeded at a cell density of 3.5×10^4 cells/ml

(700 cells /well). Cells without hydrogen peroxide and EP treatment were used as a negative Control and cells treated with the highest concentration of hydrogen peroxide were used as a positive control. Data represent the mean +/- standard deviation from three replicate measurements from one experiment *p<0.05.. 192

Figure 6.8 LDH assay of 3T3 cells seeded onto alginate scaffolds. The cells were either seeded into dry scaffolds or pre-wetted with cell media (n=5). Cells were seeded at a cell density of 3.5×10^4 cells/ml (700 cells /well). Cells with no scaffolds were used as a control. Data represent the mean +/- standard deviation from three replicate measurements from one experiment *p<0.05. 194

Figure 6.9 Representative images of Live/dead staining of 3T3 cells seeded onto alginate scaffolds after 5 days in culture. a) Live/dead (PI/CFDA) staining of cells seeded onto a dry alginate scaffold; b) Live/dead staining of cells seeded onto a pre-wetted alginate scaffold. The live/dead staining differentiate the live (green) and dead (red) cells. Images representative of 5 separate scaffolds for each group. 195

Figure 6.10 Representative images of Live/dead staining of the 3T3 cells seeded onto a pre-wetted sample using z-stacking method. Images of planes were taken at various depths. Cells were seeded at a cell density of 3.5×10^4 cells/ml (700 cells /well). Moving through the sequence (from left to right) it is possible to see the cells distributed through the scaffold, from the top surface until a depth of 135µm. Images obtained from a single scaffold..... 196

Figure 6.11 Cell viability measurement of cardiac fibroblasts seeded onto four groups of scaffolds; Alginate alone; Alginate:EP; RGD-Alginate alone; RGD-Alginate:EP. The scaffolds were produced with method 6 at -20°C and - 80°C. Cells were seeded at a cell density of 3.5×10^4 cells/ml (700 cells /well). After 5 days of incubation, Neutral Red assay was used to measure cell viability (n=3) Cells only in 20% serum media were used as a negative Control, cells only in serum-free media were used as a positive Control (n=3). Data represent the mean +/- standard deviation from three replicate measurements from one experiment *p<0.05. 198

Figure 6.12 LDH activity measurement of cardiac fibroblasts seeded onto four groups of scaffolds; Alginate alone; Alginate:EP; RGD-Alginate alone; RGD- Alginate: EP. Cells were seeded at a cell density of 3.5×10^4 cells/ml (700 cells /well). The scaffolds were produced with method 6 at: a) - 20 and b) - 80°C. At day 1, day3 and day 5 of incubation LDH was measured. Data represent the mean +/- standard deviation from three replicate measurements from one experiment *p<0.05. 199

Figure 6.13 Fluorescence microscopy images (10X) following PI (Dead cells, red)/ CFDA (Live cells, green) staining of rat cardiac fibroblasts seeded onto scaffolds produced with method 6 at -20C: a) Alginate alone; b) Alginate:EP; c) RGD- Alginate alone d) RGD-Alginate:EP; and on scaffolds prepared at -80C: e) Alginate alone; f) Alginate:EP; g) RGD-Alginate alone h) RGD-Alginate:EP. Cells were seeded at a cell density of 3.5×10^4 cells/ml (700 cells /well). At the end of the incubation period of 5 days, the patches were taken forward for evaluation by fluorescent microscopy Images are representative of 5 independent images from each sample. 201

Figure 6.14 Fluorescence microscopy images (10X) following PI (Dead cells, red)/ CFDA (Live cells, green) staining of rat cardiac fibroblasts seeded onto scaffolds produced with method 6 at -20°C: a) RGD-Alginate:EP; and on scaffolds prepared at -80°C: b) RGD-Alginate:EP. Cells were seeded at a cell density of 3.5×10^4 cells/ml (700 cells /well). At the end of the incubation period of 5 days, the patches were taken forward for evaluation by fluorescent microscopy. 202

List of tables

Table 1. Summary details of different methodologies used to produce macro-porous alginate scaffolds.....	46
Table 2 Summary of the experiments carried out during the optimisation of the alginate hydrogel phase of the study.....	93
Table 3 EP loading efficiency (%) in alginate hydrogels. Data represent the mean \pm stdev (n=3)	106
Table 4 Summary of the methodology used to prepare EP alginate scaffolds, .n=5	117
Table 5 Drug loading efficiency of alginate scaffolds. n=5.....	162
Table 6 Measurement of the porous size of alginate scaffolds. n=5.....	171

List of abbreviations

ABTS: 2, 2'-Azino-Bis (3-Ethylbenzthiazoline-6-Sulfonic Acid)

ACE: Angiotensin-Converting Enzyme

ACS: Acute Coronary Syndrome

AMI: Acute Myocardial Infarction

ATP: Adenosine Triphosphate

BRDU: Bromodeoxyuridine

CABG: Coronary Artery Bypass Graft

CaCl₂: Calcium Chloride

Caglu: Calcium Gluconate

CPB: Cardio Pulmonary Bypass

CVD; Cardiovascular Diseases

DMEM: Dulbecco's Modified Eagle's Medium

DPPH: 2,2-Diphenyl-1-Picrylhydrazyl

ECM: Extra Cellular Matrix

EF: Ejection Fraction

EP: Ethyl Pyruvate

EU: European Union

FBS: Foetal Bovine Serum

FGF: Fibroblasts Growth Factor

G: Guluronate

GSH: Glutathione

GSSG: Glutathione Disulphide

GSHPx: Glutathione Peroxidase

HF: Hearth Failure

hTM: Human Trabecular Meshwork Cells

IGF-1: Insulin-Like Growth Factor 1

LDH: Lactate Dehydrogenase

LDL: Low-Density Lipoprotein

LV: Left Ventricle

M: Mannuronate

MI: Myocardial Infarction

MMP: Matrix metalloproteinases

NEAA: Non Essential Amino Acids

NR: Neutral Red

OH: Hydroxyl Radical

PBS: Phosphate Buffer Solution

PCI: Percutaneous Coronary Intervention

PEG: Poly (Ethylene Glycol)

PLGA: Poly (Lactic-Co-Glycolic Acid)

RGD: Arginine-Glycine-Aspartic Acid

ROS: Reactive Oxygen Species

SOD: Superoxide Dismutase

STEMI: ST-Myocardial Infarction

TCA: Tri-Carboxyl Acid

VEGF: vascular Endothelial Growth Factor

XO: Xanthine Oxidase

1 CHAPTER ONE

LITERATURE REVIEW

1.1 Introduction

Cardiovascular diseases (CVD) are the main cause of death in the European Union (EU) and the leading cause of illness and disability (Wilkins, *et al.*, 2017). The European Heart Network estimates that the number of deaths caused by CVD each year in EU is over 1.8 million, 37% of all deaths in EU (Wilkins, *et al.*, 2017). The term cardiovascular disease is the general term that includes a category of diseases of the heart and the circulatory system such as myocardial infarction, stroke, cardiomyopathies and heart failure (Nichols, *et al.*, 2012). Heart disease and stroke are respectively the first and the second most common causes of death in the EU (Wilkins, *et al.*, 2017). In addition, the social and economic cost of CVD is estimated to be almost €200 billion per year for the EU economy (Wilkins, *et al.*, 2017). In particular, around half of the total cost (€111 billion) is the cost of direct health care, €54 billion is the estimation of the cost for productivity losses and the remaining €45 billion is the cost for the care of people living with CVD morbidities (Wilkins, *et al.*, 2017).

1.2 Clinical needs for cardiac regeneration

1.2.1 Myocardial Ischemia and left ventricular remodelling

Coronary arteries provide oxygen and nutrients to the cardiac tissue (Nabel & Braunwald, 2012). These arteries can be affected by atherosclerosis, a chronic inflammation which develops over time in response to biochemical stimuli and various inflammatory factors (Nabel & Braunwald, 2012). The endothelium is affected by such inflammation, undergoing a transformation in permeability, allowing access and the retention of monocytes and LDL molecules within the vessel wall (Nabel & Braunwald, 2012). The subsequent accumulation of cholesterol, calcium, collagen and other components within the wall creates a plaque, so called atherosclerotic plaque, which compromises the blood flow in the affected artery. In some cases, the plaque may rupture, followed by a formation of a thrombus and consequently the partial or

complete interruption of the blood flow to the surrounding tissue (Nabel & Braunwald, 2012). When the blood flow is interrupted, the oxygen and the nutrients cannot reach the cells. The subsequent lack of oxygen into the myocardium is referred to as myocardial ischemia, while in the brain this is referred to as stroke. A prolonged oxygen deprivation leads to cell death in the affected area of the heart which is known as myocardial infarction (Nabel & Braunwald, 2012).

After myocardial infarction, it is important to restore the blood flow that has been compromised. Thrombolysis treatment can be used to unblock the coronary arteries by dissolving the thrombus in the acute phase, but ultimately a longer term solution involves a revascularisation procedure. Percutaneous coronary intervention (PCI) and coronary artery bypass graft (CABG) are generally the preferred revascularization options for such ischaemic hearts (Deb, *et al.*, 2013). PCI consists of the insertion of a catheter through the radial or femoral artery, reaching the point where the atherosclerotic plaque caused ischaemia. The blood flow is restored through the initial expansion of a balloon and a stent is then implanted permanently to keep the lumen open. This is often the preferred method to restore the blood flow, as long as it is performed in the first 90 minutes after MI (Smith, *et al.*, 2015). However, about 30% of the patients with acute myocardial infarction are not eligible for PCI (Dasari, *et al.*, 2016). There are cases when it is either not possible to perform PCI or when the outcome is likely to be enhanced by the use of CABG. CABG is a more invasive surgical method to restore the blood flow. The bypass is performed by using a healthy artery or vein to create a second passage for the blood, bypassing the blockage (Deb, *et al.*, 2013). In order to perform the CABG, cardiopulmonary bypass (CPB) is generally used to support the circulation during the procedure (Zakkar, *et al.*, 2015). Once isolated, the heart is perfused with cardioplegia solution, which stops the heart (Knott, *et al.*, 2006). Even though cardioplegia is used to reduce cell damage during CPB, ischaemic injury still occurs (Zakkar, *et al.*, 2015).

Although the reperfusion strategies outlined above are generally successful in restoring the blood flow to the ischaemic area, they can also increase cell death in the myocardium, a condition known as ischaemia/reperfusion injury (Nikolic-Heitzler, *et al.*, 2006). After ischaemia/reperfusion, the heart may undergo a progressive

transformation in the anatomy and in the physiology of the myocardium, and this process is called ventricular remodelling (Gajarsa & Kloner, 2011). At the infarcted area where the cardiomyocytes died, the necrotic tissue is replaced by connective tissue which presents little or no contractile function.

An increase of cardiac fibroblasts density has been observed in the proximity of the scar tissue after myocardial infarction (Camelliti, *et al.*, 2005). During the process of scar formation, cardiac fibroblasts undergo a phenotypic modulation to myofibroblasts, which are thought to be responsible for cardiac remodelling that may ultimately lead to heart failure (Baum & Duffy, 2011). In fact, myofibroblasts have a greater ability to synthesise ECM proteins compared to cardiac fibroblasts. The increase of collagen deposition by myofibroblasts leads to the formation of the hypertrophic fibrotic scar in the infarcted heart (Calderone, *et al.*, 2006). This increase in fibrotic accumulation at the infarcted area may result in sliding displacement (slippage) of cardiomyocytes, with a decrease in muscular layers in the ventricular wall, leading to ventricular dilatation and consequent cardiac dysfunction (Kong, *et al.*, 2014).

Myofibroblasts also secrete inflammatory cytokines, such as IL-6, IL-10, TNF α , IL-1 α and IL-1 β , which maintain the local inflammatory response to cardiac injury (Baum & Duffy, 2011). At this point, the heart cannot efficiently contract anymore. To overcome this problem, and to maintain the oxygen supply, the heart undergoes remodelling, resulting in important changes in its anatomy (Gajarsa & Kloner, 2011). In particular, in the first day after MI the myocardial cells undergo necrosis and the collagen fibres start to degenerate. From day three to four the inflammatory response occurs, with the migration of macrophages to the necrotic tissue. This period is followed by infarct expansion, which leads to left ventricular remodelling (Gajarsa & Kloner, 2011). At the beginning, these responses have beneficial effects because the heart can compensate for the contractility loss of the infarcted area. Unfortunately, over time this process may lead to left side heart failure with an increase of wall stress and oxygen demand (Gajarsa & Kloner, 2011). In some cases, LV function can be improved using cardiac resynchronisation, β -blockers therapy or revascularisation, such as CABG (Bonow, *et al.*, 2015).

In the prospective Surgical Treatment for Ischemic Heart Failure (STICH) trial, 1,212 patients with coronary artery disease and LV dysfunction (with low EF, $\leq 35\%$) were randomly assigned to either a medical therapy alone (602 patients) or to medical therapy with CABG (610 patients) (Carson P & Investigators., 2013). Results of this study showed that the use of CABG statistically reduced sudden death and fatal pump failure events, compared with medical therapy alone. This protective effect of CABG principally occurred after 24 months (Carson P & Investigators., 2013). In another study, revascularisation in patients with marked LV remodelling and low ejection fraction (EF) did not improve LV function or survival (Moreyra, *et al.*, 2013). Data from 65,377 patients who underwent CABG surgery in New Jersey from 1998 to 2007 were analysed, in order to identify the factors related to heart failure after CABG (Moreyra, *et al.*, 2013). They registered that the admission rate for heart failure (HF) post-CABG was 15.7% after 1 year and 18.8% 2 years after surgery. Patients that had low EF ($< 35\%$) before CABG had 1.5-2.7 times higher risk of in-hospital and 2 year mortality compared to the patients with higher EF (Moreyra, *et al.*, 2013).

1.2.2 Oxidative stress and inflammation in injured hearts

Oxidation and reduction reactions are fundamental to various different metabolic processes (Rodrigo, *et al.*, 2013). Oxidants, also called reactive oxygen species (ROS), are the product of the aerobic cellular metabolism by reduction of the oxygen molecule (Tsutsui, *et al.*, 2011). ROS include free radicals such as hydroxyl radical (OH \cdot), superoxyde (O $_2^{\cdot-}$) lipid radicals (ROO \cdot) and nitric oxide (NO), and non-free radicals such as hydrogen peroxyde (H $_2$ O $_2$) and peroxyxynitrite (ONOO \cdot) (Elahi, *et al.*, 2009). When there is an imbalance between oxidants and antioxidants, with the oxidants being most abundant, this gives rise to a state known as oxidative stress. Under physiological conditions, ROS produced are easily scavenged by endogenous enzymes, such as catalase, superoxide dismutase (SOD) and glutathione peroxidase (GSHPx) (Tsutsui, *et al.*, 2011). High level of ROS can open the mitochondrial membrane permeability transition pore (PTP), causing the release of the cytochrome c and other factors, leading to apoptotic cell death (Elahi, *et al.*, 2009).

Under normal pathological conditions, ROS are produced by mitochondria respiration, neutrophil activation, xanthine oxidase (XO) and arachidonic acid metabolism

(Rodrigo, *et al.*, 2013). ROS is also involved in the initiation at cellular level of the inflammation activity during the cardiovascular disease process (Figure 1.1).

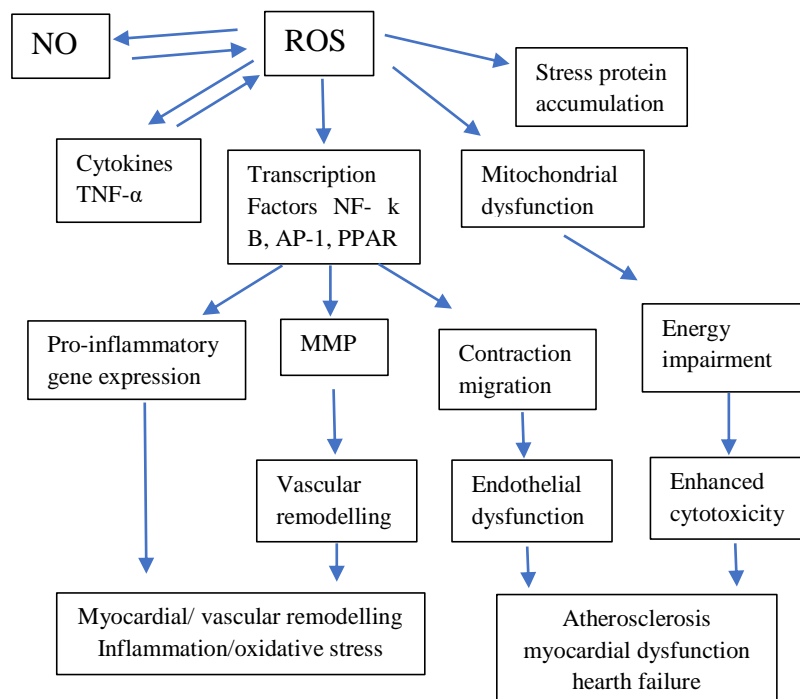


Figure 1.1 Schematic representation of the ROS and NO involvement of the initiation of the inflammation state at the cellular level and consequent development of cardiac diseases. Adapted from (Elahi, *et al.*, 2009).

The inflammation that occurs after ischemia/reperfusion leads to high levels of oxidative stress which produce deleterious effects in the myocardium (Hori & Nishida, 2009). ROS and inflammatory cytokines, such as TNF alpha and beta and interleukin-6 (IL-6) are produced at the infarcted area of the myocardium. During the reperfusion, the presence of Xanthine Oxidase, a derived form of the enzyme xanthine oxidoreductase which generates ROS, is increased and this produces more ROS (Rodrigo, *et al.*, 2013). The presence of oxidative stress in the infarcted area is not limited to the period post MI, but it lasts during cardiac repair and LV remodelling (Sia, *et al.*, 2002).

Whilst it is difficult to describe the temporal nature of this oxidative stress response in detail, in a clinical study carried out by Nikolic-Heitzler, *et al.*, 2006, the level of

peroxide in the blood was measured in patients who had experienced an acute myocardial infarction (Nikolic-Heitzler, *et al.*, 2006). The patients underwent emergency PCI and the samples were taken before the procedure and then after two hours, four hours, three days and seven days (Nikolic-Heitzler, *et al.*, 2006). The results of this study showed that the level of peroxide in the blood increased progressively, reaching a peak after 7 days (end point) when the patients were discharged from the hospital (Nikolic-Heitzler, *et al.*, 2006).

The levels of inflammation (TNF-alpha and beta) have also been measured in different rat models of acute myocardial infarction (Ono, *et al.*, 1998) (Sia, *et al.*, 2002). Ono *et al.* discovered that a week after myocardial infarction, the level of TNF- beta showed the highest peak (Ono, *et al.*, 1998), while Sia *et al.*, 2002, demonstrated a sustained increase of TNF-alpha for the following 3 weeks after MI (Sia, *et al.*, 2002).

Matrix metalloproteinase (MMP) are a group of enzymes responsible for the extracellular matrix turnover (Vanhoutte, *et al.*, 2006). In infarcted hearts, MMPs are activated by the inflammatory cytokines, leading to the progressive degradation of the extracellular matrix (Vanhoutte, *et al.*, 2006). In one study conducted on transgenic mice with a cardiac overexpression of TNF-alpha, hearts were found to have high levels of inflammation, left ventricular enlargement and myocardial fibrosis (Sivasubramanian, *et al.*, 2001). The overexpression of TNF-alpha in mice was also accompanied by an increase in the activity of MMPs with this corresponding to a decrease in myocardial collagen content (Sivasubramanian, *et al.*, 2001). In the same study, it was also demonstrated that MMP activity decreased over time, due to the increase in tissue inhibitors of MMPs (TIMP) (Sivasubramanian, *et al.*, 2001). In fact, TIMPs are thought to play a crucial role in preservation of the ECM, balancing the effect of MMPs. Consequently, an imbalance between the levels of MMPs and TIMPs can have damaging effects in the ECM, as shown after myocardial infarction (Sakata, *et al.*, 2004).

In conclusion, ROS and inflammatory cytokines not only damage cell membranes causing cell death, but they also create a cascade of damaging effects in the myocardium, leading disease progression. (Hori & Nishida, 2009).

1.2.3 Current treatments for damaged myocardium

Patients that present with ST-myocardial infarction (STEMI), are treated acutely with PCI to restore the blood flow, as mentioned in section 1.2.1. If this treatment is not available in the 120 minutes after STEMI, it is recommended that a fibrinolytic therapy should be administered to the patients within 30 minutes of hospital arrival (Smith, *et al.*, 2015). The management of acute coronary syndrome (ACS), which includes different myocardial ischaemic states such as unstable angina, STEMI and non-STEMI, is very important in both acute and long-term stages. Antiplatelet therapy, such as aspirin with a P2Y₁₂ antagonist, is given as soon as possible to the patients and should be continued indefinitely to reduce the risk of thrombosis (Smith, *et al.*, 2015). The antiplatelet therapy is given to patients with ACS which are both medically managed or undergoing PCI (Smith, *et al.*, 2015). Statins, which are lipid lowering agents, are also commonly given to patients who have suffered from MI (Smith, *et al.*, 2015).

Beta-adrenergic blockers (β -blockers) are used to lower myocardial contractility, by targeting the beta receptors in the myocardium. The main benefit of using β -blockers is the decrease of oxygen demand, by reducing the heart work (Smith, *et al.*, 2015). β -blockers are administered in the 24 hours after an acute coronary event, but it is not recommended in patients with HF, with low cardiac output state or high chance of cardiogenic shock (Smith, *et al.*, 2015). The carvedilol post infarction survival-controlled evaluation (CAPRICORN) trial showed that the β -blocker carvedilol with ACE inhibitors improved mortality by decreasing systolic volume in post infarction patients (Gajarsa & Kloner, 2010).

Angiotensin-converting enzyme (ACE) inhibitors are used to decrease blood pressure through an inhibition of angiotensin I mediated blood vessel constriction (Smith, *et al.*, 2015). These should be administered in the first 24 after an ACS event in patients with HF, low EF, STEMI or pulmonary congestion (Smith, *et al.*, 2015). ACE inhibitors have been demonstrated to reduce left ventricular remodelling in different clinical studies (Sharpe, *et al.*, 1988) (Pfeffer, *et al.*, 1988). In a study conducted on 60 patients with left ventricular dysfunction, 1 week after Q wave-myocardial infarction the ACE inhibitor captopril was given three times per day. Left ventricular

volume was measured every 3 months for 1 year (Sharpe, *et al.*, 1988). The results showed that in patients treated with captopril the left ventricular end-diastolic volume index remained unchanged, while the left ventricular end-systolic volume index was reduced. The stroke volume and the ejection fraction index increased from month 1. In contrast, the placebo group showed a significant increase in left ventricular volume, with ejection fraction reduced and stroke volume unaltered (Sharpe, *et al.*, 1988). In another study, patients who underwent cardiac catheterization 11 to 31 days after infarction, were treated with either captopril or placebo (Pfeffer, *et al.*, 1988). After 1 year of follow up, the increase in the ventricular end-diastolic volume was reduced in the captopril group compared to the placebo (Pfeffer, *et al.*, 1988). Although captopril has shown to attenuate left ventricular dilatation after infarction, another study conducted on patients with HF and angina showed that treatment with captopril increased the symptoms of angina and compromised myocardial reperfusion because of its hypotension effect (Cleland, *et al.*, 1991).

Although some pharmacological treatments above have been shown to reduce the ventricular remodelling, these treatments are not always successful with many patients still going on to develop heart failure (Smith, *et al.*, 2015). For this reason, novel strategies to alleviate cardiac injury have been investigated, such as cell therapy, gene therapy, growth factors/protein delivery and pharmacological targeting of inflammation and oxidative stress.

1.3 Novel strategies to alleviate cardiac injury

1.3.1 Cell therapy for cardiac regeneration

Cardiac cellular transplantation is a broad term that is used to describe the use of different types of cells to regenerate damaged myocardial tissue (Zhang, *et al.*, 2015). Many different cell types have been investigated so far including adult stem cells, embryonic and induced pluripotent stem cells (Zhang, *et al.*, 2015).

1.3.1.1 *Adult stem cells*

The initial studies on cellular transplantation were focussed on the use of adult stem cells. Adult stem cells, also known as somatic stem cells, are undifferentiated cells

which have the ability to renew themselves and to differentiate into different cell types to replenish dying cells (Montagnani, *et al.*, 2016). Early animal studies showed promising results when they injected skeletal myoblasts into the injured myocardium (Taylor, *et al.*, 1998) (Murry, *et al.*, 1996). The results showed that cell transplantation into cryo-infarcted hearts improved left ventricular function and reduced scar formation. It was suggested that this positive effect was due to cells trans-differentiation into cardiac myocytes in rats (Taylor, *et al.*, 1998) and rabbits (Murry, *et al.*, 1996), although this view has been challenged (Reinecke, *et al.*, 2002).

A study conducted on infarcted mice reported that bone marrow-derived (Lin- c-kit⁺) stem cells, delivered into the myocardium, differentiated into cardiomyocytes and regenerated the myocardium (Orlic, *et al.*, 2001). Based on such positive findings, adult stem cell and progenitor cells transplantation was soon translated into clinical studies (Assmus, *et al.*, 2002) (Strauer BE, 2002). In a small study, autologous mononuclear bone marrow cells were transplanted via a balloon catheter placed into the artery related to the infarct during balloon dilatation into AMI patients. After 3 months follow-up, the patients treated with cells showed improved ejection fraction, and smaller infarct size, compared to the patients treated with the standard therapy (Strauer BE, 2002). In the Transplantation of Progenitor Cells and Regeneration Enhancement in Acute Myocardial Infarction (TOPCARE-AMI) study, patients with re-perfused acute myocardial infarction were treated with an intracoronary infusion of either bone marrow cells or autologous progenitor cells after 4 days from MI. At 4 months follow-up, cell treatment improved the global left ventricular ejection fraction and systolic left ventricular volume, with no difference between the two different cell types used (Assmus, *et al.*, 2002).

The mechanism proposed by Orlic, *et al.*, 2001, to explain the positive effects observed following cell treatment, was then called into question by two independent studies (Balsam, *et al.*, 2004) (Murry, *et al.*, 2004). Balsam *et al.*, 2004 transplanted c-kit-enriched bone marrow cells, Lin- c-kit⁺ bone marrow cells and c-kit⁺ Thy1.1^{lo} Lin- Sca-1⁺ long-term reconstituting haematopoietic stem cells into the infarcted mouse heart. They found that after 30 days the transplanted cells showed no cardiac tissue markers (Balsam, *et al.*, 2004). Similar results were reported in the study by Murry

et al., 2004, which transplanted bone marrow-derived Lin- c-kit⁺ cells into infarcted mice hearts by catheterisation. 1-4 weeks after infarction, the cells transplanted did not differentiate into cardiomyocytes. A more recent animal study suggested that the positive effects manifested in rat hearts treated with mesenchymal stem cells, could be attributed to the paracrine effect that transplanted cells have on the endogenous cells (Tang, *et al.*, 2010). Cytokines and growth factors, such as hepatocytes growth factors and insulin-like growth factor-1, secreted by the transplanted cardiac progenitor cells, may result in a paracrine effect on endogenous cells and this effect may persist after the transplanted cells disappear. In fact, it has been reported that after the injection of mesenchymal stem cells, only 5% of cells survived after their transplantation in pig's hearts (Freyman, *et al.*, 2006), while only 6% of bone marrow cells survived after 3 days from transplantation in infarcted rat hearts (Yasuda, *et al.*, 2005) (Hayashi, *et al.*, 2004).

1.3.1.2 Embryonic stem cells

Embryonic stem cells have been studied for their potential to differentiate into any cell type with the correct growth factors exposure. A study conducted on mice showed that the injection of embryonic stem cells into mice infarcted hearts lead to large teratomas rather than new mature cardiomyocytes (Nussbaum, *et al.*, 2007). After several weeks from cell transplantation, the hearts were characterised by inflammation and the implanted cells were immunologically rejected (Nussbaum, *et al.*, 2007). To avoid the immune response obtained with implanted embryonic stem cells, a new approach was to use *ex-vivo* pre-differentiated human embryonic stem cell derived cardiac myocytes (Laflamme, *et al.*, 2007). The transplantation of these cells in rat models of infarcted hearts showed that the grafted cells survived and proliferate. A reduction in ventricular remodelling was observed with an improvement in ejection fraction of 20-40% (Laflamme, *et al.*, 2007). Although positive results have been obtained from the studies on rats, the first long-term (12-weeks) study on mice showed that the positive effects of transplanted cells were not visible after 12 weeks of implantation (van Laake, *et al.*, 2007). In another study, human embryonic stem cells derived cardiomyocytes were transplanted into non-human primate model of myocardial ischaemia (Chong, *et al.*, 2014). After ischaemia and reperfusion, around a billion human embryonic stem cells

derived cardiomyocytes were injected into the myocardium. The transplanted cells presented a progressive but incomplete maturation over the following 3 months. The engrafted cells generated new tissue although non-fatal ventricular arrhythmia was observed (Chong, *et al.*, 2014).

1.3.1.3 Induced pluripotent stem cells

Somatic cells can be programmed to resemble embryonic stem cells. This type of cell, called induced pluripotent stem cell, has been investigated as a treatment for damaged myocardium. Initially, induced pluripotent stem cells were obtained by transferring the somatic cell nucleus in an unfertilised egg (Cowan, *et al.*, 2005). It was discovered that somatic cells were converted into embryonic stem cell like cells when specific genes, which are responsible for maintaining the pluripotent state in embryonic stem cells, were expressed in mice fibroblasts using retrovirus (Takahashi & Yamanaka, 2006). In a similar way, human fibroblasts have also been converted into induced pluripotent stem cells (Takahashi, *et al.*, 2007) (Yu, *et al.*, 2007) (Huangfu, *et al.*, 2008) (Nakagawa, *et al.*, 2008). New methods to obtain such stem cells have been studied, such as non-viral (O'Doherty R, 2013) or substituting the original genes with some molecules (Huangfu, *et al.*, 2008). Several studies in which mice were subjected to myocardial infarction showed that fibroblasts present in infarcted hearts can be programmed to become cardiomyocytes *in vivo* by using certain cardiogenic transcript factors, such as GATA4, Hand2, MEF2C, and Tbx5 (GHMT) (Song, *et al.*, 2012) or Gata4, Mef2c and Tbx5 (GMT). (Qian, *et al.*, 2012). After 3 months from the treatment with cardiogenic transcript factors, an increase in fibrosis (Song, *et al.*, 2012), a reduced infarcted area and some attenuation of cardiac dysfunction (Qian, *et al.*, 2012) have been observed.

1.3.2 Summary of current limitations in cell therapy

Despite the fact that several studies on cell therapy for damaged myocardium have shown promising results, a number of important challenges remain (Zhang, *et al.*, 2015). Studies have shown that approximately 5-7% of mesenchymal stem cells delivered by needle injection into the myocardium survive after 3 days from implantation in infarcted hearts (Freyman, *et al.*, 2006) (Yasuda, *et al.*, 2005) (Hayashi, *et al.*, 2004). This can be explained by the fact that cells are exposed to a

hostile environment characterized by inflammation, hypoxia and ECM matrix degradation (Pereira, *et al.*, 2011). After cell transplantation only a small number of cells differentiate into cardiomyocytes and this number is thought to be too low to explain the beneficial effects of stem cells in myocardial tissue regeneration (Gnecchi, *et al.*, 2008). Data has suggested that the significant functional improvement may be resulting from the release of biological molecules and growth factors, (Gnecchi, *et al.*, 2008), autocrine and paracrine factors from the transplanted cells (Karantalis, *et al.*, 2012) rather than cell differentiation.

1.3.3 Gene therapy

Gene therapy consists of the delivery of DNA/RNA to target specific cell cycle processes in order to treat heart failure (Vinge, *et al.*, 2008). The investigations carried out in this area to date have been mostly in animals. This approach is valuable because humans and animals have common biological signal pathways in damaged cardiomyocytes (Vinge, *et al.*, 2008). One of the promising targets for gene therapy is Ca^{2+} handling during the excitation-contraction coupling of the cardiomyocytes. Ca^{2+} cycling is crucial for cardiomyocyte function and when it is altered, it may lead to arrhythmias and heart remodelling (Vinge, *et al.*, 2008). The cardiac SERCA2a and Na^{+} - Ca^{2+} exchanger (NCX) play an important role in Ca^{2+} cycling in larger animals (Vinge, *et al.*, 2008). SERCAa gene transfer has shown potential therapeutic effects in small animal studies (Vinge, *et al.*, 2008). In the CUPID 2 trial phase 2b, double-blind, placebo-controlled, randomized study, recombinant adeno-associated virus serotype 1 (AAV1)/SERCA2a was delivered intracoronary to patients with heart failure and reduced ejection fraction (Greenberg, *et al.*, 2015). The trial suggested that this approach led to an improvement of systolic and diastolic functions by increasing SERCA2a protein levels (Greenberg, *et al.*, 2015). In a more recent study, BNP116.I-1c was delivered intracoronary in volume-overload HF induced pigs. One month after the treatment, pigs showed improved left ventricular ejection fraction compared to the saline treated group (Watanabe, *et al.*, 2017).

1.3.4 Protein delivery

Growth factors are secreted by cells and help regulate the regeneration of tissue and various related aspects of cell activity (Rebouças, *et al.*, 2016). For this reason, growth

factors have been studied as a treatment to stimulate myocardial regeneration after myocardial infarction (Rebouças, *et al.*, 2016). Angiogenesis is part of the process of tissue regeneration in the infarcted heart and it is regulated by growth factors, such as vascular endothelial growth factor (VEGF) and fibroblast growth factor (FGF) (Formiga, *et al.*, 2012). The VEGF family has been demonstrated to reduce wall thickening in both pig (Pearlman, *et al.*, 1995) and rat models (Schwarz, *et al.*, 2000) of acute myocardial ischaemia, by stimulating new vessel formation. In another study using the mouse corneal angiogenesis model, VEGF was shown to increase angiogenesis, although the new vessels were found to be immature and disorganized (Cao, *et al.*, 2004). On the other hand, in the same study FGF induced mature and organised vessels formation (Cao, *et al.*, 2004). The FGF family of growth factors has also been shown to induce angiogenesis when injected into the myocardium in a pig (Laham, *et al.*, 2000) and in a rabbit model (Bougioukas, *et al.*, 2007).

Anti-apoptotic factors, such as hepatocyte growth factor (HGF) and insulin-like growth factor I (IGF-I) have also been investigated for their potential to reduce myocardial injury (Rebouças, *et al.*, 2016). Intravenous administration of HGF in a rat model of ischaemia/reperfusion showed a reduction in the infarct size (Nakamura, *et al.*, 2000). IGF-1 delivered as bolus during reperfusion after regional ischaemia, improved cardiac function in mice (Heinen, *et al.*, 2017). The myocardial injection of HGF and IGF- I in combination showed cardio-protective effects in infarcted pig hearts (Ellison, *et al.*, 2011). In fact, the injection of HGF and IGF-I improved left ventricular function and produced a reduction in infarct size 2 months post MI (Ellison, *et al.*, 2011).

It is therefore clear that growth factors have been shown to have the potential to reduce ventricular remodelling in infarcted hearts, although the development of an optimal protein therapy remains challenging (Rebouças, *et al.*, 2016). In fact, the therapeutic potential of growth factors is limited by their short biological half-life, low accuracy to target specific organs and their low plasma stability. These challenges have been described in a study by Hwang & Kloner, 2011, in which a combination of growth factors was delivered into chronic infarcted myocardium in rats. After four weeks post-

surgery there was no difference in cardiac functions between the treated rats and the control group (Hwang & Kloner, 2011).

1.3.5 Novel Pharmacological Therapies

Infarcted hearts present high level of inflammation and oxidative stress, which lead to a progressive cell death, as discussed in section 1.22. Anti-inflammatory and antioxidant treatments have been therefore investigated as a possible therapy to limit tissue damage after MI (Hori & Nishida, 2009).

1.3.5.1 Antioxidants

There are several animal studies indicating the efficacy of antioxidant strategies in reducing left ventricular remodelling (Hori & Nishida, 2009). The overexpression of antioxidant superoxide dismutase (SOD) in transgenic mice, showed a reduction in infarct size after ischaemia/reperfusion injury (Chen, *et al.*, 1998) (Wang, *et al.*, 1998). In an *in vivo* model of MI in rabbits, the radical scavenger 3-methyl-1-phenyl-2-pyrazolin-5-one (edaravone) was injected into the ischaemic myocardium before reperfusion (Onogi, *et al.*, 2006). In the rabbits that received the edaravone bolus, the infarct size was reduced and the overall cardiac function was improved after 14 days of MI by reducing the level of superoxide and hydroxyl radicals (Onogi, *et al.*, 2006). Edaravone has been used to prevent reperfusion injury in patients with acute MI in a randomized, controlled, open-label clinical study (Tsujita, *et al.*, 2004). In this study, Edaravone was intravenously injected for 10 minutes before reperfusion. The results showed a reduced infarct size and better outcomes in patients treated with edaravone compared to the placebo treatment (Tsujita, *et al.*, 2004). In addition, the level of the oxidative stress marker thioredozin was reduced by the presence of edaravone (Tsujita, *et al.*, 2004).

Carvedilol is a non-selective beta blocker which differs from the other beta blockers because of its ability to scavenge ROS (Book, 2002). In isolated rabbit hearts, carvedilol was delivered 30 min before ischaemia and throughout the reperfusion. The use of carvedilol showed a marked decrease in oxidative stress (GSH/GSSG) after reperfusion, compared to propranolol (Cargnoni, *et al.*, 2000). In a canine model of ischaemia/reperfusion, carvedilol showed a decrease of 78% in infarct size compared

to controls (Hamburger, *et al.*, 1991). Although several animal models suggested that the antioxidant activity of carvedilol might be responsible for the enhanced effect of carvedilol compared to other β -blockers, a feline study suggested that the carvedilol has a protective effect due to the blockade of adrenoceptors (Brunvand, *et al.*, 1996).

Aspirin is normally given to MI patients to prevent blood clot formation. In the Multicenter Oral Carvedilol Heart failure Assessment (MOCHA) trial, the effect that aspirin has on the carvedilol treatment in patients with heart failure was assessed (Lindenfeld, *et al.*, 2001). In this study, aspirin significantly reduced the positive effect that carvedilol had on the left ventricular ejection fraction (Lindenfeld, *et al.*, 2001). In an animal study of MI, aspirin was used to prevent ventricular remodelling by reducing the oxidative stress (Adamek, *et al.*, 2007). In this study, high doses of aspirin delivered after MI by Alzet mini-osmotic pumps for 4 weeks did not stop ventricular remodelling in mice, although it reduced the expression of pro-inflammatory cytokines (Adamek, *et al.*, 2007).

Xanthine oxidase is one of the sources of reactive oxygen species in mammalian hearts. The high level of xanthine oxidase found after MI has been proposed to be used as a marker for MI in different studies (Raghuvanshi, *et al.*, 2007). Allopurinol is normally used to reduce uric acid levels by decreasing xanthine oxidase in the prevention of the gout (Mackenzie, *et al.*, 2016). In contrast to other studies, in which the antioxidants were just injected in one dose, allopurinol was given after MI for an extended period of time in mice (Engberding, *et al.*, 2004) and humans (Rekhranj, *et al.*, 2013) (Mackenzie, *et al.*, 2016). In a study conducted on mice, after induced MI, allopurinol was given by gavage for 4 weeks starting 1 day after MI (Engberding, *et al.*, 2004). The ROS level was found to be raised immediately after MI, but it was reduced with the allopurinol treatment. Echocardiography indicated that there was a reduction in left ventricular remodelling in the group treated with allopurinol compared to the control (Engberding, *et al.*, 2004). High doses of allopurinol administered orally for 9 months has also been demonstrated to reduce left ventricular hypertrophy in MI patients (Rekhranj, *et al.*, 2013) and reduced mortality in patients with heart failure (Wei, *et al.*, 2009). The ALL-HEART trial, a large prospective randomised study of allopurinol is currently in progress in UK, started in the 2013

(Mackenzie, *et al.*, 2016). The aim of the trial is to finally address if allopurinol improves the outcomes in patients with ischaemic heart disease (Mackenzie, *et al.*, 2016).

Vitamin C and E supplementation have also been investigated for their antioxidant and anti-inflammatory properties in different clinical studies (Jaxa-Chamiec, *et al.*, 2005) (Basili, *et al.*, 2010) (Tsutsui, *et al.*, 2011) (Rodrigo, *et al.*, 2014). A significant reduction in malonyldialdehyde, an end product of membrane lipid peroxidation, and superoxide anion has been observed in patients with heart failure following treatment with 4 weeks oral administration of vitamin E (α -tocopherol) (Ghatak, *et al.*, 1996). In the Myocardial Infarction and Vitamins (MIVIT) trial, acute myocardial infarction (AMI) patients were given a vitamin c infusion followed by a vitamin C and E supplement for 30 days (Jaxa-Chamiec, *et al.*, 2005). Although the study showed some positive effects on the patients, such as reduced incidence of cardiac mortality or new MI, the authors suggested that a larger study is still needed to confirm the efficacy of the treatment (Jaxa-Chamiec, *et al.*, 2005). On the other hand, the GISSI-Prevenzione trial showed that long term (3.5 years) administration of vitamin E supplements to MI patients with left ventricular dysfunction was associated with an increased risk of developing heart failure (Marchioli, *et al.*, 2006).

The hypertrophy following MI is thought to be mediated, at least in part, by the by G proteins of the Rho family, which are important for the cytoskeletal dynamics of the cells (Wang, *et al.*, 2006). Statins, used for lowering the cholesterol in MI patients, have been studied for their antioxidant effects in the prevention of cardiac hypertrophy (Takemoto, *et al.*, 2001). In a rat model of cardiac hypertrophy, Simvastatin was injected percutaneously into the heart for 14 days (Takemoto, *et al.*, 2001). Rats treated with Simvastatin showed a reduction in cardiac hypertrophy, superoxide anion and membrane Rho activity, compared to the saline treated rats (Takemoto, *et al.*, 2001). Although the statin treatment showed good results in the prevention of cardiac hypertrophy in animal studies, in clinical trials (CORONA study and GISSI-HF study) a daily intake of Rousvastatin failed to showed any improvement in patients with heart failure (Kjekshus, *et al.*, 2007).

Probucol is another antioxidant that has been studied as a treatment for ventricular remodelling (Oskarsson, *et al.*, 2000) (Sia, *et al.*, 2002) (Nakamura, *et al.*, 2002). Clinically it has been used (it is still used in certain Asian countries) to lower the cholesterol level in the blood, but it has also been studied as a possible treatment for ventricular remodelling (Keyamura, *et al.*, 2014). In a rat model of heart failure, three doses of probucol were injected into the peritoneal cavity 3 days after MI for 7 weeks (Oskarsson, *et al.*, 2000). The results showed that the treatment attenuated oxidative stress and myocytes apoptosis compared to the control (Oskarsson, *et al.*, 2000). In another rat model of MI, probucol was delivered 24h after MI for 4 weeks (Sia, *et al.*, 2002). The results of the study showed that probucol reduced oxidative stress levels and the expression of pro-inflammatory cytokines interleukin (IL)-1 β and IL-6, although it failed to reduce left ventricular hypertrophy (Sia, *et al.*, 2002). In a study conducted by Betge *et al.*, 2007, probucol treatment did not improve mortality after MI in rats with chronic heart failure (Betge, *et al.*, 2007).

1.3.5.2 Anti-inflammatory strategies

After MI, high levels of cytokines contribute to the detrimental damage of the myocardium, as discussed in section 1.2.2. One of the strategies used to reduce the level of cytokines has been anti-TNF therapy (Hori & Nishida, 2009). The anti-TNF Therapy Against Congestive Heart Failure (ATTACH) trial demonstrated that a 2h intravenous infusion of infliximab, a chimeric monoclonal antibody to TNF- α , not only did not improve the clinical conditions of the patients with heart failure and low ejection fraction, but at high doses it had detrimental effects on patients, with an increase of all cause of death or hospitalization for heart failure (Chung, *et al.*, 2003).

The use of anti-inflammatory drugs/antioxidants as a treatment to prevent and possibly reverse tissue damage after MI has been widely studied and the results obtained are often quite contradictory, as discussed in this section. In fact, although in some animal studies, the use of an antioxidant was effective to reduce the oxidative stress levels after MI (Onogi, *et al.*, 2006) (Tsujiita, *et al.*, 2004) (Cargnoni, *et al.*, 2000), it also failed to reduce ventricular hypertrophy (Probucol) (Betge, *et al.*, 2007), (Aspirin) (Adamek, *et al.*, 2007) and sometimes led to an increase in heart failure (vitamin E) (Marchioli, *et al.*, 2006). In most of the studies presented, the antioxidants were short

term delivered in a small number of doses mostly by percutaneous injection, such as statins, probucol, by IV infusion, such as infliximab, or orally, such as allopurinol, vitamin C and E. Long-term delivery of vitamin E was associated with an increase in heart failure. The studies described thus far also failed to demonstrate that the antioxidant used was able to inhibit ventricular remodelling. A potential explanation for this is that the drug delivery methods or the short duration of the treatment studied so far was not effective to improve outcomes. On the other hand, the studies conducted on allopurinol showed more promising results, with allopurinol orally delivered for 9 months reducing left ventricular hypertrophy in MI patients (Rekhranj, *et al.*, 2013) and reducing mortality in patients with heart failure (Wei, *et al.*, 2009). The lack of consistent beneficial effect of the strategies described may result from suboptimal duration of delivery and dose, but this also suggests that alternative drugs may be necessary to control left ventricular remodelling after MI.

1.4 Pyruvate

Pyruvate is the final product of glycolysis and the substrate for the production of tri-carboxyl Acid (TCA) in the Krebs cycle (Flink, 2007). It is therefore essential for cellular metabolism. Pyruvate has been investigated as a potential therapeutic in various settings (Flink, 2007). In isolated intact guinea pigs hearts perfused with 5 mM pyruvate enriched media, pyruvate increased myocardial ATP levels and consequently enhanced ATP-dependent sarcoplasmic reticular Ca^{++} transport (Mallet & Bünger, 1994). Pyruvate is also capable of scavenging reactive oxygen species like hydrogen peroxide (H_2O_2) and hydroxyl radical (OH^\cdot) in a non-enzymatic reaction as shown in Figure 1.2. In a prospective, randomized, clinical trial, either lactate or pyruvate (10 mM) enriched cardioplegia was used in patients undergoing CABG surgery (Olivencia-Yurvati, *et al.*, 2003). Cardiac troponin I and CPK-MB contents, which are indicators of myocardial damage, did not increase during bypass in patients treated with pyruvate, compared to the patients treated with lactate cardioplegia (Olivencia-Yurvati, *et al.*, 2003). Pyruvate also increased ventricular stroke work in the 4 hours after CPB, while in the same period patients treated with lactate showed a decrease in stroke work. Ultimately, pyruvate reduced postoperative hospitalization by more than 1 day (Olivencia-Yurvati, *et al.*, 2003).

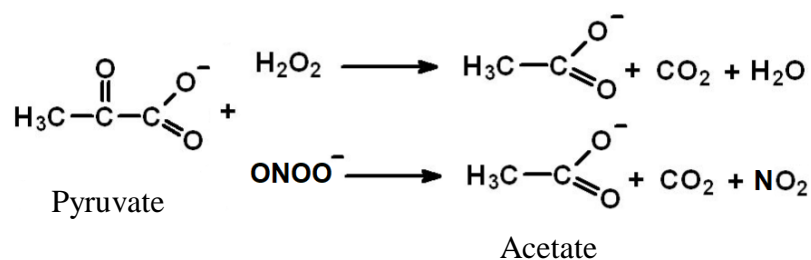


Figure 1.2 Schematic Mechanism of ROS scavenging by Pyruvate.

Despite the promising results obtained by using sodium pyruvate as a ROS scavenger, its instability in aqueous solutions remains its main limitation (Montgomery & Webb, 1956) (Von Korff, 1964) (Willems, *et al.*, 1978). In fact, in such solutions sodium pyruvate can undergo spontaneous transformations and form new compounds like parapyruvate and pyruvate hydrate. Once sodium pyruvate becomes either parapyruvate or pyruvate hydrate, it loses its ability to scavenge ROS (Montgomery & Webb, 1956) (Von Korff, 1964) (Willems, *et al.*, 1978). For this reason, pyruvate is not used for a prolonged period of time.

1.5 Ethyl Pyruvate

1.5.1 *In vitro* effects of Ethyl Pyruvate

Ethyl pyruvate (EP), a more stable derivate of pyruvate, has been widely investigated as a new therapeutic agent, with more than 300 articles published on this to date (Yang, *et al.*, 2016). EP is not only more stable in water than pyruvate, but it was shown that it is also far more potent (Kao & Fink, 2010). In one study conducted by Johansson *et al.*, 2008, human umbilical vein endothelial cells were exposed to pro-inflammatory agents, lipopolysaccharide (LPS), IL-1 β and TNF- α (Johansson, *et al.*, 2008). The cells were treated with 10 mM EP before or after the cytokines exposure. The results showed that EP reduced neutrophil adhesion and the expression of the adhesion molecules, such as VCAM-1, ICAM-1 and E-selectin, (Johansson, *et al.*, 2008). On the other hand, when 10 mM of pyruvate was used to treat the cells, it did not have any protective effect. The authors also accounted for the fact that hydrolysis of EP gives one molecule of pyruvate for one mole of ethanol, so they repeated the experiments using an equimolar concentration of ethanol and pyruvate mixed together

(Johansson, *et al.*, 2008). The results showed that the co-treatment with ethanol and pyruvate was not effective against the cytokines, and this confirmed the superior anti-inflammatory effects of EP (Johansson, *et al.*, 2008). The same group obtained similar results in another study, conducted on A549 human transformed pulmonary epithelial cells (Johansson & Palmblad, 2009). Similarly, Mizutani *et al.*, 2010 demonstrated that EP inhibited the activation of the nuclear factor NF- κ B signalling pathway in cultured A549 human alveolar epithelial cells, while pyruvate and pyruvate with ethanol were ineffective (Mizutani, *et al.*, 2010).

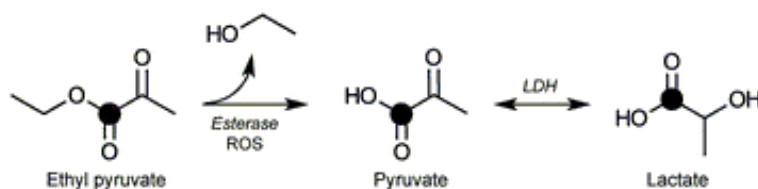


Figure 1.3 Metabolism of Ethyl Pyruvate. EP can be hydrolysed by Esterase enzymes or ROS. Adapted from (Keshari & Wilson, 2014).

EP is not only an anti-inflammatory agent, it is also known to have antioxidant properties, such as being able to scavenge hydrogen peroxide (Yang, *et al.*, 2016). In one study conducted by Famili *et al.*, 2013 the antioxidant property of EP (1 - 20 mM) was evaluated in cultured human trabecular meshwork (hTM) cells when exposed to hydrogen peroxide (Famili, *et al.*, 2013). The cells were either co-treated with hydrogen peroxide for 24h or treated only with hydrogen peroxide for 24h after the EP treatment for 24h (Famili, *et al.*, 2013). The results obtained by Famili *et al.* showed that the co-treatment of EP and hydrogen peroxide increased the cell viability, compared to hydrogen peroxide challenged cells without EP treatment or cells with a EP pre-treatment (Famili, *et al.*, 2013). In the presence of peroxide stress, EP increased cell survival and maintained metabolic activity. Despite its antioxidant properties, EP was not able to enhance the endogenous antioxidant capacity of the cultured cells in the EP pre-treated cells. For that reason, the authors suggested that it would be potentially advantageous if EP levels could be maintained for an extended period of time (Famili, *et al.*, 2013). The protective effect of EP on rat neural cells when exposed to H₂O₂ has been demonstrated in different studies (Kim, *et al.*, 2005)

(Zeng, *et al.*, 2007). In particular, in the study conducted by Kim *et al.*, neuron and microglia cells were exposed to 200 μ M H₂O₂ for 30 minutes and then they were treated with 5- 20 mM EP. After 4 hours of incubation with EP, cells showed an increase in cell viability, indicating that EP helped the cells recover after H₂O₂ exposure (Kim, *et al.*, 2005).

1.5.2 *In vivo* effects of Ethyl Pyruvate

EP has been investigated as a novel treatment in a range of different injury models (Yang, *et al.*, 2016). It reduced nuclear factor NF- κ B expression in liver and colonic mucosa after resuscitation in a mice model of haemorrhagic shock (Yang, *et al.*, 2002). EP has also been shown to reduce severe sepsis in mice, by inhibiting the secretion of High Mobility Group Box-1 (HMGB-1), a late-acting mediator of LPS and sepsis induced death (Ulloa, *et al.*, 2002). A single dose of EP (28 mM) in 0.4 mL Ringer's solution injected intraperitoneally at 0, 6, or 12 hours after cecal puncture, attenuated sepsis-induced acute renal failure in aged mice (Miyaji, *et al.*, 2003). In various rat models of severe acute pancreatitis, EP has been demonstrated to reduce the expression of TNF- α , IL-6, HMGB1 and ROS, all factors that are thought to contribute to the development of acute renal failure (Luan, *et al.*, 2015) (Yang, *et al.*, 2008) (Cheng, *et al.*, 2007). EP has also been shown to ameliorate acute alcohol-induced liver injury in mice (Yang, *et al.*, 2003), acute-on-chronic liver failure in rats (Wang, *et al.*, 2012) and hepatic ischemia-reperfusion injury in mice (Shen, *et al.*, 2013).

EP was also used to attenuate ischaemia/reperfusion injury in various animal studies. In a study conducted on a rat model (Woo, *et al.*, 2004), a 1.5 mL/kg intravenous bolus of EP (28 mM) was administered intravenously immediately before inducing ischemia followed by reperfusion. The study showed that EP reduced oxidative stress, increased myocardial ATP levels and decreased infarct size (Woo, *et al.*, 2004). EP enhanced tissue ATP levels, preserved cardiac function, attenuated myocardial oxidative injury in a Langendorff perfused heart experiment. The rat hearts were treated with 2 mM EP which was added to the cardioplegic solution during ischaemia, to the storage solution and to the Krebs–Henseleit solution during reperfusion (Guo, *et al.*, 2014). After ischaemia/reperfusion, there are high levels of TNF- α , IL-6, and HMGB-1, which triggers a cascade of inflammation (Lin, *et al.*, 2015). EP attenuated

all these factors following a (40 mg/kg) single IV injection prior to a 48h reperfusion in a rat model of ischaemia/reperfusion (Lin, *et al.*, 2015). In another rat model of ischaemia/reperfusion, a 40 mg/kg single intraperitoneal injection of EP prior to ischaemia/reperfusion inhibited the activation of the nuclear factor NF- κ B signalling pathway, cytokines production and consequently reduced infarct size (Jang, *et al.*, 2010). In a rat model of Adriamycin-induced cardiomyopathy, after exposure to Adriamycin, rats were treated with 50 mg/Kg/day of EP delivered via gastric lavage for 30 days (Liu, *et al.*, 2016). Results showed that rats treated with EP reduced ADR-induced fibrosis by increasing mRNA levels of MMPs and reducing TGF β -1 and TIMPs, suggesting that EP can be used as a potential therapeutic agent for ADR-induced myocardial damage (Liu, *et al.*, 2016).

In a double-blind, randomized, placebo-controlled clinical study, EP has been administered intravenously in high-risk patients undergoing coronary artery bypass graft and/or cardiac valvular surgery with CPB (Critical Therapeutics Inc, Lexington, MA, USA) (Bennett-Guerrero, *et al.*, 2009). Patients received a dose of 7,500 mg intravenously over 60 minutes every 6 hours for 6 doses, where the first dose was given before CPB. In this study, EP did not significantly reduce the incidence of the post-operative adverse outcomes and it failed to decrease the systemic inflammatory markers (Bennett-Guerrero, *et al.*, 2009). The authors suggested that possibly the dose administered to the patients was not adequate to reduce the inflammation. They also suggested that the length of the treatment might have been insufficient (Bennett-Guerrero, *et al.*, 2009).

1.6 Hydrogels for cardiac repair and regeneration

1.6.1 Introduction

In addition to the role that pharmacological approaches might play in encouraging cardiac regeneration following injury, it is also important to consider the impact of the delivery mechanism and potentially beneficial effects of local drug delivery technologies. In this section, the role of hydrogels in this context will be explored.

The infarcted area of the myocardium comprises a scar made of connective tissue, as previously discussed in section 1.2.1. It has been seen how this fibrotic component

does not allow implanted stem cells to create electromechanical connections with the native cardiomyocytes, which are essential for myocardial contraction (Laflamme & Murry, 2011). Hydrogels have been extensively investigated for cardiac repair and regeneration (Li & Guan, 2011). Hydrogels used to treat damaged tissue are either biomaterial scaffolds that are prepared *in-vitro* and subsequently implanted *in-vivo*, or injectable biomaterials that turn into scaffolds *in-situ* (Venugopal, *et al.*, 2012). Scaffolds used for cardiac application should mimic the properties of the cardiac tissue, helping the regeneration of the myocardium (Venugopal, *et al.*, 2012). The biomaterials used to prepare the scaffolds must be biocompatible, to minimise immune response and inflammation following implantation (Cui, *et al.*, 2016). Where the biomaterials proposed are biodegradable, it is important that the degradation products are not toxic and can be physiologically removed by the body (Cui, *et al.*, 2016). At the same time, biomaterials need to be stable for a therapeutic period of time to allow cell proliferation or to act as a reservoir for the sustained release of a therapeutic drug/protein (Cui, *et al.*, 2016). It has been suggested that such scaffolds should have a porous structure with interconnected pores of 50 μm minimum of diameter to allow cell infiltration and proliferation, but also the free movement of nutrients and waste (Cui, *et al.*, 2016). Once the cells proliferate into the scaffold, the scaffold should degrade, leaving space for the newly formed tissue (Cui, *et al.*, 2016).

Biomaterials used for the purposes outlined above are generally either natural hydrogels, such as collagen, alginate, matrigel, fibrin, chitosan or synthetic materials, such as polyurethane, and poly (glycolide-co-caprolactone) (Venugopal, *et al.*, 2012). The advantage of using synthetic biomaterials is that they are easy to control in terms of molecular weight, mechanical characteristics and protein delivery, although their potential cytotoxicity can be a limitation (Li & Guan, 2011). An example of a very widely used synthetic biomaterial is the degradable copolymer Poly (Lactic-Co-Glycolic Acid) or (PLGA). PLGA nanocomposites were used to deliver growth factors to treat damaged myocardium (Wang, *et al.*, 2009) (Simón-Yarza, *et al.*, 2012). In one study conducted by Mukherjee *et al*, 2011, isolated adult rabbit cardiomyocytes were seeded onto a PLA-co-poly (ϵ -caprolactone)/collagen bio-composite scaffold and cell organization resembled the native myocardium *in-vitro* (Mukherjee, *et al.*, 2011).

Natural hydrogels are the most studied hydrogels, because they are generally biocompatible and have similar structure and properties to the biological tissue (Li & Guan, 2011). The most commonly used hydrogels for cardiac regeneration to date have been extracellular matrix derivatives, such as collagen, gelatin and materials derived from plants, such as alginate extracted from seaweed (Li & Guan, 2011). These natural hydrogels have been used to form scaffolds that can be stitched onto the heart where the infarcted area is. In this way, scaffolds can be used for the delivery of cells or growth factors *in situ* for cell/protein delivery (Li & Guan, 2011). Such natural hydrogels have been shown to improve the delivery of cells and growth factors by acting as a protective barrier against the inflamed host tissue (Li & Guan, 2011). As discussed in section 1.3.1, stem cells have been studied as a treatment of damaged tissue, although their use is very challenging, due to the fact that they generally have poor *in-vivo* survival, differentiation, and maturation (Gnecchi, *et al.*, 2008). For this reason, hydrogels have been investigated not just for their ability to deliver cells, but also for other positive effects that they may have on the myocardium that are independent of cells. In fact, the implantation of patches, such as collagen (Serpooshan, *et al.*, 2013), alginate (Sabbah, *et al.*, 2013) or alginate and fibrin (Yu, *et al.*, 2009) hydrogels without any drug into the myocardium has shown a reduction in infarct expansion and preserved wall thickness in various animal models.

1.6.2 Collagen

Collagen consists of a third of the total protein in humans and it is the main component of the extracellular matrix (Shoulders & Raines, 2009). The collagen structure is characterised by a triple helix of three parallel strands of polypeptides (Shoulders & Raines, 2009). Twenty-eight different types of collagen have been identified in vertebrates (Shoulders & Raines, 2009). Type I-V collagen are the most common and they are the main constituent of dermis, tendons, ligaments and bones (type I), cartilage (type II), skin, blood vessels (type III), basement membrane (type IV) and bone, placenta, dermis (type V) (Shoulders & Raines, 2009). In the heart, cardiac fibroblasts are the main cell responsible for the production of different extracellular matrix components, including collagen (Souders, *et al.*, 2009), with the predominant types of collagen in the cardiac ECM being the fibrillar collagen types I and III (Fan, *et al.*, 2012).

Collagen is one of the most studied biomaterials used for cardiac regeneration (Cui, *et al.*, 2016). For biomaterial applications, the most common sources of collagens are rat tail, porcine skin, bovine tendon, human cadavers and the new approach of human recombinant protein production (Shoulders & Raines, 2009). Collagen has been used alone or as a delivery system of cells and proteins in different animal studies (Cui, *et al.*, 2016). In a murine model of MI, a collagen patch prepared with sterile rat tail-derived type I collagen was sutured onto the infarcted area immediately after ligation of the left anterior descending artery (Serpooshan, *et al.*, 2013). The patches were shown to preserve heart contractility and reduced ventricular remodelling compared to the hearts with no treatment (Serpooshan, *et al.*, 2013). In the study conducted by Miyagi *et al.*, 2011, collagen patches (Ultrafoam, Davon) incorporated with vascular endothelial growth factor (VEGF)-165 were used to replace a full right ventricular wall defect in rats. At day 28, the scaffolds with VEGF showed an increase in vascularisation compared to the control (Miyagi, *et al.*, 2011). A collagen patch made from sterile rat tail type I collagen was also used to deliver the cardio-protective factor Follistatin-Like-Protein 1 (FSTL1) in mouse and swine models of MI (Wei, *et al.*, 2015). FSTL1 stimulated cell cycle and division of cardiomyocytes and improved cardiac function (Wei, *et al.*, 2015).

1.6.3 Chitosan

Another abundant natural biomaterial is chitosan, derived from seashells. Chitosan has also been used in cardiac regeneration. In a recent study conducted by Fiamingo *et al.*, 2016, chitosan patches were tested on a rat model of MI (Fiamingo, *et al.*, 2016). One month after scaffold placement, the authors investigated the level of inflammation. The scaffolds prepared at lower chitosan concentration (1.5%) showed no signs of inflammation, while the scaffolds prepared at higher chitosan concentration (2%) were encapsulated by fibrous tissue accompanied by multinucleated giant cells (Fiamingo, *et al.*, 2016). A chitosan-hyaluronan/silk fibrin patch was also tested in a rat model of MI (Chi, *et al.*, 2013). 8 weeks after implantation, the patch reduced the diameter of the LV and increased the ventricular wall thickness compared to the control hearts with no patch (Chi, *et al.*, 2013).

Collagen and chitosan present some limitations in cardiac regeneration, such as the low elastic modulus of collagen, which reduces their mechanical integration (Deng, *et al.*, 2010) or the low cell retention of chitosan hydrogels (Blan & Birla, 2008). Apart from collagen and chitosan, many other natural biomaterials have been used to treat damaged myocardium. One of the most studied natural hydrogels is alginate. Alginate properties and application are discussed in detail in the following section.

1.7 Alginate as tissue engineering scaffold

1.7.1 Introduction

Alginate is a natural polysaccharide extracted from the intercellular matrix of brown seaweed. This biocompatible anionic and hydrophilic copolymer is composed of homopolymeric blocks of mannuronate (M) and guluronate (G) residues (as shown in **Figure 1.4**).

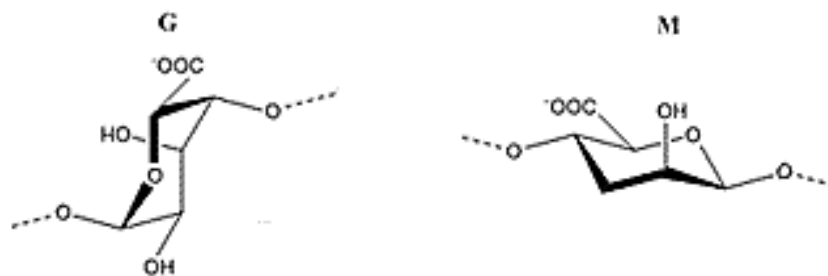


Figure 1.4 Alginate homopolymeric blocks of mannuronate (M) and guluronate (G) residues. Adapted from (Pereira, *et al.*, 2013)

The level of the residues depends on the species of seaweed used (Lee & Mooney, 2012). Alginates are characterised by a wide range of molecular weights, chemical composition and physical characteristics.

1.7.2 Alginate hydrogel formation

Alginate becomes a hydrogel by forming cross-linked junctions between the G block residues and divalent cations, such as Ca²⁺, Ba²⁺, and Sr²⁺, resulting in an “egg box” structure as shown in Figure 1.4 (Pereira, *et al.*, 2013). Because only the G blocks are responsible for the crosslinking, the alginate ratio of G/M blocks affects the structural

characteristics of the hydrogel produced. A higher G/M ratio alginate will correspond to more crosslinks which result in a more stable hydrogel. For tissue engineering applications Ca^{2+} is often preferred as cross-linking agent because it is well accepted in physiological environment (Lee & Mooney, 2012). One of the most used ionically cross-linkers is calcium chloride (CaCl_2). When CaCl_2 is used to cross-link alginate, the hydrogel formation is very quick, due to the fact that CaCl_2 is highly hydrophilic. This easy and fast reaction makes this type of hydrogel very suitable for the preparation of cardiac patches for clinical application. However, a rapid gelation time can also negatively affect the uniformity of the hydrogel structure, resulting in a poorly controlled gelation (Lee & Mooney, 2012). In order to increase the gelation time, other cross-linkers with lower solubility can be used, such as calcium gluconate (Caglu), calcium carbonate (CaCO_3) or calcium sulphate (CaSO_4).

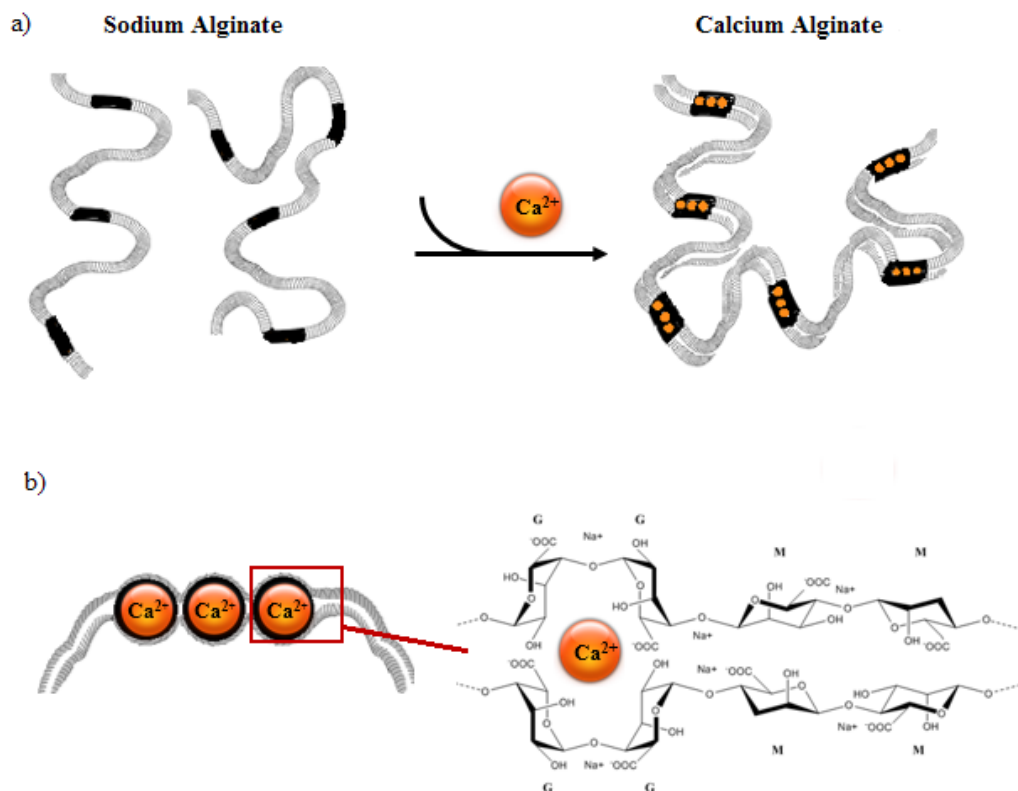


Figure 1.5 Schematic representation of a) sodium alginate cross-linked with Calcium ions; b) molecular structure of sodium alginate, with the alginate blocks (G=guluronate residues, M=mannuronate residues) and the cross-linked junction between the positively charged calcium ions and the negatively charged G blocks (egg-box structure).

The physical characteristics of alginate hydrogels can be modulated chemically by covalent crosslinking of alginate. In fact, alginate can be chemically modified by covalently crosslinking methacrylate groups onto the alginate backbone (Andersen, *et al.*, 2015). Alginate hydrogels with different mechanical properties were prepared by covalently crosslinking poly (ethylene glycol) (PEG) (Eiselt, *et al.*, 1999). The choice of the cross-linking molecules not only leads to a different mechanical characteristics, but also modifies the swelling behaviour of the gel (Lee, *et al.*, 2000).

Alginate is composed of inert monomers which lack bioactive ligands, that are necessary for cell attachment (Sun & Tan, 2013). When scaffolds are used for tissue regeneration, it is important that the biomaterial used promotes cell proliferation. In order to overcome this limitation, alginate can be chemically modified by adding a ligand, such as the Arginine-Glycine-Aspartic acid (Arg-Gly-Asp, RGD) sequence to the alginate, using water soluble carbodiimide chemistry (Sun & Tan, 2013). The interaction between cells and RGD modified alginate contributes to the formation of the hydrogel structure, and for this reason this reaction is called cell-crosslinking (Sun & Tan, 2013). This type of crosslinking was investigated in the study conducted by Lee *et al.*, 2003. When MC3T3-E1 mouse calvarial osteoblasts were added to RGD alginate solutions, this led to hydrogel formation, without the use of external cross-linkers (Lee, *et al.*, 2003).

Alginate gels have also been prepared in the form of macro-beads. These beads have been studied as an alternative method to deliver proteins, small drugs and cells in tissue engineering. They are formed by dripping alginate solution into a cross-linking bath. This method is called extrusion-dripping (Chan, *et al.*, 2009).

1.7.3 Biocompatibility

Since alginate is a bio-product, it may contain bacteria and various other impurities. For this reason, alginate goes through different steps of filtration as a first stage of sterilisation or it can also be obtained commercially as an ultrapure product (Lee & Mooney, 2012). Alginate scaffolds can be sterilised by applying a UV light for 1 hour, without damaging the integrity of the alginate structure. Gas, such as Ethylene Oxide (EtO), can be used but it might be retained, and it can be toxic *in vivo* (Lee & Mooney, 2012). The biocompatibility of alginate has been extensively studied both *in vitro* and

in vivo, and it is a U.S. Food and Drug Administration (FDA)-approved material (Sun & Tan, 2013).

1.7.4 Biodegradability of alginate hydrogels

Alginate is not readily degraded in mammals due to the fact that they lack the enzyme alginase that degrades the polymer chain. Despite this, the ionically cross-linked alginate hydrogels can be dissolved in physiological solution with a gradual exchange of ions between the hydrogel and the media. The calcium ions that are bonded to the COO⁻ residues in the hydrogel are replaced with the sodium ions present in the physiological solution. The high concentration of the negatively charged COO⁻ residues start an electrostatic repulsion that leads to relaxation of the chains and consecutively swelling of the gel (Bajpai & Sharma, 2004). Alginate hydrogels placed in physiological solution increase the water intake in a process called swelling. This step is characterised by an increase in weight proportional to the water intake. This stage is followed by a decrease in hydrogel weight called syneresis, until the complete dissolution of the gel (Bajpai & Sharma, 2004).

Most of the alginates available have a molecular weight above the renal clearance threshold (~50,000 g/mol) and likely will not be completely removed from the body (Al-Shamkhani & Duncan, 1995). Very low viscosity sodium alginate with a molecular weight below 75,000 g/mol (Landa, *et al.*, 2008) is now available. The molecular weight of alginate influences the mechanical characteristics and the degradation characteristics of the hydrogels. In fact, a lower molecular weight corresponds to an increase in reactive positions for hydrolysis degradation, which reduces the degradation time (Sun & Tan, 2013). In order to speed degradation of alginate gel, alginate can be modified chemically (Balakrishnana, *et al.*, 2005). For this purpose, sodium alginate can be oxidised, by using sodium periodate to cleave the carbon-carbon bond, which reduces the molecular weight of alginate (Balakrishnana, *et al.*, 2005).

1.7.5 Porous alginate scaffolds

The ideal scaffold for tissue regeneration should have a porous structure with interconnected pores to allow cell infiltration and proliferation, as previously discussed in section 1.5. For this reason, in addition to simple alginate hydrogels, alginate has

been used to prepare macro-porous scaffolds. There are different methods to prepare porous alginate hydrogels, such as solvent casting, gas foaming, particulate leaching, lyophilisation and phase separation (Sun & Tan, 2013). The easiest and the most used method to prepare porous alginate hydrogels is lyophilisation (Sun & Tan, 2013). Alginate solution or alginate gels are frozen at -20°C or below and then placed into a freeze-drier. In the process of freeze-drying, the water crystals obtained by freezing are sublimed, leaving pores in the structure. The freezing temperature affects the scaffold internal structure, as shown in the study of Zmora *et al.*, 2002. They investigated the pore shape and size of porous alginate gels under different conditions, such as freezing slowly at -20°C in a freezer, a quick freezing at -196°C in liquid nitrogen or at -35°C in an oil bath. The results showed that the alginate gels that were slowly frozen at -20°C presented round and interconnected pores, while gels frozen with liquid nitrogen or oil bath showed uneven pore shapes (Zmora, *et al.*, 2002).

1.7.6 Alginate hydrogels for protein/small drug delivery

Alginate hydrogels have been used for different biomedical applications, due to their similarity to extracellular matrices of living tissues. Alginate has been used in wound healing, cell transplantation and as a delivery system of bioactive agents such as growth factors and small chemical drugs (Lee & Mooney, 2012). The regeneration of the myocardium after ischemia/reperfusion injury is one of the main applications of alginate gels. In the clinical AUGMENT-HF study Algisyl (injectable calcium alginate hydrogel) was delivered by several injections in the left ventricular wall through an anterior thoracotomy in patients affected by advanced heart failure (Mann, *et al.*, 2016). 1-year follow-up showed an improvement in exercise capacity and reduced symptoms in patients treated with alginate hydrogels compared with the control group which was treated with standard medical therapy only. The gel improved ventricular wall thickness and reduced myocardial wall stress, however cardiovascular deaths at 12-months follow up was higher for the Algisyl-treated group compared to the group treated with standard medication (Mann, *et al.*, 2016).

Alginate gels have also been used to deliver growth factors into the myocardium in different animal studies (Lee, *et al.*, 2003) (Ruginov, *et al.*, 2010) (Ruginov, *et al.*, 2011) (Lee & Mooney, 2012). In the study conducted by Lee *et al.*, 2003, alginate

hydrogel was used to deliver vascular endothelial growth factor (VEGF) and basic fibroblast growth factor (bFGF) into ischemic cardiac muscle tissue. The VEGF was released by the hydrogel for more than 14 days, resulting in new capillaries formation surrounding the gel (Lee, *et al.*, 2003). In the study conducted by Ruvinov & Cohen 2011, alginate hydrogels were used to deliver insulin-like growth factor-1 (IGF-1) and hepatocyte growth factor (HGF) into the myocardium. A rat model of acute MI was used in the study and alginate hydrogel with IGF-1/HGF was delivered with an intra-myocardial injection. After 4 weeks, this alginate biomaterial prevented scar formation, and at the same time increased angiogenesis at the infarcted area (Ruvinov, *et al.*, 2011).

Alginate gels have been investigated for the delivery of small drugs in different applications (Lee & Mooney, 2012). Antineoplastic drugs have been released *in-vitro* by oxidised alginate gels cross-linked with adipic dihydrazide in the study conducted by Bouhadir *et al.*, 2001 (Bouhadir, *et al.*, 2001). In this study 3 antineoplastic agents (methotrexate, doxorubicin, and mitoxantrone) were loaded into the hydrogel via three different mechanisms. Methotrexate was contained within the pores of the hydrogel and was released after a few hours by diffusion. Doxorubicin was covalently bonded to the backbone of the hydrogel and it was released when the chemical hydrolysis of the linker started (3 days). Mitoxantrone was ionically bonded to alginate and it was released when the gel started degrading (after 7 days) (Bouhadir, *et al.*, 2001). Alginate gels were used to deliver the adrenergic drug dobutamine to the left ventricle of rats in the study conducted by Lovich *et al.*, 2011 (Lovich, *et al.*, 2011). Dobutamine is usually delivered by IV injection during cardiac surgery (Lovich, *et al.*, 2011). IV inotrope injection is of great benefit to patients with reduced ventricular function, but it is associated with negative effects of tachycardia and hypertension (Lovich, *et al.*, 2011). Alginate gels loaded with dobutamine were immersed in water and the drug release measured after 15 minutes. Although the release of the drug from the gel was achieved, the duration of the release was limited to a 15 minutes interval (Lovich, *et al.*, 2011). The gels were then tested *in vivo* in rats. Dobutamine was added to alginate hydrogels and then placed onto the rat ventricle. *In vivo* results showed that the drug released by the patch had the same positive effect on contractility but with far fewer side effects (Lovich, *et al.*, 2011).

Alginate has been used to prepare macro-porous ferrogels, prepared with alginate and magnetic particles, as a drug release device (Zhao, *et al.*, 2011). The scaffolds were shown to have the ability to deliver small drugs such as the chemotherapy drug mitoxantrone with and without magnetic stimulation over 3 hours *in vitro* (Zhao, *et al.*, 2011) and drugs with high molecular weight, such as proteins and plasmid DNA over 10 hours *in vitro* (Zhao, *et al.*, 2011).

1.8 Summary of study rationale

The inflammation that occurs after ischemia/reperfusion leads to high levels of oxidative stress which produce deleterious effects in the myocardium (Hori & Nishida, 2009). In fact, a sustained increase in TNF-beta levels in the first 3 weeks after MI has been reported in a rat study (Sia, *et al.*, 2002), while in a clinical study patients with acute myocardial infarction presented a progressive increase in oxidative stress levels in the blood, reaching a peak after 7 days (end point) when the patients were discharged from the hospital (Nikolic-Heitzler, *et al.*, 2006).

The use of anti-inflammatory drugs/antioxidants as a treatment to prevent and possibly reverse tissue damage after MI has been widely studied and the results obtained are quite contradictory, as discussed previously in section 1.3.4. In most of the studies presented, the antioxidants were short term delivered in a limited number of doses by either percutaneous injection (statins, probucol), IV infusion (infliximab), or orally (allopurinol, vitamin C). Those studies also failed to demonstrate that the antioxidant used was able to inhibit ventricular remodelling. This suggests that perhaps the drug used, the drug delivery methods or the duration of the treatment studied so far was not effective to improve damaged hearts.

EP has been shown to reduce oxidative stress and increase myocardial ATP levels and decreased infarct size in rats (Woo, *et al.*, 2004). EP enhanced tissue ATP levels, preserved cardiac function and attenuated myocardial oxidative injury in a Langendorff perfused heart experiment (Guo, *et al.*, 2014). In rat models of ischaemia/reperfusion, one injection of EP was shown to inhibit TNF- α , IL-6, HMGB-1 (Lin, *et al.*, 2015) and inhibited the activation of the nuclear factor NF- κ B signalling pathway, cytokines production and consequently reduced infarct size (Jang, *et al.*, 2010). Despite the encouraging results obtained in animal models of

ischaemia/reperfusion injury, EP failed to reduce the incidence of the post-operative adverse outcomes and it did not decrease the systemic inflammatory markers when administered intravenously in high-risk patients undergoing heart surgery (Bennett-Guerrero, *et al.*, 2009). Although EP was ineffective in the clinical trial, the authors suggested that possibly the dose administered to the patients was not adequate and the length of the treatment might have been insufficient (Bennett-Guerrero, *et al.*, 2009). This suggests that the drug delivery methods used were not effective to reduce oxidative stress after myocardial injury. The delivery of an antioxidant, in this case EP, from an implanted material *in situ* would not only minimise any unwanted systemic effects, but also be potentially more effective in the tissue area that needs to be treated (Dikmen, *et al.*, 2011). EP has never been delivered locally in a sustained manner over several days or weeks.

Alginate hydrogels have been used for different biomedical applications, due to their similarity to extracellular matrices of living tissues. Although alginate hydrogels have been extensively used for drug delivery and shown promising results when injected into the myocardium in patients with heart failure, they have never been used for a sustained delivery of antioxidants onto the myocardium for cardiac regeneration. Therefore, in this study the use of alginate to prepare an implantable patch that has the ability to deliver EP *in-vitro* over time will be investigated. Although the ideal release time of EP into the myocardium is still unknown, it is recognised that the increase of oxidative stress production takes place in the first 3 weeks after MI. This suggests that EP delivered over 3 weeks may be sufficient to reduce oxidative stress and consequently improve the patient outcomes.

As well as providing a delivery vehicle for EP, alginate may also serve as a scaffold to promote tissue regeneration. The ideal scaffold for tissue regeneration should have a porous structure with interconnected pores to allow cell infiltration and proliferation as previously discussed in section 1.5. For this reason, porous alginate scaffolds that can deliver EP over time would have potential improve cell attachment and proliferation, which are essential for tissue regeneration.

1.9 OBJECTIVES

The overall aim of this study was to develop alginate macro-porous scaffolds loaded with EP, which have the ability to deliver EP over a period of weeks and allow cell attachment and proliferation *in-vitro*. In order to achieve this, the following specific objectives were set:

- Investigate the development of an optimal alginate hydrogel for the sustained delivery of EP;
- Investigate the development of an optimal porous alginate patch for sustained delivery of EP;
- Characterise the effects of EP on cardiac cell viability under various levels of oxidative stress *in vitro*;
- Evaluate the effects of EP-loaded alginate scaffolds on cardiac cell viability *in vitro*.

2 CHAPTER TWO

MATERIALS AND GENERAL METHODS

2.1 *In-vitro* cell culture studies

2.1.1 Materials

Versene EDTA (*Lonza, UK*), Phosphate Buffer Saline (PBS) (*Sigma Aldrich, UK*), Dulbecco's Modified Eagle Medium (media) with Non-Essential Amino Acids (NEAA) (*Gibco®, Thermo Fisher Scientific*), trypsin (*Gibco®, Thermo Fisher Scientific*), Foetal Bovine Serum (FBS) (*Gibco®, Thermo Fisher Scientific*), penicillin/streptomycin (*Gibco®, Thermo Fisher Scientific*), TrypLE™ (*Gibco® Thermo Fisher Scientific*).

2.1.2 3T3 cell culture

3T3 cells is the abbreviation of “3-day transfer, inoculum 3×10^5 cells”, which refers to the protocol used to obtain the cell line from mouse primary embryonic fibroblasts. This protocol consisted of transferring the cells every 3 days and incubating them in a fixed density of 3×10^5 cells per 20 cm² dish. After 20 – 30 generations in culture the immortalised cells grow at a constant rate. This cell line was used to evaluate the biocompatibility of the alginate patches developed in this study. The cells were kindly made available to the project by Prof Helen Grant (Biomedical Engineering).

Cells were cultured under standard conditions (37°C, 5% CO₂ in humidified atmosphere) in standard sterile cell culture plastic ware. When cells were sub-confluent, they were passaged or split into 96 well plates for use in experimental studies. Media was removed, and the cells were washed twice with 5 mL of versene EDTA in PBS, to remove any trace of media. 1 mL of trypsin in versene was added into the 25 cm² flask to detach the cells from the flask. Once the cells were completely detached 5 mL of complete medium was added to the cells to stop the reaction. Cell counting was performed, and cells were split or seeded at the appropriate seeding density, depending on whether they were being simply passaged or being used in experiments. Cells were used between passage 30 and passage 60. Experiments on

these cells were carried out in 96 well plates in 200 μ L of 10% FBS 1% penicillin/streptomycin, 1% NEAA media. Cells were incubated under standard conditions for 24 hours to allow cell attachment and proliferation before each experiment.

2.1.3 Cardiac fibroblasts cell culture

Cardiac fibroblasts used in this study were harvested from adult rats according to an established protocol (Martin, *et al.*, 2018). They were kindly made available to the project by Dr Susan Currie (Strathclyde Institute of Pharmacy and Biomedical Sciences) and Prof Helen Grant (Biomedical Engineering).

When cells were sub-confluent, they were passaged or split into 96 well plates. Media was removed, and the cells were washed twice with 5 mL of versene (EDTA) in PBS, to remove any trace of media. 3 mL of TrypLE™ was added into the 25 cm³ flask and placed in the incubator for 5 minutes, to allow cell detachment from the flask. Once the cells were completely detached, they were transferred into a 15-mL tube and 3 mL of complete medium was added to the cells to stop the reaction. Cells were centrifuged at 800 RPM for 5 minutes until a pellet of cells was formed at the bottom of the tube. The supernatant was discarded, and 2 mL of complete medium was added to the pellet, pipetting up and down to break up cell clumps. Cell counting was performed, and cells were split or seeded at the appropriate seeding density, depending on the study to be carried out.

Cells were used from passage 1 and 2 and were grown in 96 well plates in 200 μ L of 20% FBS 2% penicillin/streptomycin media. Cells were incubated at 37 °C in 5% CO₂ for 48 hours to allow cell attachment and proliferation before each experiment.

A range of viability, proliferative and toxicity assays were performed and the following sections describe these.

2.1.4 Cell assays

2.1.4.1 AlamarBlue™ Cell Viability Assay

AlamarBlue™ Cell Viability Assay (Thermo Fisher Scientific) was used as an indirect indicator of cell viability through measurement of the cell metabolic activity. The active ingredient of AlamarBlue™ is resazurin, a blue dye which is stable and not toxic to the cells. For this reason, it can be used to monitor cell activity over time. This dye has a blue colour in its original oxidised state. The colour changes from blue to the fluorescent pink in its reduced form. If the cells are healthy, they reduce the resazurin, but if the cells are unhealthy and not viable, their metabolic activity is reduced. The overall change from oxidised to reduced state therefore results in a colour change, measurement of which is used to represent the number of viable cells.

The specific details of the procedure used are as follow. Cell media was removed from the wells and substituted with 200 µL/well serum free media. 20 µL of AlamarBlue™ solution was added to each well and incubated under standards conditions for 4 hours. After the incubation, the media with AlamarBlue™ was removed and transferred to a new 96 well plate for colorimetric analysis. Fresh media, with replacement of the initial EP starting concentration where appropriate, was added to cells for the continuation of the experiment.

A Multiskan™ GO Microplate Spectrophotometer was used to measure the absorbance of the removed media samples at 570 and 600 nm, which correspond to the reduced and oxidised state respectively. In order to determine the percentage of the reduced AlamarBlue™, the following calculation was then performed:

Equation 1

$$\text{Difference in reduction (\%)} = \frac{\text{Abs}_{570} - (\text{Abs}_{600} \times R_0) \text{for sample}}{\text{Abs}_{570} - (\text{Abs}_{600} \times R_0) \text{for positive control}} \times 100$$

Where Abs_{570} is the absorbance of the sample at 570 nm minus the absorbance at 570 nm of the media only, Abs_{600} is the absorbance of the sample at 600 nm minus the absorbance at 600 nm of the media only, and R_0 is the correction factor, which is calculated as follows:

$$R_0 = \frac{Abs_{570} \text{ media with Ab} - Abs_{570} \text{ media only}}{Abs_{600} \text{ media with Ab} - Abs_{600} \text{ media only}}$$

Cells in medium containing 20% FBS without EP were used as a positive control and cells without FBS were used as a negative control.

2.1.4.2 BrdU Cell proliferation assay

The evaluation of cell proliferation was performed by the measurement of BrdU (5-bromo-2-deoxyuridine) incorporation in newly synthesised DNA. BrdU is a synthetic nucleoside that is an analogue of thymidine. During DNA replication, BrdU is incorporated into the DNA in place of thymidine. BrdU antibodies can be used to detect the BrdU incorporated into the cells, which will indicate the number of cells that were actively replicating their DNA.

The BrdU assay was used to investigate the effect of EP on cardiac fibroblasts proliferation. At the time points of interest, 20 μ L of BrdU labelling solution, provided by the manufacturer of the kit, was added to each well of a 96 well plate and incubated for 2 hours. After the incubation, the labelling medium was removed and 200 μ L/well of fixation solution, provided by the manufacturer of the kit, was added to each well. After 30 minutes, the fixation solution was removed and 100 μ L of 1:100 anti-BrdU-POD working solution, provided by the manufacturer of the kit, was added to each well and left to incubate for 90 minutes at room temperature. The wells were then rinsed with washing solution (PBSx1) and 100 μ L of fixation solution was then added to each well. After about 30 minutes a blue colour develops that is indicative of DNA replication. To stop the reaction, 25 μ L of 1M H₂SO₄ was added to each well. With the addition of the stop solution, provided by the manufacturer of the kit, the colour changes from blue to yellow.

A Multiskan™ GO Microplate Spectrophotometer was used to measure the absorbance at 450 nm and 690 nm within 5 minutes of adding the stop solution.

In order to determine the percentage of BrdU incorporation, the following calculation was then performed:

$$\text{BrdU incorporation (\%)} = \frac{\text{Abs}_{450} - \text{Abs}_{690} \text{ for sample}}{\text{Abs}_{450} - \text{Abs}_{690} \text{ for positive control}} \times 100$$

Where Abs_{450} is the absorbance of the sample at 450 nm minus the absorbance at 450 nm of the media only, Abs_{690} is the absorbance of the sample at 690 nm minus the absorbance at 690 nm of the media only. The positive control used in this assay was the cells in 20% FBS media with no EP treatment. The negative control was the cells in 0 /FBS media with no EP.

2.1.4.3 MTT assay

MTT assay was used to measure the metabolic activity of 3T3 cells as an indirect measure of cell number.

This assay involves the conversion of the water soluble MTT (3-(4,5-dimethylthiazol-2-yl)-2,5-diphenyltetrazolium bromide) (Sigma Aldrich) to an insoluble formazan by NAD(P)H-dependent cellular oxidoreductase enzymes. In this reaction, the yellow colour of MTT is converted into the deep purple colour of the insoluble formazan. Only viable cells cause this deep change, so the measurement of the concentration of formazan corresponds to the number of living cells.

10 mM of MTT solution in PBS was prepared and filtered with a 0.2 μm filter and stored at 4 °C. At the time point of interest, 50 μL of MTT solution was added to each well of the 96-well plate and incubated at 37 °C for 4 hours. Cell culture media with MTT was then removed and 200 μL of DMSO was added to each well to dissolve the formazan product. The amount of formazan in the samples was measured at 540 nm using a Multiskan™ GO Microplate Spectrophotometer.

2.1.4.4 Neutral red assay

Neutral red assay (Basic Red 5, Toluylene Red) is a dye that is incorporated into only the lysosomes of viable cells, thereby excluding in this way the non-viable cells. This assay was used to measure the viability of cardiac fibroblasts in presence of alginate scaffolds loaded with EP.

A stock solution of 40 mg/ml of Neutral Red in PBS was prepared and stored at room temperature. The day before performing the assay, the neutral red solution was diluted 1:100 in 20% FBS media. The solution was filtered with a 0.2 µm filter and stored at 37 °C overnight.

Cell culture medium was removed from the wells and 200 µL of 40 µg/mL Neutral Red solution was added to each well. The plates were incubated at 37 °C for 3 hours. At the end of the incubation, the solution was removed and the wells were rinsed once with 200 µL of PBS per well. The dye retained by the cells was extracted with 100 µL/well of destain solution (1% glacial acetic acid, 50% Ethanol, 49% distilled H₂O). The amount of formazan in the samples was measured at 540 nm using a Multiskan™ GO Microplate Spectrophotometer.

2.1.4.5 LDH activity

Necrosis is a type of cell death which consists of swelling of the cell and subsequently leakage of plasma across the membrane. Once this happens intracellular molecules are released into the extracellular space. Lactate dehydrogenase (LDH) is a cytoplasmic enzyme which is present in cells. Once the cytoplasmic membrane undergoes breakage, LDH is released into the external environment. Measurement of this enzyme in the cell culture medium therefore gives an estimation of the number of cells going through cell death. LDH activity measurement was used to measure the toxicity of EP loaded alginate scaffolds on cardiac fibroblasts.

LDH coupled with pyruvic acid converts NADH to NAD⁺ through an enzyme - catalysed oxidation reaction. The amount of NADH converted into NAD⁺ can be easily determined by measuring the absorbance at 340 nm using a Multiskan™ GO Microplate Spectrophotometer.

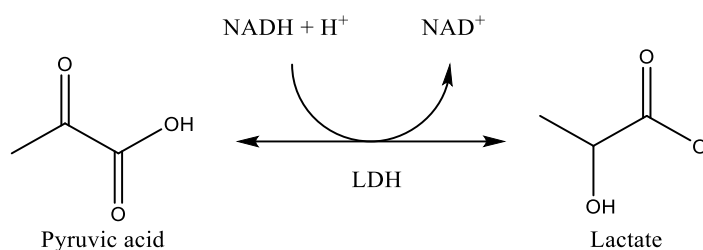


Figure 2.1 Schematic representation of the Lactate Dehydrogenase (LDH) reaction.

A stock solution of 0.1 M of Sodium Phosphate (NaPi) buffer at pH 7.6 was prepared and stored in the cold room at $-4\text{ }^{\circ}\text{C}$. NaPi buffer was used to prepare a 3 mg/mL pyruvic acid/NADH solution. Growth medium was collected from the wells and replaced with fresh medium at day 1, 3 and 5 of cell culture. LDH assay was performed immediately after the collection of the samples.

The reaction was started by adding 100 μL of the culture medium collected from the samples to 40 μL of the pyruvic acid/NADH solution and 860 μL of NaPi buffer solution. NaPi buffer solution was used as a blank. The absorbance was measured at 340 nm on time course mode over 60 seconds. The Point pick function within the UV-Spectrophotometer was used to take the readings of the absorbance at time zero and at a time of 60s.

A high difference in absorbance indicates that a high amount of LDH leaked out of the cell membrane, indicating that the material or drug tested is toxic to the cells. The enzymatic activity of LDH was measured using the equation below:

Equation 4

$$\text{Enzyme activity} = \frac{((t = 60s) - (t = 0s))/min}{E}$$

Where (E) is a constant and represents the NADH molar extinction coefficient, which is 6.22 mM^{-1} at 340 nm; $t=60s$ is the absorbance measured after 1 minute, when the reaction occurred and $t=0s$ is the absorbance measured before the start of the reaction.

2.1.5 Live/dead staining and confocal imaging

Live/dead staining is another method that can be used to test the potential cytotoxicity of a drug or material on cells. Cells are stained with two fluorescent dyes which will distinguish dead cells from the alive cells. Propidium Iodide (PI) is a red-fluorescent dye that binds to the DNA. Because this dye is not absorbed through the membrane, this will exclude the live cells. For this reason, it is commonly used to detect dead cells in a cell population. On the contrary, Carboxyfluorescein Diacetate, Acetoxymethyl Ester (CFDA) is a cell permeable dye, cleaved by intracellular esterase enzymes to form Carboxyfluorescein succinimidyl ester (CFSE) which produces a green-fluorescence. In this way only the live cells are stained. Cardiac fibroblasts were seeded at 2.7×10^3 cells/cm² cell density into three 9.2 cm² petri dishes. One petri dish was used as a control (media only), one with 3 mM EP media and the other one with 10 mM EP media. After 5 days Propidium Iodide with CFDA were used to perform a live/dead staining.

2.2 Alginate hydrogel for EP delivery

2.2.1 Alginate hydrogel production

Materials

Sodium alginates with low viscosity (LV) and medium viscosity (MV) (39% guluronate, 61% mannuronate), EP (C₅H₈O₃, 98% purity, Mw = 116.12 g/mol), and Calcium Chloride (CaCl₂, 99% purity, Mw = 110.98g/mol) were purchased from Sigma-Aldrich, UK. PRONOVA™ UP LVG, ultrapure low viscosity sodium alginate (Mw = 75,000 - 200,000 g/mol) with a minimum 60% of the monomer units being guluronate, was purchased from FMC BioPolymer AS / NovaMatrix, Industriveien, Sandvika. Ultrapure water was used to prepare all gel solutions.

Methods

All percentage concentrations are weight per volume (w/v) unless stated otherwise. The preparation of the hydrogels containing EP was carried out in the fume cupboard, in order to eliminate the risk of fumes or vapour that would be an irritant. 1% (w/v) and 2% (w/v) alginate solutions were prepared by adding high mannuronate content

or high guluronate content sodium alginate to water. In the study conducted by Famili *et al.*, 2013, the toxicity of EP in cultured trabecular meshwork cells was assessed (Famili, *et al.*, 2013). It was found that cells were well tolerant to EP concentration at or below 10mM while higher doses were shown to be toxic (Famili, *et al.*, 2013). For this reason, the aim of the study was to prepare alginate hydrogels that can deliver up to 10 mM EP. In the first batch of alginate hydrogels prepared with high mannuronate alginate, a lower EP concentration was used. 1 mL of alginate solution was poured into each well/ vial and 1.11 μL of EP was added to it to provide 10 mM EP. The plate/vials were then stirred with a vortex shaker to allow the mixing of alginate solution with EP. A solution of 0.6%, 1% and 1.5% of CaCl_2 respectively was then added to each well/vial with a 1:1 ratio, making a final EP concentration of 5 mM. At that point the hydrogel was visible, and the extra liquid solution left was removed. The Alginate scaffolds prepared with high guluronate alginate were prepared in a similar way as the high mannuronate alginate hydrogels. 0.5 mL of alginate solution was poured into each well/ vial and EP (2.78 μL added to 0.5 mL of alginate solution) was added to have 50 mM EP concentration in alginate solution, which became 25 mM EP concentration when a 1:1 ratio CaCl_2 solution was added to the alginate solution. Alginate hydrogels were prepared to be used for a stability study and an EP release study which required the immersion of the hydrogels in a 1:1 ratio PBS solution. Once the hydrogels were placed in PBS, the maximum EP concentration could be estimated as being around 12.5 mM, close to the 10 mM of the target set out.

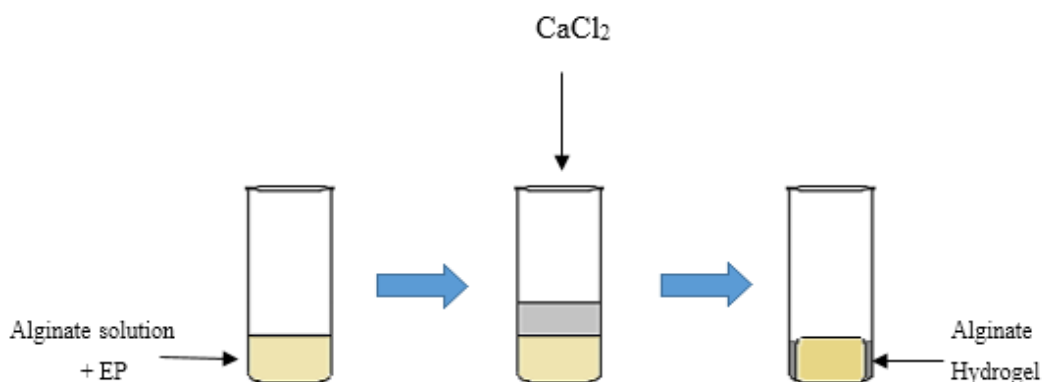


Figure 2.2 Schematic representation of alginate gel preparation steps

2.2.2 Alginate Hydrogel stability in PBS

Alginate hydrogel degradation was studied by measuring the weight change over time (Sarker, *et al.*, 2014). Alginate hydrogels were placed in 1 mL of PBS solution and incubated at 37 °C for 28 days. At each time point (1 hour, 1 day, 3 days, 5 days, 7 days, 14 days 21 days, 28 days) all the incubation medium was removed and the samples were weighed within the glass vial. The formula used to measure the weight change (or swelling ratio) is as follows:

Equation 5

$$\text{Swelling ratio}(\%) = \frac{\text{Final weight} - \text{Initial weight}}{\text{Initial weight}} \times 100$$

where the “initial weight” is the weight of the hydrogel at the start of the experiment, before adding the PBS into the container and the “final weight” is the weight of the hydrogel at each time point after removing the PBS solution.

2.3 Alginate scaffolds for EP delivery

Materials

EP (C₅H₈O₃, 98% purity, Mw = 116.12 g/mol), Calcium Chloride (CaCl₂, 99% purity, Mw = 110.98 g/mol) and Calcium D-gluconate monohydrate (C₁₂H₂₂CaO₁₄ · H₂O, ≥98% purity, Mw= 448.39 g/mol) were purchased from Sigma-Aldrich. PRONOVA™ UP VLVG, ultrapure very low viscosity sodium alginate (Mw < 75,000 g/mol) where minimum 60% of the monomer units are guluronate and NOVATACH™ VLVG 4GRGDSP, 4GRGDSP-coupled very low viscosity sodium alginate (Mw < 75,000 g/mol) where minimum 60% of the monomer units are guluronate were purchased from FMC BioPolymer AS / NovaMatrix, Industriveien, Sandvika. Ultrapure water was used to prepare all gel solutions.

Methods

Lyophilisation or freeze-drying is the extraction of water from a substance. Samples are frozen and a vacuum pump reduces the surrounding pressure, allowing the water contained in the samples to sublime, changing from the solid state to the gas state. In

this study, the samples were prepared in 24 well plates and stored in the freezer at either -20 °C or -80 °C overnight. The lid of the plates was removed and the plates were covered with PARAFILM® M (Sigma Aldrich), to keep the samples in place. The PARAFILM® M was then pierced several times, to allow the extraction of water from the scaffolds (Figure 2.3-c). The scaffolds were then freeze-dried at -50 °C for 24 hours using a MicroModulyo Freeze Drier 1.5L (Thermo Savant) (Figure 2.3-a). A series of different alginate scaffolds were prepared using different methodologies that are described in detail below. The concentration of EP was kept constant (25 mM in the scaffold).

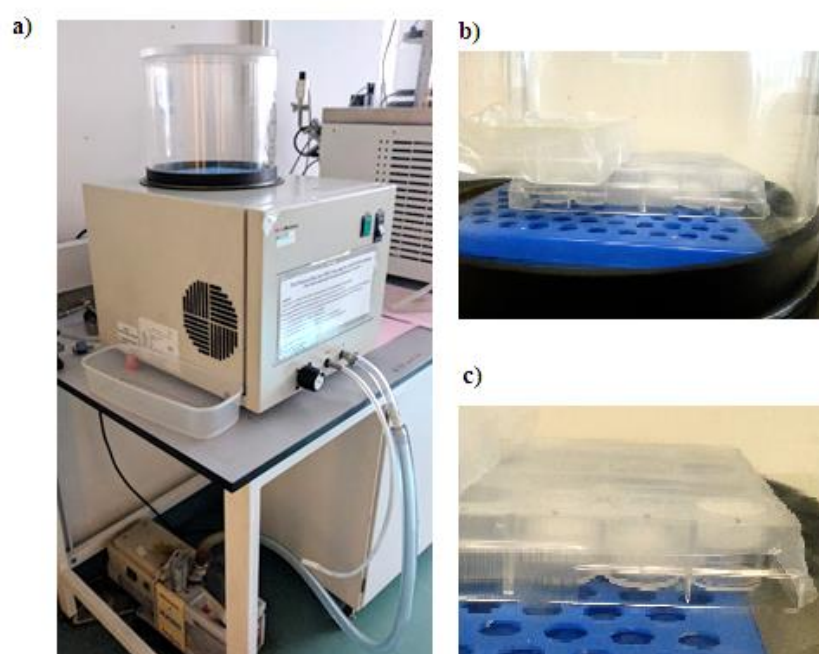


Figure 2.3 Freeze-drying method used to prepare macro-porous alginate scaffolds. **a)** Micro Modulyo Freeze Drier 1.5L (Thermo Savant); **b)** Frozen samples were placed in the freeze-drier and freeze-dried at -50 °C. **c)** Alginate scaffolds were then ready after 24h of freeze-drying.

In the preliminary method, alginate solution was cross-linked with calcium gluconate and freeze-dried. In subsequent methods 1 to 4, a single cross-linker (Calcium chloride) was used to create the bonds with alginate. On the other hand, in the methods 5 and 6 double cross-linking was used to produce the scaffolds (calcium gluconate and calcium chloride). These methods are summarised in Table 1. For each type of scaffold two 24 well plates were used, one for the control samples, and one with samples containing EP, in order to reduce any possible exchange of EP between the samples.

For each method, four plates in total were used, two stored at -20 °C, the other two stored at -80 °C.

Table 1. Summary details of different methodologies used to produce macro-porous alginate scaffolds.

Alginate scaffolds produced with 1 cross-linker					
Method 1	0.5mL 2% VLVG alginate solution frozen at -20°C/-80°C overnight	Freeze-dried at -50°C for 24h	2.78 µL of EP (to have 25mM EP in the scaffold) added the scaffold was placed in 1 mL of 0.2M CaCl ₂ bath for 30 mins Frozen at -20°C/-80°C overnight	Freeze-dried at -50°C for 24h	
Method 2	0.5mL 2% VLVG alginate solution was frozen at -20°C/-80°C overnight	Freeze-dried at -50°C for 24h	2.78 µL of EP added the scaffold was placed in 1 mL of 0.2M CaCl ₂ bath for 30 mins		
Method 3	2.78 µL EP+0.5mL 2% VLVG alginate solution was frozen at -20°C/-80°C overnight	Freeze-dried at -50°C for 24h	the scaffold was placed in 1 mL of 0.2M CaCl ₂ bath for 30 mins Frozen at -20°C/-80°C overnight	Freeze-dried at -50°C for 24h	
Method 4	2.78 µL EP + 0.5mL 2% VLVG alginate solution was frozen at -20°C/-80°C overnight	Freeze-dried at -50°C for 24h	the scaffold was placed in 1 mL of 0.2M CaCl ₂ bath for 30 mins		
Alginate scaffolds produced with double cross-linking					
Method 5	5.56 µL (to have 25mM EP in the scaffold) EP + 0.5mL 2% VLVG alginate solution + 0.5mL 0.4%-1% Calcium gluconate solution frozen at -20°C/-80°C overnight	Freeze-dried at -50°C for 24h	the scaffold was placed in 1 mL of 0.2M CaCl ₂ bath for 30 mins Frozen at -20°C/-80°C overnight	Freeze-dried at -50°C for 24h	
Method 6	5.56 µL EP + 0.5mL 2% VLVG alginate solution + 0.5mL 0.4%-1% Calcium gluconate solution frozen at -20°C/-80°C overnight	Freeze-dried at -50°C for 24h	the scaffold was placed in 1 mL of 0.2M CaCl ₂ bath for 30 mins		

2.3.1 Calcium gluconate alginate scaffolds preparation

Alginate scaffolds were prepared by adding 0.5 mL of 2 % VLVG alginate solution in a 24 well plate and cross-linked by adding 0.5 mL of 0.4% or 1% calcium gluconate solution to each well. After 30 minutes, the samples were frozen overnight and then freeze-dried for 24 hours.

For the production of alginate scaffolds containing EP, 2.78 μL of EP was added to each scaffold as explained in Table 1.

2.3.2 Calcium chloride alginate scaffolds preparation

Alginate scaffolds were prepared by adding 0.5 mL of 2 % VLVG alginate solution in a 24 well plate. The plate was then stored in the freezer at $-20/-80\text{ }^{\circ}\text{C}$ overnight. The scaffolds were then freeze-dried for 24 hours (see section 2.3.3). The scaffolds were then cross-linked by adding 1 mL of 0.2 M of CaCl_2 solution to each scaffold. After 30 minutes, the CaCl_2 solution was removed and the samples were either frozen again overnight for the following cycle of freeze-drying or used straight away.

For the production of alginate scaffolds containing EP, 2.78 μL of EP was added to each scaffold as explained in Table 1.

2.3.3 Double cross-linked alginate scaffolds preparation

Double cross-linked alginate scaffolds were prepared by adding 0.5 mL of 2% VLVG alginate solution to each well of a 24 well plate. The solution was cross-linked by adding 0.5 mL of 0.4% or 1% of calcium gluconate solution to each well and mixed it with an immersion mixer and left for 20 minutes in the fridge before placing the plates in the freezer at $-20/ -80\text{ }^{\circ}\text{C}$ overnight. After 24 hours of freeze-drying, the scaffolds were further cross-linked by adding 2 mL of 0.2 M of CaCl_2 solution to each scaffold. After 30 minutes, the CaCl_2 solution was removed and the samples were either ready to be used or frozen again overnight for the following cycle of freeze-drying. In the study of EP release, 5.56 μL of EP was added to each scaffold as explained in the Table 1.

2.3.4 Degradation study of alginate scaffolds

Alginate scaffolds degradation was studied by measuring the weight change over time, as explained earlier in section 1.3.2. Briefly, different formulations of alginate scaffolds were placed in 1.5 mL of PBS solution and incubated at 37 °C for 28 days. This time the volume of PBS used for the experiment was 1.5 mL, maintaining 1:1 ratio between PBS and alginate solution with cross-linking solution (0.5 mL of alginate solution + 1 mL CaCl₂ solution). The scaffolds were weighed at the beginning of the experiment, before placing them in PBS. At each time point (1 hour, 1 day, 3 days, 7 days, 14 days, 21 days, 28 days) all the medium was removed and the samples were weighed within the glass vial. Equation 5 was used to measure the swelling ratio.

In this study, the “initial weight” is the weight of the scaffold in its dry form, before adding the PBS in the container and the “final weight” is the weight of the scaffold at each time point after removing the PBS solution.

2.4 EP release studies

2.4.1 Sample preparation

The methodology used to prepare the alginate hydrogels for this study is explained in section 2.2.1, while alginate macro-porous scaffolds used in this study were prepared with the methodology described in section 2.3.2 and 1.3.3. The concentration of EP (25mM) was the same in both hydrogels and macro-porous scaffolds.

2.4.2 Sample collection

The samples were placed in a 1:1 PBS solution and stored in an incubator at 37 °C at a constant gentle agitation. At different time points (1 hour, 1 day, 3 days, 7 days, 14 days, 21 days, 28 days) the vials were removed from the incubator and half of PBS solution collected from each sample. The solution was transferred in an Eppendorf and stored in the freezer at -20 °C for future measurement. In order to maintain the volume of the release solution constant, the same volume of solution removed was replaced by an equal amount of fresh PBS solution and the vial returned to the incubator. A schematic representation of the methodology is shown in Figure 2.4.

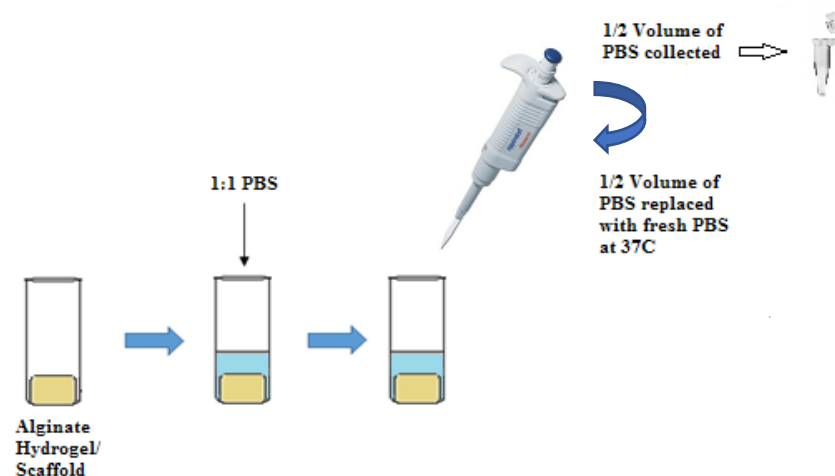


Figure 2.4. Schematic representation of the sample collection for EP release study. Alginate hydrogels and alginate scaffolds were placed in a 1:1 PBS solution and stored in an incubator at 37 °C at a constant gentle agitation. At different time points (1 hour, 1 day, 3 days, 7 days, 14 days, 21 days, 28 days) half of PBS solution was collected and stored in an Eppendorf -20 °C for future measurement. In order to maintain the volume of the release solution constant, the same volume of solution removed was replaced by an equal amount of fresh PBS solution and the vial returned to the incubator.

2.5 Measurement of EP

There has been little investigation into the optimal methods of detecting and quantifying easily the concentration of EP in physiological solution. Several methods were thus investigated for measurement of EP, as discussed in more details in Chapter 3. These include the use of direct methods, such as UV-Spectroscopy (UV/Vis-spectrophotometry, Nano-spectrophotometry) and High Performance Chromatography, and indirect methods based on the antioxidant activity of the compound (DPPH assay, ABTS assay) and based on the measurement of pyruvate (pyruvate assay). Further details on each technique and how it was used in this study are included below.

2.5.1 Direct measurement of EP

2.5.1.1 UV/Vis-spectrophotometry

Ultraviolet/visible-spectrophotometry is a widely used analytical technique to measure quantitatively a compound in a solution. A beam of light in the range of visible and/or

UV light is separated into distinct wavelengths by a prism or diffraction grating. Each single wavelength beam is split into two equal beams by a half mirror. One of the beams passes through a cuvette containing only the solvent, the other beam passes through another cuvette containing the compound being studied in a solution of the same solvent. The absorbance of the light by the solution and the solvent is measured by an electronic detector and compared. The absorbance of the solvent is used as blank and is subtracted from the absorbance of the compound solution. Each compound has a characteristic peak of absorbance, which is the maximum absorbance at a certain wavelength.

A UV 2401 PC UV/VIS Recording Spectrophotometer was used to measure EP in PBS solution. UV-Cuvette UV-Transparent Spectrophotometry Cuvettes were purchased from BrandTech Scientific, Inc. (Essex, CT).



Figure 2.5 UV 2401 PC UV/VIS Recording Spectrophotometer used to measure EP in PBS solution.

A set of EP standards in PBS in the range of 36 μM – 20 mM was prepared and a standard calibration curve produced. Briefly, 0.5 mL of each standard was pipetted into the quartz cuvette and the absorbance of the spectrum was measured. PBS was used as a blank and the standards were measured in the spectra from 190 to 300 nm.

2.5.1.2 Nano-spectrophotometry

Genova Plus Spectrophotometer (Bibby Scientific Ltd. UK) was also investigated as a method for measuring the absorbance of EP in PBS. Briefly, 2 μ L volume of sample or standard was pipetted onto the sample holder and the absorbance of the spectrum was measured. The peaks of absorbance were identified as indication of the absorbance of the drug. PBS was used as a blank and the standards were measured in the spectra from 190 to 300 nm.

2.5.1.3 HPLC

Reverse phase high performance liquid chromatography (HPLC) is widely used to measure the amount of drug in various solutions. A mixture of solvents, known as the mobile phase, and the drug is injected in a column at high pressure. The sample is automatically collected with a needle and transferred to the detector by passing through the column. The column is filled with an adsorbent that leads to the separation of the different components. The time taken by the sample to pass from the column to the detector is called retention time. Every substance has a specific retention time which varies depending on the initial conditions such as temperature and dimensions of the column, pressure, adsorbent material characteristics and solvents used. The detector is a UV spectrophotometer which measures the absorbance of compound at a certain wavelength. Each component of the formulation can give rise to a distinctive peak.

HPLC was used to measure EP standards in the range of 70 μ M – 50 mM produced respectively in methanol and PBS. The flow rate used was 0.3mL/min for 10 minutes using a C18 column of 5 μ m particle size. The absorbance was measured at different wavelengths (203, 205, 210, 300 nm). The mobile phase used comprised 30% methanol 10% acetonitrile and 60% double distilled water, as previously described by Kim *et al*, 2011. The height of the peaks was used to obtain a calibration curve.

2.5.1.4 Determination of EP concentration in experimental samples

The peaks of absorbance were identified as an indication of the absorbance of the drug and PBS was used as a blank. The three different detection methods described above produced linear calibration curves of the type shown below.

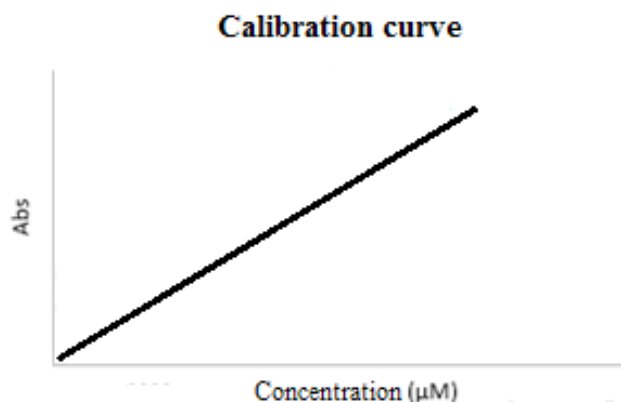


Figure 2.6 Example of linear calibration curve.

The samples from the release experiments were then analysed and the unknown EP concentration in each inferred from the equation of the calibration curve best fit line. In order to determine the cumulative release amount, the following calculations were performed.

The concentration of the EP released from the alginate scaffolds was calculated from the curve of the regression equation

Equation 6

$$y = mx + b$$

Where (y) is the absorbance, (m) is the slope, (b) is the intercept and (x) is the unknown sample concentration. This is a linear equation and it is obtained by creating a trend line which passes through the data points of the calibration curve.

The (x) unknown concentration can be calculated from this equation, which becomes

$$x = (y - b)/m$$

In order to remove any interference from this measurement, the absorbance of the media from alginate scaffolds without EP was measured and the absorbance removed from the absorbance of the sample.

The cumulative mass of EP released is calculated as follow:

$$M = CVM_w$$

In this equation, M is the mass of EP released, C is the concentration of EP calculated in the previous step, V is the volume of release media and M_w is the molecular weight of EP (116.12 g/mol).

Half of the media was collected at every time point and replaced with fresh PBS. In this way, the mass (M) of EP measured is half the actual amount of EP in the media. For this reason, the partial mass of EP released (M_1) is double the mass measured in the previous step.

$$M_1 = M * 2$$

The calculation of the partial mass of the sample collected at the following time point is more complex than the previous case. When the first sample is collected, half of media is left and it contributes to the mass measured in the following time point sample. For this reason, half of the mass of the previous sample should be removed from the mass of the followed time point sample. The partial mass is also double the mass measured, as explained previously. This partial mass of the following time point sample (M_2) is expressed in the equation below:

$$M_2 = M * 2 - \left(\frac{M_1}{2}\right)$$

The M_2 value was calculated for each time point. The cumulative Mass released over time is calculated by adding the partial mass to the cumulative mass of the previous time point. The average of the cumulative mass of the scaffolds (n=5) is calculated for each time point. Standard deviation is calculated as a measure of uncertainty in the values.

2.5.2 Indirect measurement of EP

2.5.2.1 Pyruvate assay

A Pyruvate Assay Kit from Sigma Aldrich was investigated as an indirect method to measure pyruvate concentration in solution. In this study, this assay was used to measure EP by measuring its pyruvate component. EP concentration was determined by the coupled enzyme assay, which resulted in a colorimetric change observable at a wavelength of 570 nm, proportional to the pyruvate present. Pyruvate standards and EP standards in the range of 40-400 μ M were prepared and used to plot the calibration curve. All standards were run in duplicate. EP content in the samples was measured by using the calibration curve method.

2.5.2.2 DPPH assay

DPPH assay has been used to measure the antioxidant activity of different agents, although it has not previously been used for EP measurement (Garcia *et al*, 2012). In this study it was assessed to determine if this method can measure EP concentrations.

DPPH (2, 2- diphenyl-1-picryl-hydrazyl-hydrate) is a free radical which presents a deep violet colour when dissolved in ethanol. In presence of an antioxidant agent, the radical is reduced and the colour changes from violet to colourless (Garcia *et al*, 2012). The change in colour was measured by a spectrophotometer plate reader at 517nm after 100 minutes of incubation. The assay was run according to methodology used by Garcia *et al*, 2012. AGI-1067, a known anti-inflammatory drug used to treat atherosclerosis with well-defined anti-oxidant activity (Crim, *et al.*, 2010) was used as a positive control. EP and AGI-1067 standards were prepared in the range of (0.06 – 0.4 mM) for AGI-1067 and (0.06 – 12.8 mM) for EP in PBS. 0.5 mM DPPH solution

in ethanol was used as a reaction solution that was added to the standards. The negative control used was the 0.5 mM DPPH solution in ethanol.

The percentage of antioxidant activity (AA %) of AGI-1067 and EP was calculated according to Garcia *et al*, 2012 (Garcia, *et al.*, 2012):

Equation 11

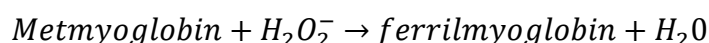
$$AA\% = 100 - [(Abs\ Standard - Abs\ Blank) \times 100 / Abs\ Control]$$

The calibration curve was obtained from the absorbance of the EP standards. The equation of the calibration curve was used to measure EP in the samples.

2.5.2.3 ABTS assay

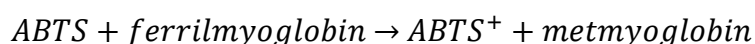
The ABTS antioxidant assay (Zen-Bio, Inc.) is widely used to measure the antioxidant activity of different substances (Dong, *et al.*, 2015). In the presence of hydrogen peroxide and metmyoglobin, a ferril myoglobin radical is produced.

Equation 12



This radical can oxidise ABTS (2, 2'-azino-bis (3-ethylbenzthiazoline-6-sulfonic acid) forming the radical cation ABTS⁺. This reaction produces a green colour and the absorbance can be measured at 405 nm with a colorimeter.

Equation 13



In presence of an antioxidant, the reaction is stopped, therefore the concentration of the antioxidant is indirectly proportional to the radical produced. Trolox (6-hydroxy-2,5,7,8-tetramethylchroman-2-carboxylic acid) (Zen-Bio, Inc.) is an antioxidant and it was used as a positive control. The reaction was allowed to proceed for 5 minutes and then the stop solution was added to the wells, in order to stop the reaction. The plate reader was used to measure the absorbance at 405 nm.

EP standards were prepared fresh in PBS and in buffer solution in the range of 40 – 10,000 μM . Trolox standards were used as a positive control. The quantification of EP was calculated from its ability to stop the oxidation of ABTS.

2.6 EP stability study

EP is hydrophilic and it is preferred to the normal pyruvate because of its stability in solution, as discussed in section 1.5. EP also has a high thermal degradation point, which makes it ideal for being released over time *in vivo*. To confirm the stability of EP in solution, in this study it was investigated the stability of EP *in-vitro* at body temperature.

EP standards in PBS in the concentration range of 78 μM to 10 mM were prepared. The standards were then split into 2 batches which were then stored at 2 different temperatures. The reference standards were stored at -20°C , while the others were stored in the oven at 37°C . The absorbance of both batches was measured at different time points over 21 days. The absorbance of the standards was measured with two different spectrophotometers, the UV-spec (190 to 300 nm spectra) and the Nanospec (198 nm).

Standards were placed at room temperature for 2 hours before use in order to reach the same temperature, avoiding any possible interactions that temperature could have with the absorbance. PBS was used as a blank.

2.7 Morphological analysis

2.7.1 Porosity

The porosity of the alginate scaffolds was calculated for each formulation. The equation used to calculate the porosity is

Equation 14

$$\text{Porosity (\%)} = \frac{\text{Final weight} - \text{Initial weight}}{\text{Final weight}} \times 100$$

Where the “final weight” is the weight of the wet scaffolds and the “initial weight” is the weight of the scaffold when dry.

2.7.2 SEM analysis

A Scanning Electron Microscope (SEM) (HITACHI TM-1000 Tabletop Microscope) was used to investigate the morphology of the alginate structures.

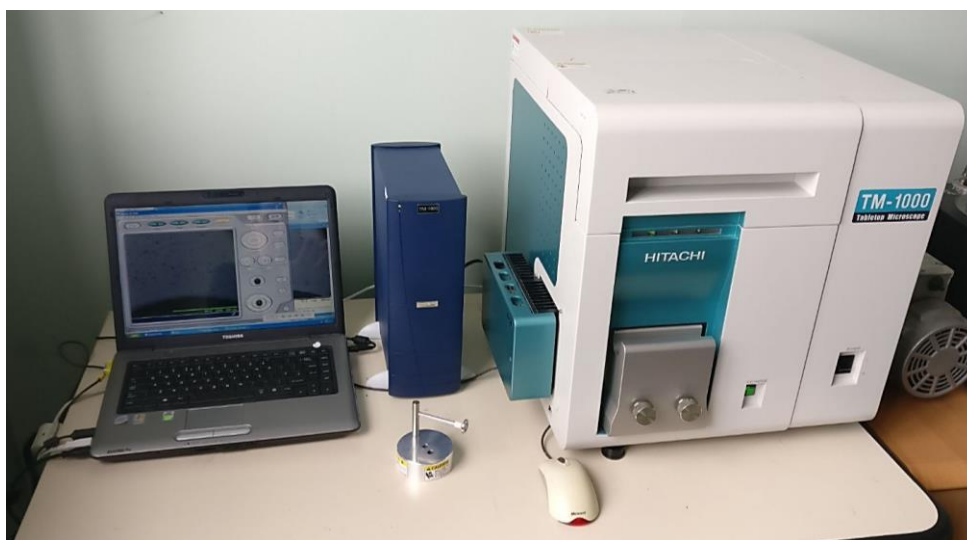


Figure 2.7 Scanning Electron Microscope (SEM) (HITACHI TM-1000 Tabletop Microscope) used to investigate the morphology of the alginate structures.

Alginate samples were fixed onto the specimen mount by using carbon conductive tape. The samples were placed in the SEM either wet (for the alginate hydrogels) or dry (for the macro-porous scaffolds). The scaffolds were then analysed and several images were taken at different magnifications (x150 – x300) of the surface. The scaffolds were also cut with a surgical scalpel to obtain the cross-section views using the same methodology used for the surface.

3 CHAPTER THREE

ETHYL PYRUVATE DETECTION METHOD AND STABILITY STUDY

3.1 Introduction

Ethyl pyruvate (EP) has been studied for its antioxidant properties and ability to enhance ATP levels and reduce tissue damage in a range of different injury models (Yang, *et al.*, 2016). A single dose of EP (40mg/ml or other units of concentration) injected intraperitoneally 12 h after cecal puncture, attenuated sepsis-induced acute renal failure in aged mice (Miyaji, *et al.*, 2003). In various rat models of severe acute pancreatitis, EP has been demonstrated to reduce the expression of TNF- α , IL-6, HMGB1 and ROS, all factors that are thought to contribute to the development of acute renal failure (Luan, *et al.*, 2015) (Yang, *et al.*, 2008) (Cheng, *et al.*, 2007). EP has also been shown to ameliorate acute alcohol-induced liver injury in mice (Yang, *et al.*, 2003), acute-on-chronic liver failure in rats (Wang, *et al.*, 2012) and hepatic ischemia-reperfusion injury in mice (Shen, *et al.*, 2013). In the study conducted on a rat model (Woo, *et al.*, 2004), a 1.5 mL/kg intravenous bolus of ethyl pyruvate was administered intravenously immediately before inducing ischemia followed by reperfusion. The study showed how ethyl pyruvate reduces oxidative stress and increases myocardial ATP levels and decreased infarct size (Woo, *et al.*, 2004). EP enhanced tissue ATP levels, preserved cardiac function and attenuated myocardial oxidative injury in a Langendorff perfused heart experiment (Guo, *et al.*, 2014).

It is clear that EP therefore has great therapeutic potential for the treatment of a wide range of conditions. As with any compound, the dose delivered to the target tissue will be an important determinant of efficacy. In a double-blind, randomized, placebo-controlled study, EP has been administered intravenously in high-risk patients undergoing coronary artery bypass graft and/or cardiac valvular surgery with CPB. (Critical Therapeutics Inc, Lexington, MA, USA) (Bennett-Guerrero, *et al.*, 2009). In this study EP did not significantly reduce the incidence of the post-operative adverse outcomes and it failed to decrease the systemic inflammatory markers (Bennett-

Guerrero, *et al.*, 2009). The authors suggested that the dose administered to the patients was potentially too low to reduce the inflammation. They also propounded that the period of the treatment might have been insufficient (Bennett-Guerrero, *et al.*, 2009).

In order to be able to fully explore the relationship between drug dose and efficacy, it is important that there are robust methods in place to allow measurement of EP *in-vitro*. In the previous studies mentioned above, after EP treatment, the concentration of EP in blood has not been measured. In fact, there has been little investigation into the optimal methods of detecting and quantifying easily the concentration of EP in physiological solution. To date, there appears to be only one method that has been reported for the measurement of EP in physiological solution. Kim *et al*, 2011 described the use of a High-Performance Liquid Chromatography-Electrospray Ionisation/Mass Spectrometry method (HPLC-ESI/MS) to quantify EP concentrations in rat plasma (Kim, *et al.*, 2011). This method of EP measurement requires several specialist items of equipment, which were not available to this project and indeed are not always readily available in many laboratories. There is thus the need to investigate alternative methods to detect and measure EP in physiological solutions.

It has been shown that EP has greater stability than sodium pyruvate, making it the candidate selected for investigation in this study (see section 1.5). However, given the final application of EP envisioned in this study, it was necessary to investigate its stability over prolonged periods in physiological solution.

3.1.1 Aim and objectives

The aim of this study was to investigate the development of an easy and quick method to measure EP in physiological solution. Several methods of EP quantification were investigated, and this chapter will describe the results of this work. The methods used can be allocated into two groups, with the first group based on the indirect measurement of EP, such as pyruvate, DPPH and ABTS assays, and the second group being methods based on direct spectroscopy, such as UV/Vis spec analysis, Nano-spectroscopy and HPLC. Given that it is important for EP to remain effective over prolonged periods of release *in vivo*, it was therefore decided to investigate the stability

of this drug at body temperature over time. The specific objectives have been summarised as follows:

- To identify a suitable method for measurement of EP in physiological solution;
- To determine the stability of EP in physiological solution at body temperature for a period of 2 weeks.

3.2 Methods

The materials and methods used have been described earlier (section 2.5). Briefly, a series of EP standards in different ranges of concentrations were prepared in PBS. These were analysed by various different detection techniques and calibration curves generated for each measurement method. The first assay investigated was the pyruvate assay, used to determine the amount of pyruvate in solution. Subsequent assays assessed were antioxidant assays, specifically the DPPH assay and the ABTS assay. Those assays were used to measure EP indirectly, by measuring the antioxidant effect of EP. Finally, a range of different direct spectroscopic techniques were investigated.

3.3 Results

3.3.1 Pyruvate assay

Pyruvate assay is a method used to detect pyruvate in solution. In this study, the assay was used to determine the EP concentration by measuring the pyruvate component of ethyl pyruvate. The method used was discussed in more detail in the section 2.4.2.1. The calibration curves generated for pyruvate and EP are shown in Figure 3.1-a. It can be seen that the assay was capable of measuring both pyruvate and EP. There is a near linear relationship between the absorbance and the drug concentration between 40 to 160 μM for both compounds, while there was little further increase in the absorbance recorded above 160 μM (see Figure 3.1-a). Excluding the highest concentration, it was possible to fit a linear curve through each set of data (Figure 3.1-b)

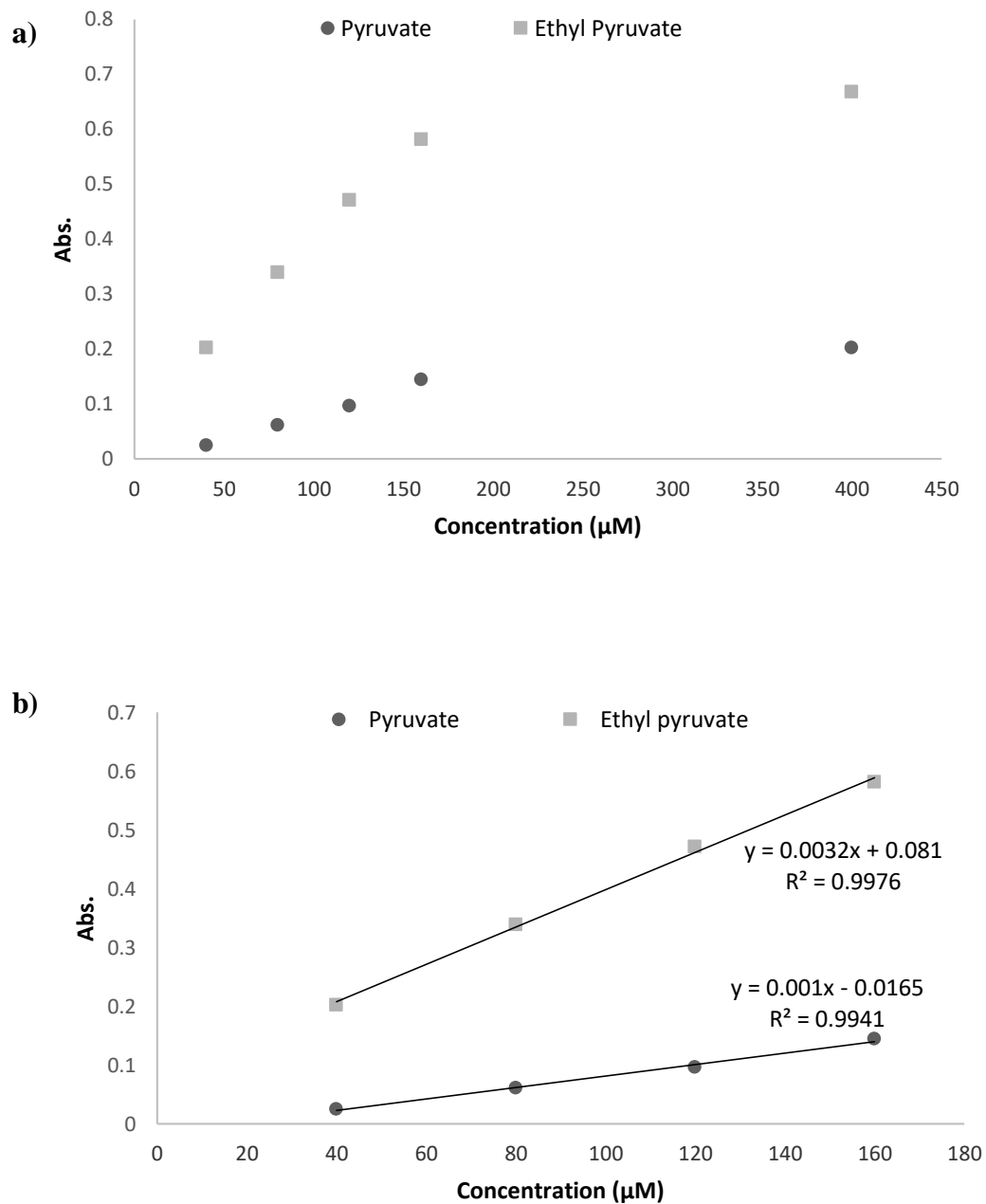


Figure 3.1 Calibration curve of Ethyl pyruvate and pyruvate using the Pyruvate assay. Pyruvate standards and ethyl pyruvate standards in the range of 40-400 μM were prepared and used to plot the calibration curve. **a)** Calibration curve of pyruvate and ethyl pyruvate; **b)** Calibration curve of pyruvate and ethyl pyruvate excluding the highest concentration value. All standards were run in duplicate and the data presented represent the mean of these measurements.

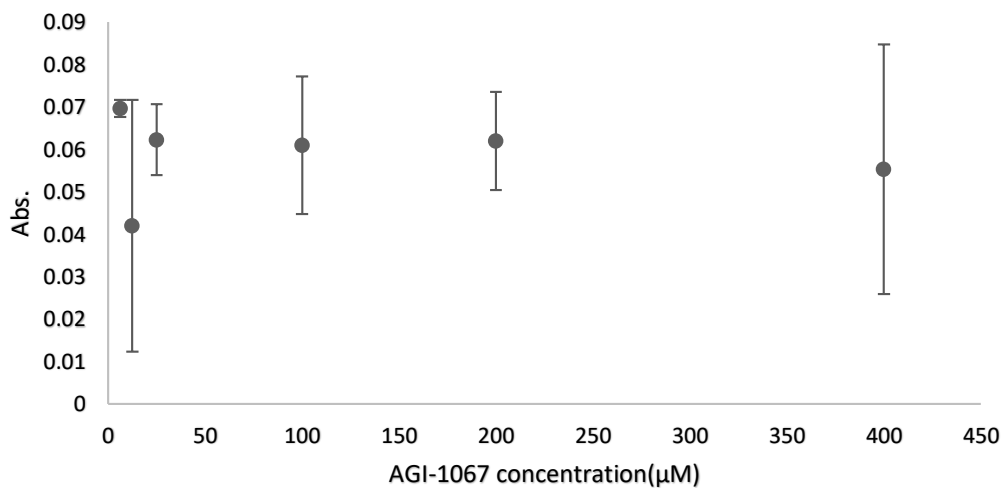
The assay successfully detected EP in PBS, although the range of EP concentrations that can be measured is very limited. In fact, from the calibration curve shown in Figure 3.1-a it is clear that the EP concentration of 400 μ M is close to saturation. This result suggests that this method of EP detection is not ideal for EP concentration higher than 160 μ M. For this reason, other methods of EP detection were investigated.

3.3.2 DPPH antioxidant assay

The DPPH assay has been widely used to measure the antioxidant activity of a particular agent (Garcia, *et al.*, 2012). In this section, this assay was used to measure EP indirectly, by measuring the antioxidant effect of EP on DPPH. The reduction of DPPH by EP causes a change in colour that can be measured by a spectrophotometer at 517 nm after 100 minutes of incubation (Garcia, *et al.*, 2012). AGI-1067, a known anti-inflammatory drug used to treat atherosclerosis with well-defined anti-oxidant activity (Crim, *et al.*, 2010), was used as a positive control. The methodology used in this section is explained in more detail in section 2.4.2.2.

The calibration curve obtained with this assay is essentially the quantification of the DPPH scavenged by EP. An increase in EP concentration is expected to correspond to a lower DPPH absorbance. Graphically, this reduction in DPPH will be expressed as a descending curve. The range of AGI-1067 concentrations examined was 6 μ M - 400 μ M), while for EP a wider concentration range of (6 μ M - 12.8 mM) was used, due to the fact that the antioxidant ability of EP to scavenge DPPH was unknown. The AGI-1067 calibration curve obtained with this assay is shown in Figure 3.2-a, while EP calibration curve is shown in Figure 3.2-b.

a)



b)

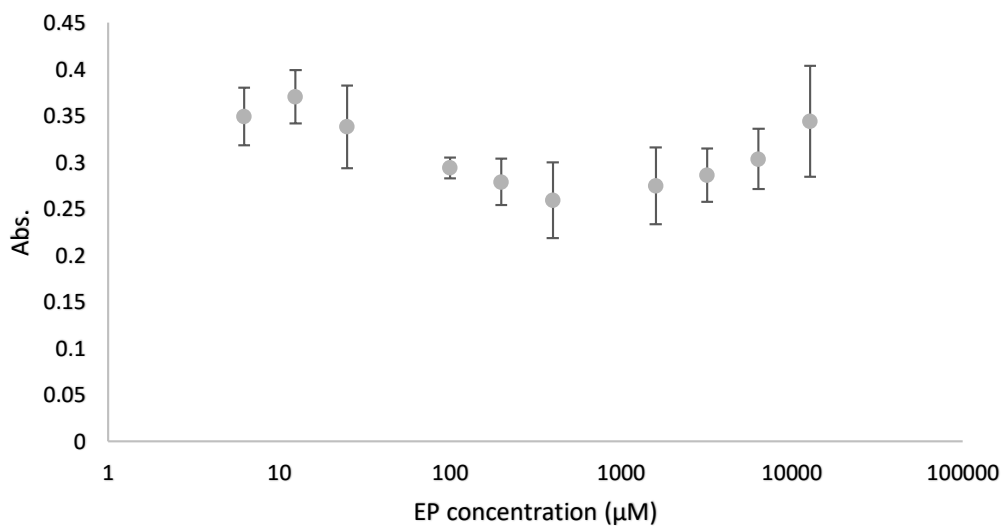
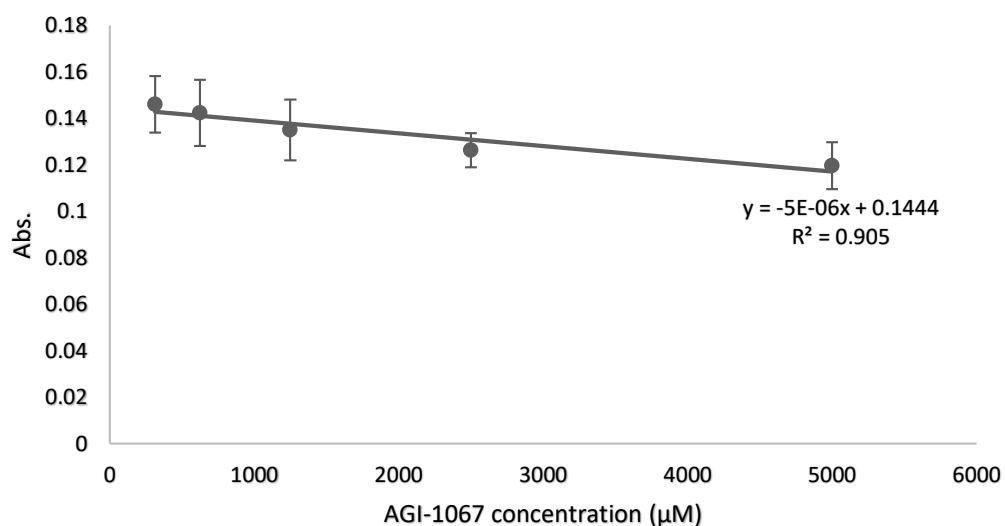


Figure 3.2 Calibration curve of a) AGI-1067 and b) Ethyl pyruvate using the DPPH assay. AGI-1067 and ethyl pyruvate were determined by measuring their ability to scavenge DPPH. AGI-1067, was used as a positive control and DPPH without antioxidants as a negative control. The absorbance values correspond to the reduction in DPPH in presence of one of the antioxidants. Standards were prepared in PBS in the range of 6 - 400 µM for AGI-1067, 6 µM - 12.8 mM for EP. All standards were run in triplicates, with the data presented representing the mean of these samples \pm Stdev

AGI-1067 was not effective at scavenging DPPH in the range of 25-400 μM , as shown in the calibration curve (Figure 3.2-a). The curve shows no relationship between AGI-1067 concentration and reduction in DPPH.

The EP calibration curve obtained in this study presents a descending trend line in the first part and then it changes direction, ascending in the second part (Figure 3.2-b). In particular, the first part of the curve shows that DPPH decreases proportionally with the increase in EP concentration in the range of 12-400 μM . Surprisingly, at higher EP concentrations (1.6-12.8 mM) EP gradually lost its effect on DPPH, showing an increase in DPPH when EP concentration increased (Figure 3.2-b). The EP calibration curve obtained which descends and then changes direction is unsuitable for use as a calibration curve. A wider concentration range (6.4 - 100 mM) was subsequently examined as a repeat experiment, in order to understand if this loss of antioxidant effect by EP is continued at higher concentrations. A calibration curve was created and it is shown in Figure 3.3-b. AGI-1067 was also tested at a higher concentration range (0.3 – 5mM) and a calibration curve was created, as shown in Figure 3.3-a. This time, at higher concentrations, both AGI-1067 and EP calibration curves showed a linear relationship between the individual antioxidant and the reduction in DPPH (Figure 3.3-a, -b). Although the results obtained showed the ability of EP to scavenge DPPH, this assay did not demonstrate a sensitivity that was expected and with the discrepancy between Figure 3.2 and Figure 3.3 there is sufficient uncertainty to demand that alternative methods of EP detection should be explored. For this reason, another antioxidant assay was assessed for EP measurement, as discussed in the next section.

a)



b)

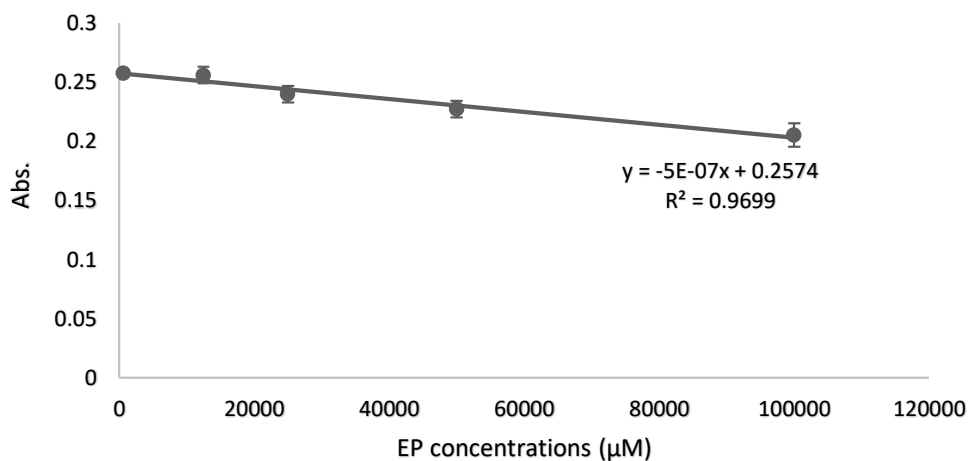


Figure 3.3 Calibration curve of **a)** AGI-1067 and **b)** Ethyl pyruvate using the DPPH assay. Ethyl pyruvate was determined by measuring their ability to scavenge DPPH. In presence of an antioxidant agent DPPH is reduced and the colour changes from violet to colourless (Garcia, *et al.*, 2012). The change in colour was measured by a spectrophotometer plate reader at 517 nm after 100 minutes of incubation. The standards were prepared in PBS in the range of 25-6,400 μM and used to plot the calibration curve. All standards were run in triplicate.

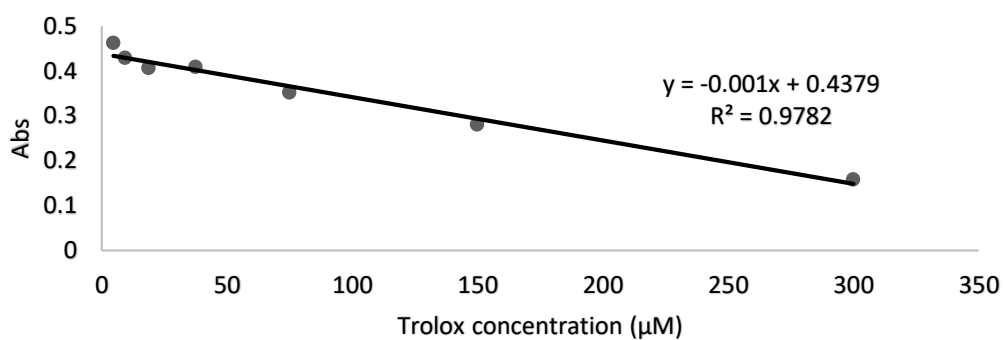
3.3.3 ABTS antioxidant assay

The ABTS assay has been widely used to measure the antioxidant activity of a variety of different substances (Dong, *et al.*, 2015). In the presence of hydrogen peroxide and myoglobin, a ferril myoglobin radical is produced. Graphically, this reduction in $ABTS^+$ will be expressed as a descending curve. Therefore, the concentration of EP is indirectly proportional to the radical produced.

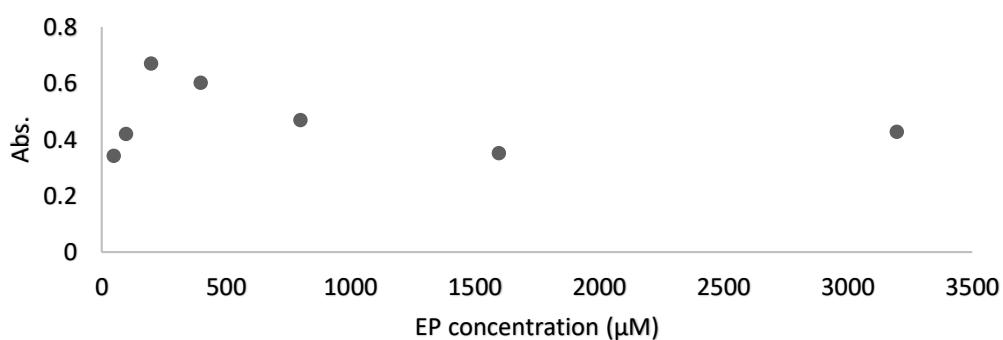
Trolox standards (4.6-300 μ M) were used as a positive control. The methodology used has been explained in detail in section 2.4.2.3. Briefly, EP standards were prepared fresh in PBS in the range of (0.05 – 3.2 mM). In the assay previously used, EP showed an increase and then a decrease in antioxidant activity (see Figure 3.2-b) in the range of 0.2- 1.6 mM. In order to investigate if EP shows the same loss in antioxidant activity with the ABTS assay, the EP concentrations were chosen to be close to this range.

The Trolox calibration curve obtained with this assay is shown in Figure 3.4-a, while the EP calibration curve is shown in Figure 3.4-b.

a)



b)



c)

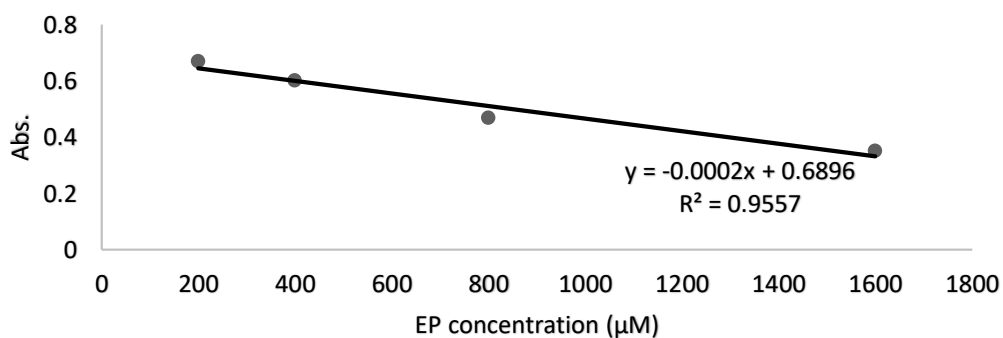


Figure 3.4 Calibration curve of **a)** Trolox and **b)** Ethyl pyruvate using the ABTS assay. ABTS can be oxidised, producing a green colour and the absorbance can be measured at 405 nm with a colorimeter. Trolox is an antioxidant and it was used as a positive control. EP standards were prepared in PBS in the range of 0.5-3.2 mM and used to plot the calibration curve. **c)** EP calibration curve narrowing the concentration range of the graph in **b)** to 200-1,600 μM. All standards were run in duplicate and the data presented represent the mean of these measurements.

The Trolox calibration curve showed a linear relationship between the antioxidant and the reduction in radical cation ABTS⁺ formation (Figure 3.4-a).

The EP calibration curve obtained in this study presents an ascending trend line in the first part and then it changes direction, descending in the second part (Figure 3.4-b). In particular, the first part of the curve in the range of 50-200 μM , EP showed a decrease in antioxidant effect, with the concentration (50 μM) of EP having the same antioxidant effect as the 1.6 mM concentration, suggesting either that they are having the same level of inhibition or the assay is not sensitive to detect differences. At higher EP concentrations (200-1,600 μM) EP gradually increased its antioxidant effect, showing a decrease in the radical cation ABTS⁺ absorbance directly proportional to the increase in EP concentration (Figure 3.4-b). Surprisingly, EP antioxidant activity dropped at the highest concentration of 3.2 mM.

The EP calibration curve shown in figure 3.4-c was extrapolated from the calibration curve in figure 3.4-b. This curve was prepared by using the absorbance values of the EP standards used to prepared the calibration curve in Figure 3.4-b, but in this case only the values of the EP standards in the range of 0.2-1.6 mM were presented.

Although the results obtained show the potential ability of EP to reduce the radical cation ABTS⁺ formation, the relationship between EP concentration and ABTS radical formation is unclear. The uncertainty in the relationship between EP and ABST shown in these results suggests that the ABTS assay, like the DPPH assay discussed before, is not a suitable method to measure EP in solution. For this reason, a different approach was taken in the following section.

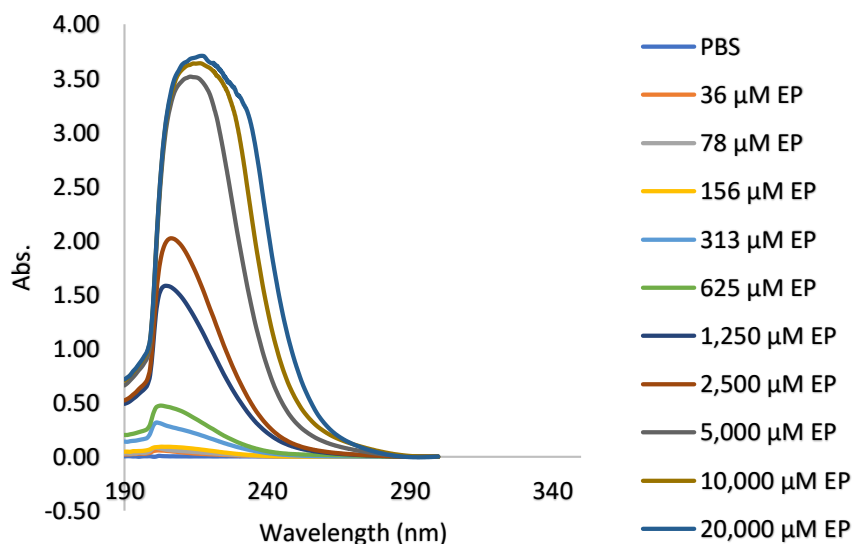
3.4 Measurement of EP using UV spectroscopy

3.4.1 UV/Vis spectrophotometer

Ultraviolet/visible-spectrophotometry is a widely used analytical technique to quantitatively measure a compound in a solution. The complete methodology used in this section is described in detail in section 2.4.1.1. A set of EP standards in PBS were prepared within a broad range of concentrations, 40 – 20,000 μM , and a standard calibration curve generated. PBS was used as a blank control. UV/Vis

spectrophotometric measurement of EP in PBS in the spectra from 190 to 300 nm is shown in Figure 3.5-a. A calibration curve was subsequently obtained by plotting the Absorbance value at the peak against the concentration for each EP standard (Figure 3.5-b).

a)



b)

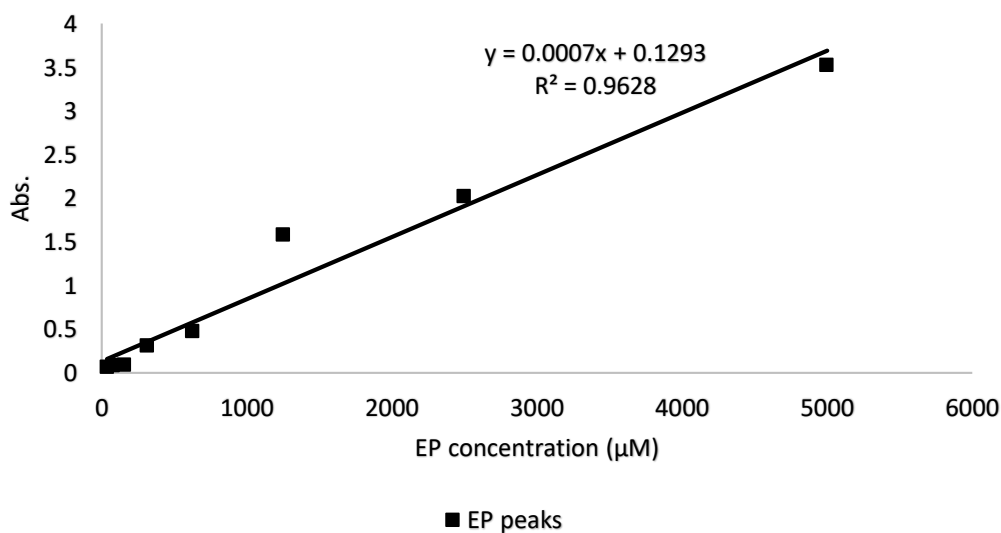


Figure 3.5 UV/Vis spectrophotometric measurement of ethyl pyruvate in PBS. **a)** Ethyl pyruvate absorption spectra (190 -300 nm). EP standards were prepared in PBS in the range of 40-20,000 μM and PBS was used as a blank. **b)** EP calibration curve obtained by plotting the value of the peaks against the concentration for each EP standard. EP calibration curves were prepared by narrowing the concentration range of the graph in a) to 40-5,000 μM , due to saturation at higher concentration. Note that this is preliminary data and that more validation is required.

The EP absorption spectra (190 -300 nm) shows the peaks of EP absorbance in the range of 203-213 nm (Figure 3.5-a). The peak values increase proportionally with the increase in EP, in the EP concentration range of 40-5,000 μM . At concentrations higher than 5,000 μM the peaks are close to the same value, which is an indication of saturation (Figure 3.5-b). The linear relationship between EP concentration and absorbance is shown in the calibration curve shown in Figure 3.6-b. At high EP concentrations (5-20 mM) the reading of the absorbance is shifted, as shown in Figure 3.6-a. The results demonstrated that if the EP samples are in that range of 5- 20 mM, dilution should be performed before the measurement of EP. Ultimately, dilution of samples is an additional step that can introduce errors in the measurement, and for this reason an alternative UV-spectrophotometer was investigated to determine if the effective concentration range could be extended.

3.4.2 Nano-spectrometer

A Nanospectrometer was used to measure EP in PBS. The methodology used is discussed in the section 2.5.1.2. Briefly, a broad range of EP standards (78 μM -20 mM) were prepared in PBS. The concentration range was chosen in order to investigate the detection limits of the device. 2 μL of standard was pipetted onto the sample holder and the absorbance of the spectrum was measured. PBS was used as a blank and the standards were measured across a wavelength range from 198 to 300 nm. The obtained spectra showed a peak in the range of 198-200 nm. For this reason, the following measurements were made at the peak wavelength of 198 nm. The absorbance at 300nm was also recorded as a baseline. The absorbance values obtained were normalised by subtracting the the baseline absorbance at 300nm from the absorbance at 198 nm. The calibration curve produced with the final values is shown in Figure 3.6.

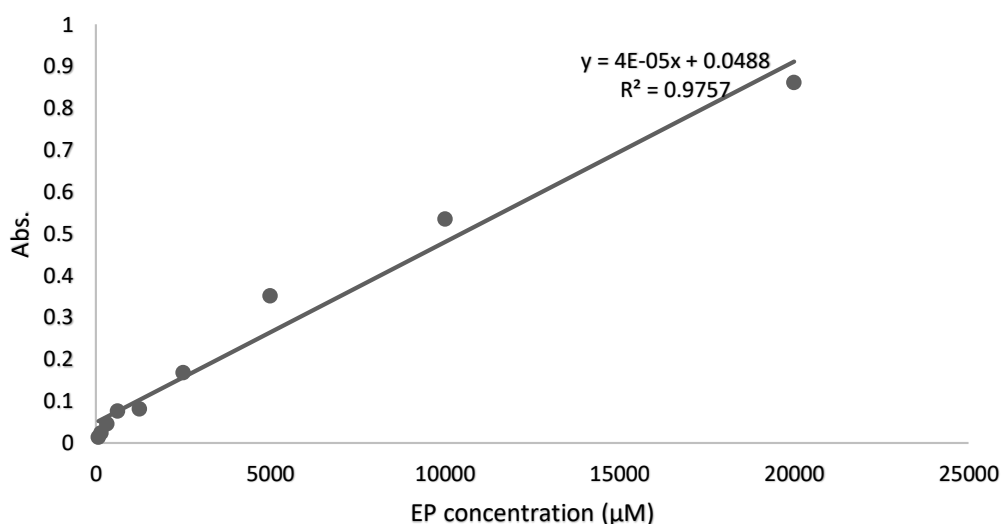


Figure 3.6 Calibration curve of Ethyl pyruvate using the Nanospec. Calibration curve of Ethyl pyruvate prepared with the absorbance values measured at the wavelength of 198 nm. EP standards were prepared in PBS in the range of 78-20,000 µM and used to plot the calibration curve. PBS was used as a blank and the standards were measured at two wavelengths, the peak wavelength at 198 nm and the zero wavelength at 300 nm. The values obtained were normalised by subtracting the zero absorbance from the absorbance at 198 nm before plotting the calibration curve.

With the Nanospec it was possible to obtain an EP calibration curve in the range of 78 µM -20 mM EP concentration. The maximum peak of absorption was registered at 198 nm, very close to the wavelength range where the peaks were obtained with the UV/Vis spectrophotometer in section 3.3.1.

3.4.3 HPLC

HPLC was used to additionally confirm the validity of the method to measure EP obtained with UV spectroscopy and Nano-spectroscopy. The methodology used in this section is described in detail in section 2.4.1.3. Briefly, HPLC was used to measure EP standards in the range of 70 – 50,000 µM, produced respectively in either methanol or PBS. The flow rate used was 0.3 mL/min for 10 minutes. The absorbance was measured at different wavelengths (203, 205, 210, 300 nm). The wavelengths were chosen in the range previously used to detect EP with the UV/Vis spec in section 3.3.1.

A representative sample of the HPLC readings of the EP standards in PBS obtained are showed in Figure 3.7. The results obtained at 203 and 205 nm demonstrated similar

results to each other. The standards prepared in PBS showed several peaks and it was not clear which one corresponded to EP (Figure 3.7). For this reason, it was not possible to prepare a calibration curve for these samples.

In figure 3.8, a representative sample of the HPLC readings of the EP standards in methanol is shown. In this case, EP in methanol demonstrated a clear peak at 5.4 minutes (Figure 3.8) at the wavelength of 205 nm. This result confirmed the EP absorbance measured with the UV/Vis spectrophotometer and the Nanospec in section 3.4.1 and 3.4.2 respectively, with the EP peaks detected in the same range of wavelengths. The size of the peak increased with the increase in EP concentration (Figure 3.8).

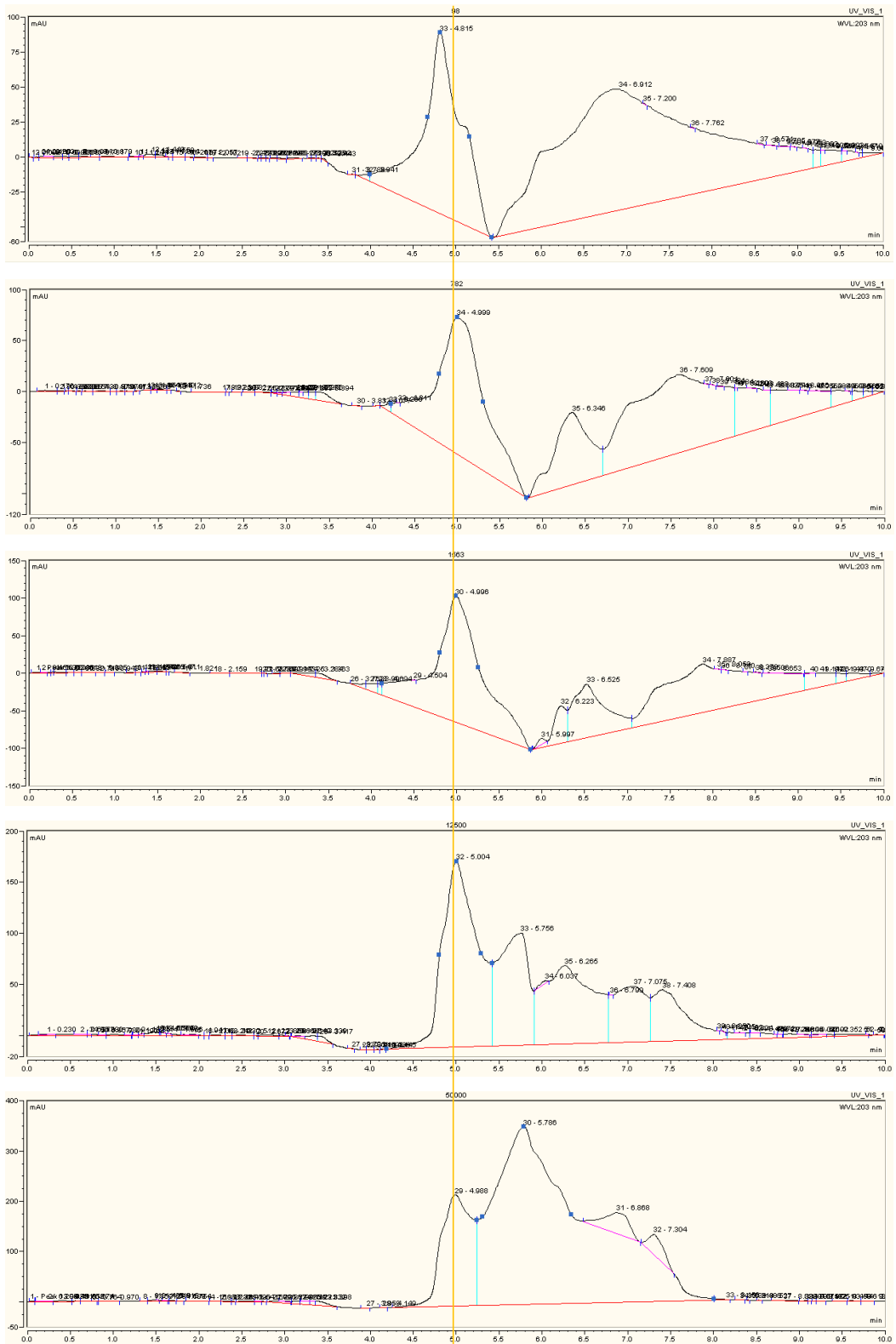


Figure 3.7 HPLC graphs of EP measurement in PBS at different EP concentrations. Milli absorbance unit (mAU) versus retention time. HPLC was used to measure EP standards in the range of 70 – 50,000 μM in PBS, although here are shown the graphs of some of the standards measured (from top to bottom, 98, 782, 1563, 12,500 and 50,000 μM EP). The flow rate used was 0.3mL/min for 10 minutes. The absorbance was measured at the wavelength of 203 nm.

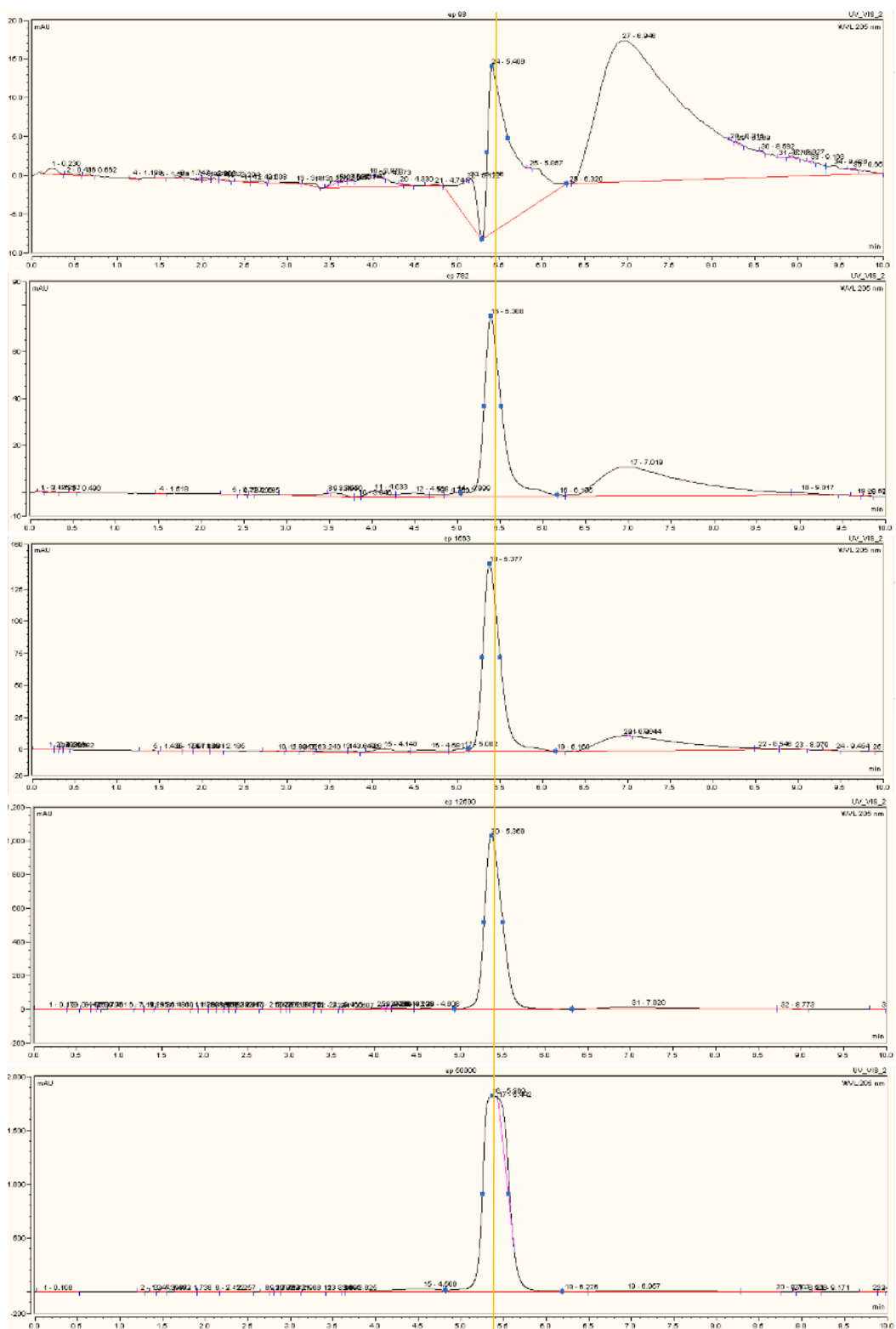
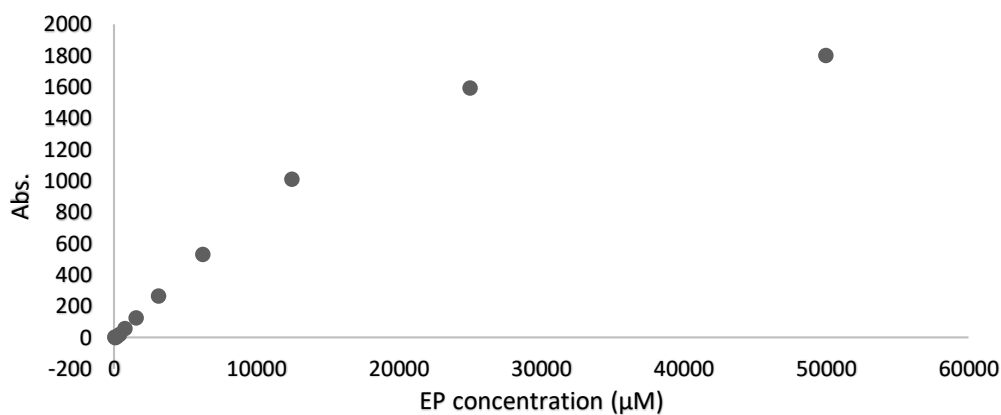


Figure 3.8 HPLC graphs of ethyl pyruvate measurement in methanol at different EP concentrations. Milli absorbance unit (mAU) versus retention time. HPLC was used to measure EP standards in the range of 70 – 50,000 μM in methanol, although here are shown the graphs of some of the standards measured (from top to bottom, 98, 782, 1563, 12,500 and 50,000 μM EP). The flow rate used was 0.3mL/min for 10 minutes. The absorbance was measured at the wavelength of 205 nm.

A calibration curve (Figure 3.9-a) was obtained by plotting the value of the peaks measured against the concentration for each EP standard in methanol (Figure 3.9). It can be seen that the curve is linear in the range of 70-12,500 μM , while it shows saturation at higher concentrations (25-50 mM). For that reason, another calibration curve was plotted from the same HPLC readings, but in this case EP calibration curve was prepared by narrowing the concentration range of the graph to 70-12,500 μM .

a)



b)

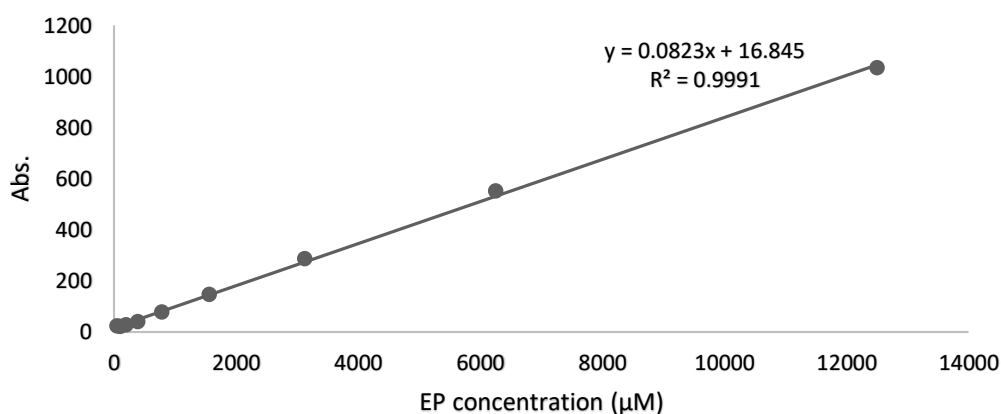


Figure 3.9 Calibration curve of ethyl pyruvate in methanol (HPLC). HPLC was used to measure EP standards in the range of 70 – 50,000 μM in methanol. The absorbance was measured at the wavelength of 205 nm. a) EP calibration curve obtained by plotting the value of the peaks against the concentration for each EP standard in the range of 70 – 50,000 μM in methanol. b) EP calibration curve prepared by narrowing the concentration range of the graph in a) to 70-12,500 μM , due to saturation at higher concentration. Note that this is preliminary data and that more validation is required.

In order to have an additional confirmation that the peak obtained with the HPLC at the absorbance of 205 nm corresponded to EP, a set of EP standards in methanol were prepared and analysed with the UV-spec, using the methodology discussed in section 3.4.1. The calibration curve obtained with the measurement of EP from the standards is shown in Figure 3.10. The results confirm the absorbance of EP in methanol previously obtained with the HPLC at the 205 nm wavelength.

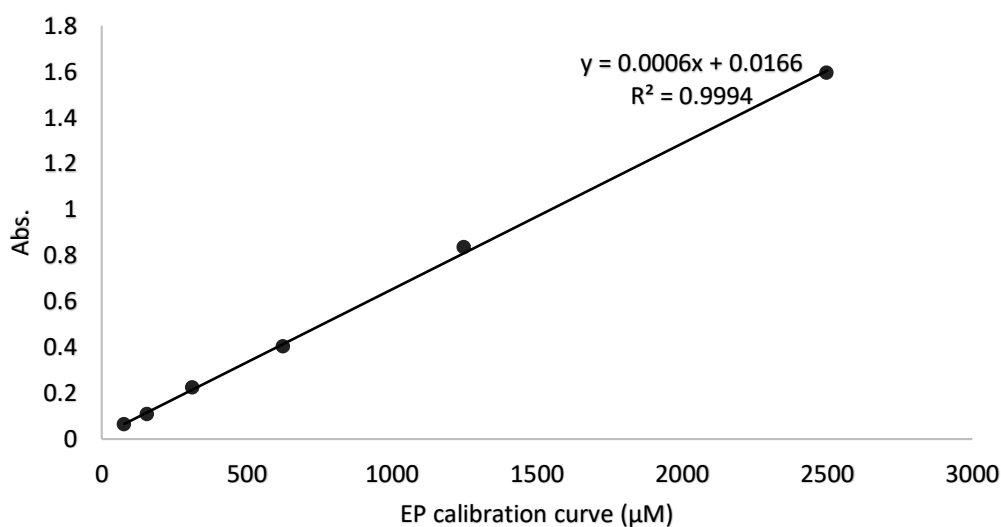


Figure 3.10 Calibration curve of ethyl pyruvate in methanol (UV/Vis spec). UV/Vis spec was used to measure EP standards in the range of 78 – 2,500 µM in PBS. The absorbance was measured at the wavelength of 205 nm. Data represent the mean \pm st dev of three consecutive measurements.

3.5 EP stability *in vitro*

3.5.1 Introduction

EP has been preferred to sodium pyruvate because of its enhanced stability in solution (Flink, 2007), as discussed in section 1.5. However, the stability of EP in a physiological solution at body temperature does not appear to have been previously reported. The overall aim of this study was to create a vehicle that is capable of delivering EP over a period of weeks at 37°C. For this reason, it was therefore important to investigate if the UV-spectra for EP remains stable at this temperature. During the release studies the release samples will be stored at -20°C for analysis, so it was also important to investigate if freezing/ thawing has an effect on the EP spectra.

3.5.2 Methodology

The methodology used in this aspect of the study is described in section 2.4.3. Briefly, a set of EP standards in PBS were prepared in the concentration range of 0.078 to 2.5 mM. The standards were then split into 2 batches which were then stored at 2 different temperatures. One batch of standards were stored at -20°C , while the other one was stored in the incubator at 37°C . The absorbance was measured at different time points, at 1, 3, 7 and 14 days. The absorbance of the standards was measured with two different spectrophotometers, the UV-spec and the Nanospec as explained in section 3.3.1 and 3.3.2 respectively.

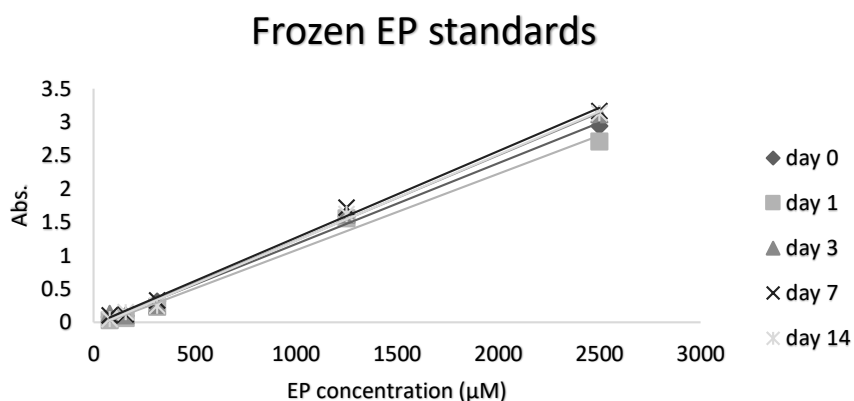
At each time point the frozen standards were thawed, measured and frozen again. All the standards were placed at room temperature for 2 hours before use in order to reach the same temperature, avoiding any possible interactions that temperature could have on the absorbance measurement. The standards were measured by spectrophotometry and the absorbance values were used to plot a calibration curve.

In order to investigate if the freezing/ thawing of the reference standards affected EP, a comparison was made between the calibration curves obtained by analysing the thawed EP at each time point and freshly made EP standards.

3.5.3 Results

The effects of freezing/ thawing on EP standards are shown in Figure 3.11-a. The curves obtained from the thawed standards show a similar linear trend-line. EP stability in PBS at 37°C was also measured with the UV/Vis spec. The results of these measurements are shown in Figure 3.11-b. EP standards stored at -20°C were used as a reference for each time point. The curves obtained by the standards stored at 37°C for a period of 2 weeks did not show any obvious signs of degradation. In fact, the curves look very similar to the reference curve (Figure 3.11-b).

a)



b)

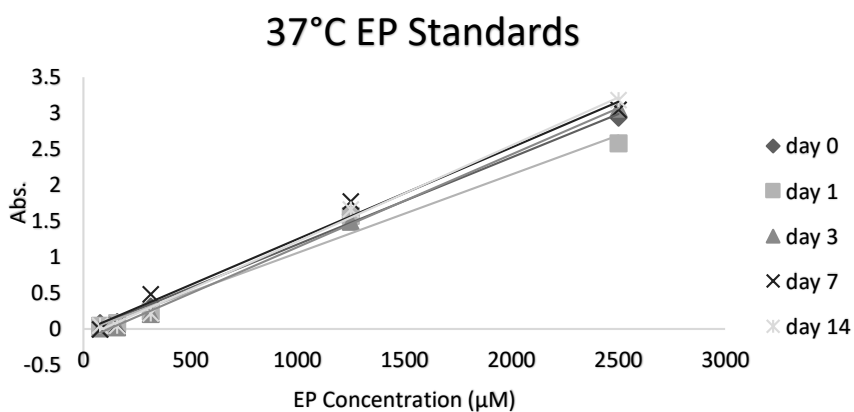
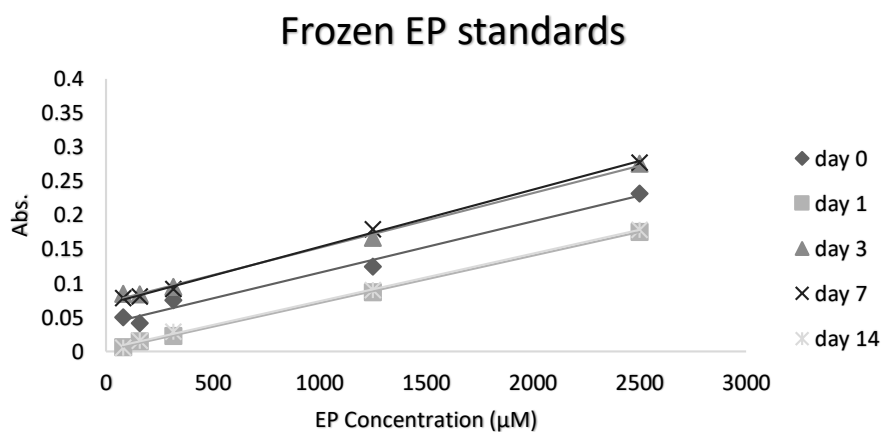


Figure 3.11 Stability study of ethyl pyruvate in PBS a) after freezing/thawing; b) at 37°C over time (UV/Vis spec). EP standards in PBS were prepared in the concentration range of 0.078 to 2.5 mM. The standards were then split into 2 batches which were then stored at 2 different temperatures. The reference standards were stored at -20°C, while the others were stored in the incubator at 37°C. The absorbance was measured with the UV/Vis spec at 205nm at different time points, at 1, 3, 7 and 14 days. Day 0 curve is the reference curve. Note that this is preliminary data and that more validation is required.

In order to confirm the results obtained with the UV/Vis spec, the same samples were then measured with the Nanospec. The effects of freezing/ thawing on EP standards were measured with the Nanospec and the results are shown in Figure 3.12-a. The measurement of the EP stability in PBS at 37°C measured with the Nanospec, is shown in Figure 3.12-b.

a)



b)

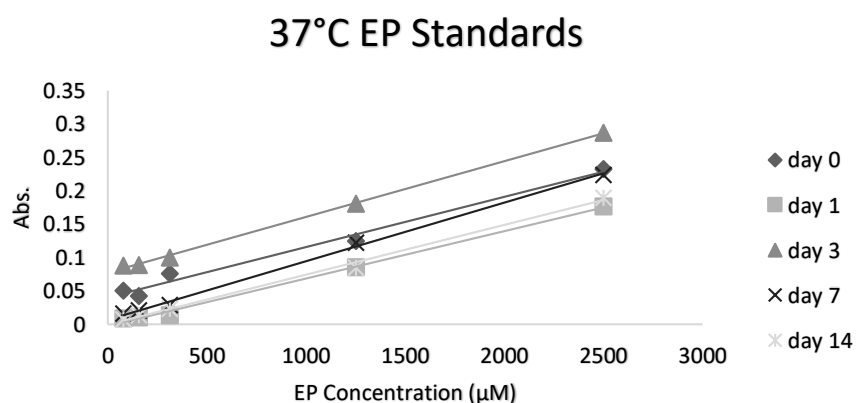


Figure 3.12 Stability study of ethyl pyruvate in PBS **a)** after freezing/thawing; **b)** at 37°C over time (Nanospec). EP standards in PBS were prepared in the concentration range of 0.078-2.5 mM. The standards were then split into 2 batches which were then stored at 2 different temperatures. The reference standards were stored at -20°C, while the others were stored in the incubator at 37°C. The absorbance was measured with the Nanospec at 198 nm and the wavelengths 300 was used as the zero point. The measurement was performed at different time points, at 1, 3, 7 and 14 days. Note that this is preliminary data and that more validation is required.

The calibration curves obtained show a shift in the standards values for each time point in both freeze/thawing standards (Figure 3.12-a) and 37°C standards (Figure 3.12-b). This suggests that the shift may not be related to the EP degradation but to the measurement variability of the instrument.

3.6 Discussion

3.6.1 Introduction

EP has been recently studied for its potential therapeutic effects in several studies as discussed in section 1.5. Although a clinical trial has shown that EP is safe to use in patients, EP did not significantly reduce the incidence of the post-operative adverse outcomes and it failed to decrease the systemic inflammatory markers in patients treated with EP (Bennett-Guerrero, *et al.*, 2009). The authors suggested that possibly the length of the treatment and the dose administered to the patients were not adequate to reduce the inflammation (Bennett-Guerrero, *et al.*, 2009).

In order to be able to fully explore the relationship between drug dose and efficacy over time *in vitro*, it is important that there are robust methods in place to allow measurement of EP. Therefore, there was a need to identify an alternative method that would not only be suitable for the current project, but which could be adopted more widely by other research groups active in this area.

Stability of EP in physiological solution is crucial if EP is to be delivered into the body and remain effective over time. For that reason, in this section EP stability in physiological solution at body temperature was investigated over 2 weeks. This timescale was selected because it is relevant to the EP release studies that will be described in subsequent chapters. In such drug release experiments, the samples are usually frozen and then thawed for measurement, for this reason, the stability of EP in physiological solution when frozen/ thawed was also investigated.

3.6.2 EP measurement *in vitro*

EP was measured using 6 different approaches in total. Due to a lack of previous literature on EP detection with these methods, a prior comparison is difficult to achieve. Pyruvate assay was the first assay used to determine the amount of EP in solution. Although the assay successfully detected EP in PBS (see Figure 3.1-b), the range of EP concentrations that can be measured was very limited. In fact, from the calibration curve shown in Figure 3.1-a, it is clear that the EP concentration of 400 μM

is close to saturation. This result suggests that this method of EP detection is not ideal for EP concentration higher than 160 μM . For this reason, other methods of EP detection were investigated.

EP is well known for its antioxidant effects, so it may be possible to measure it indirectly through the use of antioxidant assays, although this has not previously been investigated. In this way, the measurement of the antioxidant effect of EP can be translated into an amount of EP present within the samples tested. Based on this principle, two antioxidant assays, specifically the DPPH assay and the ABTS assay, were used to measure indirectly the amount of EP, by measuring its antioxidant effect. The DPPH assay is a widely used method to measure the antioxidant activity of a specific compound (Garcia, *et al.*, 2012), but it has never been used with EP. The EP calibration curve obtained in this study (Figure 3.2-b) starts with a negative relationship before turning into a positive relationship, which suggests that this assay is not sensitive to changes in the standard concentration. On the other hand, when the experiment was repeated at higher EP concentrations (6.4 - 100 mM), a linear response was obtained (Figure 3.3-c). The results further confirm this lack of a consistent relationship across the concentration range examined, demonstrating the unsuitability of the method to measure EP.

The antioxidant ABTS assay was then investigated as an alternative to the DPPH assay for the indirect measurement of EP. In the study conducted by Olek *et al.*, 2001, ABTS assay was used to measure the antioxidant activity of EP under *in vitro* conditions by using a model of cell membrane transport deletion (Olek, *et al.*, 2011). The study of Olek *et al.*, 2011 was limited to the measurement of the anti-oxidant activity of EP, while in this study EP antioxidant effect was used to measure indirectly the quantity of EP present in solution. The calibration curves obtained with this method are shown in Figure 3.4. The EP calibration curve shown in Figure 3.4-b starts with a positive relationship before turning into a negative relationship and then changes again at the highest concentration. This suggests that this assay is not sensitive to changes in the standard concentration. In Figure 3.4-c there is a linear part of the trendline of Figure 3.4-b, in the EP range of 0.2-1.6 mM. Although the results obtained indicated that EP may be able to reduce the radical cation ABTS^+ formation, the relationship between

EP concentration and ABTS radical formation was not constant. This suggests that the ABTS assay, like the DPPH assay discussed before, is not the ideal method to measure EP in solution. For this reason, a different approach was taken in the following section.

Given that none of the assays described above appeared to be suitable for EP measurement, it was decided to investigate UV spectroscopy-based methods. To our knowledge, such methods have not been used to measure EP, so no information on the most appropriate wavelength to select for EP detection was available in the literature. For this reason, UV spectroscopy was performed over a relatively wide wavelength to identify characteristic peaks. EP standards in PBS were prepared and then measured with a UV/Vis spec in the spectra range of 190-300 nm (see section 3.3.1). The UV spec detected a peak in the range of 203-213 nm, which increased in height with the increase of EP concentration as shown in Figure 3.5-a. At higher EP concentration of 5-20 mM, the peaks have the same height, which is an indication of saturation (Figure 3.5-b). The calibration curve obtained shows clearly a linear relationship between the absorbance and EP concentration in the range of 0.078-2.5 mM (Figure 3.5-b). The results demonstrate that if the EP samples are in the range of 5- 20 mM, dilution would have to be carried out before the measurement of EP in order to ensure that saturation of the absorbance reading did not occur. However, such dilution of the samples can introduce further errors into the measurement, and this therefore represents a potentially important limitation of this method. Another possible limitation of this method of measurement is the minimum volume needed (0.5ml) to run the test, which can be a limit if smaller volumes are used in the experiments.

Nanospectroscopy involves the application of UV spectroscopy with nanometric resolution (Ostertag, *et al.*, 2014). With the Nanospec device, it was possible to obtain a usable EP calibration curve over a concentration range of 78-20,000 μM , (Figure 3.6). The maximum peak of absorption was registered at 198 nm, very close to the wavelength at which the peak value was observed with conventional UV-spectroscopy (section 1.3.1). The use of the Nanospec introduced several advantages compared to the UV spec. Firstly, at higher concentrations of EP (above 2.5 mM) there was no saturation, which eliminates the need to dilute the samples or to apply corrections to the values obtained. Secondly, the volume of the standard necessary for the

measurement is as little as 2 μL with the Nanospec, compared to a minimum of 500 μl with the standard UV-spec. This introduces an important advantage when the samples obtained have a small volume, or if the measurement of the same sample needs to be repeated. Finally, an important advantage is that the Nanospec does not need the samples to be transferred into cuvettes ahead of measurement scans being performed. The use of such cuvettes can introduce errors in the measurement, including artefacts in readings due to the presence of particulate matter on the vessels walls. Similarly, the expense of Quartz cuvettes meant that they needed to be washed out thoroughly between each sample, so any failure in this process has the potential to contaminate subsequent samples. Ultimately, the Nanospec was demonstrated to be a simple, inexpensive and reliable method to measure EP in physiological solution, ideal for the measurement of small volumes.

HPLC was used to additionally confirm the validity of the method to measure EP obtained with UV spectroscopy and Nano-spectroscopy. HPLC was part of the complex method that had been previously used to measure EP in rat plasma in the study conducted by Kim *et al*, 2011 (Kim, *et al.*, 2011). The mobile phase used by Kim *et al* (30% methanol, 10% acetonitrile, 60% water) was used to perform the measurement. The rest of the methodology differed from Kim *et al*, such as the EP standards, which were prepared in PBS and methanol in this study, while in Kim *et al* they were prepared in acetonitrile and blank rat plasma. Although this method failed to detect EP in PBS (Figure 3.7), the measurement of EP was successfully demonstrated in standards prepared in methanol (Figure 3.8). In this case EP in methanol showed a clear peak after an elution time of 5.4 minutes (Figure 3.8) at a wavelength of 205 nm. This result gives confidence in the EP absorbance data measured with the UV spec, with peaks detected at the same wavelength. With the height of the peaks registered with the HPLC, it was possible to create a linear EP calibration curve (Figure 3.9). An additional confirmation that the peak obtained with the HPLC at the absorbance of 205 nm corresponded to EP, was given by the measurement of EP standards in methanol with the UV spec (Figure 3.10), which showed the same trend.

3.6.3 EP stability study

The enhanced stability of EP in comparison to standard pyruvate means that it has been the preferred drug in a number of investigations (Flink, 2007). Stability of EP in physiological solution at body temperature is crucial if EP is to be delivered into the body over time, as is the case for the intended application within the present study. For that reason, in this section EP stability in physiological solution at body temperature was investigated over 2 weeks. The period of time of 2 weeks was used as a standard time used to evaluate the stability of the drug *in-vitro*. During the release studies the release samples will be stored at -20°C for analysis, so it was also important to investigate if freezing/ thawing has an effect on EP.

The effects of freezing/ thawing on EP standards were measured with the UV/Vis spectrophotometer and the results are shown in Figure 3.11-a. EP standards were measured when fresh, before being frozen and the curve obtained was used as a reference curve. The absorbance was measured at different time points, at 1, 3, 7 and 14 days. In case of degradation, the calibration curve would differ from the reference calibration curve. The curves in Figure 3.11-a showed no difference between the calibration curves. This suggests that EP is stable in physiological solution even when it is frozen and thawed several times. This is valuable information for the future experiments.

EP stability in PBS at 37°C was also measured with the UV/Vis spec. EP standards were stored in the incubator at 37 °C, to simulate the body temperature. The results of these measurements are shown in Figure 3.11-b. Because it was demonstrated that freezing/thawing does not affect EP, the EP standards stored at -20°C were used as a reference curve for each time point. The curves obtained by the standards stored at 37°C for a period of 2 weeks did not show any important signs of degradation. In fact, the curves look very similar to the reference curve (Figure 3.11-b). The EP stability was also measured with the Nanospec, and the results are shown in Figure 3.11-Figure 3.12. The calibration curves obtained show a shift in the standards values for each time point in both freeze/thawing standards (Figure 3.12-a) and 37°C standards (Figure 3.12-b). Although the curves are shifted in the graphs (Figure 3.12- a, -b), the

calibration curves still show a linear relationship between the EP concentration and the absorbance. This suggests that the shift is not related to the EP degradation, but possibly to the measurement variability due to the instrument. Irrespective, these results demonstrate the importance of performing a calibration step prior to sample analysis.

From the results obtained, EP in physiological solution did not show any sign of degradation either when it was frozen/thawed or when it was stored at 37°C for 2 weeks. This is an important result because it not only it confirms the stability of the EP in solution discussed in literature (Yang, *et al.*, 2016), but it provides a firm basis for the future release studies of EP *in vitro* that are detailed later.

3.7 Limitations

The use of UV traces to investigate the EP stability has some limitations. The degradation products of EP might be not detected with a UV spec. HPLC does not have this limitation, but it was not suitable for EP measurement because it cannot be used to analyse EP in PBS. In this preliminary study the stability of EP in PBS was investigated, but the stability may be different in plasma, blood, and cell culture media. EP stability at different temperatures was investigated over a period of 2 weeks and not further. Although this represents a limitation of this study, the results provide an indication of the potential EP stability in PBS at body temperature.

Despite the limitations, the results obtained in this chapter make an important contribution to ongoing research efforts within this field, and are particularly valuable in the context of the present study, since they provide the confidence in the analytical methods adopted in subsequent chapters.

3.8 Future work

In this study it was demonstrated that EP UV traces remain consistent at body temperature over a period of 2 weeks. This finding will be used as a strong starting point to the preparation of alginate gels for the sustained delivery of EP over time. In

this study, spectrophotometry was successfully used to detect EP in solution. In particular, Nanospec is ideal for the measurement of small volumes for drug release measurement. For this reason, it will be used in the next study where the *in vitro* release of EP from the gel will be measured.

3.9 Summary conclusions

In this chapter, EP was successfully measured in physiological solution with spectrophotometry, an easy and readily available analytical method. The results obtained with the spectrophotometry were confirmed with three different devices, demonstrating the robustness of the results. UV/Vis spec was able to detect and measure EP in a range of 78-2,500 μM while the Nanospec was shown to be more sensitive at higher concentrations (78-20,000 μM). Some of the measurement devices were shown to have some limitations compared to others. The HPLC failed to detect EP in physiological solution, which would be a limitation for the future EP release studies. With the UV spec it was possible to measure EP in physiological solution, but the results showed saturation at EP concentrations above 2.5 mM. On the other hand, the Nanospec demonstrated to be a simple, inexpensive and reliable method to measure EP in physiological solution, ideal for the measurement of small volumes.

EP was shown to be stable in physiological solution at body temperature for 2 weeks. This is an important result because it may suggest a possible application as a sustained release treatment *in-vivo*. EP was also demonstrated to be stable when frozen/thawed, which is an important factor for carrying out release studies of EP *in-vitro*.

4 CHAPTER FOUR

ALGINATE HYDROGEL AS DELIVERY SYSTEM

4.1 Introduction

The inflammation that occurs after ischemia/reperfusion leads to high levels of oxidative stress which produce deleterious effects in the myocardium (Hori & Nishida, 2009). ROS and inflammatory cytokines not only damage cell membranes causing cell death, but they also create a cascade of damaging effects in the myocardium, as discussed in section 1.2.2. The level of TNF-alpha and beta have been measured in different rat models of acute myocardial infarction (Ono, *et al.*, 1998)(Sia, *et al.*, 2002). Ono *et al.* discovered that one week after myocardial infarction, the level of TNF- beta showed the highest peak (Ono, *et al.*, 1998), while Sia *et al.*, 2002, demonstrated a sustained increase of TNF-alpha for the following 3 weeks after MI (Sia, *et al.*, 2002). The presence of oxidative stress in the infarcted area is not limited to the period post MI, but it lasts during cardiac repair and LV remodelling (Sia, *et al.*, 2002). The level of peroxide in the blood was measured in patients who had experienced an acute myocardial infarction (Nikolic-Heitzler, *et al.*, 2006). This study showed that the level of oxidative stress in the blood increased progressively, reaching a peak after 7 days (end point) when the patients were discharged from the hospital (Nikolic-Heitzler, *et al.*, 2006). Anti-inflammatory and antioxidant treatments have been investigated as a possible therapy to limit tissue damage after MI, as discussed in detail in section 1.3.4.

The use of anti-inflammatory drugs/antioxidants as a treatment to prevent and possibly reverse tissue damage after MI has been widely studied and the results obtained are often quite contradictory, as discussed in this section. In fact, although in some animal studies, the use of an antioxidant was effective to reduce the oxidative stress levels after MI (Onogi, *et al.*, 2006) (Tsujiata, *et al.*, 2004) (Cargnoni, *et al.*, 2000), it also failed to reduce ventricular hypertrophy (Probuco) (Betge, *et al.*, 2007), (Aspirin)

(Adamek, *et al.*, 2007) and sometimes led to an increase in heart failure (vitamin E) (Marchioli, *et al.*, 2006). In most of the studies presented, the antioxidants were short term delivered in a small number of doses mostly by percutaneous injection, such as statins, probucol, by IV infusion, such as infliximab, or orally, such as allopurinol, vitamin C and E. Long-term delivery of vitamin E was associated with an increase in heart failure. The studies described thus far also failed to demonstrate that the antioxidant used was able to inhibit ventricular remodelling. A potential explanation for this is that the drug delivery methods or the short duration of the treatment studied so far was not effective to improve outcomes. On the other hand, the studies conducted on allopurinol showed more promising results, with allopurinol orally delivered for 9 months reducing left ventricular hypertrophy in MI patients (Rekhranj, *et al.*, 2013) and reducing mortality in patients with heart failure (Wei, *et al.*, 2009). The lack of consistent beneficial effect of the strategies described may result from suboptimal duration of delivery and dose, but this also suggests that alternative drugs may be necessary in controlling left ventricular remodelling after MI.

Ethyl pyruvate (EP) has been studied for its antioxidant properties and ability to enhance ATP levels and reduce tissue damage in a range of different injury models (Yang, *et al.*, 2016). The beneficial effects of EP have been studied *in vitro* and *in vivo*, as extensively discussed in section 1.5. EP enhanced tissue ATP levels, preserved cardiac function and attenuated myocardial oxidative injury in a Langendorff perfused heart experiment (Guo, *et al.*, 2014). The rat hearts were treated with 2 mM EP which was added to the cardioplegic solution during ischaemia, to the storage solution and to the Krebs–Henseleit solution during reperfusion (Guo, *et al.*, 2014).

In a double-blind, randomized, placebo-controlled clinical study, EP has been administered intravenously in high-risk patients undergoing coronary artery bypass graft and/or cardiac valvular surgery with CPB. (Critical Therapeutics Inc, Lexington, MA, USA) (Bennett-Guerrero, *et al.*, 2009). Patients received a dose of 7,500 mg intravenously over 60 minutes every 6 hours for 6 doses, where the first dose was given before CPB. In this study EP did not significantly reduce the incidence of the post-operative adverse outcomes and it failed to decrease the systemic inflammatory markers (Bennett-Guerrero, *et al.*, 2009). The authors suggested that possibly the dose

administered to the patients was not adequate to reduce the inflammation. They also propounded that the length of the treatment might have been insufficient (Bennett-Guerrero, *et al.*, 2009). In fact, although EP has been extensively studied for its cardio-protective effect, it has never been delivered locally to the myocardium in a sustained manner.

The method of delivery, dose and timing are all believed to be crucial to the effectiveness of these compounds in the treatment of the oxidative stress (Hori & Nishida, 2009). The delivery of an antioxidant from an implanted material *in situ* would not only minimise any unwanted systemic effects, but also be potentially more effective in the tissue area that needs to be treated. This method of delivery would therefore allow the use of a lower amount of drug and a sustained delivery over several days and potentially weeks.

Alginate has been widely used in tissue engineering, due to its biocompatibility and its tuneable physical characteristics. It is typically used in the form of a hydrogel, a three-dimensional structure that contains mostly water. Alginate becomes gel when it is cross-linked with multivalent cations (e.g., Ca^{+2} or Ba^{+2}), as described in section (1.7.2). The stability of the resultant gel in physiological solution depends on different factors, such as the viscosity of the alginate and the type of cross-linker used, but also the chemical structure of the alginate (Lee & Mooney, 2012). In fact, alginates extracted from different sources differ in their mannuronate (M) or guluronate (G) content. The differences in chemical structure result in different characteristics, with the high M alginate gel being quite malleable while the high G alginate gel is more stable and rigid (Lee & Mooney, 2012).

Alginate has been used in wound healing, cell transplantation and as a delivery system of bioactive agents, such as growth factors and small chemical drug molecules (Lee & Mooney, 2012). The regeneration of the myocardium after ischemia/reperfusion injury has been one application of alginate gels that has received considerable attention. An alginate gel was used to deliver various growth factors into the myocardium in different animal studies (Lee, *et al.*, 2003)(Ruvinov, *et al.*, 2010)(Ruvinov, *et al.*, 2011)(Lee & Mooney, 2012). In the study conducted by Lee *et al.*, 2003, an alginate hydrogel was used to deliver vascular endothelial growth factor (VEGF) and basic

fibroblast growth factor (bFGF) into ischaemic muscle tissue of severe combined immunodeficient (SCID) mice.(Lee, *et al.*, 2003) The VEGF was released by the hydrogel for more than 14 days, resulting in new capillary formation surrounding the gel (Lee, *et al.*, 2003). In the study conducted by Ruvinov & Cohen 2011, alginate hydrogels were used to deliver insulin-like growth factor-1 (IGF-1) and hepatocyte growth factor (HGF) into the myocardium. A rat model of acute MI was used in the study and alginate hydrogel with IGF-1/HGF was delivered with an intra-myocardial injection. After 4 weeks, this alginate biomaterial reduced scar formation, and at the same time increased angiogenesis at the infarcted area (Ruvinov, *et al.*, 2011).

Alginate gels have been investigated for the delivery of small drugs in different applications (Lee & Mooney, 2012). Antineoplastic agents have been delivered by alginate gels *in vitro* in a study conducted by Bouhadir *et al.*, 2001 (Bouhadir, *et al.*, 2001). Other drugs, such as the anti-inflammatory Flurbiprofen, have been incorporated into alginate gels and released *in vitro* over relatively short time periods of 1.5 hr (Lee & Mooney, 2012). Alginate gels were used to deliver dobutamine to the left ventricle of rats in a study conducted by Lovich *et al.*, 2011. Before the *in vivo* application, the drug release was measured *in vitro*. It was found that the duration of the release was limited to a 15 minute period (Lovich, *et al.*, 2011). Alginate-CaCl₂/chitosan+ glyoxal coatings on medicated (diclofenac) contact lenses, have been shown to produce a controlled release of the drug from soft contact lens and intraocular lens for at least one week *in vitro* (Silva, *et al.*, 2016). Alginate gels were also able to release fibroblast growth factors (FGFs) in PBS over a period of 2 weeks (Lee, *et al.*, 2013). Although alginate hydrogels have been extensively used for drug delivery, they have never been investigated for their potential to deliver an antioxidant onto the myocardium for cardiac regeneration.

4.1.1 Aim and objectives

High levels of oxidative stress have been found to be present one week after ischaemia reperfusion (Nikolic-Heitzler, *et al.*, 2006). This suggests that in order to reduce oxidative stress within the myocardium, the antioxidant should have the highest release in week one with a slower release thereafter during the healing phase

The overall aim of this aspect of the study was therefore to prepare a range of implantable alginate hydrogel patches that would provide sustained delivery of EP for periods up to 3 weeks. In order to achieve this, the alginate hydrogels should be stable in physiological solution to allow the EP release over time. Two specific objectives were therefore set:

- Investigate the stability of the EP loaded alginate hydrogels *in vitro*;
- Characterise the EP release from alginate hydrogels *in vitro*;

4.2 Alginate gel preparation

The methodology used in this section has been described in detail in section 1.2.1. Briefly, the preparation of the alginate hydrogels was achieved by mixing alginate solution with calcium chloride solution. Two types of alginate were used in this study, the high mannuronate (M) content sodium alginate and the high guluronate (G) content sodium alginate (Novamatrix).

4.2.1 High mannuronate content sodium alginate (preliminary study)

Methods

In this section, high M alginate (61% Mannuronate) was used to prepare the gels. The gels were prepared using 2 different concentrations of alginate (1% (w/v) and 2% (w/v)) in order to understand the effect of concentration on hydrogel formation and degradation rate in a physiological environment. 1% (w/v) and 2% (w/v) alginate solution were prepared by adding sodium alginate to deionised water. 1 mL of alginate solution was poured into either a well of a 6-well plate or a 5 mL plastic vial (see Table 2) and 1.11 μ L of EP was added to it to provide a final EP concentration of 10 mM. The gels were initially prepared in a 6-well plate because they could be then taken forward to *in vitro* cell culture experiments. The plate/vials were then stirred with a vortex shaker to allow the mixing of alginate solution with EP. A solution of either 0.6%, 1% or 1.5% of CaCl₂ respectively was then added to each well/vial with a 1:1 ratio. At that point the hydrogel formation was clearly visible and the surplus solution left was removed. Different volumes of PBS (as detailed in Table 2) at 37°C

were added to each well/vial. The plate/vial was then placed in an incubator at a constant level of agitation at 37°C.

Results

The successful preparation of the gels was not immediately achieved and several challenges were faced during these preliminary experiments, such as early dissolution of the gel and evaporation of the surrounding medium. A summary of the various attempts to obtain hydrogels are shown in Table 2.

Table 2 Summary of the experiments carried out during the optimisation of the alginate hydrogel phase of the study.

Gel Composition	Type of container used	Gel degradation methodology	Degradation time
1 mL of 1% and 2% M-alginate (LV, MV) + 1 mL of 0.6% CaCl₂ 10 mM EP (n=3)	A 6 well plate was used to produce the gels.	5 mL of PBS preheated at 37°C was added to each well. The plate was then placed in the incubator at constant stirring	1 day
1 mL of 1% and 2% M-alginate (LV, MV) + 1 mL of 0.6% CaCl₂ (5, 7, 10) mM EP (n=2)	6 well plate	The volume of PBS was decreased to 4ml to achieve better gel stability	1 day/evaporated
1 mL of 1% and 2% M-alginate LV + 1 mL of (0.6%, 1%, 1.5%) CaCl₂ No EP (n=2)	2 x 6 well plate	The volume of PBS was decreased to: 3 mL in the plate 1 2 mL in the plate 2 to achieve better gel stability	5 days/evaporated
1 mL of 1% and 2% M-alginate LV + 1 mL of (0.6%, 1%, 1.5%) CaCl₂ No EP(n=2)	Sealed 5 mL vials were used to stop evaporation	2 mL PBS	5 days
1 mL of 1% and 2% M-alginate LV + 1 mL of (0.6%, 1%, 1.5%) CaCl₂ + 10mM EP(n=2)	Sealed 5 mL vials	2 mL PBS	5 days

The first formulation (1ml of 1% and 2% M-alginate (LV) 1ml of 0.6% CaCl₂, 10 mM EP (n=3) was used to prepare the first set of gels in a 6 well. 5ml of PBS preheated at 37°C was added to each well. The plate was then placed in the incubator at constant stirring. After 1 day, the gels were completely dissolved. In order to reduce the dissolution of the gel, medium viscosity (MV) sodium alginate was investigated instead of the low viscosity alginate. However, these gels were also found to be fully dissolved after just 1 day of incubation.

Because the use of medium viscosity alginate did not improve the endurance of the gels in PBS, other factors that may affect the stability of the gels were investigated. It is known that in physiological solution, alginate hydrogels gradually relax and increase their water intake in a process called swelling (Bajpai & Sharma, 2004). High volumes of PBS may speed the swelling process of the gels. For this reason, the volume of PBS used for the study was reduced (from 5 to 4 mL). This had little impact on the gel behaviour, with complete dissolution observed after 1 day.

The next step was to further reduce the volume of PBS, from 4 to 3 and then to 2 mL. In these experiments, the concentration of the cross-linker CaCl_2 was increased from 0.6% to 1% and 1.5%, (as shown in Figure 4.1), in order to produce a gel more stable in solution. In all formulations examined, the gels completely dissolved after 5 days. The stability of the gels was increased by 4 days, but this was still not ideal for the drug release application intended.

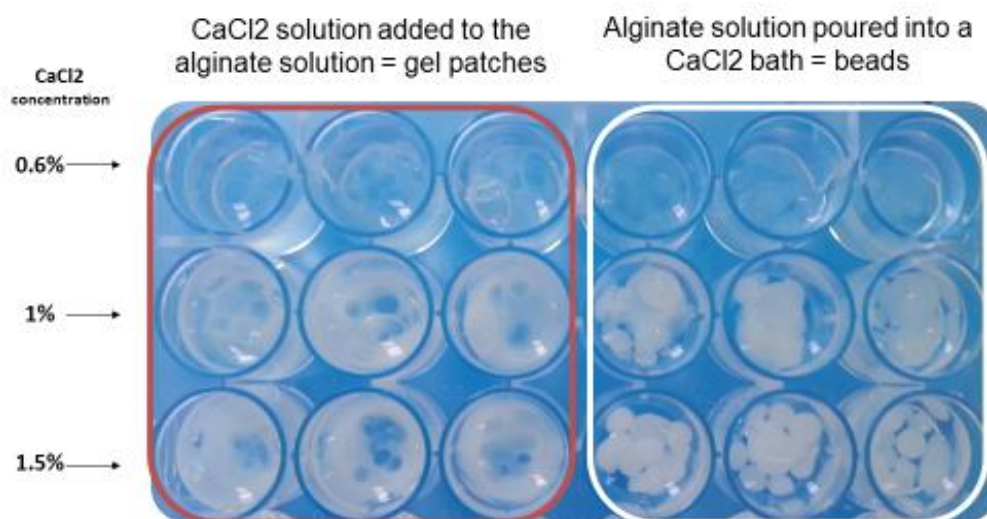


Figure 4.1 Alginate gels prepared with 1% LV alginate solution (Sigma) and different CaCl_2 concentrations $n=3$.

Figure 4.1 shows the impact of the order of alginate and cross-linker addition on the form that the hydrogel takes. When the cross-linker is added to the alginate solution gel patches were formed over the majority of the well area. In contrast, if the alginate solution is added to the cross-linker, beads were formed. With higher CaCl_2

concentration, the gels prepared showed a more robust structure, consistent with an increase in calcium bonding between the alginate and the cross-linker. This effect can be seen in a gradual change in colour when a higher concentration of calcium was present in the gel (Figure 4.1).

Another challenge that was encountered was evaporation. Although the cover of the plate was on the plate during incubation, it was clear that evaporation of the gel had occurred overnight. For that reason, a sealed 5 mL vial was then used in the remaining experiments.

The last formulation of gels (1% 2% alginate (LV), cross-linked using either 0.6%, 1%, 1.5% CaCl₂) were prepared again but this time they were placed in sealed 5 mL vials. Even although the evaporation problem was solved this time, the gels were completely dissolved by day 5. In order to investigate if EP incorporation within the gels would have an effect on the degradation of the gels, another set of gels were prepared in the presence of EP (10mM). The results showed that the gels with EP dissolved at the same rate as the gels without EP. This suggests that EP did not affect the degradation time of the gels.

Since the overall aim of the study was to prepare alginate gels which are stable in PBS for at least 3 weeks to allow EP delivery *in vitro*, it was therefore decided to investigate the use of an alginate with a high guluronate content.

4.2.2 High guluronate content sodium alginate (preliminary study)

Methods

NovaMatrix Pronova UP ultrapure sodium alginate (low viscosity LV) with high G content ($\geq 60\%$) was used to produce a new set of hydrogels. Due to the preliminary nature of the study, the gels were prepared without EP. The methodology used was similar to that used for the preparation of hydrogel with high mannuronate sodium alginate explained in the previous section. Briefly, 1 mL of alginate solution (1% or 2%) was poured into a 5 mL vial. 1 mL of the cross-linking solution (0.6%, 1%, 1.5% CaCl₂) was added to the alginate solution to start the crosslinking reaction. The excess of crosslinking solution was removed and 1 mL PBS solution was added to each vial.

The gels were then placed in an incubator at 37 °C. The stability of the gels in PBS at 37°C was monitored visually over periods up to 30 days.

Results

Gels were successfully prepared using this methodology. An example of the gels prepared is shown in Figure 4.2.

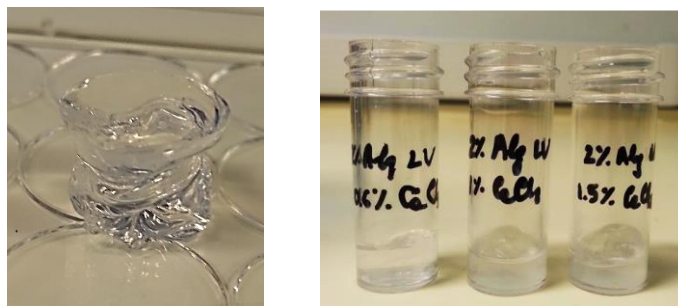


Figure 4.2 Examples of Alginate hydrogels prepared high G content. Left panel shows an alginate hydrogel prepared with 1:1 1% alginate (LVG Novamatrix) solution and 0.6% CaCl_2 solution. The right panel shows alginate hydrogels prepared with 1:1 1%-2% alginate (LVG Novamatrix) solution and 0.6%, 1%, 1.5% CaCl_2 solution.

The gel stability was examined over 30 days. Due to the preliminary nature of the study, the stability was assessed by simple visual inspection of the vials to determine if the gel structure was still visible. The gels did not dissolve over a period of 30 days. This result demonstrates that the gels exhibited stability that would be suitable for the intended application. In this section EP was not added to the gels, so the next step was to prepare gels with EP and to examine if this impacted on gel stability.

4.3 Stability study of alginate hydrogels *in vitro*

Methods

In the section 4.2, alginate hydrogels without EP were prepared and their overall stability in PBS was observed over time on a visual basis. In this section, high G content alginate hydrogels containing EP (10 mM) were placed in PBS and in addition to visual inspection, their change in weight was also monitored over time. The

methodology used to prepare EP loaded gels was the same as the method used to prepare the EP-free hydrogels (section 4.2). Briefly, EP (10mM) was added to 1 mL of the relevant alginate solution. A solution of either 0.6%, 1% or 1.5% of CaCl₂ respectively was then added to each vial with a 1:1 ratio of cross-linker to alginate solution. Two types of vials were used to produce the hydrogels, plastic and glass vials. It was quickly found that EP left evident marks on the plastic vial's wall when it was poured. This suggested that the EP reacted in some way with the vials. To avoid this, only glass vials were therefore used for the remainder of the study.

The gels were then placed in 1 mL PBS and incubated at 37 °C for 28 days. At each time point (1 hour, 1 day, 3 days, 5 days, 7 days, 14 days, 21 days, 28 days) half of the medium (0.5mL) was collected for drug release measurements (see section 4.5), and replaced every time with an equal volume of fresh PBS. Before weighing the gels, all the incubation medium was removed, and then the same medium was reinserted within the vial to allow the incubation to continue.

Results

The results of the hydrogels stability study are shown in Figure 4.3.

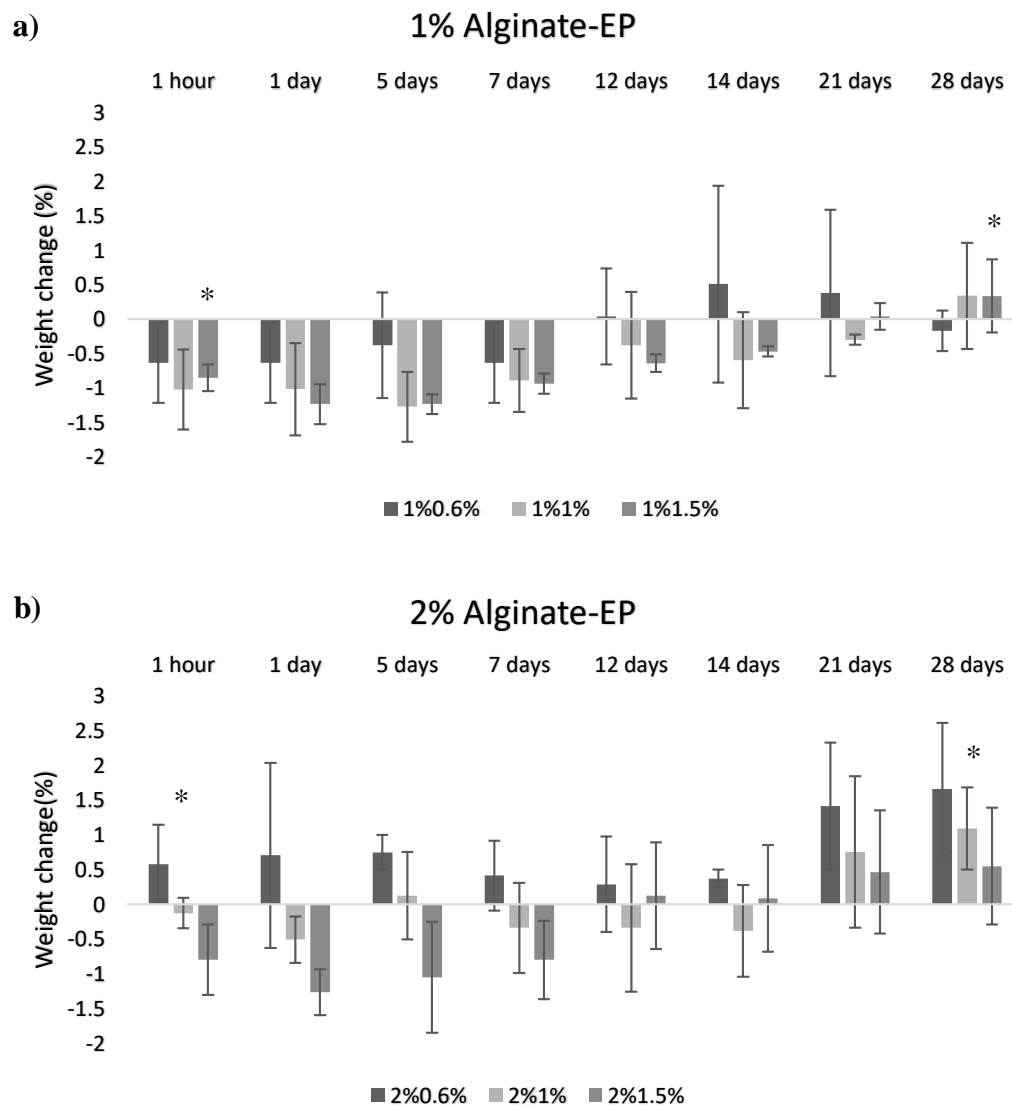


Figure 4.3 EP (10mM) loaded alginate hydrogels stability in PBS over 28 days. Alginate gels were placed in PBS and incubated at 37°C at constant agitation. Alginate gels were prepared with **a)** 1%alginate and **b)**2% alginate solution using different CaCl₂ concentrations (0.6%, 1%, and 1.5%). The change in weight of the gels was measured at different time point (1 hour, 1 day, 3 days, 5 days, 7 days, 14 days 21 days, 28 days). The weight change (%) is shown in figure as a measurement of hydrogel stability. Data represent the mean ± st dev from three samples. The weight change at the beginning of the experiment (1 hour) was compared to the one at the end of the experiment (28 days) (* $p < 0.05$).

It can be seen that the hydrogels prepared with 1% alginate showed a small reduction in weight within the first hour following incubation. This phenomenon is associated with the release of water from the hydrogel into the release media. The mass then remained relatively stable for up to 7 days for the 0.6% CaCl₂ formulation gels. There

was a slight reduction in mass observed in the 1% and 2% CaCl₂ formulations over the first 5 days, before a slight recovery after 7 days (Figure 4.3). A t-test, two tailed distribution, paired analysis ($p \leq 0.05$) showed no statistical difference between the initial weight (1 hour) and the final weight (28 days) of each scaffold, except for the scaffolds prepared with 1% alginate and 1.5% CaCl₂ and 2% alginate and 1% CaCl₂, as shown in Figure 4.3. The hydrogels prepared with 2% alginate and 1%-1.5% CaCl₂ showed a similar behaviour trend, with a reduction of weight in the first 2 weeks, followed by a swelling of the hydrogels from day 21. On the other hand, the scaffolds prepared with 2% alginate 0.6% CaCl₂ showed a constant increase in swelling over 28 days with the scale of this being particularly evident in the last two weeks of the experiment. A t-test two tailed distribution analysis ($p \leq 0.05$) showed that the change in weight of the scaffold prepared at different alginate concentrations (1% and 2% alginate) were statistically different only for the scaffolds cross-linked at lower CaCl₂ concentration (0.6%), as shown in Figure 4.4.

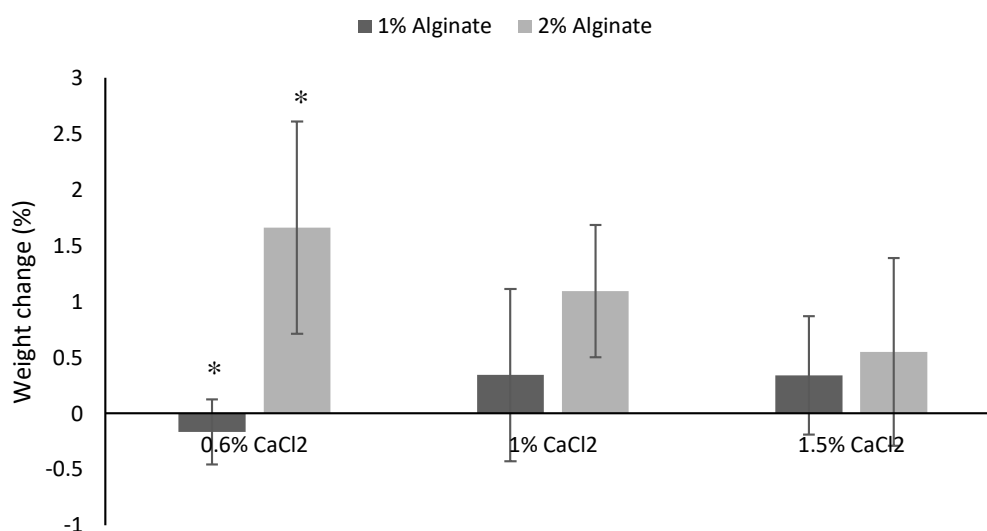


Figure 4.4. Comparison of the stability of EP loaded alginate hydrogels prepared with 1%alginate and 2% alginate in PBS at 28 days. Alginate gels were placed in PBS and incubated at 37°C at constant agitation. Alginate gels were prepared with either 1%alginate or 2% alginate solution using different CaCl₂ concentrations (0.6%, 1%, and 1.5%). The change in weight of the gels was measured at different time point (1 hour, 1 day, 3 days, 5 days, 7 days, 14 days 21 days, 28 days). The weight change (%) is shown in figure as a measurement of hydrogel stability. Data represent the mean \pm st dev from three samples(* $p < 0.05$).

The change in weight of the 1% and 2% alginate gels measured over 28 days showed an overall weight change between -1.5% and 1.5% (Figure 4.3). This result demonstrates that the overall swelling of the gels was relatively small. A one-way ANOVA analysis ($p \leq 0.05$) showed that there was no statistical difference in weight change between scaffolds prepared at different cross-linker concentrations, which suggests that the cross-linker concentration in this range did not affect the stability of the hydrogels.

4.4 SEM imaging of ethyl pyruvate loaded alginate gels

The morphology of a limited number of alginate gels with and without EP was investigated with SEM imaging using the method described in 2.5.2. Alginate hydrogels were prepared with 2% alginate and 1.5% CaCl_2 , as per the method used to produce the gels used in the stability testing detailed above. The results of this work are shown in Figure 4.5.

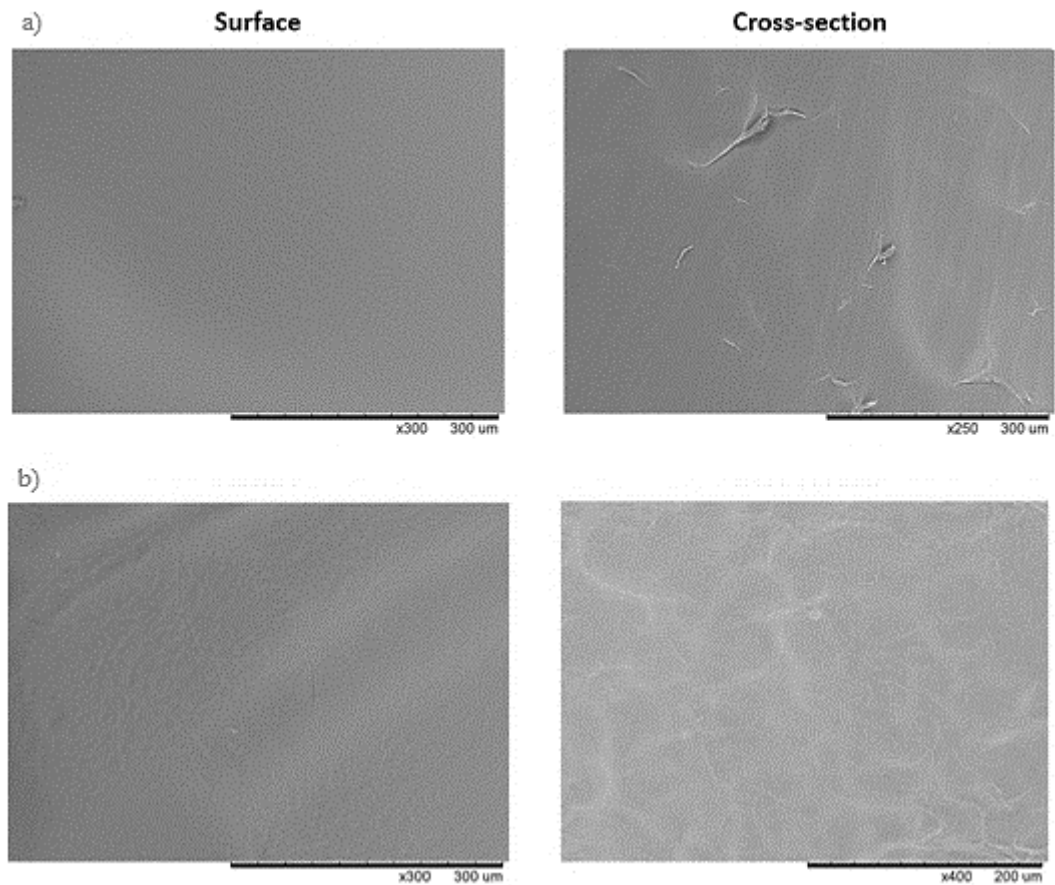


Figure 4.5 SEM imaging of alginate hydrogels. **a)** SEM images of the surface and the cross-section of alginate hydrogel without EP; **b)** SEM images of the surface and the cross-section of alginate hydrogel with (10mM) EP. The hydrogels were prepared with 2% alginate and cross-linked with 1.5% CaCl_2

It can be seen that the gels prepared with EP displayed little difference in morphology compared to the gels with no EP. Both gels showed a smooth surface, with no macropores visible, although the cross section images of the gels with EP showed a different pattern compared to the gels without EP. The results suggest that the presence of EP did not change the final morphology of the hydrogel. Both of them presented a smooth structure not only on the surface but also in the cross-sectional areas examined.

4.5 *In-vitro* ethyl pyruvate release study from alginate gels

Methods

The hydrogels prepared for the stability study (section 4.3) were also used for the measurement of EP released by the hydrogels in PBS. The methodology used in this study is described in section 1.4. Two sets of gels were prepared, one set with EP, the other set without EP, to provide a negative control. At different time points (1 hour, 1 day, 3 days, 7 days, 14 days, 21 days, 28 days) the vials were removed from the incubator and 0.5 mL of PBS solution collected from each sample. The removed solution was transferred to an Eppendorf and stored in the freezer at -20 °C for future measurement using the Nanospec spectrophotometer (section 2.5.1.2). In order to maintain the volume of the release solution constant, 0.5 mL of solution removed was replaced with 0.5 mL of fresh PBS solution and the vial returned to the incubator.

Results

4.5.1 1% alginate hydrogels

The profiles of EP release from the 3 formulations of alginate hydrogels are shown in Figure 4.6. Alginate hydrogels prepared with 1% alginate successfully released EP over a 3 week period (Figure 4.6-a). The total EP released by the different hydrogel formulations was $1856 \pm 658 \mu\text{g}$ (0.6% CaCl_2), $2112 \pm 317 \mu\text{g}$ (1% CaCl_2) and $1934 \pm 346 \mu\text{g}$ (1.5% CaCl_2). In Figure 4.6-b the percentage EP release profile follows the same pattern as the cumulative mass release data (Figure 4.6-a) with about 85% of EP ($81 \pm 12\%$ for gels prepared with 0.6% calcium chloride; $83 \pm 9\%$ for gels prepared with 1% calcium chloride; $87 \pm 1\%$ for gels prepared with 1.5% calcium chloride) released in the first week, and the remaining EP over the following weeks. A one-way ANOVA ($p \leq 0.05$) showed no statistical difference between the EP releases from the hydrogels prepared with different CaCl_2 concentrations.

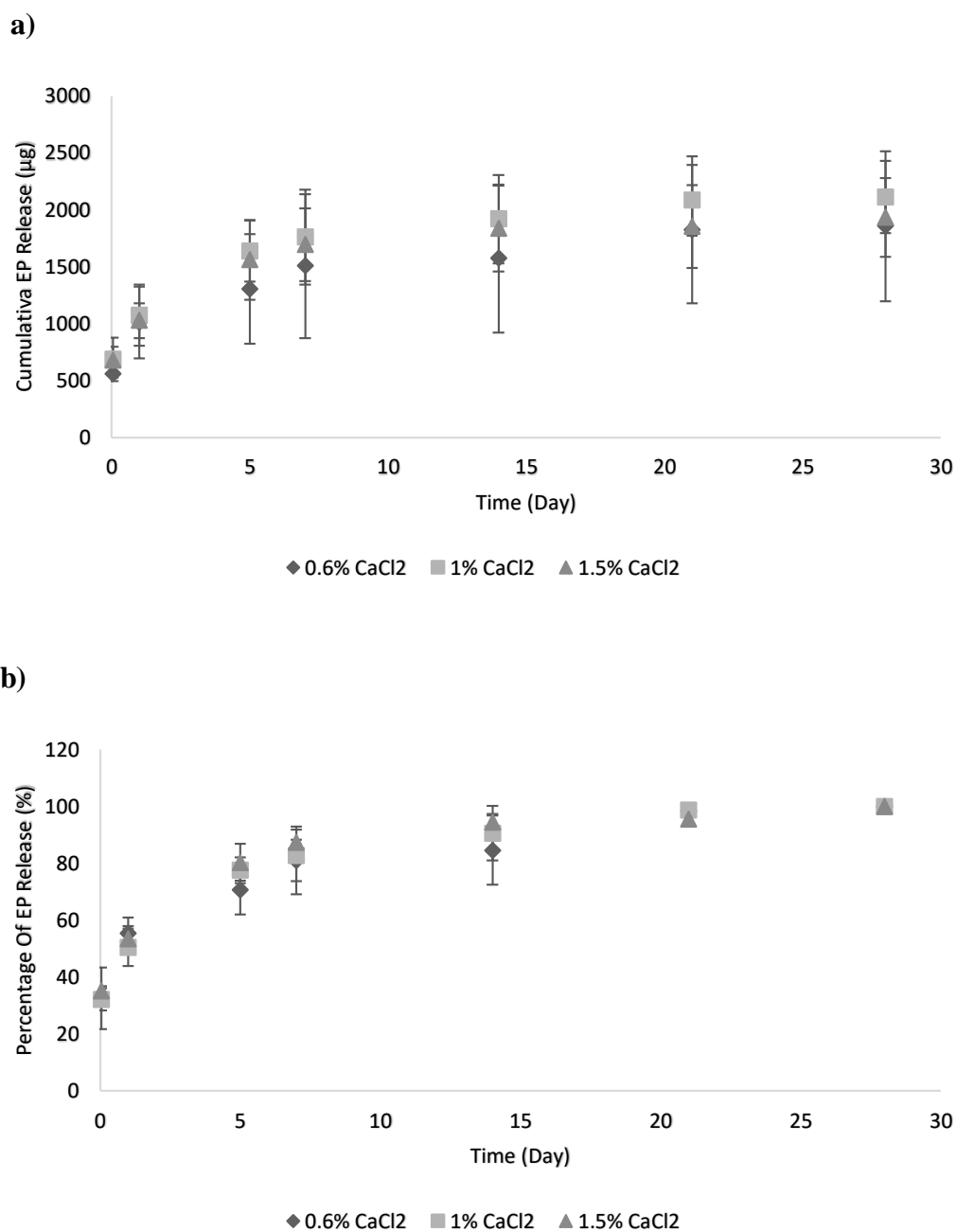


Figure 4.6 Cumulative EP released from 1% alginate hydrogels over 28 days. a) Cumulative EP release from the gels over time; b) Percentage of EP release over time. The gels were immersed in PBS and incubated at 37 °C at a constant level of agitation. At different time points (1 hour, 1 day, 3 days, 7 days, 14 days, 21 days, 28 days) the samples were collected and stored in the freezer at -20°C. The EP contained in the samples was measured with the Nanospec at 198 nm wavelength. The percentage was calculated using the total amount of EP released by the hydrogel as the total EP present in the hydrogel.

4.5.2 2% alginate hydrogels

Hydrogels were produced with 2% sodium alginate and three different calcium chloride concentrations (0.6%, 1% and 1.5%). The profiles of the EP release from these 3 formulations are shown in Figure 4.7.

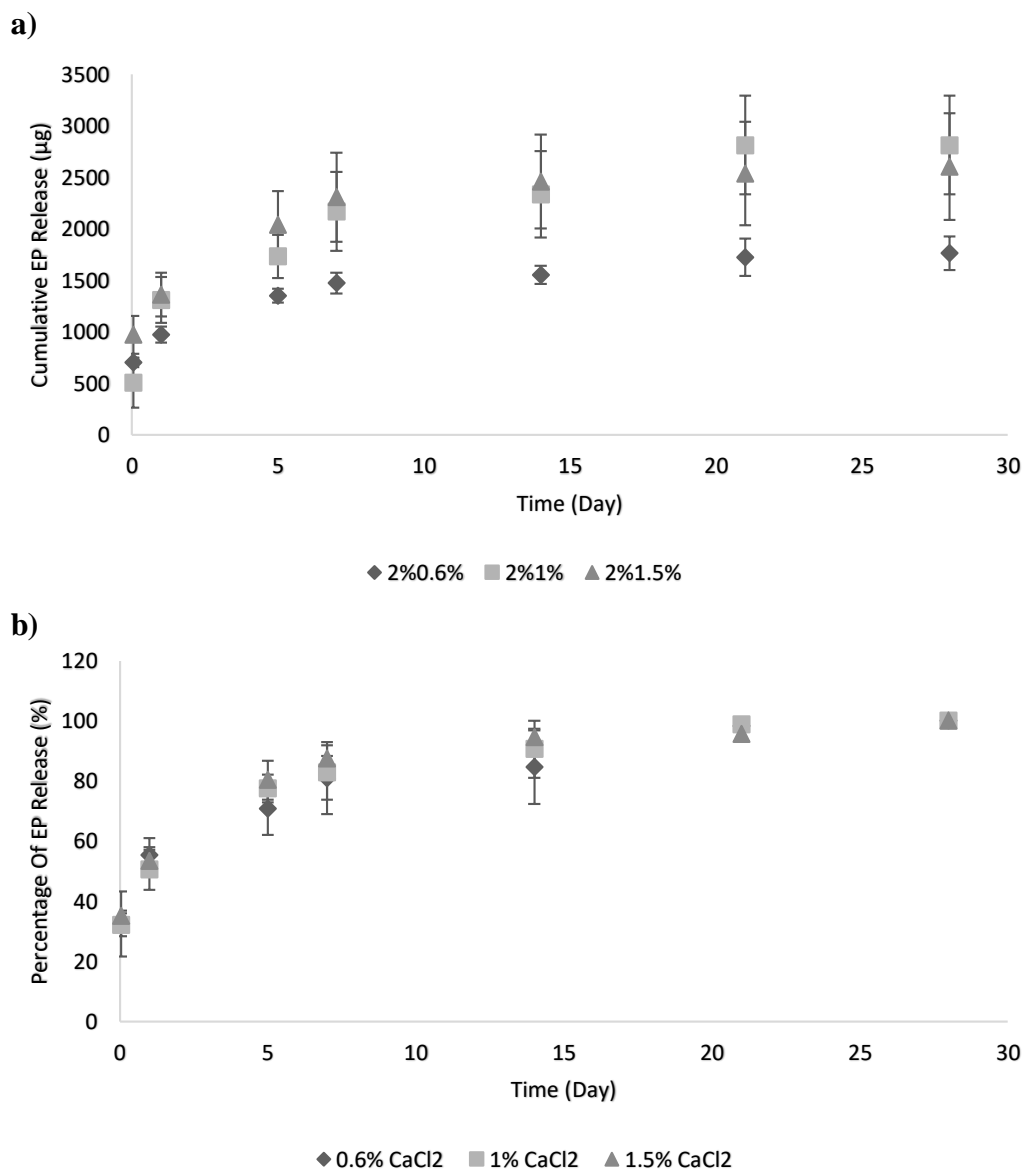


Figure 4.7 EP released from 2% alginate hydrogels over 28 days. a) Cumulative EP release from the gels over time; b) Percentage of EP release over time. The gels were immersed in PBS and incubated at 37 °C at a constant level of agitation. At different time points (1 hour, 1 day, 3 days, 7 days, 14 days, 21 days, 28 days) the samples were collected and stored in the freezer at -20°C. The EP contained in the samples was measured with the Nanospec at 198 nm wavelength. The percentage was calculated using the total amount of EP released by the hydrogel as the total EP present in the hydrogel. Data represent the mean \pm st dev from three samples.

The hydrogels prepared with 2% alginate and different CaCl₂ successfully released EP over a 4 week period (Figure 4.7). The hydrogels prepared with higher CaCl₂ concentrations (1%, 1.5%) showed a total EP release of 2813 ±830 µg (1% CaCl₂) and 2606 ±893 µg (1.5% CaCl₂) respectively, while the hydrogels prepared at lower CaCl₂ concentration (0.6%CaCl₂) released 1767 ±282 µg of EP. A one-way ANOVA analysis (p<0.05) showed no statistical difference in EP release at 28 days between the scaffolds prepared with different CaCl₂ concentrations.

In the Figure 4.7-b alginate hydrogels presented a similar EP release profile, with about 85% of EP (84 ± 4% for the gels prepared with 0.6% CaCl₂; 77 ± 3% for the gels prepared with 1% CaCl₂; 89 ± 1% for the gels prepared with 1.5% CaCl₂) released in the first week, and the remaining EP over the following weeks. This release profile was almost identical to the EP profile of the hydrogels prepared with 1% (Figure 4.6-b). In fact, a t-test two tailed distribution analysis (p<0.05) showed that the scaffolds prepared at different alginate concentration were not statistically different, which suggests that the alginate concentration in this range did not affect EP release, as shown in Figure 4.8.

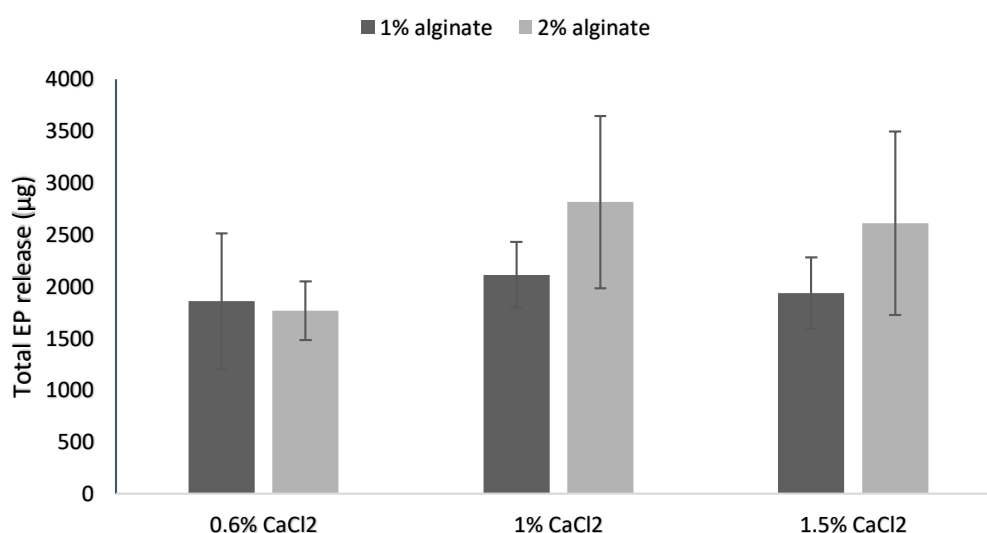


Figure 4.8. Comparison of total EP released from 1%alginate hydrogels and 2% alginate hydrogels at 28 days. The gels were immersed in PBS and incubated at 37 °C at a constant level of agitation. At different time points (1 hour, 1 day, 3 days, 7 days, 14 days, 21 days, 28 days) the samples were collected and stored in the freezer at -20°C. The EP contained in the samples was measured with the Nanospec at 198 nm wavelength. Data represent the mean ± st dev from three samples. No Significant differences were observed between the datasets.

4.6 Drug loading efficiency

The amount of EP added to the alginate solution (2.78 μL of EP in 1mL of alginate solution) during the gel preparation may differ from the EP ultimately retained by the gel. The measure of the amount of EP not taken into the gel during production can be used not only as an indication of the efficiency of the gel preparation, but also to measure the repeatability of the gel preparation method. For this reason, in this section it was decided to investigate the amount of EP retained by the gel compared to the amount of EP added into the hydrogel by calculating the drug loading efficiency of each hydrogel. The values were calculated considering the EP added in each scaffold during the hydrogel preparation as 100% efficiency.

Equation 15

$$EP \text{ loading efficiency (\%)} = \frac{\text{Total EP released by the scaffold}}{\text{EP added to each scaffold}} \times 100$$

The loading efficiency values calculate for each of the formulations are shown in Table 3.

Table 3 EP loading efficiency (%) in alginate hydrogels. Data represent the mean \pm stdev (n=3)

Alginate	Calcium Chloride	EP loading efficiency (%)	st dev
1%	0.6%	64%	23
	1%	73%	11
	1.5%	67%	12
2%	0.6%	61%	10
	1%	97%	29
	1.5%	90%	31

Alginate scaffolds prepared with higher CaCl_2 concentration (1%, 1.5%) presented a higher loading efficiency compared to the scaffolds prepared at lower CaCl_2 concentration within the same group (Table 3). This suggests that the increase of the cross-linker concentration leads to an increase in crosslinks in the gel, thereby

increasing retention of EP within the gel matrix. Similarly, the use of 2% alginate appears to have increased the capacity of the gel to uptake and retain EP, as observed by the consistently higher loading efficiencies observed at this concentration compared to the 1% alginate gels. Indeed, the gels prepared with 2% alginate and 1% CaCl₂ have the highest EP loading efficiency of 97%.

4.7 Discussion

4.7.1 Introduction

The presence of oxidative stress in the infarcted area is not limited to the period post MI, but it lasts during cardiac repair and LV remodelling (Sia, *et al.*, 2002). It has been shown that the level of peroxide in the blood reached a peak after 7 days in patients who had experienced an acute myocardial infarction (Nikolic-Heitzler, *et al.*, 2006), while pro-inflammatory cytokines measured in rat models of acute myocardial infarction showed a sustained increase for the following 3 weeks after MI (Sia, *et al.*, 2002). Anti-inflammatory and antioxidant treatments have been investigated as a possible therapy to limit tissue damage after MI, as discussed in detail in section 1.3.4. Although the optimal release time for EP, or indeed other similar potential therapeutics, into the myocardium is still unknown, this suggests that EP delivered over 3 weeks would be appropriate to reduce inflammation and oxidative stress, thereby offering potentially improved patient outcomes. Although alginate hydrogels have been extensively used for drug delivery, they have never been studied as a delivery system of an antioxidant onto the myocardium for cardiac regeneration (Lee & Mooney, 2012). EP has been extensively studied for its cardio-protective effect following application during surgery (Yang, *et al.*, 2016) but it has never been delivered in a sustained manner (Guo, *et al.*, 2014)(Jang, *et al.*, 2010). The overall aim of this study was therefore to prepare a hydrogel which was stable in physiological solution over a minimum period of 3 weeks to allow a sustained release of EP.

4.7.1 Alginate hydrogels preparation

Different approaches were taken to prepare the hydrogel (Table 2). The gels were obtained using 1:1 volumes of alginate solution (1%-2%) and CaCl₂ solution (0.6%,

1% and 1.5%). The problem of evaporation was the main challenge encountered during the initial stability studies. Initially, a 6 well plate and a 12 well plate were used to produce and store the gels in the incubator. Although a plastic sheet was used and a tray with water was placed in the incubator to limit the evaporation, after 4 days the gels and the media evaporated completely. To overcome this problem, sealed containers were used in all subsequent studies.

Two different types of sodium alginate were used in this study, a high M content alginate and a high G content. The high M alginate was initially investigated due to its ready availability at low cost. In this study, the first set of hydrogels were prepared using high M sodium alginate. Hydrogels produced with high M sodium alginate and 0.6% calcium chloride degraded after 5 days at 37°C in PBS. Alginate concentrations higher than 2% were not considered in this study because with high alginate concentrations, alginate solution would have been more difficult to prepare (alginate solubility). The concentration of the cross-linker was increased from 0.6% to 1% and 1.5%, in order to increase the stability of the gels in PBS. The results showed that although the cross-linker concentration was increased, this did not improve the stability of the gels, which dissolved by day 5 (Table 2). For this reason, high G ultrapure alginate was purchased from Novamatrix. This sodium alginate is widely used for tissue engineering, pharmaceutical, biomedical applications due to the ultrapure formulation. In the preliminary study conducted on the alginate hydrogels prepared with the high G alginate, the gels did not dissolve for more than 30 days at 37°C in PBS. This result is consistent with previous observations by Mooney et al., 2012, which described how sodium alginate with high M content creates a less stable hydrogel, compared to the hydrogels prepared with high G content alginate, due to the fact that the G component of alginate is responsible for the crosslinks with calcium, so higher G content corresponds to higher crosslinking (Lee & Mooney, 2012). The results presented here further demonstrate the importance of using alginate with high G content (Novamatrix) for the preparation of alginate hydrogels, where long term structural stability following immersion is required.

4.7.2 Stability study of alginate hydrogels

In the preliminary study alginate gels did not dissolve for 30 days at 37°C in PBS, as discussed before. The results suggested that the methodology used to prepare the gels was optimal for the preparation of EP loaded gels. EP (2.78 µL) was successfully loaded into the alginate hydrogels by adding EP to the alginate solution before the crosslinking. Different alginate concentrations (1-2%) and different CaCl₂ concentrations (0.6%, 1% and 1.5%) were used to prepare the gels. In this way it was possible to investigate how those variables can affect the stability of the gels. Alginate concentrations higher than 2% were not considered in this study not only because alginate solution would have been more difficult to prepare, as previously discussed, but also because only a limited amount of alginate was available for the study, due to the expensive type of alginate used. The visual observations outline above provided a qualitative measure of such stability. However, in order to provide a quantitative indication of this, the change in gel mass of the gels was measured at various time points over a 28-day period. The change in weight of the 1% and 2% alginate gels measured over 28 days showed an overall weight change between -1.5 and 1.5% (Figure 4.3). This result shows that the swelling of the gels was relatively small. The results showed that the effect that alginate and the cross-linker concentration may have on the stability was not visible in this time frame under the experimental conditions used. This suggests that the alginate gels prepared may be suitable for the delivery of EP in the same time frame of 28 days.

The SEM images of the gels suggest that the presence of EP did not interfere with the final morphology of the hydrogel (see Figure 4.5). Both of them presented a smooth structure not only on the surface but also in the cross-section (Figure 4.5).

4.7.3 EP delivery study

Ethyl pyruvate, a more stable derivate of sodium pyruvate, has been widely studied for its antioxidant properties in several recent studies (Woo *et al*, 2004; Famili *et al*, 2013). However, the effectiveness of ethyl pyruvate has been measured only for short term release in animal studies (Woo *et al*, 2004; Famili *et al*, 2013) and in humans (Bennett-Guerrero, *et al.*, 2009), therefore the long term effect of locally delivered ethyl

pyruvate on damaged myocardial tissue has not yet been studied either *in vitro* or *in vivo*. EP has also never been loaded into a hydrogel for the sustained release over time.

In the present study, long term *in vitro* release of EP over a period of 21 days was successfully achieved by loading EP into alginate hydrogels (Figure 4.6- Figure 4.7). Such sustained release of EP has not previously been achieved. Alginate has been used to deliver small drugs but it has never been used to deliver an antioxidant, in particular EP.

Various alginate gels were produced, with all of them demonstrating the ability to provide sustained release of EP over time. 1% alginate gels release approximately 2000 μg after 28 days, which appeared to be independent of the cross-linker concentration (Figure 4.6-a). However, increasing the concentration of alginate to 2% lead to an increase in EP release to approximately 3000 μg (Figure 4.7-a). There was no statistical difference between the scaffolds prepared at different alginate concentration, indicating that within the concentration of alginate used in this study alginate concentration did not significantly affect drug release. The amount of EP retained by the gel during gel production was used not only as an indication of the efficiency of the gel preparation, but also to measure the repeatability of the gel preparation method. The scaffolds prepared with 2% alginate and 1% -1.5% CaCl_2 were shown to have the best loading efficiency of 90-97%. This suggests that an increase in density of cross links within the gel has contributed to increased EP retention.

Alginate gels have been used as drug delivery systems to deliver small compounds, such as the anti-inflammatory Flurbiprofen, (Lee & Mooney, 2012), or dobutamine (Lovich, *et al.*, 2011), with a very limited release of several minutes to hours *in vitro*. Instead, the alginate gels loaded with EP prepared in this study released EP over a much longer period of time. The aim of the project was to prepare a gel that could release EP with an initial burst in the first week in order to counteract the ROS production that follows MI, followed by a slow release along with the healing process. The gels prepared meet these requirements, with both the 1% and 2% alginate gels releasing about 85% of EP in the first week, and the remaining EP over the following weeks (Figure 4.6-b – Figure 4.7-b). In clinical translation, the initial burst of EP would

be potentially beneficial to combat the increase of oxidative stress in ischaemic hearts. The following release of the remaining EP by the gels would provide not only antioxidant protection, but also ATP, necessary for cell metabolism. In fact, after ischaemia/reperfusion, not only is there a burst of ROS production, but this phase is also characterised by ATP depletion. The recovery of ATP upon reperfusion may limit cell damage and help cell recovery (Taylor, *et al.*, 2005).

EP has already been shown to have beneficial effects in different applications, not only on ischaemic hearts, but also on reducing brain injury, kidney injury, combating human leukaemia cells, ameliorating pancreatic and liver injury, lung injury, bowel disease and inhibiting tumour growth (Yang, *et al.*, 2016). The possibility of releasing EP *in situ* over time may improve the efficacy of EP and reduce any possible peripheral accumulation of the drug. As a U.S. Food and Drug Administration (FDA)-approved polymer, alginate is biocompatible and biodegradable *in vivo*. In this context, the EP-alginate gel formulations developed here have potential for use in a wide range of treatment areas.

4.8 Limitations

Alginate gel stability was studied by measuring the change in weight (swelling ratio) of the gels over time. The effect of errors in weight measurements due to surface liquid retention upon swelling ratio represents a limitation of this study. The results do however provide an indication of the potential gel stability in PBS at body temperature. Alginate used in this study to prepare hydrogels had a molecular weight of 75,000-200,000 g/mol, which exceeds the renal clearance threshold (~50,000 g/mol) and likely will not be completely removed from the body (Al-Shamkhani & Duncan, 1995). The results do however provide an indication of the potential for such gels to provide sustained release of EP. Future work should therefore investigate whether the results obtained here extend towards the use of sodium alginate with a lower molecular weight, thereby allowing this concept to move closer towards clinical translation. An important part of such translation would be further characterisation of the EP release, since the *in vitro* system used here does not capture the complexity of the *in vivo* environment.

4.9 Summary conclusions

In this chapter, EP was successfully loaded into alginate hydrogels. The hydrogels were stable in physiological solution over 28 days, allowing the delivery of EP over a potentially therapeutic period of time. EP was released by the hydrogels in a sustained manner, characterised by an initial burst in the first week, followed by a slow release for the remaining 2 weeks. The sustained release of EP from hydrogels has not been reported previously. In clinical translation, the initial burst of EP could be beneficial to counteract the increase of oxidative stress in ischaemic hearts. The subsequent release of the remaining EP by the gels would provide not only antioxidant protection, but also ATP, necessary for cell metabolism. With further development, the patch may be used surgically by applying it directly onto the myocardial surface or due to the nature of the gel, alginate solution could be injected into the heart and cross-linked *in situ* (Landa, *et al.*, 2008). However, it has been suggested that the presence of macropores in the scaffolds might improve cell attachment and proliferation (Dar, *et al.*, 2002), with a possible improvement in the regeneration of the affected area *in vivo*. Therefore, the next step will be the preparation of EP loaded alginate scaffolds with low molecular weight for biodegradability *in vivo*. Dry scaffold would also have prolonged shelf life, which is an important factor in the product development.

5 CHAPTER FIVE

ALGINATE MACRO-POROUS SCAFFOLDS FOR CARDIAC REGENERATION

5.1 Introduction

Alginate hydrogels have been used for different biomedical applications, due to their similarity to extracellular matrices of living tissues. Examples include the use of alginate in wound healing and cell transplantation studies and as a delivery system for bioactive agents, such as growth factors and small molecule drugs (Lee & Mooney, 2012). In the previous chapter, alginate hydrogels loaded with EP were successfully prepared. EP was released by the hydrogels in a sustained manner, characterised by an initial burst in the first week, followed by a slow release for the remaining two weeks. It is envisioned that future clinical application of this technology would involve the developed hydrogels being placed onto the myocardium following CABG surgery or other cardiac procedures where ischaemic damage may be present. This could provide an initial burst of EP, to inhibit the increase of damaging oxidative stress in ischaemic hearts. The continued release of the remaining EP within the gels could also provide not only antioxidant protection, but also elevate ATP levels, thereby supporting a return to normal cell metabolism. The hydrogel would then gradually dissolve *in vivo* over time, so no surgery would be needed to remove it.

It is therefore clear that the hydrogels described may have clinical utility, with their capacity to provide sustained EP release having potential therapeutic benefit. In addition to this, the use of alginate as the delivery vehicle opens up the possibility of using the hydrogel to encourage cell integration, improving performance yet further. It has previously been shown that scaffolds that have a porous structure with interconnected pores allow cell infiltration and proliferation, as well as the free movement of nutrients and waste. Once the cells populate and proliferate within the scaffold, it should then gradually degrade, leaving space for the newly formed tissue (Cui, *et al.*, 2016). Macro-porous alginate scaffolds have been shown to support the

culture of different primary cells, such as rat fibroblasts (Shapiro & Cohen, 1997), cardiomyocytes and cardiac fibroblasts (Dar, *et al.*, 2002).

As discussed previously in section 1.7.6, *in vitro* studies have shown that alginate scaffolds have the ability to deliver small molecules, such as the chemotherapy drug mitoxantrone (Zhao, *et al.*, 2011) and other higher molecular weight bioactive agents, such as proteins and plasmid DNA (Zhao, *et al.*, 2011). However, no study has investigated the use of alginate macro-porous scaffolds for provision of sustained release of EP. In this chapter, the optimal method of producing macro-porous alginate scaffolds that can deliver EP over 3 weeks was therefore investigated.

Various aspects of the alginate scaffold preparation method may influence both EP retention during the preparation of the scaffolds and subsequent release following *in vitro* incubation. Both the freeze-drying technique and crosslinking conditions may play an important role in retention. The internal morphology of the scaffold, such as pore size and shape is a critical factor for drug retention and release (Zhao, *et al.*, 2011). The freezing regime, which is part of the freeze drying process, was shown to influence the pore size of the scaffolds in previous studies (Kang *et al.*, 1999) (Zmora *et al.*, 2002). In fact, Kang *et al.* showed how the use of low temperature (-80 °C) in the freezing process can lead to smaller pore size formation in gelatin hydrogels.

5.2 Aims

The overall aim of this part of the study was to prepare a range of implantable alginate patches with a macro-porous structure that could allow cell infiltration and would provide sustained delivery of EP for periods up to 3 weeks. In order to achieve this, the alginate scaffolds should be stable in physiological solution to allow the EP release over this time period. The following four specific objectives were set:

- Investigate the optimal method for production of macro-porous alginate scaffolds
- Investigate the stability of the EP loaded alginate macro-porous scaffolds *in vitro*;
- Characterise the EP release from alginate macro-porous scaffolds *in vitro*;
- Characterise the scaffold morphology.

5.3 Methodology

5.3.1 Preliminary study - Calcium gluconate alginate scaffolds

The methodology described previously in section 2.3.1 was used to produce alginate scaffolds, cross-linked with calcium gluconate. Briefly, scaffolds were prepared by adding 0.5 mL of 2% VLVG alginate solution in a 24 well plate and cross-linked by adding 0.5 mL of 0.4% or 1% calcium gluconate solution to each well. After 30 minutes, the samples were frozen overnight and then freeze-dried for 24 hours. The alginate scaffolds produced with this method were placed in 1.5 ml of PBS at 37°C. The stability of the scaffolds was examined in a preliminary study, where the dissolution was evaluated daily. Due to the preliminary nature of the study, the stability was simply assessed by visual inspect of the vials to determine if the gel structure was still visible. It was found that the scaffolds dissolved completely after 5 days of incubation. Since the target was to obtain a scaffold that maintained its structure over 3 weeks, an alternative methodology was therefore developed to prepare the scaffolds.

5.4 Alginate scaffolds preparation

5.4.1 Introduction

Several aspects of the scaffold fabrication can influence the characteristics of the final structure and consequently the degradation behaviour and drug release characteristics of the scaffolds. Temperature, type of cross-linker, concentration of calcium added to the alginate solution, freezing process and lyophilisation time are only a few examples of factors that can affect the ultimate product. The following diagram (Figure 5.1) illustrates the experimental layout used to investigate the impact of these factors on the properties of the scaffolds produced.

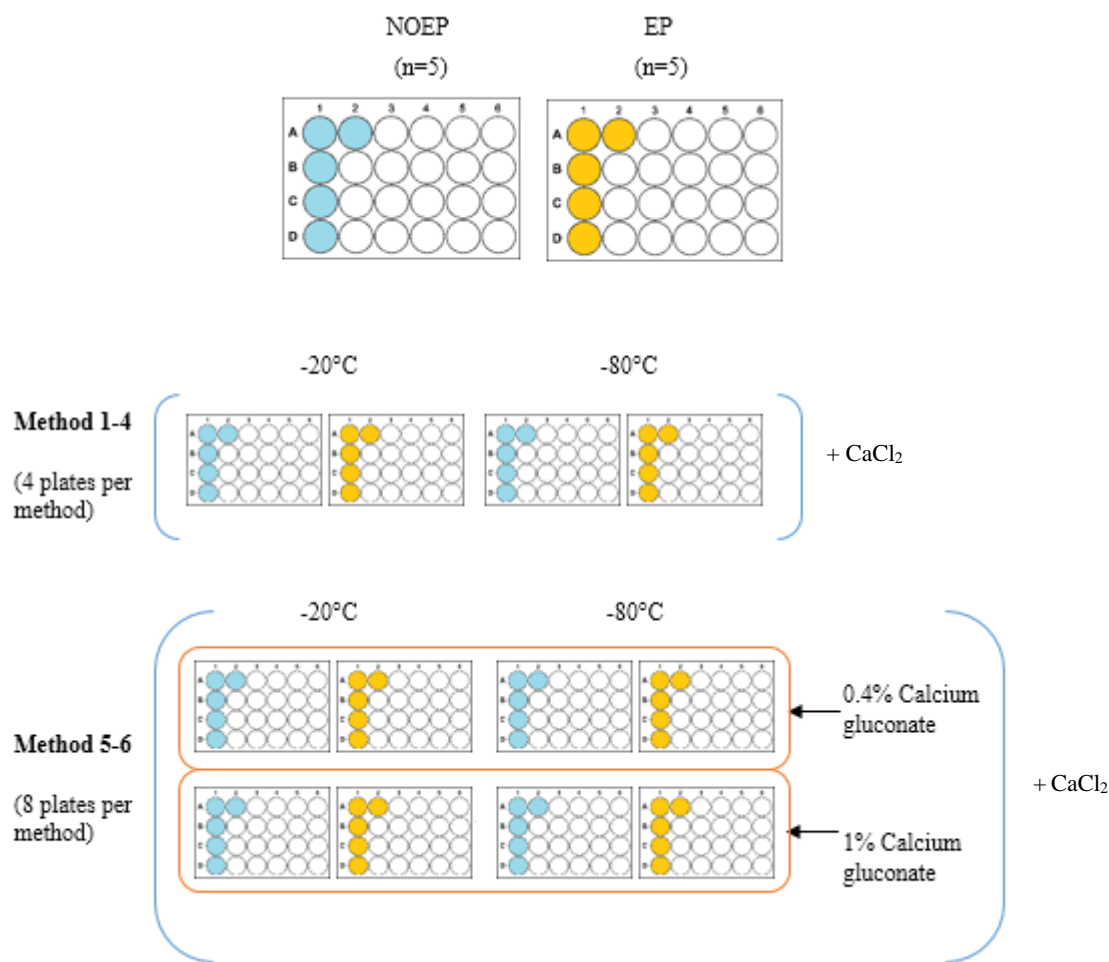


Figure 5.1 Schematic representation of the experimental design used to investigate the impact of various factors on final gel characteristics. In the methods 1 to 4, a single cross-linker (Calcium chloride) was used to create the bonds within the alginate structure. On the other hand, in the methods 5 and 6 double cross-linking was used to produce the scaffolds (calcium gluconate followed by calcium chloride). 5 replicates were prepared for every formulation.

Different methodologies were used in order to compare the degradation and the EP release profiles of the scaffolds over time. In the methods 1 to 4, a single cross-linker (Calcium chloride) was used to create the bonds with alginate. On the other hand, in the methods 5 and 6 double cross-linking was used to produce the scaffolds (calcium gluconate and calcium chloride). Full details on the concentrations of the different components used are provided in Table 1(section 2.3). In the text below each method is explained in detail.

Table 4 Summary of the methodology used to prepare EP alginate scaffolds, .n=5

Methodology	Cross-linker		Freeze-drying cycles	EP addition	
	Calcium Chloride (0.2 M)	Calcium Gluconate (0.4-1%)		Early (in alginate solution)	Late (to the freeze-dried scaffold)
Method 1	✓		2		✓
Method 2	✓		1		✓
Method 3	✓		2	✓	
Method 4	✓		1	✓	
Method 5	✓	✓	2	✓	
Method 6	✓	✓	1	✓	

5.4.2 Single cross-linked scaffold production

5.4.2.1 Introduction

The scaffolds were prepared by the addition of VLVG alginate solution and cross linker solution to individual wells of a 24-well culture plate, followed by periods of freezing and freeze-drying. For each methodology, four 24-well plates of scaffolds were produced. Two of these contained alginate scaffolds that were prepared without EP, one at -20°C and the other one at -80°C, whilst the other two contained scaffolds with EP, one prepared at -20°C and the other one at -80°C. In each plate there were 5 replicate wells. Separating out the samples in this way helped ensure that there would be no accidental exchange of EP between the samples during the various steps of production. 2.78 µL of EP was added to each well sample to provide approximately 25mM EP in each scaffold produced.

5.4.2.2 Method 1

The methodology used to prepare the alginate scaffolds is based on the work of Seung-Man Han, 2006 (Seung-Man Han, 2006) and is summarised in Figure 5.2. 0.5 mL of 2% VLVG alginate solution was added to each well in a 24 well plate. The plate was then stored in the freezer at either -20 or -80°C overnight. The scaffolds were then freeze-dried at -50°C for 24 hours. Once dried, 2.78 µL of EP was gently pipetted into

each scaffold. This mass of EP was selected as it was estimated that this could be measured during the *in vitro* release studies. The scaffolds were then cross-linked by placing them individually in a 1 mL of 0.2 M of CaCl₂ bath in a 24 well plate. After 30 minutes, the CaCl₂ solution was removed and the samples were frozen again overnight for the following cycle of freeze-drying. The use of a second freeze-dry step was used in this method to obtain a dry scaffold which would be easy to store.



Figure 5.2 Schematic representation of method 1.

However, this introduced the possibility that the amount of EP retained by the scaffolds would be reduced due to the use of a second freeze-drying step. In order to understand if this was the case, a second method was therefore investigated (method 2), in which this step was removed.

5.4.2.3 Method 2

This method is similar to method 1, with the key difference being that after the CaCl₂ bath immersion, the samples were placed immediately in 1.5 mL of PBS for the EP release study, omitting the second freeze-drying cycle, as shown in figure 5.3. A schematic representation of this method is shown in figure 5.3.

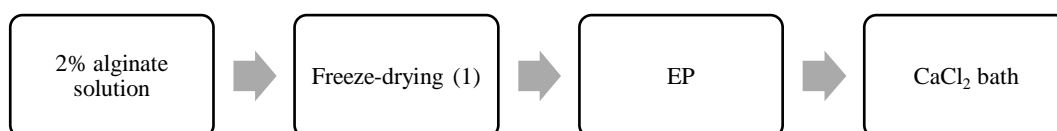


Figure 5.3 Schematic representation of method 2.

In methods 1 and 2, EP was added once the scaffolds were already formed, to avoid any possible EP loss during the first freeze-drying. However, it was unclear if mixing EP with alginate solution in the first step would lead to a better EP retention and altered release kinetics. For this reason, a series of alginate scaffolds were subsequently

produced by addition of EP to alginate solution. These methods (3 and 4) are described below.

5.4.2.4 Method 3

In this method, EP was added to the alginate solution, mixed and stored for 20 minutes at 4-5 °C before placing the plates in the freezer at either -20°C or -80°C. The remainder of the procedure is similar to method 1, with two freeze-drying cycles separated by a cross-linking step performed in a CaCl₂ bath. The schematic representation of the method is shown in figure 5.4.

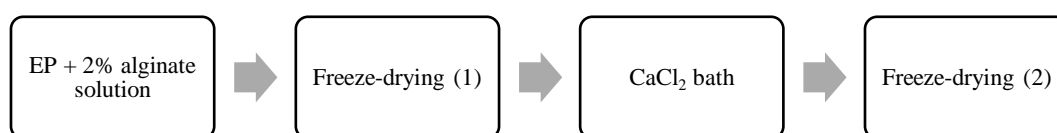


Figure 5.4 Schematic representation of method 3.

5.4.2.5 Method 4

As discussed in section 5.5.2.1.2, the second freeze-dry step may lead to a reduced amount of EP retained by the scaffolds. For that reason, method 4 was investigated, in which the second freeze-drying step was removed, compared to method 3, as shown in figure 5.5.

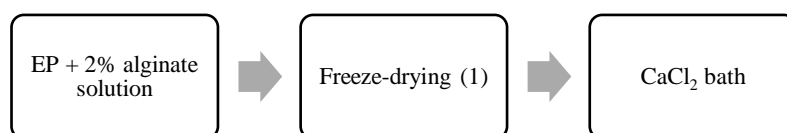


Figure 5.5 Schematic representation of method 4.

The method presented in this section is similar to method 2, but in this case EP was added to the alginate solution, in the first step. The addition of the second cross-linker

calcium gluconate in the preparation of the alginate scaffolds was investigated in method 5 and method 6.

5.4.3 Double cross-linked scaffold production

5.4.3.1 Introduction

The scaffolds were prepared by the addition of VLVG alginate solution and cross linker solution to individual wells of a 24-well culture plate, followed by periods of freezing and freeze-drying. For each methodology, four 24-well plates of scaffolds were produced. Two of these contained alginate scaffolds that were prepared without EP, one at -20°C and the other one at -80°C, whilst the other two contained scaffolds with EP, one prepared at -20°C and the other one at -80°C. In each plate there were 5 replicates. Separating out the samples in this way, helped ensure that there would be no accidental exchange of EP between the samples during the various steps of production.

5.4.3.2 Method 5

In this method double crosslinking was used to prepare the alginate scaffolds. In order to maintain the same EP concentration (25mM) in the scaffold used in the other methods, 5.56 µL of EP was added to each scaffold. The solution was cross-linked by adding 0.5 mL of 0.4% or 1% of calcium gluconate solution to each well and mixed with an immersion mixer and left to rest for 20 minutes in the fridge, before placing the plates in the freezer. The remainder of the procedure is the same as method 1. The schematic representation of method 5 is shown in figure 5.6.

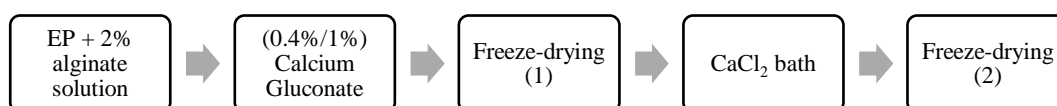


Figure 5.6 Schematic representation of method 5.

Once produced, the scaffolds were placed in 3 mL of PBS for the EP release study. The volume of PBS was doubled, in order to maintain the same scaffold to release medium volume used in the previous experiments. At each time point, half of the

release media was collected and stored in the freezer for EP release measurement. The PBS collected was replaced every time with fresh PBS, in order to maintain constant volume.

5.4.3.3 Method 6

This method is similar to method 5, the only difference being that after the CaCl₂ bath, the samples were placed directly in 3 mL of PBS for the release study, without the second freeze-drying stage, as shown in figure 5.7.

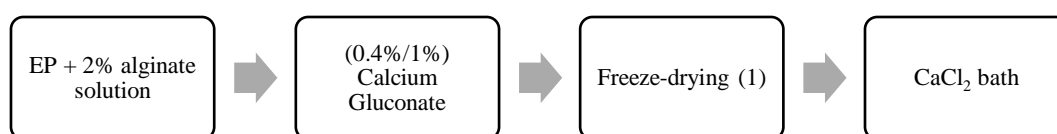


Figure 5.7 Schematic representation of method 6.

All scaffolds prepared as detailed above were stored in situ within the 24-well plates at room temperature prior to subsequent use. The scaffold stability, EP release characteristics and porosity were all then measured, as described in detail in chapter 2.

5.5 Stability of alginate scaffolds *in vitro*

5.5.1 Methodology

The methodology used in this aspect of the study is explained in detail in section 2.3. EP loaded alginate macro-porous scaffolds were prepared as described above (section 5.4.2-5.4.3). The scaffolds were then placed in 1.5 mL (for methods 1-4) and in 3 mL PBS (for method 5-6). The scaffolds were incubated at 37 °C for 28 days. At each time point (1 hour, 1 day, 3 days, 7 days, 14 days, 21 days, 28 days) half of the medium (0.75 mL- 1.5 mL) was collected for drug release measurements, and replaced every time with an equal volume of fresh PBS. Before weighing the scaffolds, all of the surrounding incubation medium was removed, and then the same medium was reinserted within the vial following weighing. The equation in section 1.3.2 was used to measure the swelling ratio, where the “initial weight” is the weight of the scaffold

in its dry form, before adding the PBS in the container and the “final weight” is the weight of the scaffold at each time point after removing the PBS solution.

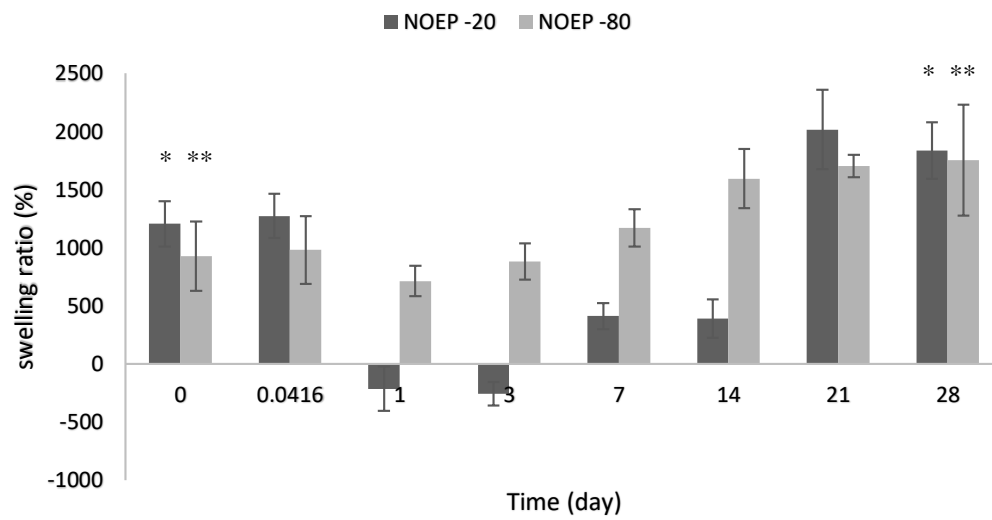
5.5.2 Results

5.5.2.1 *Single cross-linked scaffolds*

5.5.2.1.1 Method 1

The swelling ratio (SR) of the alginate scaffolds, in 1.5 mL of PBS at 37°C, over 28 days, is shown in Figure 5.8. All the scaffolds prepared without EP (Figure 5.8-a) were stable in the first hour, with a SR of approximately 1200% ($1274 \pm 192\%$ for -20°C) and 900% ($982 \pm 292\%$ for -80°C), while after 1 day, a reduction in weight for both scaffolds was observed. After 1 day, the -20°C scaffolds showed a marked reduction in swelling ratio to $-215 \pm 190\%$, followed by an increase from day 7, reaching a peak at day 21 of $2016 \pm 341\%$ (Figure 5.8-a). On the other hand, scaffolds prepared at -80°C showed a less marked reduction in SR at day 1, but then they started swelling again until they reached a maximum peak of $1755 \pm 477\%$ at day 28 of the study. A t-test two tailed distribution, paired analysis ($p < 0.05$) showed that the initial swelling ratio (day 0) and the final one (28 days) of the scaffolds were statistically different, which suggests that the scaffolds went through a change in structure over time.

a)



b)

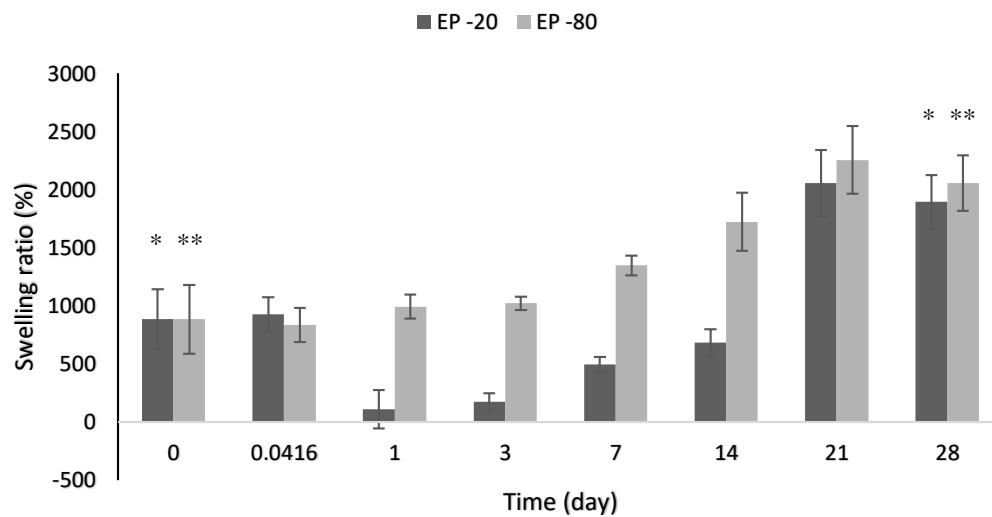


Figure 5.8 Macro-porous alginate scaffolds stability in PBS over 28 days. **A)** Alginate scaffolds without EP and **b)** EP loaded Alginate scaffolds were prepared at either -20°C (NOEP -20) or -80°C (NOEP -80) using method 1, placed in 1.5 mL PBS and incubated at 37°C at constant agitation. Alginate gels were prepared with 0.5 mL 2% alginate solution and cross-linked in a 1mL 0.2M CaCl_2 bath. The swelling ratio was measured at different time point (1 hour, 1 day, 3 days, 7 days, 14 days 21 days, 28 days). The swelling ratio (%) is shown in figure as a measurement of alginate scaffold stability. Data represent the mean \pm st dev from five samples ($*p < 0.05$, compared to zero-day dataset (paired t-test, two tailed).

The swelling ratio of the alginate scaffolds with EP is shown in Figure 5.8-b. Both the scaffolds prepared at -20/ -80°C showed a similar initial swelling ratio of approximately 800%. The scaffolds prepared at -20°C showed a reduction in SR at day one, reaching $110 \pm 166\%$, followed by a slow increase in swelling until reaching the maximum value of $2054 \pm 286 \%$ at day 21. On the other hand, the scaffolds prepared at -80 °C continued swelling from 1h and reached the maximum SR at day 21 ($2255 \pm 92\%$). Although scaffolds prepared at -20°C reduced SR in the first day while -80 °C ones did not, they showed overall a similar behaviour over 28 days, as shown in Figure 5.9, both reaching the maximum swelling point at day 21. In fact, a t-test two tailed distribution analysis ($p < 0.05$) showed no statistical difference between scaffolds prepared at -20°C and at - 80 °C at day 28.

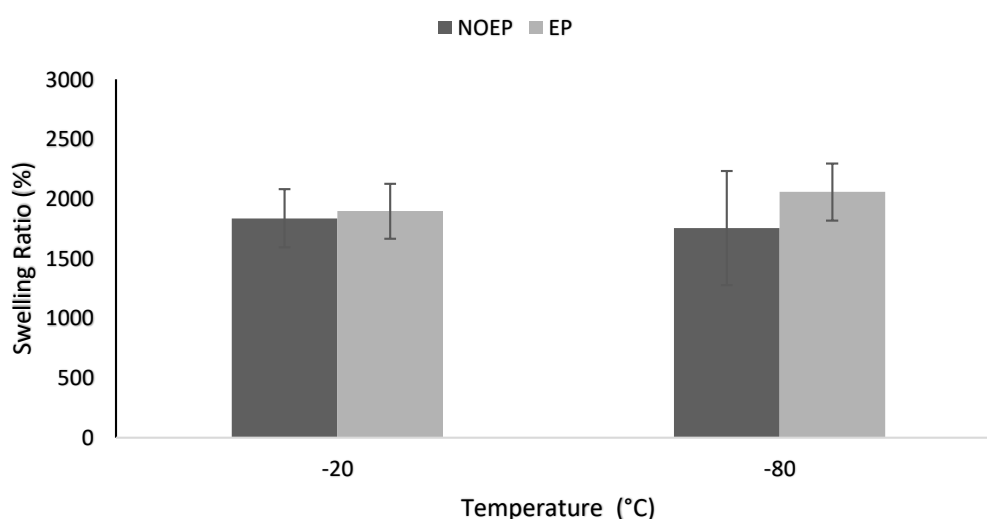


Figure 5.9. Macro-porous alginate scaffolds stability in PBS at day 28. Alginate scaffolds without EP and EP were prepared at either -20 °C or -80°C using method 1, placed in 1.5 mL PBS and incubated at 37°C at constant agitation. Alginate gels were prepared with 0.5 mL 2% alginate solution and cross-linked in a 1mL 0.2M CaCl₂ bath. The swelling ratio was measured at different time point (1 hour, 1 day, 3 days, 7 days, 14 days 21 days, 28 days) but here it is shown only at day 28. The swelling ratio (%) is shown in figure as a measurement of alginate scaffold stability. Data represent the mean \pm st dev from five samples. No significant differences were observed between the datasets.

From the results obtained it appears that the inclusion of EP in the scaffolds did not change the structural stability of the alginate gel materials produced. In fact, a paired

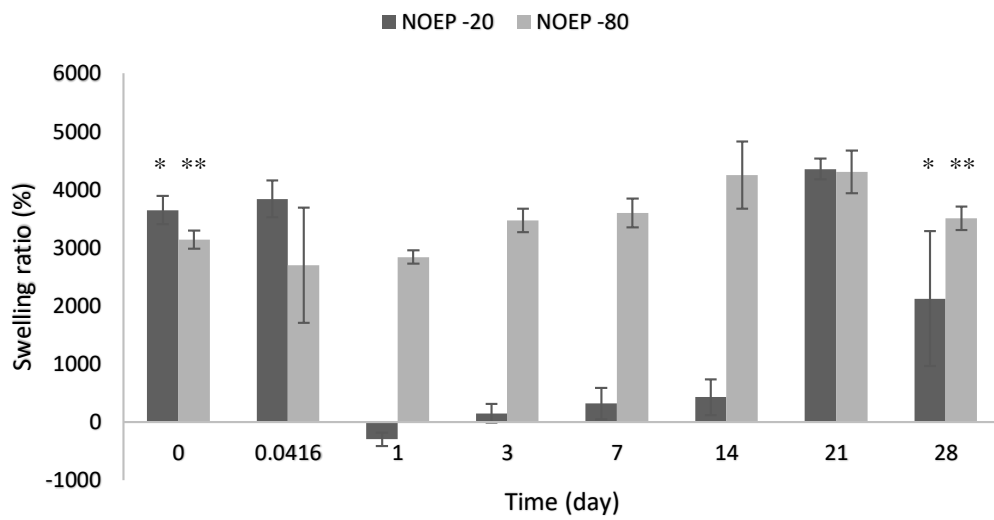
t-test two tailed distribution analysis ($p < 0.05$) showed that there was no statistical difference between scaffolds with and without EP at day 28 (Figure 5.9).

5.5.2.1.2 Method 2

The stability of the alginate scaffolds in 1.5 mL of PBS at 37°C is shown in Figure 5.10. All the scaffolds prepared without EP (Figure 5.10-a) showed an initial loss of weight in the first day of the study, followed by an increase of water intake over the following 3 weeks. A t-test two tailed distribution, paired analysis ($p < 0.05$) confirmed that the initial swelling ratio (day 0) and the final one (28 days) of each of the scaffolds were statistically different. The scaffolds prepared at -20°C showed a gradual increase in SR until they reached the maximum peak of $4355 \pm 181\%$ at day 21. The scaffolds prepared at -80°C showed a reduction in SR after 1h of $2694 \pm 992\%$, followed by a gradual increase in SR as the scaffolds prepared at -20°C, reaching the maximum peak of $4302 \pm 1165\%$ at day 21, similar to the -20°C scaffolds (Figure 5.10-a). At day 28, both the scaffolds prepared at -20°C and at -80°C presented a reduction in swelling ratio of $2124 \pm 1165\%$ and $3505 \pm 203\%$ respectively. A t-test two tailed distribution analysis ($p < 0.05$) confirmed that the scaffolds prepared at -20°C and at -80°C were statistically different at day 28 of the study.

The stability of the alginate scaffolds with EP is shown in Figure 5.10-b. Both the scaffolds prepared at -20/-80°C showed a similar initial SR of 2400%, as well as at the dissolution time (day 21). In fact, a t-test two tailed distribution, analysis ($p < 0.05$) confirmed that the scaffolds prepared at -20°C and at -80°C were not statistically different at the end of the study. The scaffolds prepared at -20°C showed a major loss of mass at day 1 and a consequent complete dissolution at day 21. On the other hand, the scaffolds prepared at -80°C, after a small reduction in SR after 1 hour, they gradually swelled until they reached the maximum peak of 2200% at day 14. After that point, the scaffolds were completely dissolved. From the results obtained, it seems that the presence of EP in these scaffolds lead to an earlier structure degradation (Figure 5.10-b). In fact, a t-test two tailed distribution analysis ($p < 0.05$) confirmed that the scaffolds with EP were statistically different at day 28 of the study as shown in Figure 5.11.

a)



b)

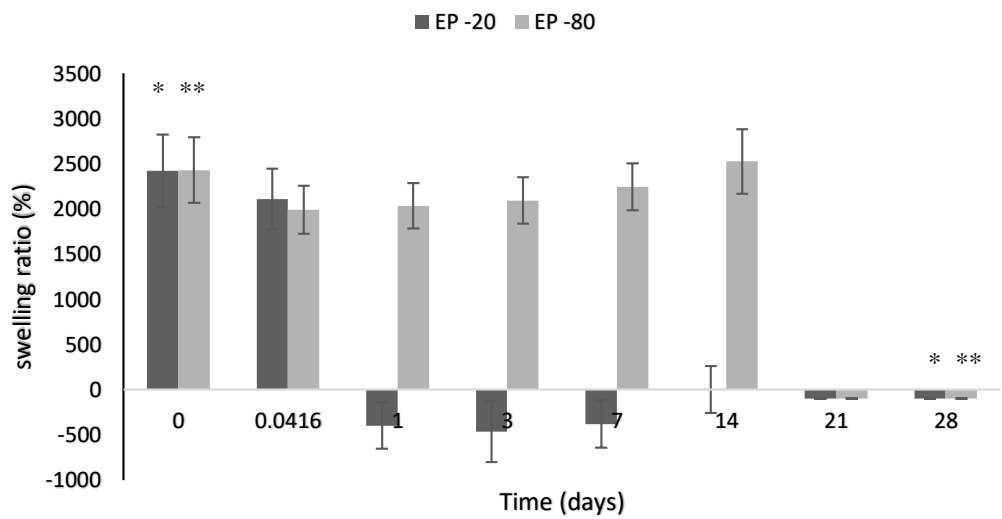


Figure 5.10 Macro-porous alginate scaffolds stability in PBS over 28 days. a) Alginate scaffolds without EP and b) EP loaded alginate scaffolds were prepared at either -20 °C or -80°C using method 2, placed in 1.5 mL PBS and incubated at 37°C at constant agitation. Alginate gels were prepared with 0.5 mL 2% alginate solution and cross-linked in a 1mL 0.2M CaCl₂ bath. The swelling ratio was measured at different time point (1 hour, 1 day, 3 days, 7 days, 14 days 21 days, 28 days). The swelling ratio (%) is showed in figure as a measurement of alginate scaffold stability. Data represent the mean \pm st dev from five samples (*p<0.05).

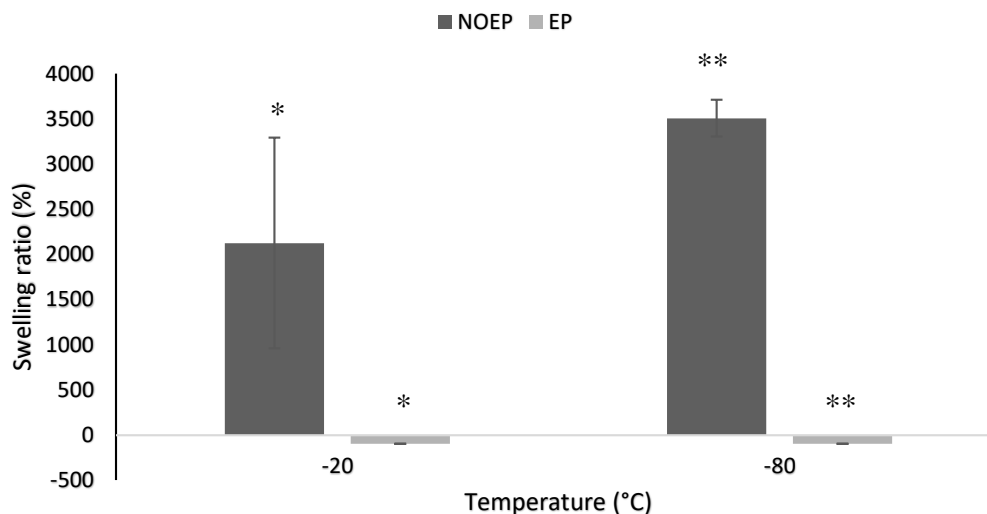


Figure 5.11. Macro-porous alginate scaffolds stability in PBS at day 28. Alginate scaffolds without EP and EP were prepared at either -20 °C or -80°C using method 2, placed in 1.5 mL PBS and incubated at 37°C at constant agitation. Alginate gels were prepared with 0.5 mL 2% alginate solution and cross-linked in a 1mL 0.2M CaCl₂ bath. The swelling ratio was measured at different time point (1 hour, 1 day, 3 days, 7 days, 14 days 21 days, 28 days) but here it is shown only at day 28. The swelling ratio (%) is shown in figure as a measurement of alginate scaffold stability. Data represent the mean \pm st dev from five samples (* p <0.05).

In method 1 (section Method 1 5.4.2.2), scaffolds were prepared with two cycles of freeze-drying. Method 2 was then used to prepare scaffolds with one cycle of freeze-drying, in order to investigate if the second freeze-drying may influence the stability of the scaffolds. Differently from scaffolds prepared with method 1, scaffolds with EP prepared with method 2 were completely dissolved at day 28. A t-test two tailed distribution, analysis ($p \leq 0.05$) of the final swelling ratio of the scaffolds prepared with method 1 and method 2 confirmed that the swelling behaviour of the scaffolds

produced with the two methods (-20°C and -80°C) are significantly different, as shown in Figure 5.12.

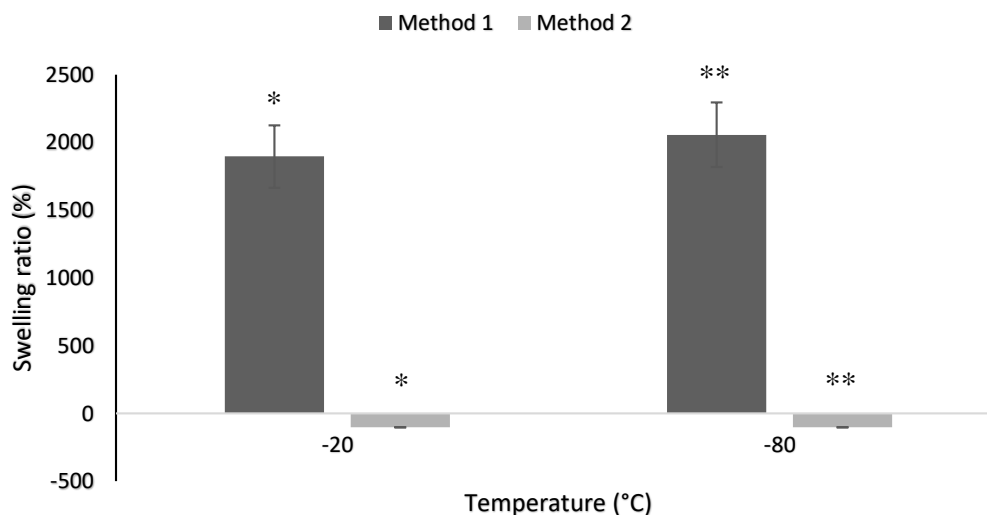


Figure 5.12 Comparison of method 1 and method 2 macro-porous alginate scaffolds stability in PBS at day 28. In method 1 scaffolds were prepared with two cycles of freeze-drying. Method 2 was then used to prepare scaffolds with one cycle of freeze-drying, Alginate scaffolds without EP and EP were prepared at either -20 °C or -80°C, placed in 1.5 mL PBS and incubated at 37°C at constant agitation. Alginate gels were prepared with 0.5 mL 2% alginate solution and cross-linked in a 1mL 0.2M CaCl₂ bath. The swelling ratio was measured at different time point (1 hour, 1 day, 3 days, 7 days, 14 days 21 days, 28 days) but here it is shown only at day 28. The swelling ratio (%) is shown in figure as a measurement of alginate scaffold stability. Data represent the mean \pm st dev from five samples (* $p < 0.05$).

5.5.2.1.3 Method 3

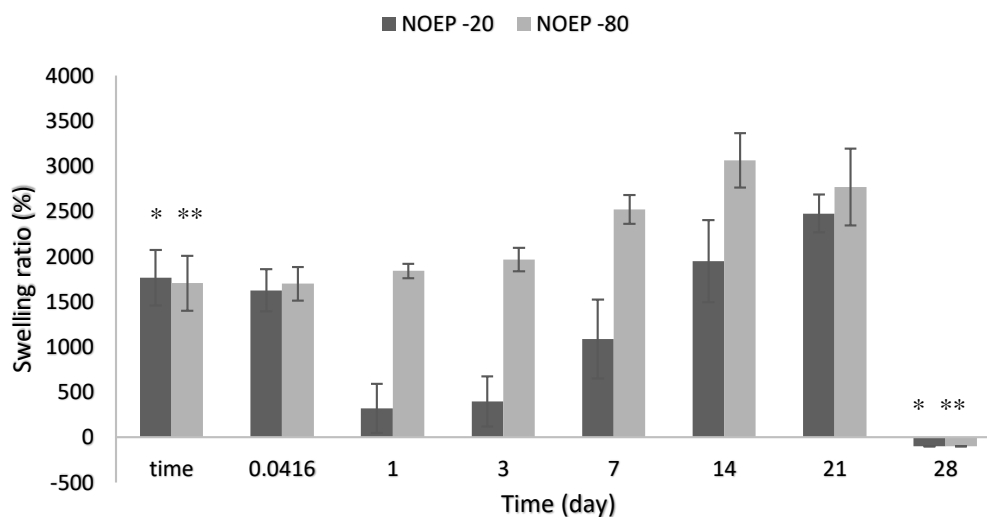
The stability of the alginate scaffolds prepared with method 3 is showed in Figure 5.13. The scaffolds prepared at -20°C without EP (Figure 5.13-a) presented a substantial reduction in SR at day 1, followed by an increase in SR with a maximum peak of $2476 \pm 210\%$ at day 21 and concluded by a complete dissolution of the scaffold at day 28. On the other hand, the scaffolds prepared at -80°C showed a sustained increase of swelling ratio until the maximum peak of $3063 \pm 300\%$ at day 14 and concluded by the complete dissolution of the scaffolds at day 28.

The stability of the alginate scaffolds with EP is shown in Figure 5.13-b. The scaffolds prepared at -20°C (Figure 5.13-b) presented a substantial reduction in SR at day 1

($52 \pm 221\%$), followed by an increase, with a maximum peak of $929 \pm 225\%$ at day 14 and a consequent complete dissolution for 4 scaffolds out of five and the partial dissolution of one scaffold from day 21. On the other hand, the scaffolds prepared at -80°C showed a sustained increase of swelling ratio until the maximum peak of $1946 \pm 147\%$ at day 14 with a consequent complete dissolution for 4 scaffolds out of five and a complete dissolution of one scaffold at day 28, similar to the scaffolds prepared at -20°C . In fact, a t-test two tailed distribution, analysis ($p < 0.05$) confirmed that there was no statistical difference in SR between scaffolds prepared at -20°C and -80°C scaffolds at the end time point of the study.

The maximum swelling ratio observed in the scaffolds without EP was about 2500% - 3000%, while the maximum swelling ratio in the scaffolds with EP decreased to around 1000%-2000% (Figure 5.13-b). It appears that the inclusion of EP lead to a decrease in the maximum swelling ratio. In fact, a t-test two tailed distribution, analysis ($p < 0.05$) showed statistical difference between the scaffolds with and without EP at day 14 (maximum value). On the other hand, a t-test two tailed distribution, analysis ($p < 0.05$) showed no statistical difference between the scaffolds with and without EP at the end of the study.

a)



b)

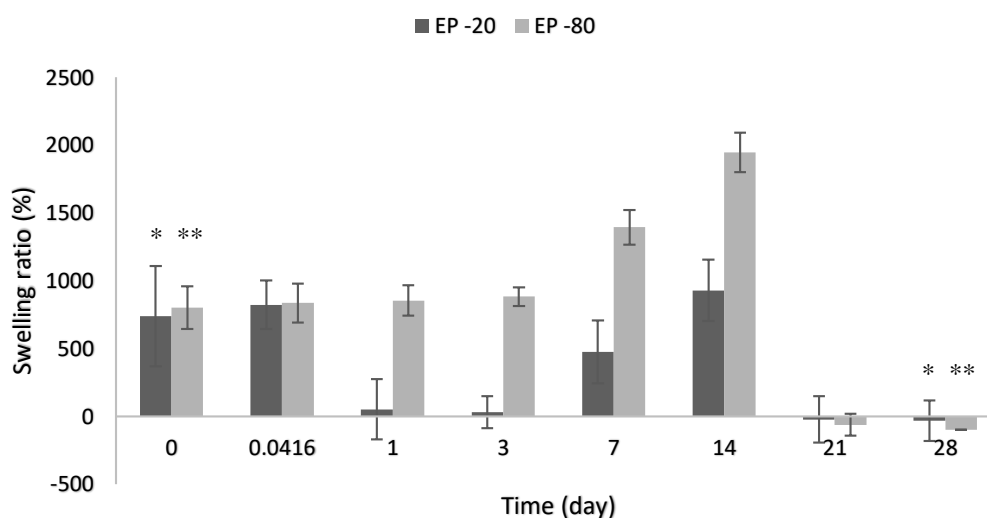


Figure 5.13 Macro-porous alginate scaffolds stability in PBS over 28 days. **a)** Alginate scaffolds without EP and **b)** EP loaded alginate scaffolds were prepared at either -20°C or -80°C using method 3, placed in 1.5 mL PBS and incubated at 37°C at constant agitation. Alginate gels were prepared with 0.5 mL 2% alginate solution and cross-linked in a 1mL 0.2M CaCl_2 bath. The swelling ratio was measured at different time point (1 hour, 1 day, 3 days, 7 days, 14 days 21 days, 28 days). The swelling ratio (%) is showed in figure as a measurement of alginate scaffold stability. Data represent the mean \pm st dev from five samples ($*p<0.05$).

Method 1 and method 3 consisted of the same steps, including 2 cycles of freeze-drying and a CaCl_2 cross-linking step. The main difference between the two methods

is that method 3 involved addition of EP to the alginate solution at the early stage of the scaffold preparation, while in method 1 EP was added once the scaffold had already formed. The two methods were used to investigate if there is a difference in scaffold stability if EP is added early (method 3) or later (method 1). A t-test two tailed distribution, two samples between method 1 and method 3 showed that the two methods were statistically different at the end of the study (day 28), with markedly increased swelling observed in method 1 scaffolds compared to method 3.

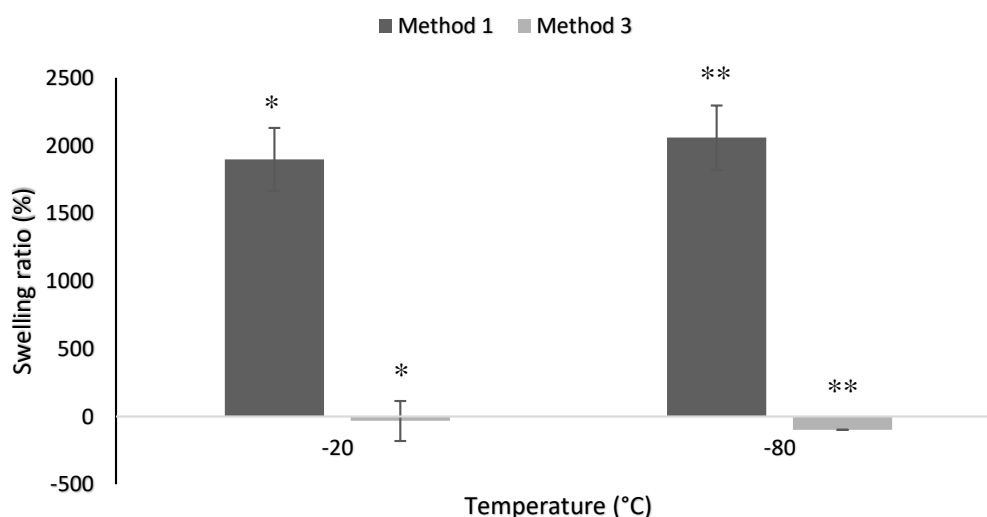


Figure 5.14. Comparison of method 1 and method 3 macro-porous alginate scaffolds stability in PBS at day 28. In method 3 was prepared by adding EP to the alginate solution at the early stage of the scaffold preparation, while in method 1 EP was added at the already formed scaffold. Alginate scaffolds without EP and EP were prepared at either -20 °C or -80°C, placed in 1.5 mL PBS and incubated at 37°C at constant agitation. Alginate gels were prepared with 0.5 mL 2% alginate solution and cross-linked in a 1mL 0.2M CaCl₂ bath. The swelling ratio was measured at different time point (1 hour, 1 day, 3 days, 7 days, 14 days 21 days, 28 days) but here it is shown only at day 28. The swelling ratio (%) is shown in figure as a measurement of alginate scaffold stability. Data represent the mean \pm st dev from five samples (*p<0.05).

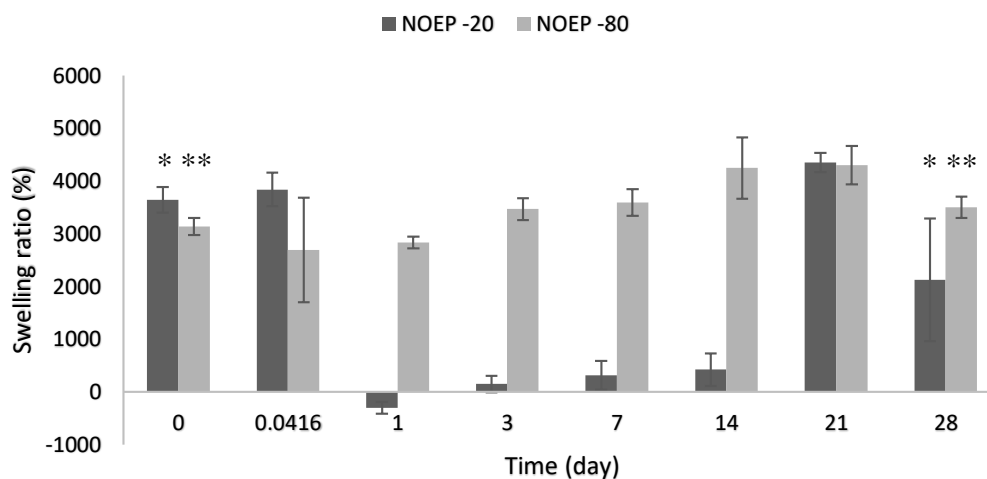
5.5.2.1.4 Method 4

The stability of the alginate scaffolds prepared with method 4 is shown in Figure 5.15. The scaffolds prepared at -20°C without EP (Figure 5.15-a) presented substantial reduction in SR at day 1, followed by an increase in SR with a maximum peak of 4355

$\pm 181\%$ at day 21 and concluded by a reduction of SR at day 28. On the other hand, the scaffolds prepared at -80°C showed a sustained increase of swelling ratio from day 1 until the maximum peak of $4302 \pm 367\%$ at day 21 and concluded by a reduction at day 28.

The stability of the alginate scaffolds with EP is shown in Figure 5.15-b. The scaffolds prepared at -20°C (Figure 5.15-b) presented substantial reduction in SR at day 1, followed by an increase in SR with a maximum peak of $2410 \pm 955\%$ at day 21 with a consequent complete dissolution of the scaffolds at day 28. On the other hand, the scaffolds prepared at -80°C showed a sustained increase of swelling ration until the maximum peak of $2711 \pm 328\%$ at day 14 with a complete dissolution at day 28, similarly to the scaffolds prepared at -20°C . In fact, a t-test two tailed distribution, analysis ($p < 0.05$) confirmed that there was no statistical difference between scaffolds prepared at -20°C and -80°C scaffolds at the end of the study.

a)



b)

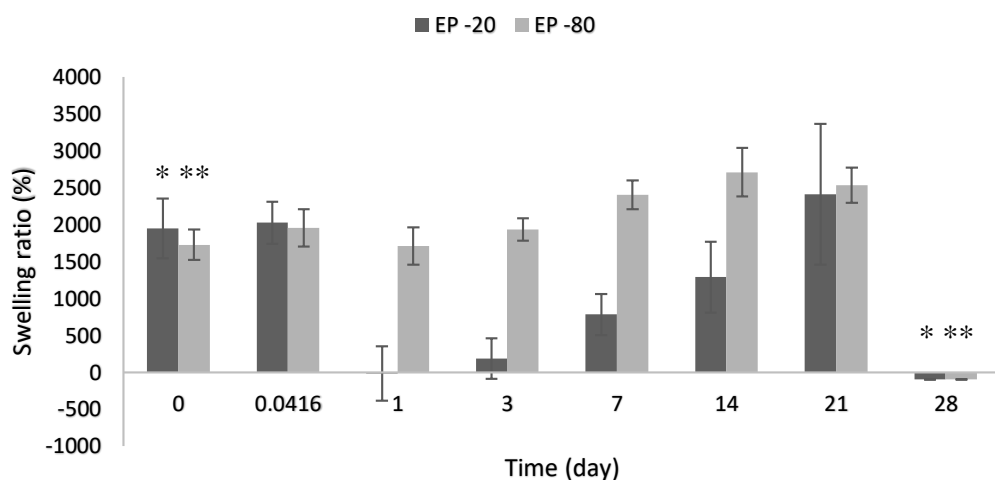


Figure 5.15 Macro-porous alginate scaffolds stability in PBS over 28 days. **a)** Alginate scaffolds without EP and **b)** EP loaded alginate scaffolds were prepared at either -20°C or -80°C using method 4, placed in 1.5 mL PBS and incubated at 37°C at constant agitation. Alginate gels were prepared with 0.5 mL 2% alginate solution and cross-linked in a 1mL 0.2M CaCl_2 bath. The swelling ratio was measured at different time point (1 hour, 1 day, 3 days, 7 days, 14 days 21 days, 28 days). The swelling ratio (%) is showed in figure as a measurement of alginate scaffold stability. Data represent the mean \pm st dev from five samples ($*p<0.05$).

The maximum swelling ratio observed in the scaffolds without EP was about 4300% (4355 \pm 181% for -20°C ; and 4302 \pm 367% for -80°C) (Figure 5.15-a), while the maximum swelling ratio in the scaffolds with EP decreased to around 2400% - 2700%

($2410 \pm 955\%$ for -20°C ; $2711 \pm 328\%$ for -80°C) Figure 5.15-b. A t-test two tailed distribution, analysis ($p < 0.05$) showed statistical difference between the scaffolds at the end of the study (28 day) **Figure 5.15**(Figure 5.16).

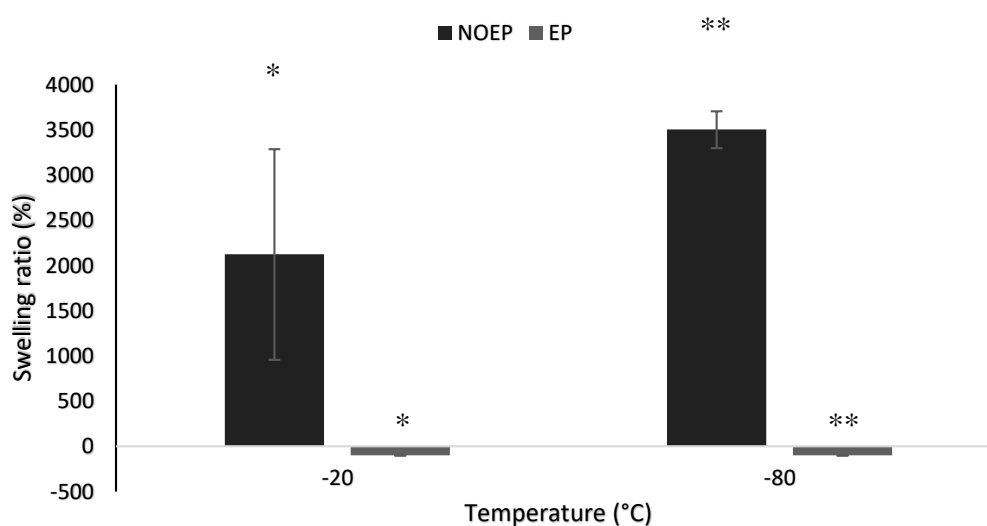


Figure 5.16 Stability in PBS of macro-porous alginate scaffolds prepared with Method 4 at day 28. Alginate scaffolds without EP and EP were prepared at either -20°C or -80°C using method 4, placed in 1.5 mL PBS and incubated at 37°C at constant agitation. Alginate gels were prepared with 0.5 mL 2% alginate solution and cross-linked in a 1mL 0.2M CaCl_2 bath. The swelling ratio was measured at different time point (1 hour, 1 day, 3 days, 7 days, 14 days 21 days, 28 days) but here it is shown the values of the peak (highest swelling ratio which was at day 21 for all the samples except for the ep-80) and the values at day 28. The swelling ratio (%) is shown in figure as a measurement of alginate scaffold stability. Data represent the mean \pm st dev from five samples ($*p < 0.05$).

In method 3 (section 5.4.2.4), scaffolds were prepared with two cycles of freeze-drying. Method 2 was then used to prepare scaffolds similarly to method 3, but with one cycle of freeze-drying, in order to investigate if the second freeze-drying may influence the stability of the scaffolds. A t-test two tailed distribution, analysis ($p < 0.05$) of the final swelling ratio of the scaffolds prepared with method 3 and method 4 showed that the swelling ratios were not statistically different, for scaffolds prepared at both -20°C and -80°C .

Method 2 and method 4 consisted of similar steps, such as 1 cycle of freeze-drying and a CaCl_2 cross-linking. The main difference between the two methods is that method 4 was prepared by adding EP to the alginate solution at the early stage of the scaffold preparation, while in method 2 EP was added at the already formed scaffold. The two

methods were prepared to investigate if there is a difference in scaffold stability if EP is added early (method 4) or later (method 2). A t-test two tailed distribution, two samples between method 2 and method 4 showed no statistical difference between the start and end of the study (day 28).

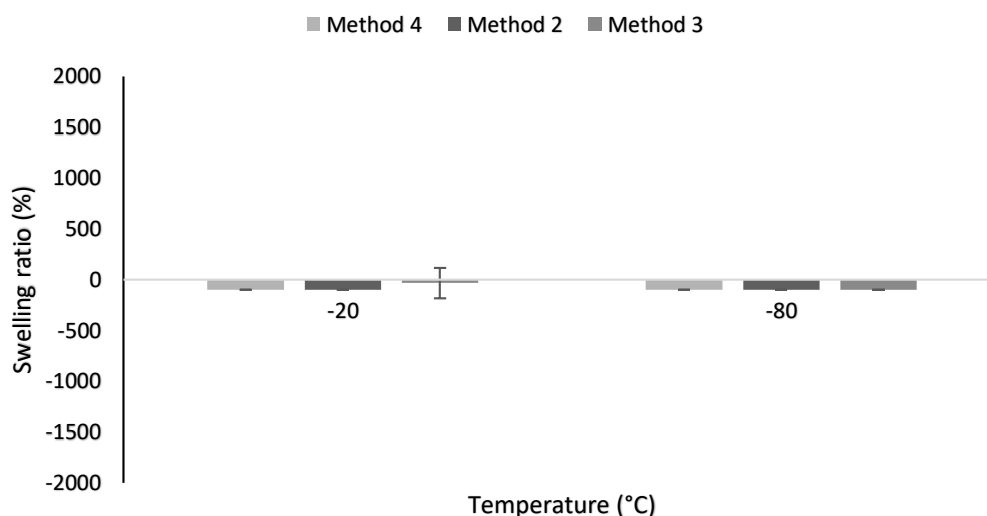


Figure 5.17. Stability study in PBS at 28 days of alginate scaffolds prepared with method 4 compared with the scaffolds prepared with method 2 and method 3. In method 3 scaffolds were prepared with two cycles of freeze-drying, while in Method 4 only one cycle of freeze-drying was used. Method 2 and method 4 consist of similar steps, such as 1 cycles of freeze-drying and CaCl₂ cross-linking bath. The main difference between the two methods is that method 4 was prepared by adding EP to the alginate solution at the early stage of the scaffold preparation, while in method 2 EP was added at the already formed scaffold. Alginate scaffolds without EP and EP were prepared at either -20 °C or -80°C, placed in 1.5 mL PBS and incubated at 37°C at constant agitation. Alginate gels were prepared with 0.5 mL 2% alginate solution and cross-linked in a 1mL 0.2M CaCl₂ bath. The swelling ratio was measured at different time point (1 hour, 1 day, 3 days, 7 days, 14 days 21 days, 28 days) but here it is shown only at day 28. The swelling ratio (%) is shown in figure as a measurement of alginate scaffold stability. Data represent the mean ± st dev from five samples. No Significant differences were observed between the datasets.

5.5.2.2 Double cross-linked scaffolds

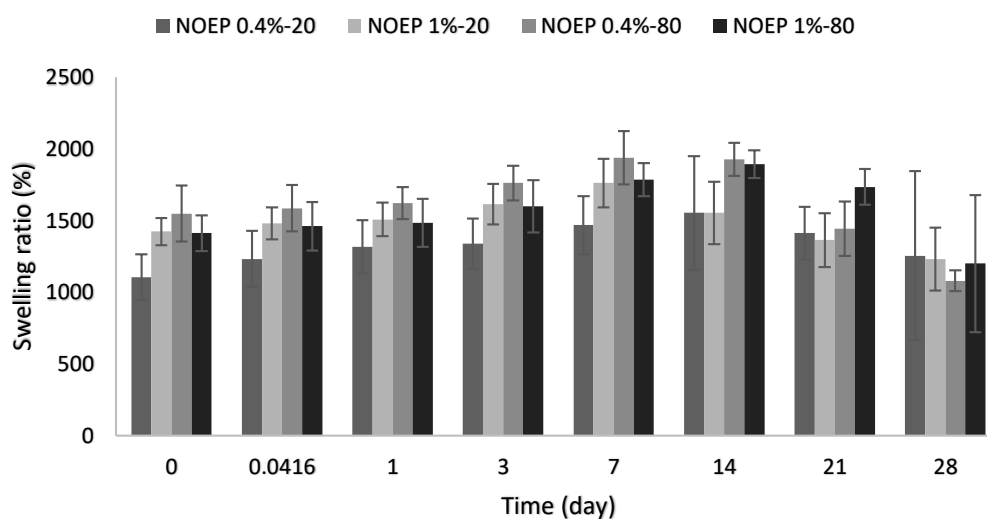
5.5.2.2.1 Method 5

The stability of the alginate scaffolds prepared with method 5 is showed in Figure 5.18. All the scaffolds without EP (Figure 5.18-a) presented a sustained increase of water intake in the first 2 weeks, followed by a gradual loss of weight in the last 2 weeks of the study. In particular, the scaffolds (prepared with 0.4% calcium gluconate at -80°C)

and the scaffolds (1% calcium gluconate prepared at -20°C) had their maximum peaks of respectively $1764 \pm 169\%$ and $1940 \pm 186\%$ at day 7 while the remaining 0.4% calcium gluconate at -20°C and 1% calcium gluconate at -80°C had their peaks of respectively $1555 \pm 397\%$ and $1893 \pm 98\%$ at day 14.

The stability of the alginate scaffolds with EP is shown in Figure 5.18-b. All the scaffolds presented a sustained increase of water intake in the first 2 weeks, reaching the maximum peak at day 14, followed by a gradual loss of weight in the last 2 weeks of the study. Overall, there was no statistical difference between scaffolds prepared at -20°C and -80°C , as well as between scaffolds prepared with different calcium chloride concentrations ($p < 0.05$). At-test two tailed distribution, two samples analysis ($p < 0.05$) showed that there was no statistical difference between the scaffolds with and without EP at 28 day, except for the scaffolds 0.4% alginate prepared at -80°C , as shown in Figure 5.19.

a)



b)

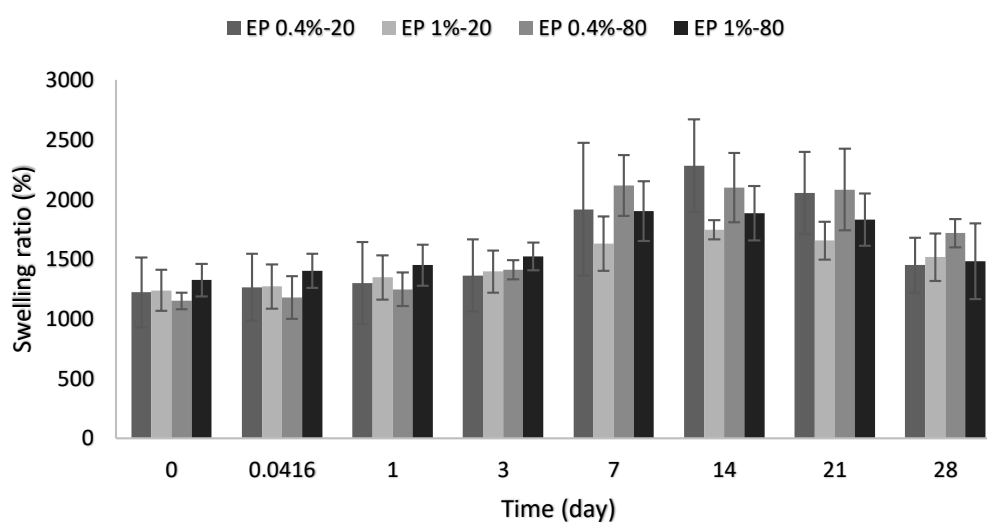


Figure 5.18 Macro-porous alginate scaffolds stability in PBS over 28 days. **a)** Alginate scaffolds without EP and **b)** EP loaded alginate scaffolds were prepared at either -20 °C or -80°C using method 5, placed in 3 mL PBS and incubated at 37°C at constant agitation. Alginate gels were prepared with 0.5 mL 2% alginate solution and double-cross-linked with 0.4-1% Calcium gluconate and 0.2M CaCl₂. The swelling ratio was measured at different time point (1 hour, 1 day, 3 days, 7 days, 14 days 21 days, 28 days). The swelling ratio (%) is showed in figure as a measurement of alginate scaffold stability. Data represent the mean \pm st dev from five samples. No Significant differences were observed between the datasets.

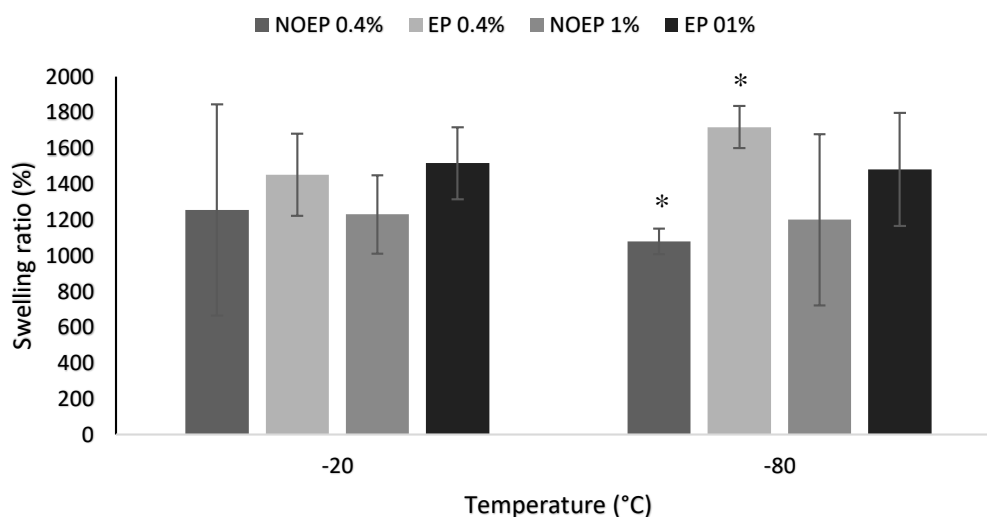


Figure 5.19. Macro-porous alginate scaffolds stability in PBS at day 28. Alginate scaffolds without EP and EP were prepared at either -20 °C (-0.4% Caglu;-1% Caglu) or -80°C (-0.4% Caglu;-1% Caglu) using method 5, placed in 3 mL PBS and incubated at 37°C at constant agitation. Alginate gels were prepared with 0.5 mL 2% alginate solution and 0.5mL of either 0.4% or 1% calcium chloride and placed in a 2mL 0.2M CaCl₂ bath. The swelling ratio was measured at different time point (1 hour, 1 day, 3 days, 7 days, 14 days 21 days, 28 days) but here it is shown only at day 28. The swelling ratio (%) is shown in figure as a measurement of alginate scaffold stability. Data represent the mean \pm st dev from five samples (* p <0.05).

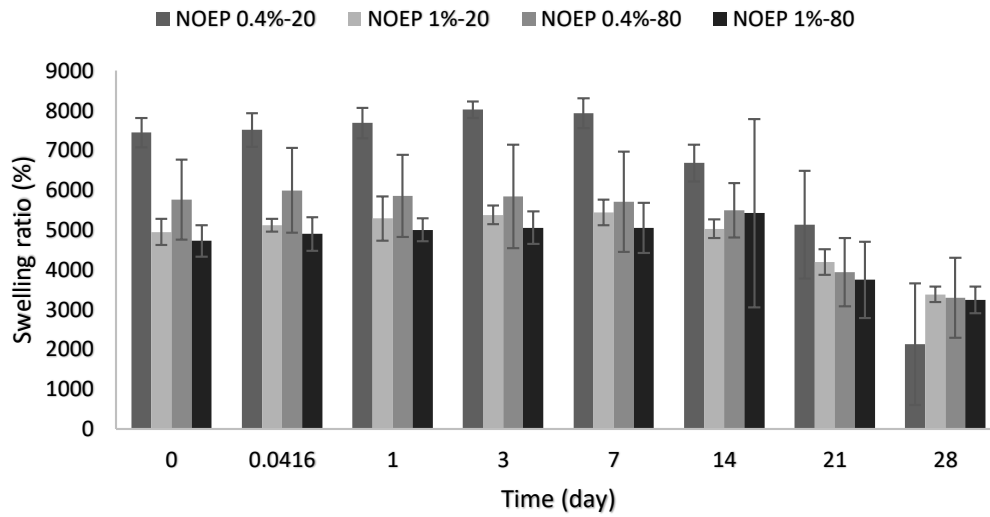
5.5.2.2 Method 6

The stability of the alginate scaffolds prepared with method 6 is shown in Figure 5.20. All the scaffolds prepared without EP (Figure 5.20-a) presented a sustained increase of water intake in the first week, followed by a gradual loss of weight in the last 3 weeks of the study. All the scaffolds presented a maximum peak around 5500% (5443 \pm 323% for the scaffolds prepared with 1% calcium gluconate at -20°C; 5993 \pm 106% for the scaffolds prepared with 0.4% calcium gluconate at -80°C; 5421 \pm 2370% for the scaffolds prepared with 1% calcium gluconate at -80°C), except for the scaffolds prepared with 0.4% calcium gluconate at -20°C, which showed a peak of about 8023 \pm 205% at day 3.

The stability of the alginate scaffolds with EP is shown in Figure 5.20-b. All the scaffolds presented a sustained increase of water intake in the first week, reaching the maximum peak at day 7, followed by a gradual loss of weight in the last 3 weeks of

the study. In particular, the scaffolds prepared with 0.4% calcium gluconate presented a higher water intake compared to the scaffolds prepared with 1% calcium gluconate, with a maximum peak of about 6000% ($6219 \pm 702\%$ for the scaffolds prepared at -20°C ; $6535 \pm 588\%$ for the scaffolds prepared at -80°C), while the scaffolds prepared with 1% calcium gluconate presented a peak of about 4500% ($4528 \pm 396\%$ for the scaffolds prepared at -20°C ; $4281 \pm 403\%$ for the scaffolds prepared at -80°C) (Figure 5.20-b). In fact, a t-test two tailed distribution, equal variance analysis showed that there was a statistical difference between the maximum peaks of the scaffolds prepared with 0.4% calcium gluconate and 1% calcium gluconate, but there was no statistical difference at the end of the study. Overall there was no statistical difference between scaffolds prepared at -20°C or at -80°C at both peaks and at the end of the study.

a)



b)

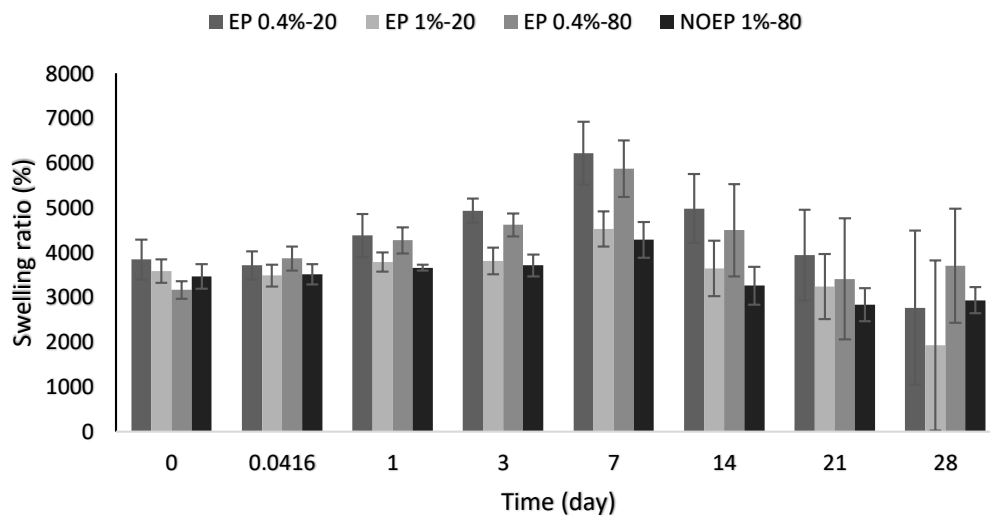


Figure 5.20 Macro-porous alginate scaffolds stability in PBS over 28 days. **a)** Alginate scaffolds without EP and **b)** EP loaded alginate scaffolds. Scaffolds were prepared at either -20°C or -80°C using method 6, placed in 3 mL PBS and incubated at 37°C at constant agitation. Alginate gels were prepared with 0.5 mL 2% alginate solution and double- cross-linked with 0.4-1% Calcium gluconate and 0.2M CaCl_2 . The swelling ratio was measured at different time point (1 hour, 1 day, 3 days, 7 days, 14 days 21 days, 28 days). The swelling ratio (%) is showed in figure as a measurement of alginate scaffold stability. Data represent the mean \pm st dev from five samples. No Significant differences were observed between the datasets.

A t-test two tailed distribution, equal variance analysis ($p < 0.05$) indicated that there was no statistical difference between the scaffolds with and without EP at the end of the study, as shown in Figure 5.21.

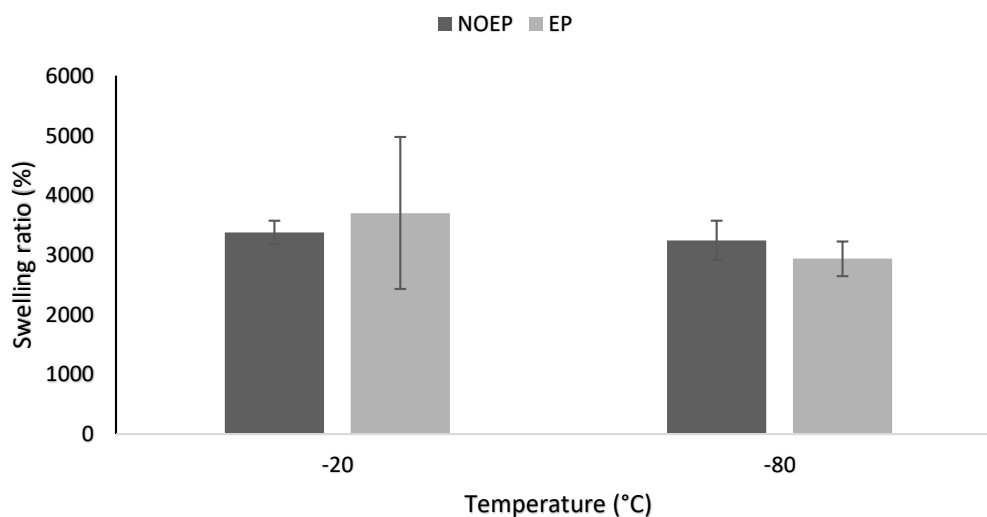


Figure 5.21. Macro-porous alginate scaffolds stability in PBS at day 28 prepared with method 6. Alginate scaffolds without EP and EP were prepared at either -20°C (-0.4% Caglu; -1% Caglu) or -80°C (-0.4% Caglu; -1% Caglu) using method 6, placed in 3 mL PBS and incubated at 37°C at constant agitation. Alginate gels were prepared with 0.5 mL 2% alginate solution and 0.5 mL of either 0.4% or 1% calcium chloride and placed in a 2 mL 0.2M CaCl_2 bath. The swelling ratio was measured at different time point (1 hour, 1 day, 3 days, 7 days, 14 days 21 days, 28 days) but here it is shown only at day 28. The swelling ratio (%) is shown in figure as a measurement of alginate scaffold stability. Data represent the mean \pm st dev from five samples. No Significant differences were observed between the datasets.

In method 5 (section 5.4.3.2), scaffolds were prepared with two cycles of freeze-drying. Method 6 was then used to prepare scaffolds similarly to method 5, but with one cycle of freeze-drying (section 5.4.3.3), in order to investigate if the second freeze-drying may influence the stability of the scaffolds. A t-test two tailed distribution, analysis ($p < 0.05$) of the final swelling ratio of the scaffolds prepared with method 5 and method 6 showed that the two methods are not statistically different for the scaffolds prepared with 0.4% calcium gluconate, while the scaffolds prepared with 1% calcium gluconate were statistically different, as shown in Figure 5.22.

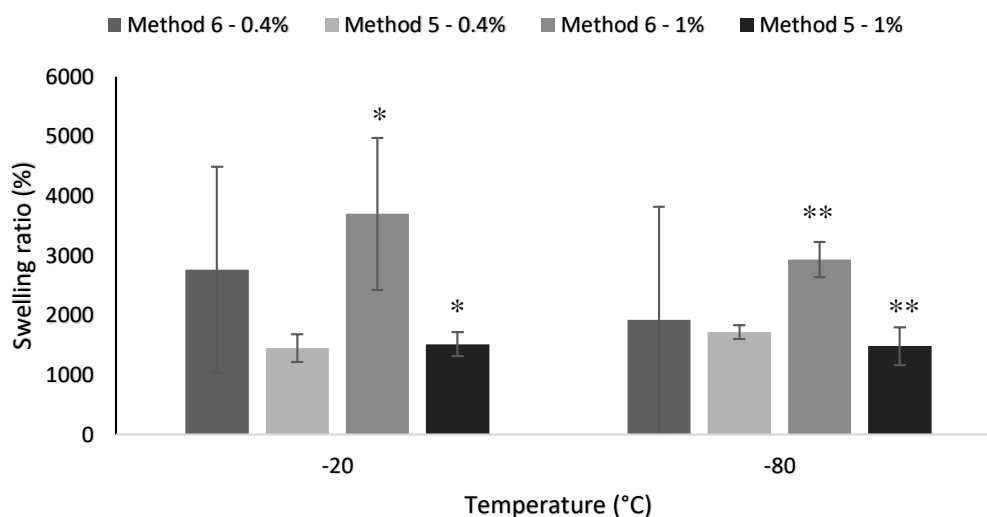


Figure 5.22. Comparison of stability of macro-porous alginate scaffolds at day 28 prepared with method 6 and method 5. In method 5, scaffolds were prepared with two cycles of freeze-drying, while in method 6 one cycle of freeze-drying was used. Alginate scaffolds without EP and EP were prepared at either -20 °C (-0.4% Caglu;-1% Caglu) or -80°C (-0.4% Caglu;-1% Caglu) using method 6, placed in 3 mL PBS and incubated at 37°C at constant agitation. Alginate gels were prepared with 0.5 mL 2% alginate solution and 0.5mL of either 0.4% or 1% calcium chloride and placed in a 2mL 0.2M CaCl₂ bath. The swelling ratio was measured at different time point (1 hour, 1 day, 3 days, 7 days, 14 days 21 days, 28 days) but here it is shown only at day 28. The swelling ratio (%) is shown in figure as a measurement of alginate scaffold stability. Data represent the mean \pm st dev from five samples (* p <0.05).

5.6 *In vitro* ethyl pyruvate release study from alginate sponges

Methods

The general methodology used in this part of the study has been explained in detail in section 2.4, so only important additional details are provided in the following description. EP loaded alginate macro-porous scaffolds were prepared as previously described (section 5.4.2-5.2.3). The scaffolds were then placed in 1.5 - 3 mL PBS (different volumes were used to maintain a constant scaffold to release medium ratio) and incubated at 37 °C for 28 days. At each time point (1 hour, 1 day, 3 days, 7 days, 14 days 21 days, 28 days) half of the medium (0.75 mL- 1.5 mL) was collected for drug release measurements, and replaced every time with an equal volume of fresh PBS. The samples collected were stored at -20°C and defrosted to allow EP

measurement. EP was measured with the Nanospec using the methodology described in section 2.5.

Results

5.6.1 Alginate scaffolds cross-linked with CaCl₂

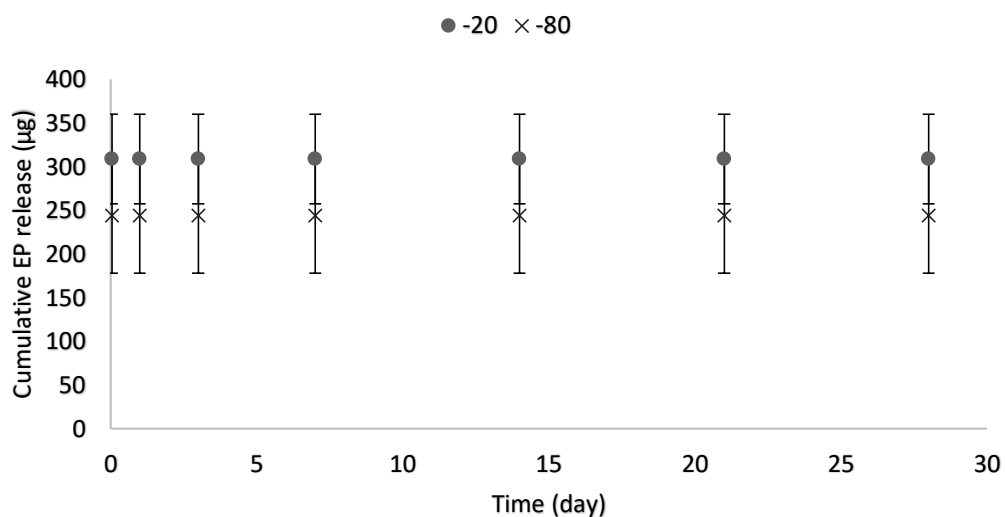
5.6.1.1 Method 1

The cumulative EP release profiles from the scaffolds produced with method 1 are shown in Figure 5.23-a. The two profiles are respectively the scaffolds produced at -20°C and the scaffolds produced at -80°C.

The scaffolds produced at -20°C appeared to release more EP than those scaffolds that were prepared at -80°C scaffolds, with approximately 300 ± 51 µg being released in the first hour from the -20°C compared to 250 ± 66 µg in the same period from the -80°C patches. A t-test two tailed, equal variance distribution analysis showed that there was no statistical difference in the EP release at day 28 from the scaffolds prepared at -20°C and those prepared at -80°C. EP release appears to be complete within the first hour, with no further release observed at later time points up to 28 days.

The percentage of EP released by the scaffolds shown in Figure 5.23-b. was calculated by using as a 100% the cumulative EP released after 28 days (n=5). Both types of scaffolds showed the same release profile, with 100% of EP released in the first hour (Figure 5.23-b).

a)



b)

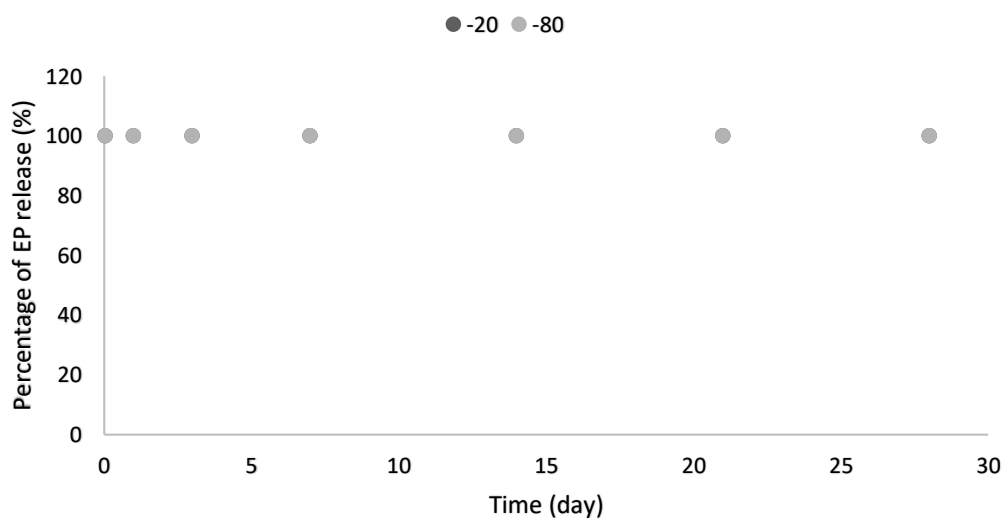


Figure 5.23 EP release study from alginate scaffolds. a) Cumulative EP release profile and b) percentage of EP released from scaffolds produce using method 1 (-20 and -80 values are shown but overlapping). Scaffolds were produced with an initial concentration of 2% alginate with two cycles of freeze-drying. EP was added to the scaffolds after the first freeze-drying cycle, before the CaCl₂ bath. Data represent the mean \pm st dev from five samples No Significant differences were observed between the datasets).

5.6.1.2 Method 2

The cumulative EP release profiles from the scaffolds produced with method 2 are shown in Figure 5.24-a. The two profiles are respectively the scaffolds produced at -20°C and the scaffolds produced at -80°C.

The scaffolds prepared at different temperature show similar EP release profiles, with an initial EP release of about 1000 µg (986± 277 µg for the scaffolds prepared at -20°C; 964 ±141 µg for the scaffolds prepared at -80°C) in the first hour, followed by a sustained release over the first week. The remaining EP was released over the following 3 weeks. The total cumulative EP released for both scaffold types was approximately 1,850 µg (1799 ± 595 µg for the scaffolds prepared at -20°C; 1805 ± 299 µg for the scaffolds prepared at -80°C). There was no statistical difference in total cumulative EP release between scaffolds prepared at -20°C and at -80°C.

The percentage of EP released by the scaffolds is shown in Figure 5.24-b. Both types of scaffolds showed similar release profile, with 55% of EP released in the first hour, reaching almost 90% (96 ± 2% for the scaffolds prepared at -20°C; 89 ± 6% for the scaffolds prepared at -80°C) after 3 days (Figure 5.24-b). The remaining EP was then released slowly over the following weeks.

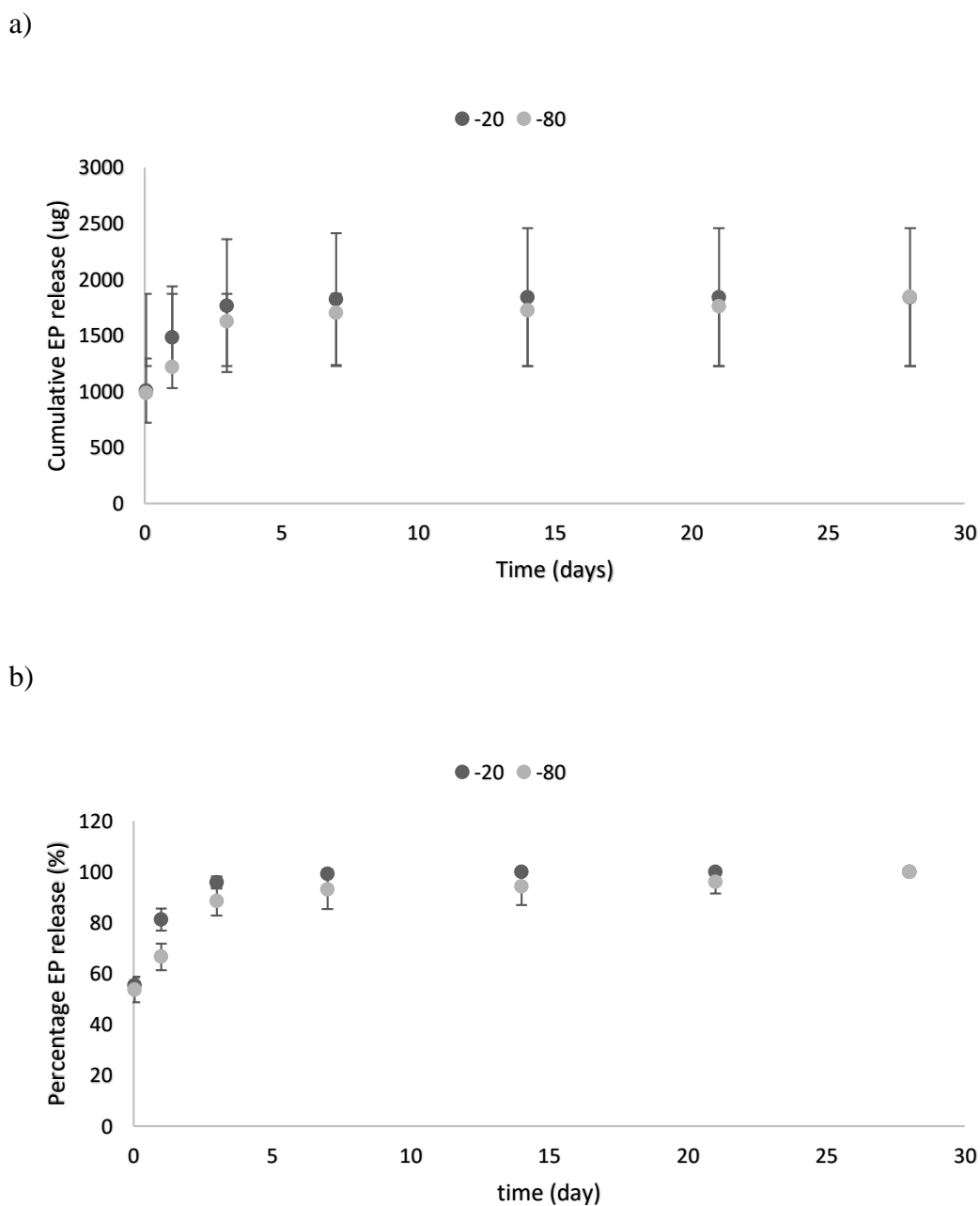


Figure 5.24 EP release study from alginate scaffolds. a) Cumulative EP release profile and b) percentage of EP released from scaffolds produce using method 2. Scaffolds were produced with an initial concentration of 2% alginate with one cycle of freeze-drying. EP was added to the scaffolds after the freeze-drying cycle, before the CaCl₂ bath. Data represent the mean \pm st dev from five samples.

In method 1 (section 5.4.2.2), scaffolds were prepared with two cycles of freeze- drying. Method 2 was then used to prepare scaffolds with one cycle of freeze-

drying, in order to investigate if the second freeze-drying may influence EP retention and release. The scaffolds produced with method 2 showed an extended EP release compared to the scaffolds produced with method 1. It appears that the second freeze-drying step performed in method 1 interfered with the EP incorporation in some way, which is maintained instead in this second method. A t-test two tailed distribution, analysis ($p < 0.05$) of the cumulative EP release of the scaffolds prepared with method 1 and method 2 showed that the two methods are statistically different, as shown in Figure 5.25.

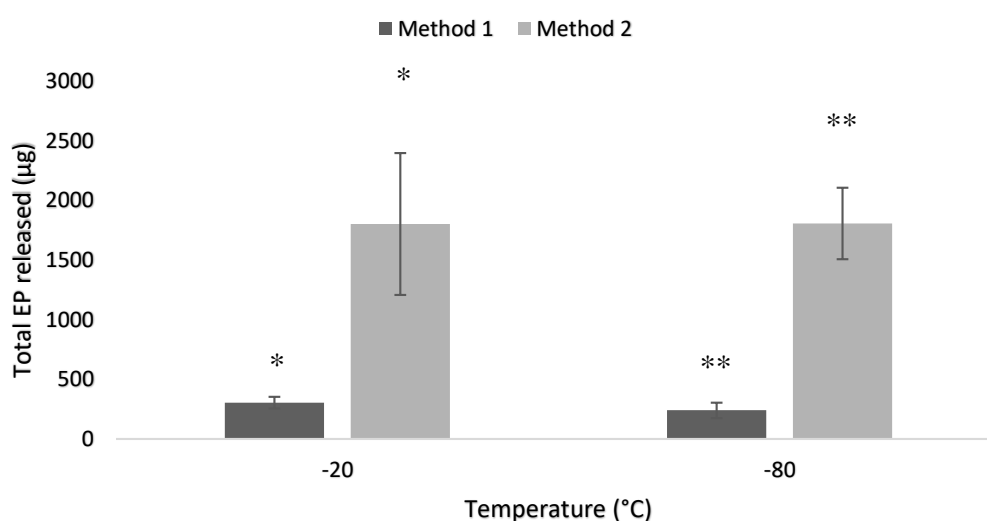


Figure 5.25. Comparison of total EP release from Alginate scaffolds prepared at either -20°C or -80°C using method 1 and method 2. In method 1 scaffolds were prepared with two cycles of freeze-drying. Method 2 was then used to prepare scaffolds with one cycle of freeze-drying, Alginate scaffolds without EP and EP were prepared at either -20°C or -80°C , placed in 1.5 mL PBS and incubated at 37°C at constant agitation. Alginate gels were prepared with 0.5 mL 2% alginate solution and cross-linked in a 1mL 0.2M CaCl_2 bath. EP release was measured at different time point (1 hour, 1 day, 3 days, 7 days, 14 days 21 days, 28 days) but here it is shown the total EP release of the scaffolds. Data represent the mean \pm st dev from five samples ($*p < 0.05$).

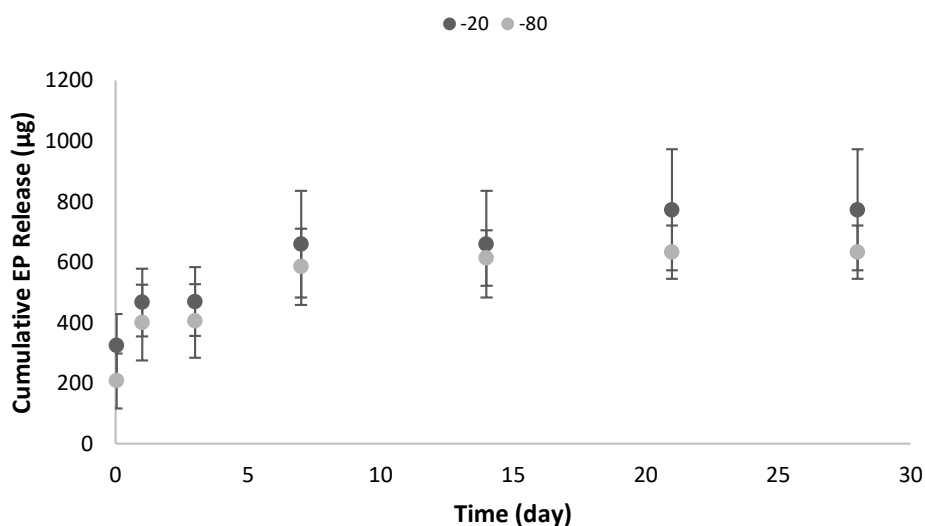
5.6.1.3 Method 3

The cumulative EP release profiles from the scaffolds produced with method 3 are shown in Figure 5.26-a. The two profiles are respectively the scaffolds produced at -20°C and the scaffolds produced at -80°C .

The scaffolds produced at -20°C showed a total EP release of $753 \pm 197 \mu\text{g}$, higher than the -80°C scaffolds which released $613 \pm 89 \mu\text{g}$, although the t-test two tailed, equal variance analysis showed no statistical difference between the scaffolds prepared at different temperatures. The -80°C scaffolds released almost all of the EP in the first 7 days, which is similar to the release profile from the scaffolds produced with method 2. On the other hand, the scaffolds produced at -20°C released most of the EP after 21 days. Both the release profiles presented intervals where EP was not released. The t-test, two tailed distribution analysis showed that there was no statistical difference in cumulative EP release between scaffolds prepared at -20°C or at -80°C .

The percentage of EP released by the scaffolds is shown in Figure 5.26-b. Both types of scaffolds showed a similar release profile, with about 60% of EP ($61 \pm 7\%$ for the scaffolds prepared at -20°C ; $64 \pm 16\%$ for scaffolds produced at -80°C) released in the first day, reaching 90% after 7 days (Figure 5.26-b). The remaining EP was then released slowly over the following 3 weeks.

a)



b)

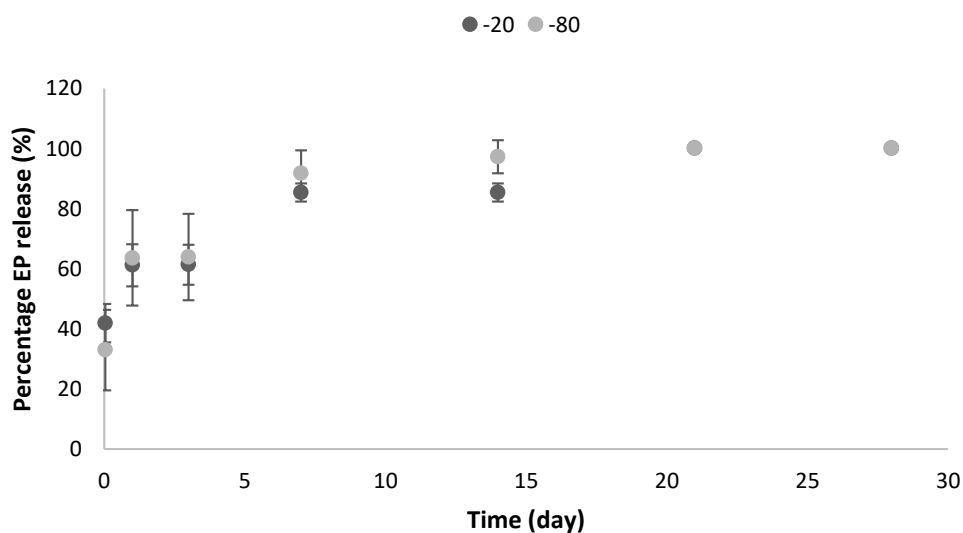


Figure 5.26 EP release study from alginate scaffolds. a) Cumulative EP release profile and b) percentage of EP released from scaffolds produce using method 3. Scaffolds were produced with an initial concentration of 2% alginate with two cycles of freeze-drying. EP was added to the alginate solution before the first freeze-drying cycle. Data represent the mean \pm st dev from five samples.

In method 1 (section 5.4.2.2), EP was added to the formed scaffolds after the first freeze-drying cycle. In order to understand if an earlier addition of EP in the process

of scaffold preparation would have led to a better EP retention, method 3 was then used to prepare the scaffolds. It appears early addition of EP to the alginate solution before the formation of the scaffold (method 3) showed an extended EP release compared to the scaffolds produced with method 1. A t-test two tailed distribution, analysis ($p < 0.05$) showed that the cumulative EP release of the scaffolds prepared with method 1 and method 3 were statistically different, as shown in Figure 5.27.

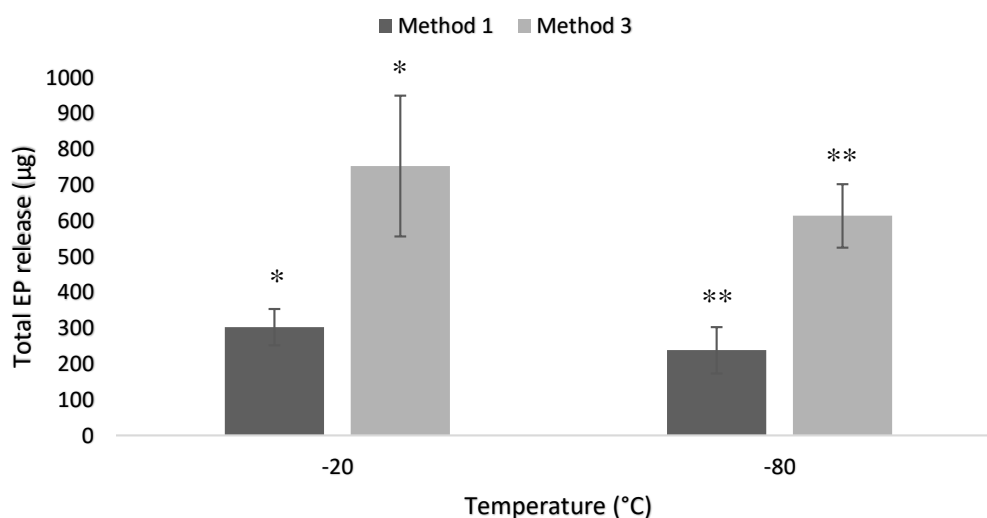


Figure 5.27. Comparison of total EP release from Alginate scaffolds prepared at either -20°C or -80°C using method 1 and method 3. In method 1 EP was added to the formed scaffolds after the first freeze-drying cycle, while in method 3 EP was added to the alginate solution, at the early stage of alginate scaffold preparation. Alginate scaffolds without EP and EP were prepared at either -20°C or -80°C , placed in 1.5 mL PBS and incubated at 37°C at constant agitation. Alginate gels were prepared with 0.5 mL 2% alginate solution and cross-linked in a 1mL 0.2M CaCl_2 bath. EP release was measured at different time point (1 hour, 1 day, 3 days, 7 days, 14 days 21 days, 28 days) but here it is shown the total EP release of the scaffolds. Data represent the mean \pm st dev from five samples ($*p < 0.05$).

5.6.1.4 Method 4

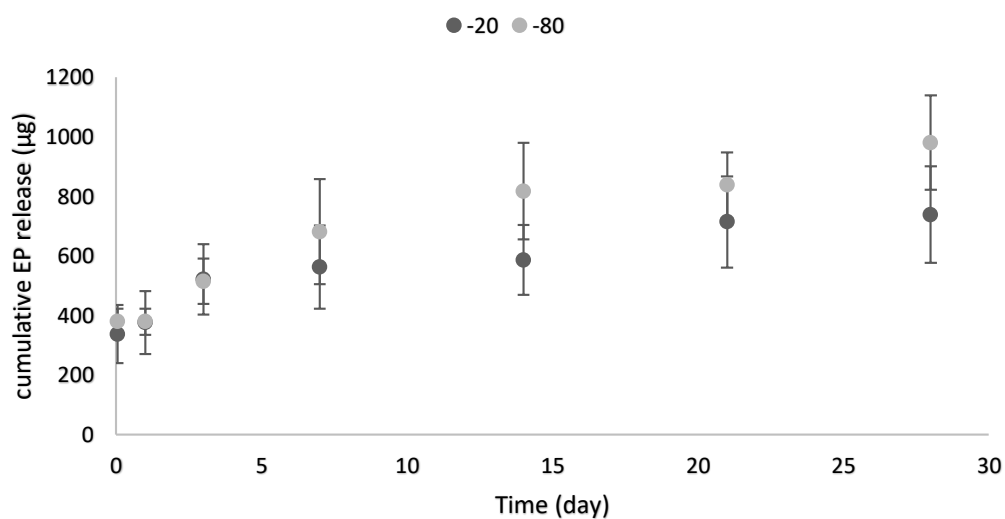
The cumulative EP release profiles from the scaffolds produced with method 4 are shown in Figure 5.28-a. The two profiles are respectively the scaffolds produced at -20°C and the scaffolds produced at -80°C .

The total cumulative EP released for the scaffolds prepared at -20°C was $716 \pm 160 \mu\text{g}$, while the scaffolds prepared at -80°C released $956 \pm 156 \mu\text{g}$ in total. A

t-test, two tailed, equal variance analysis showed that the cumulative EP release of the scaffolds prepared at -20°C and at -80°C were statistically different. Both the formulations released about $500\ \mu\text{g}$ of EP over the first 3 days ($508 \pm 118\ \mu\text{g}$ for the scaffolds prepared at -20°C ; $503 \pm 75\ \mu\text{g}$ for the scaffolds prepared at -80°C). For the scaffolds produced at -80°C , the initial burst was followed by a slow release over the following 10 days with a final burst in the third week. The formulation at higher temperature (-20°C) showed a constant release over the first 2 weeks, followed by a week of no release and a final burst of about $200\ \mu\text{g}$ in the last week (Figure 5.28-a).

The percentage of EP released by the scaffolds is shown in Figure 5.28-b. Alginate scaffolds prepared at -20°C released 40% of EP in the first hour, while the scaffolds prepared at -80°C released almost 50%. Both types of scaffolds released about 75% after 7 days (Figure 5.28-b). The remaining EP was then released slowly over the following weeks.

a)



b)

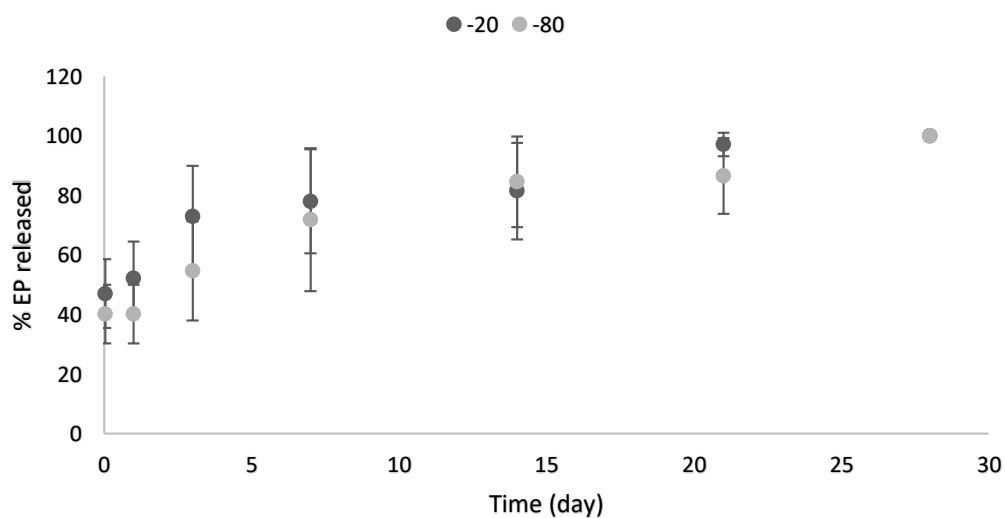


Figure 5.28 EP release study from alginate scaffolds. a) Cumulative EP release profile and b) percentage of EP released from scaffolds produce using method 4. Scaffolds were produced with an initial concentration of 2% alginate with one cycle of freeze-drying. EP was added to the alginate solution before the first freeze-drying cycle. Data represent the mean \pm st dev from five samples.

In method 3 (section 5.4.2.45.4.2.2), scaffolds were prepared with two cycles of freeze- drying. Method 4 was then used to prepare scaffolds with one cycle of freeze-

drying, in order to investigate if the second freeze-drying may influence EP retention and release. A t-test two tailed distribution, analysis ($p < 0.05$) showed that the cumulative EP release of the scaffolds prepared with method 3 and method 4 were not statistically different for the scaffolds prepared at -20°C , but they were statistically different for the scaffolds prepared at -80°C , as shown in Figure 5.29.

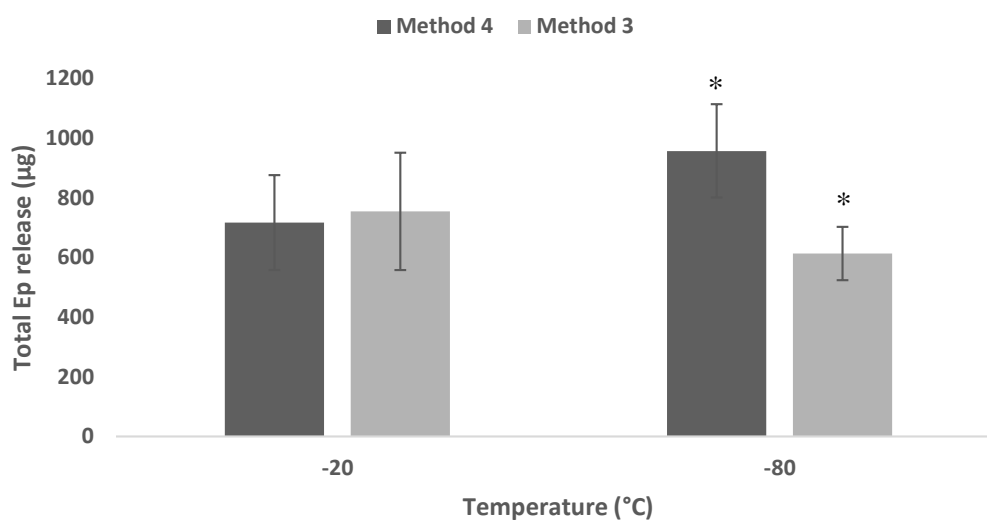


Figure 5.29. Comparison of total EP release from Alginate scaffolds prepared at either -20°C or -80°C using method 4 and method 3. In method 3 scaffolds were prepared with two cycles of freeze-drying. Method 4 was then used to prepare scaffolds with one cycle of freeze-drying. Alginate scaffolds without EP and EP were prepared at either -20°C or -80°C , placed in 1.5 mL PBS and incubated at 37°C at constant agitation. Alginate scaffolds were prepared with 0.5 mL 2% alginate solution and cross-linked in a 1mL 0.2M CaCl_2 bath. EP release was measured at different time point (1 hour, 1 day, 3 days, 7 days, 14 days 21 days, 28 days) but here it is shown the total EP release of the scaffolds. Data represent the mean \pm st dev from five samples (* $p < 0.05$).

In method 2 (section 5.4.2.3), EP was added to the formed scaffolds after the freeze-drying cycle. In order to understand if an earlier addition of EP in the process of scaffold preparation would have led to a better EP retention, method 4 was then used to prepare the scaffolds. It appears early addition of EP to the alginate solution before the formation of the scaffold (method 4) showed a statistical decrease in EP release compared to the scaffolds produced with method 2. In fact, a t-test two tailed distribution, analysis ($p < 0.05$) showed that the cumulative EP release of the scaffolds prepared with method 2 and method 4 were statistically different, as shown in Figure 5.30.

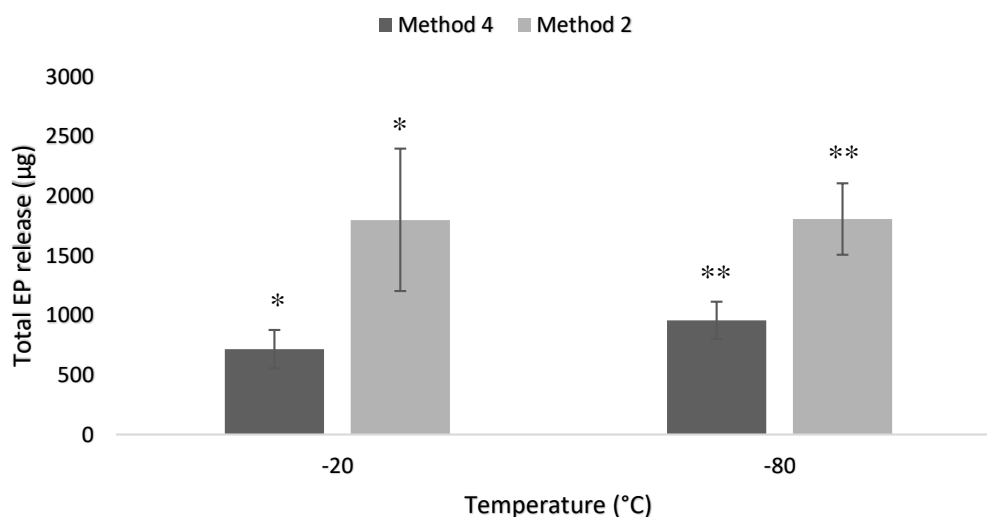


Figure 5.30. Comparison of total EP release from Alginate scaffolds prepared at either -20 °C or -80°C using method 4 and method 2. In method 2 EP was added to the formed scaffolds after the first freeze-drying cycle, while in method 4 EP was added to the alginate solution, at the early stage of alginate scaffold preparation. Alginate scaffolds without EP and EP were prepared at either -20 °C or -80°C, placed in 1.5 mL PBS and incubated at 37°C at constant agitation. Alginate gels were prepared with 0.5 mL 2% alginate solution and cross-linked in a 1mL 0.2M CaCl₂ bath. EP release was measured at different time point (1 hour, 1 day, 3 days, 7 days, 14 days 21 days, 28 days) but here it is shown the total EP release of the scaffolds. Data represent the mean \pm st dev from five samples (* $p < 0.05$).

5.6.2 Alginate scaffolds with double cross-linking

5.6.2.1 Method 5

The cumulative EP release profiles from the scaffolds produced with method 5 are shown in Figure 5.31-a. The four profiles are respectively the scaffolds produced with 0.4% calcium gluconate at -20°C (0.4%-20°C), the same calcium gluconate but prepared at -80°C (0.4%-80), 1% calcium gluconate at -20°C (1%-20), the same calcium gluconate but prepared at -80°C (1%-80). In all the formulations, EP release appears to be complete within the first hour, with no further release observed at later time points up to 28 days.

The total cumulative EP released for the scaffolds prepared with 1% calcium gluconate at -20°C was 1047 ± 288 µg, the highest compared to the other formulations. The total

cumulative EP released for the scaffolds prepared with 0.4% calcium gluconate at -20°C was $673 \pm 180 \mu\text{g}$, while the remaining two formulations prepared at -80°C released $342 \pm 193 \mu\text{g}$ for the scaffolds prepared with 0.4% calcium gluconate, $390 \pm 411 \mu\text{g}$ for the scaffolds prepared with 1% calcium gluconate (Figure 5.31-a). A t-test, two tailed analysis showed that the cumulative EP release of the scaffolds prepared at -20°C and at -80°C were statistically different for both formulations (0.4% and 1% calcium gluconate), as shown in Figure 5.32.

The cumulative EP release of the scaffolds prepared with 0.4% calcium chloride and those prepared at higher calcium chloride concentration (1%) were statistically different in the scaffolds prepared at -20°C, while they were not statistically different in those prepared at -80°C, as shown in Figure 5.32.

The percentage of EP released by the scaffolds is shown in Figure 5.31-b. All the formulations released almost 100% of EP in the first hour.

a)

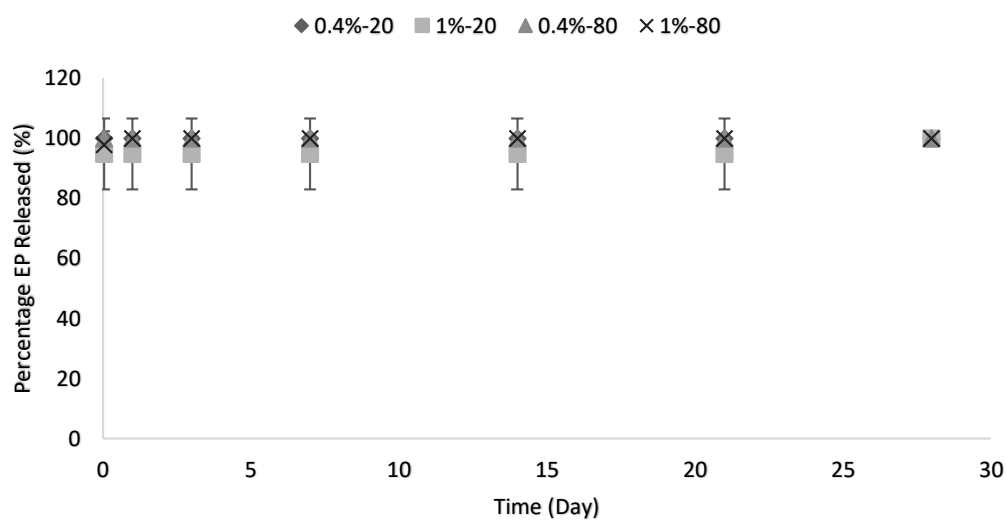
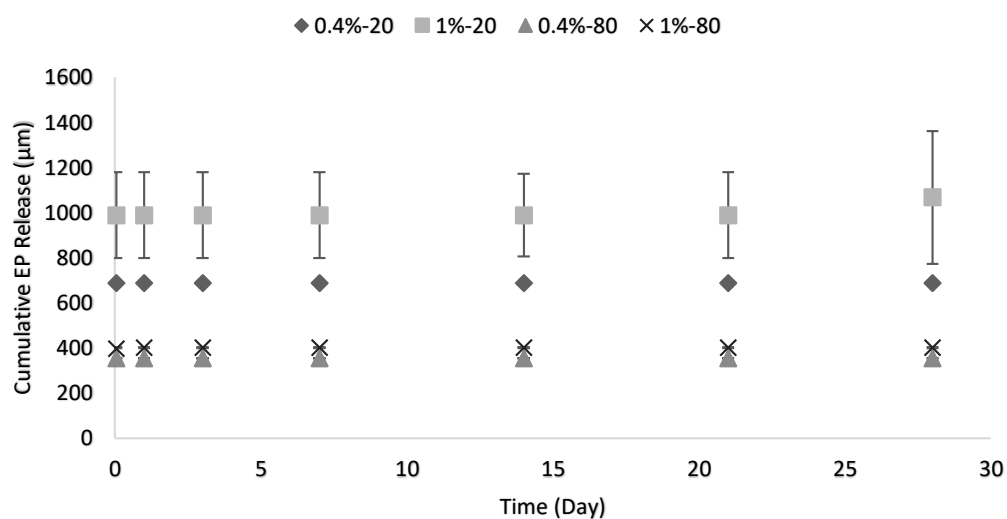


Figure 5.31 EP release study from alginate scaffolds. a) Cumulative EP release profile and b) percentage of EP released from scaffolds produce using method 5. Scaffolds were produced with an initial concentration of 2% alginate and cross-linked twice with 0.4% or 1% calcium gluconate and then with 0.2M CaCl₂. The scaffolds were produced with two cycles of freeze-drying. EP was added to the alginate solution before the first freeze-drying cycle. Data represent the mean \pm st dev from five samples.

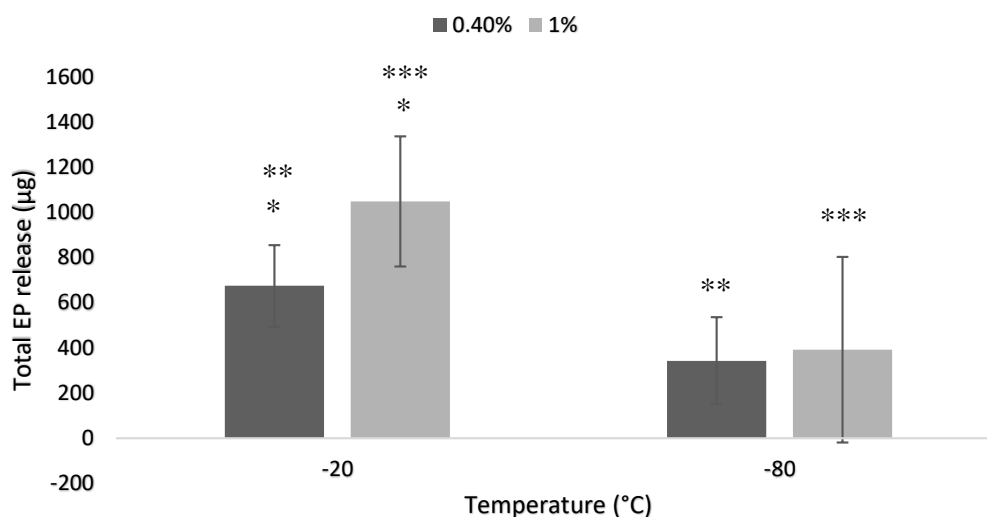


Figure 5.32. Comparison of total EP release from alginate scaffolds prepared with method 5. Scaffolds were prepared with an initial concentration of 2% alginate and cross-linked twice with 0.4% or 1% calcium gluconate and then with 0.2M CaCl₂. The scaffolds were produced with two cycles of freeze-drying. EP was added to the alginate solution before the first freeze-drying cycle. Data represent the mean \pm st dev from five samples (* p <0.05).

5.6.2.2 Method 6

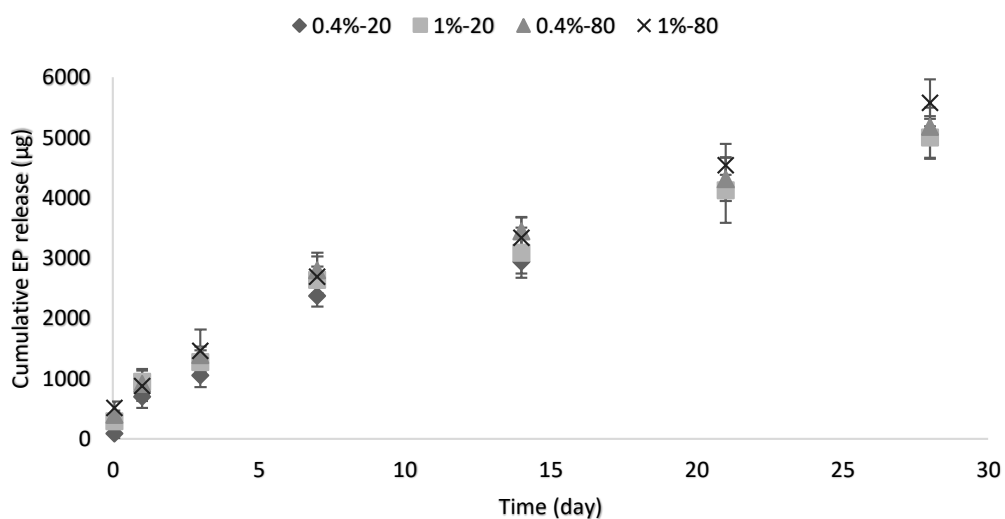
The cumulative EP release profiles from the scaffolds produced with method 6 are shown in Figure 5.33-a. The four profiles are respectively the scaffolds produced with 0.4% calcium gluconate at -20°C (0.4%-20), the same calcium gluconate but prepared at -80°C (0.4%-80), 1% calcium gluconate at -20°C (1%-20), the same calcium gluconate but prepared at -80°C (1%-80).

The scaffolds presented a similar release profile pattern, with a sustained EP release over the 28 days of the study. The total cumulative EP released for the scaffolds prepared with 1% calcium gluconate at -80°C was about 5,500 µg, the highest compared to the other formulations. The total cumulative EP released for other scaffolds was about 5,000 µg. A t-test, two tailed analysis showed that the cumulative EP release of the scaffolds prepared with 0.4% and 1% calcium gluconate were statistically not different for both formulations (at -20°C and at -80°C), as shown in Figure 5.34.

A t-test, two tailed, equal variance analysis revealed that the cumulative EP release between the scaffolds prepared at -20°C and 80 °C were statistically different for 1% calcium gluconate scaffolds, but not for 0.4% calcium gluconate scaffolds, as shown in Figure 5.34.

The percentage of EP released by the scaffolds is shown in Figure 5.33-b. All the formulations released EP in a sustained manner, with 25% of EP released after 3 days, 50% released after a week, 80% after 3 weeks.

a)



b)

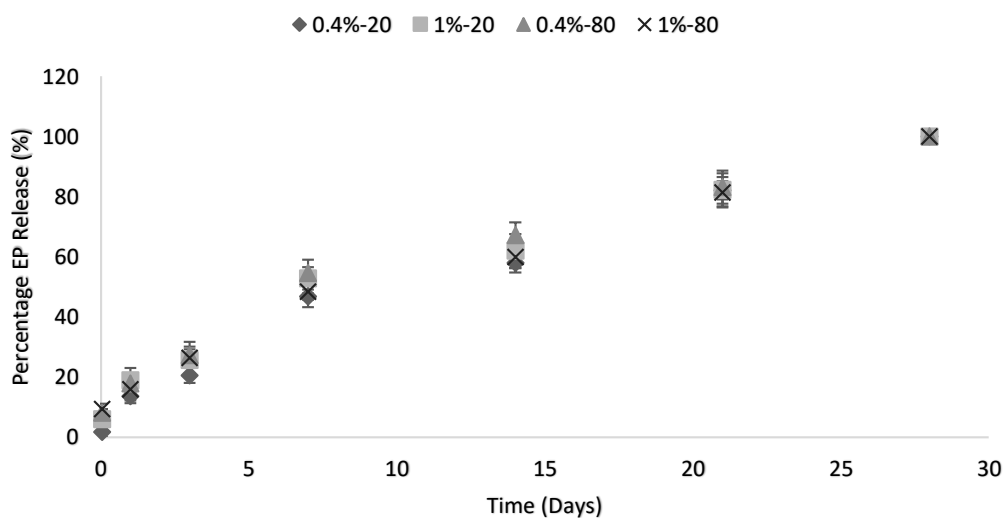


Figure 5.33 EP release study from alginate scaffolds. a) Cumulative EP release profile and b) percentage of EP released from scaffolds produce using method 6. Scaffolds were produced with an initial concentration of 2% alginate and cross-linked twice with 0.4% or 1% calcium gluconate and then with 0.2M CaCl₂. The scaffolds were produced with one cycle of freeze-drying. EP was added to the alginate solution before the freeze-drying cycle. Data represent the mean \pm st dev from five samples.

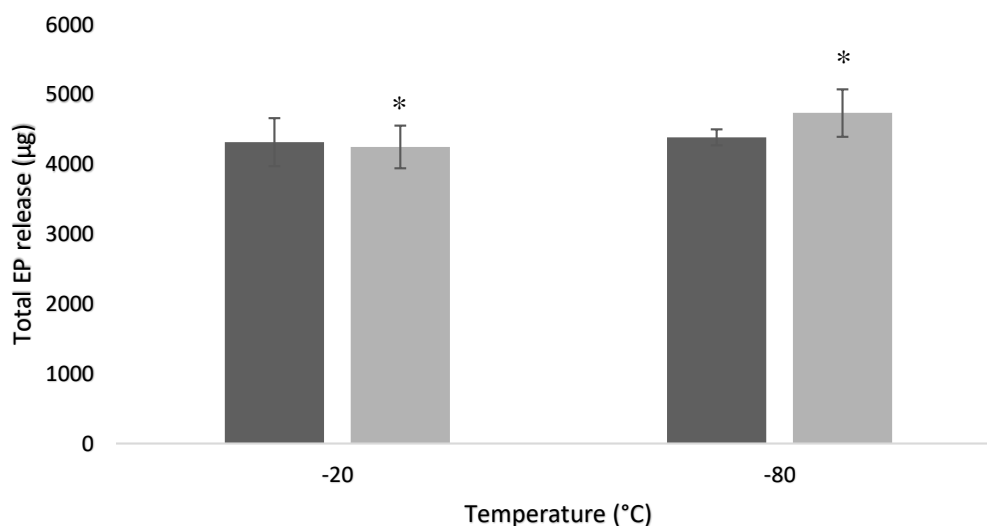


Figure 5.34. Comparison of total EP release from alginate scaffolds prepared with method 6. Scaffolds were prepared with an initial concentration of 2% alginate and cross-linked twice with 0.4% or 1% calcium gluconate and then with 0.2M CaCl₂. The scaffolds were produced with two cycles of freeze-drying. EP was added to the alginate solution before the first freeze-drying cycle. Data represent the mean \pm st dev from five samples (* $p < 0.05$).

In method 5 (section 5.4.3.2), scaffolds were prepared with two cycles of freeze-drying. Method 6 was then used to prepare scaffolds similarly to method 5, but with one cycle of freeze-drying (section 5.4.3.3), in order to investigate if the second freeze-drying may influence EP retention and release. A t-test two tailed distribution, analysis ($p < 0.05$) of the total EP release of the scaffolds prepared with method 5 and method 6 showed that the two methods are statistically different, as shown in Figure 5.35.

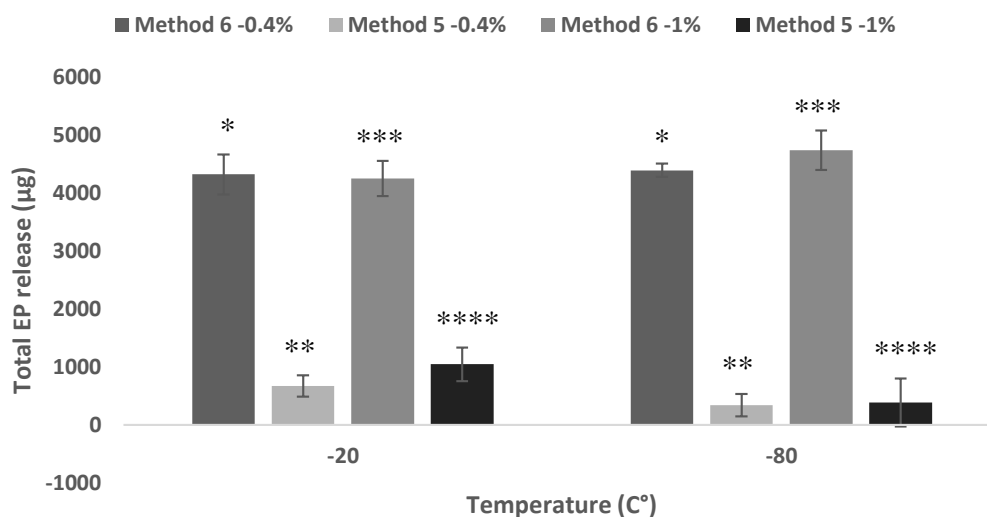


Figure 5.35. Comparison of total EP release of scaffolds prepared with method 6 and method 5. In method 5, scaffolds were prepared with two cycles of freeze-drying, while in method 6 one cycle of freeze-drying was used. Alginate scaffolds without EP and EP were prepared at either -20 °C (-0.4% Caglu;-1% Caglu) or -80°C (-0.4% Caglu;-1% Caglu) using method 6, placed in 3 mL PBS and incubated at 37°C at constant agitation. Alginate gels were prepared with 0.5 mL 2% alginate solution and 0.5mL of either 0.4% or 1% calcium chloride and placed in a 2mL 0.2M CaCl₂ bath. EP release was measured at different time point (1 hour, 1 day, 3 days, 7 days, 14 days 21 days, 28 days) but here it is shown the total EP release. Data represent the mean \pm st dev from five samples (* p <0.05).

5.7 Drug Loading Efficiency

Methods

In order to maintain the same EP concentration (25mM) in the scaffolds the volume of EP added to each scaffold was 2.78 μ L (2.66 μ g) for method 1-4, while double the amount of EP (5.56 μ L or 5.32 μ g) was added to the scaffolds prepared with method 5 and 6, as discussed in section 5.4. The amount of EP added to the scaffold during its preparation may be expected to differ from the amount of EP retained by the scaffolds (section 5.6). The measure of the amount of EP lost during the scaffold production can be used not only as an indication of the efficiency of the methodology used to prepare the scaffolds, but also to measure the repeatability of the scaffold preparation method. For this reason, in this section the amount of EP retained by the scaffolds was compared to the amount of EP added into them by calculating the drug loading efficiency of each scaffold.

Results

The drug loading efficiency of each method is shown in Table 5.

Table 5 Drug loading efficiency of alginate scaffolds. n=5

Scaffolds		Calcium Gluconate	Freezing temperature	Drug loading efficiency (\pm SD%)
Single Cross-linking (calcium chloride)	Method 1	-	-20°C	11 \pm 2%
		-	-80°C	8 \pm 2%
	Method 2	-	-20°C	38 \pm 13%
		-	-80°C	38 \pm 6%
	Method 3	-	-20°C	27 \pm 7%
		-	-80°C	22 \pm 3%
	Method 4	-	-20°C	25 \pm 6%
		-	-80°C	34 \pm 5%
Double Cross-linking (calcium gluconate + calcium chloride)	Method 5	0.4%	-20°C	12 \pm 3%
			-80°C	6 \pm 5%
		1%	-20°C	18 \pm 3%
			-80°C	9% \pm 6.95
	Method 6	0.4%	-20°C	88 \pm 7%
			-80°C	89 \pm 6%
		1%	-20°C	86 \pm 2%
			-80°C	96 \pm 7%

Alginate scaffolds prepared with method 6 (double crosslinking and one cycle of freeze-drying) presented the highest loading efficiency compared to the other

scaffolds. Within method 6 scaffolds, those prepared with high calcium gluconate concentration (1%) and at -80°C had the highest loading efficiency of $96 \pm 7\%$ (Table 5). This result was expected, due to the fact that the use of double crosslinking leads to an increase in crosslinks in the gel, which would help retain the EP within the cell matrix. On the other hand, scaffolds prepared with method 5, showed a very low loading efficiency, even although double crosslinking was used. The only difference in the methodology between method 5 and 6 is that in method 5 there were 2 cycles of freeze-drying (section 5.4.3). The results obtained in this study demonstrated that the second cycle of freeze-drying presented in method 5 is likely responsible for the loss of most of the EP added to the scaffolds during preparation. Together with method 5, method 1 showed the lowest loading efficiency over all. In particular, method 1 scaffolds had only $11 \pm 2\%$ for the scaffolds prepared at -20°C and $8 \pm 2\%$ at -80°C, while method 5 scaffolds with 0.4% calcium gluconate had $12 \pm 3\%$ (-20°C) and $6 \pm 5\%$ (-80°C) and those with 1% calcium gluconate had $18 \pm 3\%$ (-20°C) and $9 \pm 7\%$ (-80°C).

5.8 Characterisation of alginate scaffolds

5.8.1 Introduction

The porosity of macro-porous scaffolds used in tissue engineering is an important factor for new tissue formation. In fact, high porosity has been shown necessary for the proliferation and homogenous distribution of cells within the scaffold (Annabi, *et al.*, 2010). This also allows the exchange of nutrients and oxygen between the cells, promoting cell viability (Annabi, *et al.*, 2010). The characterisation of the alginate scaffolds produced in this study was carried out by measuring their porosity and by imaging the surface and the cross-sectional morphology.

5.8.2 Porosity

Methods

EP loaded alginate macro-porous scaffolds were prepared as previously described (section 5.4.2-5.2.3). The scaffolds were weighed when dry, following the last freeze drying step. They were then soaked in PBS (1.5 mL- 3 mL PBS to maintain a constant scaffold to medium ratio), removed immediately from the PBS and weighed again

when wet. The porosity of the scaffolds was then calculated for each formulation (n=5), using Equation 14 in section 2.7.1.

Results

5.8.2.1 Single cross-linked scaffolds

The values of the porosity of the single cross-linked scaffolds are shown in **Figure 5.36**.

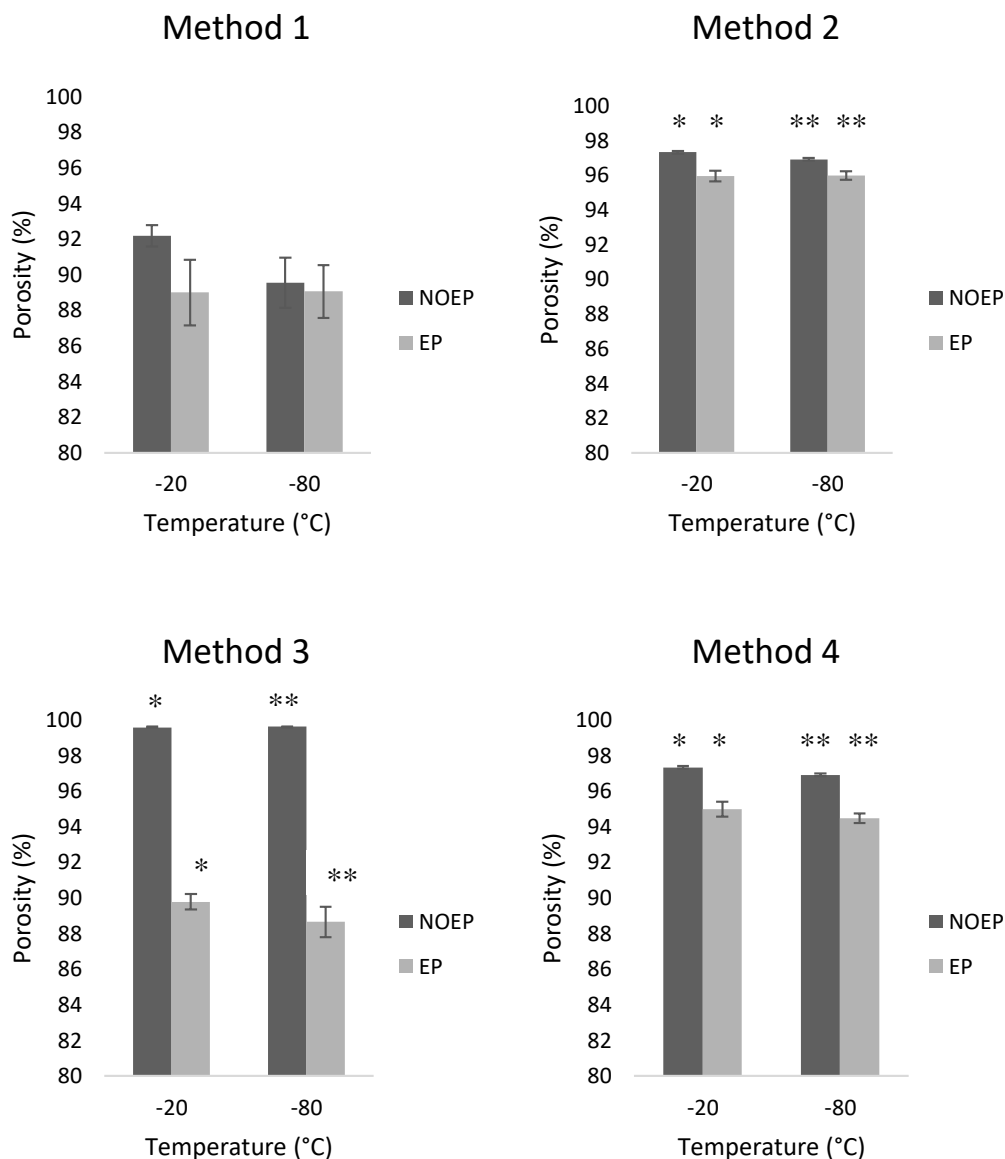


Figure 5.36 Porosity measurement of the alginate scaffolds prepared with single crosslinking. The scaffolds were prepared with methods 1-4. Data represent the mean \pm st dev from five samples (* p <0.05).

Overall, the scaffolds presented porosity higher than 88%, as shown in Figure 5.36. The scaffolds prepared with method 1 showed the lowest porosity of 88-92%. In scaffolds prepared with method 1, there was no statistical difference between the scaffolds with and without EP, as well as between scaffolds prepared at -20°C or -80°C. On the other hand, in scaffolds prepared with method 2, there was a significant difference between the scaffolds prepared with and without EP, but no statistical difference between scaffolds prepared at -20 °C and -80 °C as shown in Figure 5.36.

In method 1 (section 5.4.2.2), scaffolds were prepared with two cycles of freeze-drying. Method 2 was then used to prepare scaffolds with one cycle of freeze-drying, in order to investigate if the second freeze-drying may influence porosity. A t- test two tailed analysis ($p < 0.05$) showed that the porosity of the scaffolds prepared with method 1 and method 2 are statistically different for both scaffolds prepared at -20 °C and -80 °C and for scaffolds with and without EP.

EP scaffolds prepared using method 3 showed a porosity of $90 \pm 0.95\%$ for the scaffolds prepared at -20°C and $89 \pm 2\%$ for the scaffolds prepared at -80°C. On the other hand, the scaffolds prepared with method 3 but without EP showed the highest porosity of 99% ($99.56 \pm 0.03\%$ for the scaffolds prepared at -20°C; $99.61 \pm 0.05\%$ for the scaffolds prepared at -80°C). In scaffolds prepared with method 3, there was statistical difference between the porosity of the scaffolds with and without EP, but not between scaffolds prepared at -20°C or -80°C. Similarly to method 3, in scaffolds prepared with method 4, there was statistical difference between the porosity of the scaffolds with and without EP, but no statistical difference between scaffolds prepared at -20°C or -80°C, as shown in Figure 5.36.

In method 3 (section 5.4.2.4), scaffolds were prepared with two cycles of freeze-drying. Method 4 was then used to prepare scaffolds with one cycle of freeze-drying, in order to investigate if the second freeze-drying may influence porosity. A t- test two tailed analysis ($p < 0.05$) showed that the porosity of the scaffolds prepared with method 3 and method 4 are statistically different.

5.8.2.2 Double cross-linked scaffolds

The measured porosity of the double cross-linked scaffolds is shown in Figure 5.37.

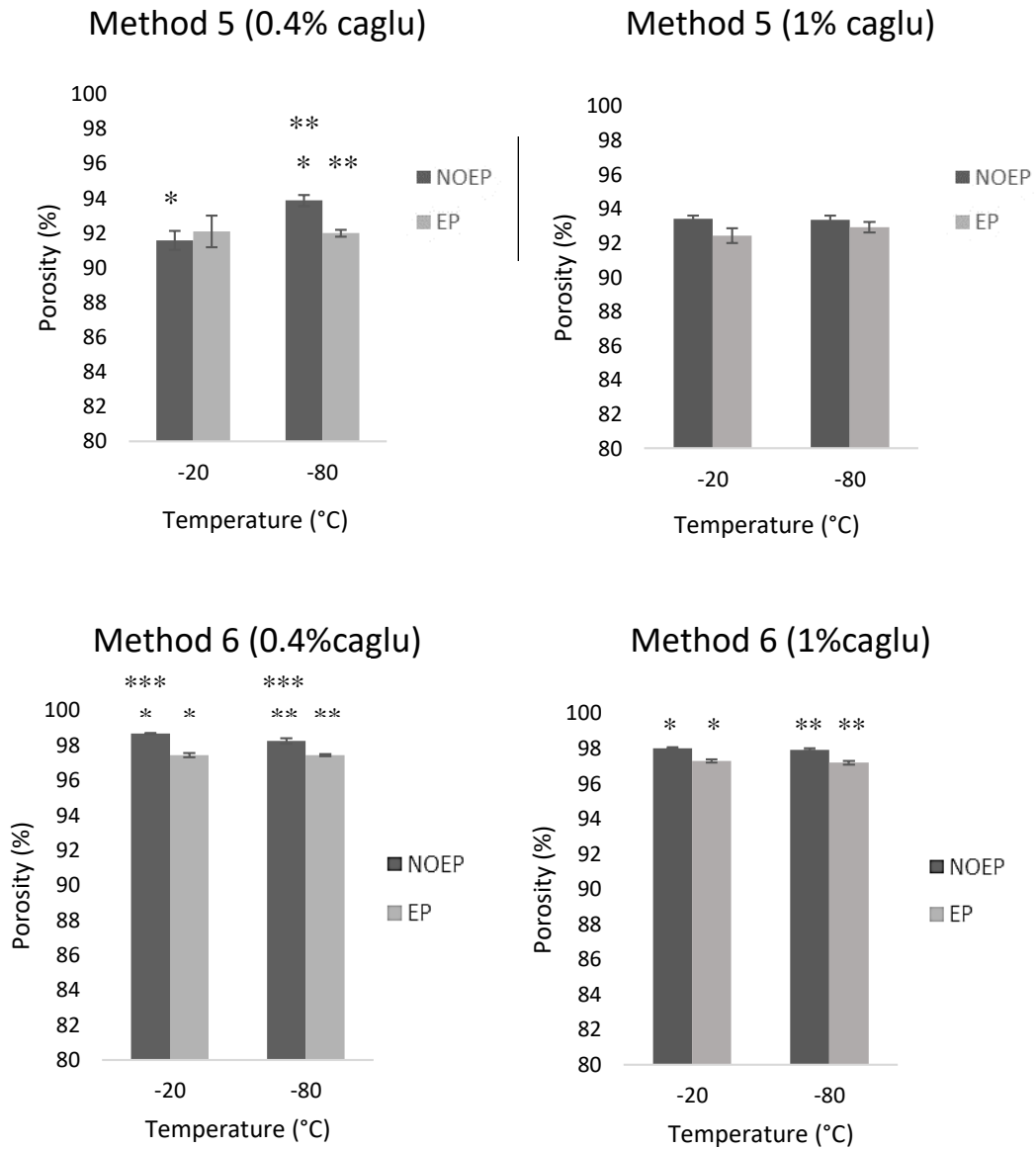


Figure 5.37 Porosity measurement of the alginate scaffolds prepared with single crosslinking. The scaffolds were prepared with methods 1-5. Data represent the mean \pm st dev from five samples (* $p < 0.05$).

Overall, the scaffolds exhibited porosity values that were consistently greater than 90%, as shown in Figure 5.37. The scaffolds prepared with method 5 showed the lowest porosity of 91-93%. A t-test two tailed analysis ($p < 0.05$) showed that the

porosity of the scaffolds prepared with method 5 at -20°C were not statistically different to the scaffolds prepared at -80°C, except for the scaffolds without EP with 0.4% calcium gluconate, as shown in Figure 5.37. The porosity of the scaffolds prepared with method 5 with 0.4% calcium gluconate were not statistically different to the scaffolds prepared with 1% calcium gluconate, except for the scaffolds without EP prepared at -20°C and the scaffolds with EP prepared at -80°C. The porosity of the scaffolds prepared without EP were not statistically different to the scaffolds prepared with EP, except for the scaffolds prepared with 0.4% calcium gluconate at -80°C.

The scaffolds prepared with method 6 showed a porosity of 97-98%, as shown in Figure 5.37. A t-test two tailed analysis ($p < 0.05$) showed that the porosity of the scaffolds prepared with method 6 at -20°C were not statistically different to the scaffolds prepared at -80°C, except for the scaffolds without EP with 0.4% calcium gluconate. The porosity of the scaffolds prepared with method 6 with 0.4% calcium gluconate were not statistically different to the scaffolds prepared with 1% calcium gluconate, except for the scaffolds without EP prepared at -20°C. The porosity of the scaffolds prepared with method 6 without EP were statistically different to the scaffolds prepared with EP for all the formulations, as shown in Figure 5.37.

In method 5 (section 5.4.3.2), scaffolds were prepared with two cycles of freeze-drying. Method 6 was then used to prepare scaffolds similarly to method 5, but with one cycle of freeze-drying (section 5.4.3.3), in order to investigate if the second freeze-drying may influence the porosity of the scaffolds. A t-test two tailed distribution, analysis ($p < 0.05$) of the porosity of the scaffolds prepared with method 5 and method 6 showed that scaffolds prepared with method 6 presented porosity statistically higher than those prepared with method 5.

5.8.3 SEM analysis

Methods

The methodology used in this study has been described in section 2.7.2. Due to the vast number of alginate scaffolds prepared in this chapter, it was necessary to narrow down the samples analysed with the SEM. The SEM study was in fact focussed on the scaffolds that showed the most promising EP release profiles and the highest EP

loading efficiency. The scaffolds were therefore prepared using method 6 (see section 5.4.3.3) but for this analysis only, the last step of the method (the second cross-linking with calcium chloride) was omitted due to the fact that the scaffolds had to be dry to perform the analysis. The scaffolds prepared with this method presented a 3D macroporous structure already before the second crosslinking step, suggesting that for imaging purpose, the core of the 3D structure of the scaffold would not change considerably with the second cross-linking. Because the EP release profiles and drug load efficiency were similar for the 2 formulations with different calcium gluconate concentrations (0.4% - 1%), only one concentration was selected (0.4%) for the SEM analysis. The scaffolds were then analysed and several images were taken at different magnifications (x150 – x300) of the surface. The scaffolds were also cut with a surgical scalpel to obtain the cross-section views using the same methodology used for the surface. The size of the pores on the surface and in the cross-section of the scaffolds was measured using ImageJ software. For each sample, 5 random pores were measured from the micrograph images captured at a magnification of x150.

Results

The images of the alginate scaffolds surface (method 6) obtained with the SEM are shown in Figure 5.38. In particular, the scaffolds prepared at -20°C without EP are shown in Figure 5.38-a, while the scaffolds prepared at -20°C with EP are shown in Figure 5.38-b. The scaffolds prepared at -80°C without EP are shown in Figure 5.38-c, while the scaffolds prepared at -80°C with EP are shown in Figure 5.38-d.

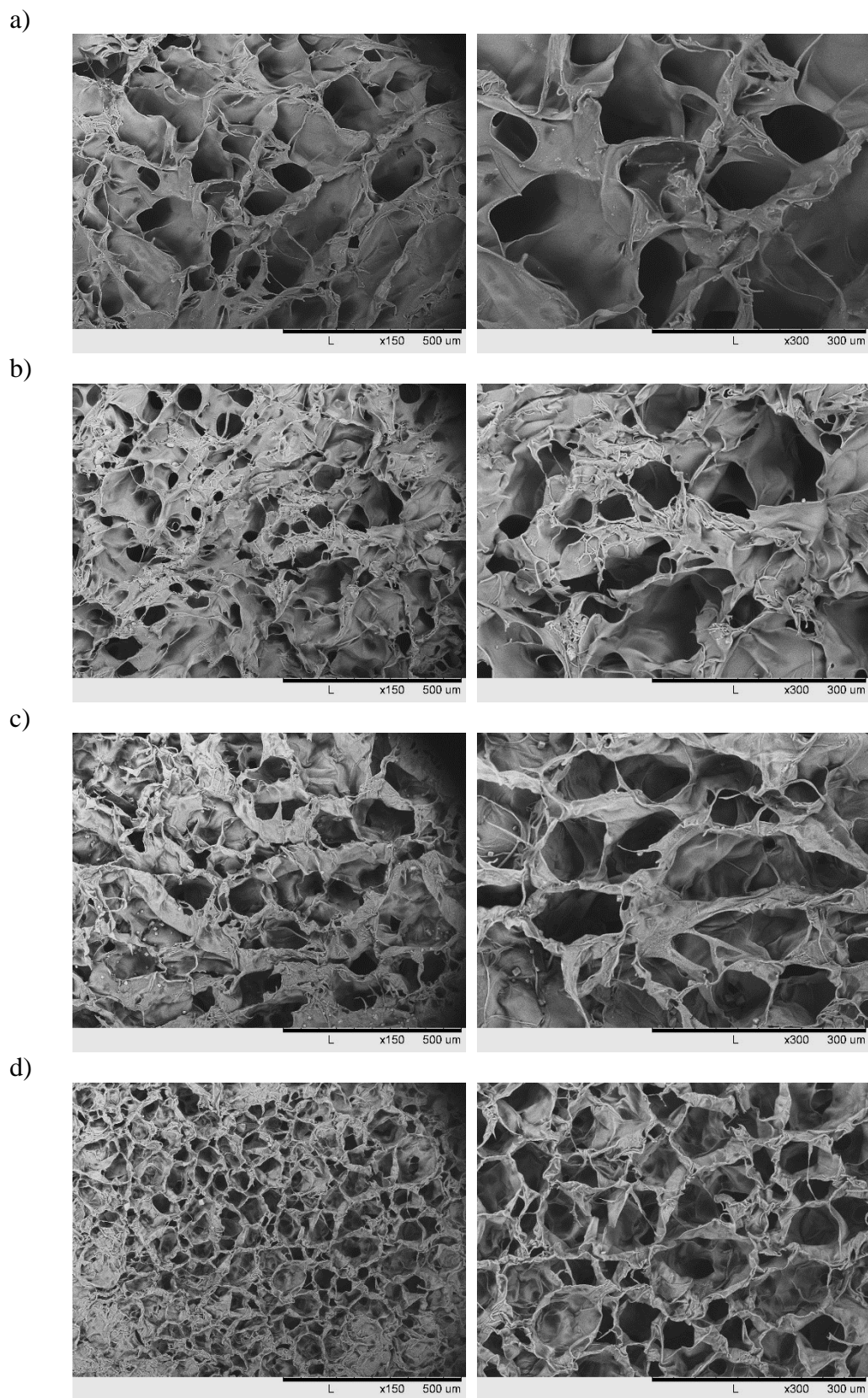


Figure 5.38 Representative SEM images of alginate scaffolds surface prepared with method 6. Scaffolds were prepared **a)** at -20°C without EP; **b)** at -20°C with EP; **c)** at -80°C without EP and **d)** at -80°C with EP. The images were obtained from dry scaffolds at different magnification (x150 and x300).

All the scaffolds presented a highly porous structure which is shown in Figure 5.38. It appears that the presence of EP in the scaffolds did not inhibit the creation of pores, as shown in Figure 5.38-b and Figure 5.38-d. In order to understand if the presence of EP or the use of different temperature affected the pore size, the average pore size was calculated for each formulation by measuring the pore diameter. The results are shown in table 6. The scaffolds prepared at -20°C showed a structure with an average pore diameter of $134 \pm 18 \mu\text{m}$ when prepared without EP, while the scaffolds with EP showed a pore size of $164 \pm 11 \mu\text{m}$. The scaffolds prepared at -80°C showed a reduced pore size compared to the scaffolds prepared at -20°C . In particular, the scaffolds prepared -80°C without EP showed a pore size average of $97 \pm 11 \mu\text{m}$, while the scaffolds with EP showed a pore size of $66 \pm 10 \mu\text{m}$.

In order to investigate the internal structure of the scaffolds, SEM cross-section images were taken of the scaffolds. The SEM images from these sections are shown in Figure 5.39. In particular, the cross-section of the scaffolds prepared at -20°C without EP are shown in Figure 5.39-a, while the scaffolds prepared at -20°C with EP are shown in Figure 5.39-b. The scaffolds prepared at -80°C without EP are shown in Figure 5.39-c, while the scaffolds prepared at -80°C with EP are shown in Figure 5.39-d.

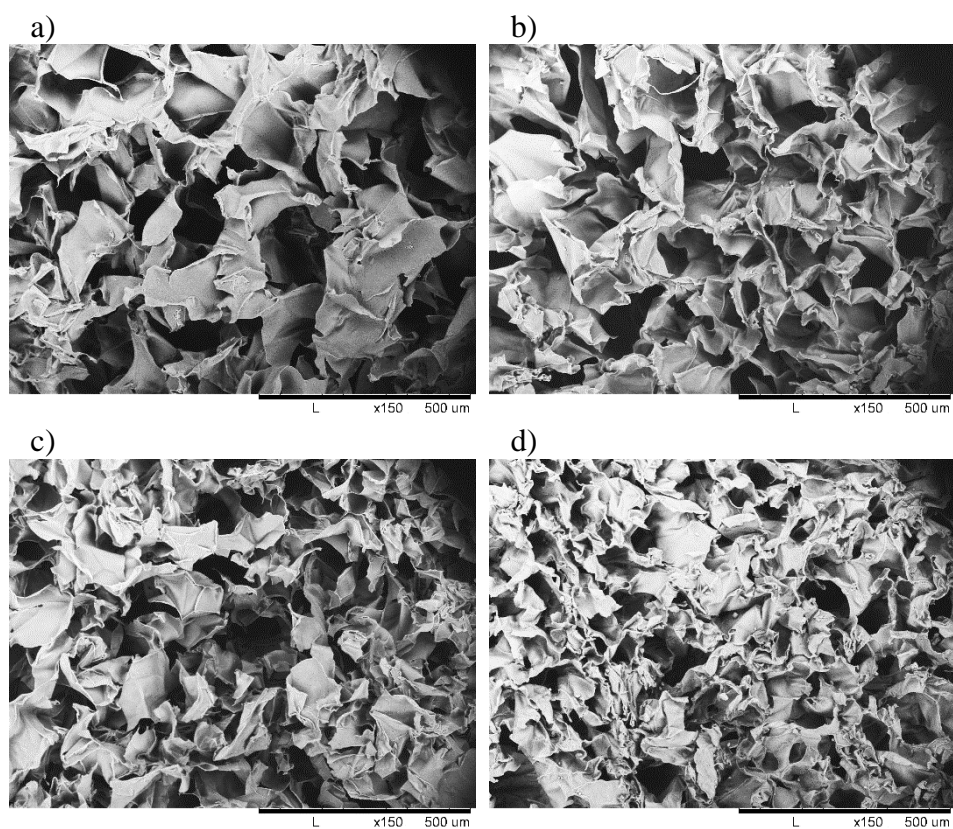


Figure 5.39 Representative SEM images of alginate scaffolds cross-section prepared with method 6. Scaffolds were prepared **a)** at -20°C without EP; **b)** at -20°C with EP; **c)** at -80°C without EP and **d)** at -80°C with EP. The images were obtained from dry scaffolds at $\times 150$ magnification.

The average of pore size in the cross-section was also calculated for each formulation by measuring the pore diameter, as discussed in section 2.7.2. The results are shown in Table 6.

Table 6 Measurement of the porous size of alginate scaffolds. $n=5$.

Freezing temperature ($^{\circ}\text{C}$)	Scaffold	Pore size ($\mu\text{m} \pm\text{SD}$)	
		Surface	Cross-section
-20	NOEP	134 ± 18	162 ± 101
	EP	164 ± 11	189 ± 30
-80	NOEP	97 ± 11	103 ± 23
	EP	66 ± 10	93 ± 12

The scaffolds prepared at -20°C showed an internal structure with an average pore diameter of $162 \pm 11 \mu\text{m}$ when prepared without EP, while the scaffolds with EP had a pore size of $189 \pm 30 \mu\text{m}$, as shown in Table 6. Both scaffolds showed slightly larger pores in the cross-section compared to the surface, with pore size of the EP scaffolds always bigger than the scaffolds without EP. The scaffolds prepared at -80°C showed a reduced pore size compared to the scaffolds prepared at -20°C . In particular, the scaffolds prepared -80°C without EP showed a pore size average of $97 \pm 11 \mu\text{m}$, while the scaffolds with EP showed a pore size of $66 \pm 10 \mu\text{m}$. Both scaffolds showed slightly bigger pores in the cross-section compared to the surface, with pore size of the EP scaffolds always smaller than the scaffolds without EP.

5.9 Discussion

5.9.1 Introduction

In the previous chapter, alginate hydrogels loaded with EP were successfully prepared. EP release from these gels was characterised by an initial burst in the first week, followed by a slow release for a further 2 weeks. This release profile may have therapeutic potential for treatment of ischaemic cardiac injury. However, it has been shown that scaffolds that have a porous structure with interconnected pores can promote cell infiltration and proliferation, whilst providing a route for the free movement of nutrients and waste. Once the cells proliferate into such a scaffold, the scaffold should ideally degrade, leaving space for the newly formed tissue (Cui, *et al.*, 2016). Given that the hydrogel formulations developed thus far in this project do not exhibit such properties, in this chapter, alginate macro-porous scaffolds were therefore developed as a new EP delivery system.

Sodium alginate is a very versatile polysaccharide. The physical characteristics of alginate scaffolds can be controlled by changing the production process. The freezing regime, which is part of the freeze drying process, influences the pore size of the scaffolds (Zmora, *et al.*, 2002). It has been shown that the choice of the cross-linker, the freezing temperature and the cycle of freeze-drying stages are all variables that can significantly affect important characteristics of the final structure of alginate scaffolds (Kang *et al.*, 1999) (Zmora *et al.*, 2002). These characteristics include the scaffold structure, porosity and swelling properties and are important to how the scaffold

performs as a potential cardiac patch material. It was therefore important to firstly investigate how these variables in the production process influenced these characteristics for the alginate grade used in this study. Crucially, the impact of incorporation of EP on the final scaffold properties has not been previously reported and so this study set out to address this important knowledge gap. Finally, the release profiles of EP from the different production methods was measured, in order to investigate how the production variables could be tuned to provide varying and potentially therapeutic EP release profiles.

5.9.2 Stability study

Alginate cannot be degraded enzymatically *in vivo*, however a slow cleavage of the glycosidic bonds will take place due to alkaline beta elimination and acid-hydrolysis in aqueous solution (Andersen, *et al.*, 2014). Renal clearance of alginate has been demonstrated for alginate with molecular weight of 50,000 g/mol (Al-Shamkhani & Duncan, 1995). For this reason, very low viscosity sodium alginate (Mw < 75,000 g/mol) was used in this study. An important initial objective of this study was to produce a scaffold which would be stable in PBS for at least 3 weeks, for the release of the EP over this time. The stability of the alginate scaffolds produced was therefore studied by incubation in PBS solution maintained at body temperature and under constant agitation.

The first batch of alginate scaffolds were prepared without EP, using similar methodology used in previous studies (Shapiro & Cohen, 1997)(Shachar, *et al.*, 2011). Alginate solution was cross-linked with calcium gluconate, frozen overnight and then lyophilised by freeze drying (section 5.3). In this preliminary part of the study, the stability of the scaffolds was assessed by visual observation. This type of scaffold demonstrated limited stability in PBS. In fact, the scaffolds dissolved completely after 5 days (section 5.3). This result is in contrast with what was observed in a previous study *in vitro*, where RGD modified alginate scaffolds prepared using a similar methodology maintained their structure over 12 days in culture medium (Shachar, *et al.*, 2011). It is possible that the presence of sodium bicarbonate within the culture medium prolonged the stability of these scaffolds *in vitro*.

The stability of the scaffolds prepared here was further assessed by the extent of swelling of the scaffold over time. It was expected that the scaffolds incubated in PBS would undergo a process of chain relaxation, followed by a period of swelling and eventual dissolution, based on previous observations (Bajpai & Sharma, 2004). The swelling is a gradual process, proceeding over time until the scaffolds reach a maximum point of swelling. After this point, the continued ion-exchange breaks the ionic crosslinking between polymer chains which ultimately leads to the final dissolution of the scaffolds (Bajpai & Sharma, 2004). The scaffolds produced using the various different methodologies described in the present study generally followed this anticipated pattern of behaviour. An increase in swelling was observed in the first weeks, followed by a relaxation period with a reduction in swelling. In particular, scaffolds prepared with method 1 showed a slow swelling increase with the peak after 21 days in both scaffolds with and without EP (Figure 5.8). The same was shown by the scaffolds prepared with method 2 without EP (Figure 5.10- a). In this case though, scaffolds with EP were statistically different from the scaffolds without EP. In fact, EP scaffolds were completely degraded at day 21 (Figure 5.10-b). The same early degradation of the EP scaffolds was also found with the scaffolds prepared with method 3 (day 21) Figure 5.13 and method 4 (28 days) Figure 5.15. These results suggest that the presence of EP, either added directly to the alginate solution or to the formed scaffolds after freeze-drying, negatively impacted upon the overall stability of the scaffolds, although this effect was not observed with method 1.

The results also showed that the different freezing regime used (-20/-80°C) and the number of freeze-drying cycles did not affect the stability of the scaffolds. The scaffolds prepared with method 5 and 6 involved a greater number of steps in the production process compared to the other methods. In fact, method 5 and 6 involved double cross-linking of alginate with calcium chloride and calcium gluconate. Two different calcium gluconate concentrations were investigated, 0.4% and 1%, but results showed no statistical difference between the scaffolds prepared at these two concentrations. Scaffolds prepared with method 5 showed a peak in the swelling ratio after 14 days, followed by a slow relaxation of the structure (Figure 5.18). On the other hand, the scaffolds prepared with method 6 showed an earlier swelling peak after one week, followed by a slow relaxation of the structure (Figure 5.20). The comparison of

the swelling ratio at the end of the study between scaffolds prepared with method 5 and 6 revealed that only the scaffolds prepared with 1% calcium gluconate were statistically different between the two methods Figure 5.22. The reason why this formulation has a different behaviour compared to the others is not clear. The only difference in methodology between method 5 and method 6 is that method 6 has only one freeze-dried cycle, but it has been shown in the results obtained from the methods 1-4 that there was no direct correlation between the number of freeze-drying cycles and change in swelling.

Although the scaffolds showed signs of degradation (relaxation of the structure), the scaffolds with one cross-linking step (method 2-4) degraded in the last weeks of the study. On the other hand, in the scaffolds prepared with double-cross-linking the structure was still present at the end of the study (28 days). This result suggested that the scaffolds prepared with methods 5-6 are potentially suitable for EP delivery over prolonged periods.

5.9.3 EP release study

EP has been shown to reduce oxidative stress and increase myocardial ATP levels and decrease infarct size when injected into the myocardium in a rat model of ischaemic injury (Woo *et al*, 2004). The effectiveness of EP has been measured only for short term release in animal studies (Woo *et al*, 2004; Famili *et al*, 2013) and in humans (Bennett-Guerrero, *et al.*, 2009). However, since EP has not previously been loaded into an implantable scaffold, the effect of its sustained and prolonged local delivery of into damaged myocardial tissue has not yet been studied either *in vitro* or *in vivo*. It was therefore important to investigate the development of a macro-porous alginate scaffold that would deliver EP in a sustained manner. The results of this aspect of the study showed that the scaffolds prepared with method 1 and method 5 were the only ones that released all of the EP in the first hour (Figure 5.23-Figure 5.31). In contrast, the scaffolds prepared with method 3 released EP over 21 days (Figure 5.26), while the remaining scaffolds released EP over 28 days (Figure 5.24; Figure 5.26; Figure 5.31). The release profile of the scaffolds prepared with method 2 and method 4 were not statistically different, even although the EP was added at different stages of scaffold formation. This result is in contrast with the result obtained with method 1

and 3. In fact, in that case, the addition of EP to the alginate solution at the early stage of scaffold formation lead to an increase in cumulative EP release (method 3).

Scaffolds prepared with method 6 showed a sustained release of EP over the 28 days, with 50% of EP released in the first week, followed by a slow release of the remaining EP (Figure 5.33). The amount of EP lost during the gel production was calculated in order to use it not only as an indication of the efficiency of the alginate scaffold preparation, but also to measure the repeatability of the preparation method. The scaffolds prepared with method 6 demonstrated the highest loading efficiency of 86-96% (Table 5). The other scaffolds instead had a much lower loading efficiency, ranging from 8-11% of the method 1 to the 38% of method 2 (Table 5).

The aim of this study was not only to find the optimal method to produce a scaffold with a sustained EP release, but also to identify what part of the production process has the greatest effects on EP retention and release. Knowledge of this can provide useful insights that will help in the future development of patches of this nature that seek to locally deliver drugs.

Freeze-drying is an important process in the preparation of the alginate scaffolds. In this study it was examined the effect that lyophilisation has on EP retention and how this effect can be reduced. It is not clear the effect that the freezing temperature used to prepare the scaffolds have on EP retention or release. In fact, only in method 4, method 5 and method 6 (1% calcium gluconate) was there a statistical difference in cumulative EP release.

It appears that the second freeze drying step used in method 1 led to a marked reduction in the cumulative mass of EP released, compared to method 2 (Figure 5.25). Similarly, for the double-cross-linked scaffolds, the cumulative EP release was statistically different between method 5 and method 6 (Figure 5.35). The reason for this reduction in EP release might be that EP was removed from the patches during the second freeze-drying process. On the other hand, the cumulative EP release of method 3 and method 4 (Figure 5.29) were not statistically different.

One factor that appears to have a positive impact on the retention of EP within the scaffold structure is the double cross-linking in method 6. Although this effect was not

visible in method 5, this likely reflects the countering effect of the second-freeze-drying step used within this particular method. Generally, the results suggested that the use of double cross-linking and one cycle of freeze-drying are the important factors for achieving the highest drug loading efficiency. Method 6 was demonstrated to not only have the ability to deliver EP in a sustained manner, but also the highest EP loading efficiency of 85-96% compared of the other methods (Table 5).

Previously, alginate has been used to prepare macro-porous ferrogels, prepared with alginate and magnetic particles, as a drug release device (Zhao, *et al.*, 2011). The scaffolds were shown to have the ability to deliver small drugs such as the chemotherapy drug mitoxantrone with and without magnetic stimulation over 3 hours *in vitro* (Zhao, *et al.*, 2011) and drugs with high molecular weight, such as proteins and plasmid DNA over 10 hours *in vitro* (Zhao, *et al.*, 2011). Although these ferrogel macro-porous scaffolds delivered drugs over time, it should be noted that the delivery of the drug was limited to few hours. On the other hand, in this chapter the new methodology used to prepare alginate scaffolds loaded with EP successfully achieved sustained release of EP over 28 days.

5.9.4 Characterisation of alginate scaffolds

The size of the crystals that are formed in the scaffolds during the freezing process depends on the freezing temperature (Kang *et al.*, 1999) (Zmora *et al.*, 2002). During lyophilisation, the water contained in the samples sublimates, changing from the solid state to the gas state. Therefore, the pore size is determined by the size of the crystals in the scaffolds (Kang *et al.*, 1999) (Zmora *et al.*, 2002).

The freeze-drying technique used in the present study led to the production of scaffolds with a macro-porous structure, with porosity being consistently around 90% or above for all scaffolds produced (section 5.8.2). It has previously been shown that this type of structure is ideal for cell attachment and proliferation (Dar, *et al.*, 2002), allowing the easy passage of cells and nutrients through the pores. In fact, Dar *et al.*, 2002 showed that rat cardiomyocytes and cardiac fibroblasts aggregated and spontaneously contracted when seeded in 90% highly porous alginate scaffolds (Dar, *et al.*, 2002).

The effects that the incorporation of small molecules, drugs, and growth factors in alginate scaffolds may have on the scaffold porosity has not been examined before. For this reason, it was therefore important to establish if EP impacted the scaffold structure. The results presented in this chapter show that overall the presence of EP reduced slightly the porosity of the scaffolds (section 5.5.1). In fact, in all of the scaffolds, except for method 1 and method 5 (0.4% calcium gluconate) the porosity of the scaffolds with EP was statistically different from the porosity of the scaffold without EP. It is possible that the presence of EP lowered the freezing point of the water contained in the alginate solution, resulting in the reduction of the porosity of the structure (Greenslade, 1933).

The scaffolds were frozen before each cycle of freeze-drying and two freezing temperatures were investigated. It appears that the different freezing temperature did not affect the overall porosity of the scaffolds, except for the scaffolds prepared with method 5 (-80°C). The use of a double cross-linking step did not increase the porosity of the scaffolds compared to the single cross-linking scaffolds (method 1 and 4) (Figure 5.36). On the other hand, it appears that there was a difference in porosity between method 5 and 6, with method 6 showing a higher porosity than the method 5 (Figure 5.37). The main difference in methodology between those two methods is the number of freeze-drying cycles used. This result suggests that the second cycle of freeze-drying not only reduced the EP retention, as discussed previously (section 5.9.3), but also reduced the porosity of the scaffolds.

SEM analysis was used to obtain images of the surface and cross/section of the scaffolds (section 5.8.3). From the SEM images it was then possible to measure the pore size of the scaffolds. Due to the vast number of alginate scaffolds prepared in this chapter, only the scaffolds prepared with method 6, which showed high porosity, the best EP release profiles and the highest EP loading efficiency discussed in the previous sections (5.6.2.1 – 5.7.2) were analysed. Because porosity, EP release profiles and drug load efficiency were similar for the 2 formulations with different calcium gluconate concentrations (0.4% - 1%), only one of these concentrations (0.4%) was selected for the SEM analysis. The SEM images showed a highly porous structure, characterised by rounded pores, in all of the samples examined, on both surface and in the internal

part of the scaffolds (horizontal cross-section), as shown in Figure 5.38 and Figure 5.39 respectively. The scaffolds prepared at -80°C presented a reduced pore size compared to the scaffolds prepared at -20°C in both scaffolds with and without EP (Figure 5.38 and Figure 5.39). This difference between the two freezing temperatures was more evident in the scaffolds produced with EP, where the scaffolds prepared at -20°C presented on average pores that were double the size of the -80°C ones, as shown in Table 6. This is in line with previous studies that have shown that the use of low temperature (liquid nitrogen at -196°C) in the freezing process can lead to smaller pore size formation in alginate macro-porous scaffolds cross-linked with calcium gluconate compared to the scaffolds prepared at -20°C (Shapiro & Cohen, 1997). Similar results were also obtained with gelatine hydrogels in the study conducted by Kang *et al*, where the scaffolds prepared at -80°C had smaller pores compared to the scaffolds prepared at -20°C (Kang *et al*, 1999).

5.10 Limitations

Alginate scaffolds stability was studied by measuring the change in weight (swelling ratio) over time. The effect of errors in weight measurements due to surface liquid retention upon swelling ratio represents a limitation of this study. The results do however provide an indication of the potential scaffolds stability in PBS at body temperature.

5.11 Summary conclusions

In this chapter, it has been shown that alginate scaffolds can be created with a porosity and stability that make them potentially suitable candidates for use as a cardiac patch to encourage regeneration. By varying the patch production conditions, and in particular the introduction of the double cross-linking and the limit of one cycle of freeze-drying it has been shown that EP can be incorporated and released from the patches in potentially therapeutic concentrations over clinically relevant time periods of up to 28 days. It was further found that this introduction of EP did not negatively impact the structural characteristics of the patches. The scaffolds produced with double cross-linking (method 6) were shown to have the optimal EP release over 28 days and porosity suitable for cell infiltration and proliferation. The patches developed therefore

have potential for use as a support for regeneration following cardiac surgery. However, their biocompatibility remains to be determined and this therefore forms the focus of the studies set out in detail in the next chapter.

6 CHAPTER SIX

IN VITRO TESTING OF ALGINATE PATCHES

6.1 Introduction

The normal myocardium is composed of around 70% cardiomyocytes by volume, representing 30-40% of the total cell number. The remaining cells are mostly cardiac fibroblasts, with other cell types, such as vascular cells, being relatively low in number (Camelliti, *et al.*, 2005). Cardiac fibroblasts have a key role in the regulation of the structure of the heart by controlling proliferation and extracellular matrix (ECM) turnover. These cells are important not only in the physiological regulation of the myocardium, but also in the remodelling process after ischaemia/reperfusion injury. An increase of cardiac fibroblasts density has been observed in the proximity of the scar tissue after myocardial infarction (Camelliti, *et al.*, 2005). During the process of scar formation, cardiac fibroblasts undergo a phenotypic modulation to myofibroblasts, which are thought to be responsible for cardiac remodelling that ultimately leads to heart failure (Baum & Duffy, 2011). Due to the high density of cardiac fibroblasts registered in proximity to the scar formation, cardiac fibroblasts can be used as a simplified *in-vitro* model of the area close to the scar.

The inflammation that occurs after ischemia/reperfusion is accompanied by high levels of oxidative stress, which produces deleterious effects in the myocardium (Hori & Nishida, 2009). In fact, a sustained increase in TNF-beta levels has been observed in the first 3 weeks after MI in a rat model (Sia, *et al.*, 2002), while another study showed that in patients with acute myocardial infarction the level of oxidative stress in the blood increased progressively, reaching a peak after 7 days (end point) when the patients were discharged from the hospital (Nikolic-Heitzler, *et al.*, 2006).

Anti-inflammatory and antioxidant treatments have been investigated as a possible therapy to limit tissue damage after MI (Hori & Nishida, 2009). There are several studies that showed promising results in using antioxidants for the inhibition of left ventricular remodelling (Hori & Nishida, 2009). EP has been shown to reduce oxidative stress and increase myocardial ATP levels and decrease infarct size in rats

(Woo, *et al.*, 2004). EP enhanced tissue ATP levels, preserved cardiac function, and attenuated myocardial oxidative injury in a Langendorff perfused heart experiment (Guo, *et al.*, 2014). In rat models of ischaemia/reperfusion, one injection of EP inhibited TNF- α , IL-6, HMGB-1 (Lin, *et al.*, 2015) and inhibited the activation of the nuclear factor NF- κ B signalling pathway, cytokine production and consequently reduced infarct size (Jang, *et al.*, 2010).

EP is also known to have antioxidant properties, such as being able to scavenge hydrogen peroxide (Yang, *et al.*, 2016). In a study conducted by Famili *et al* 2013, human trabecular meshwork (hTM) cells were treated with EP in the concentration range of 1 - 20 mM. The cells were either co-treated with hydrogen peroxide for 24h or treated only with hydrogen peroxide for 24h after the EP treatment for 24h (Famili, *et al.*, 2013). The results obtained by Famili showed that the co-treatment of EP and hydrogen peroxide increased the cell viability, compared to the cells without EP treatment or cells with EP pre-treatment (Famili, *et al.*, 2013). Ultimately, Famili suggested that in order to maintain this hydrogen peroxide scavenging effect, EP should be delivered over time in a sustained manner (Famili, *et al.*, 2013). The protective effect of EP on rat neural cells when exposed to H₂O₂ has been demonstrated in different studies (Kim, *et al.*, 2005)(Zeng, *et al.*, 2007). In particular, in the study conducted by Kim *et al*, neuron and microglia cells were exposed to 200 μ M H₂O₂ for 30 minutes and were then treated with 5-20 mM EP. After 4 hours of incubation with EP, cells showed an increase in cell viability, indicating that EP helped the cells recover after H₂O₂ exposure (Kim, *et al.*, 2005).

The cytotoxicity of EP has been tested *in vitro* on different cell types (erythrocytes, blood monocytes, neuron cells, and trabecular meshwork cells)(Birkenmeier, *et al.*, 2016)(Worku, *et al.*, 2015)(Famili, *et al.*, 2013), but not on cardiac fibroblasts. For this reason, and to better understand the therapeutic potential of the EP-releasing alginate materials detailed in chapter 5, it is necessary to investigate the effects of EP on cardiac fibroblasts. Cultures of these cells can be readily maintained over the prolonged time periods that are the focus of this investigation, making them more suitable than cardiac myocytes.

Alginate has been studied as a delivery system for cells, growth factors and active compounds directly into the myocardium (Lee & Mooney, 2012). However, alginate alone lacks mammalian cell binding sites, which is an important limiting factor for its use in tissue engineering applications (Lee & Mooney, 2012). In order to overcome this, peptides such as the arginine-glycine-aspartic acid (RGD) are commonly added to the backbone of sodium alginate using water-soluble carbodiimide chemistry (Lee & Mooney, 2012). Different methods to prepare alginate scaffolds were investigated in the previous chapter, in order to identify a formulation and methodology that would provide optimal EP release characteristics combined with sufficient porosity to permit cell infiltration. The scaffolds produced with double cross-linking (method 6) were shown to be the most promising with respect to these two important factors (see sections 5.6.2 and 5.8.1). This alginate formulation method was therefore selected to be tested in cell culture, as will be described in this chapter.

Aim and objectives

The overall aim of this study was to investigate the effects of alginate macro-porous scaffolds loaded with EP on cardiac fibroblasts *in vitro*. In order to achieve this, the following four objectives were set. These were to investigate

- the effects of EP on cardiac fibroblast viability and proliferation;
- the protective effects of EP on cardiac fibroblasts challenged with H₂O₂;
- the biocompatibility of alginate scaffolds in a 3T3 cell culture;
- the effects of alginate scaffolds loaded with EP on cardiac fibroblasts.

6.2 *In vitro* effects of EP on cardiac fibroblasts

6.2.1 Preliminary cell viability study - neutral red and MTT assay

Cardiac fibroblasts were cultured following the protocol described in section 2.1.2. Cells were seeded onto 96 well plates at a seeding density of approximately 3.5×10^4 cells/ml (700 cells /well). The cells were then left for 48 hours to settle in the wells and then treated with a range of EP concentrations (1,000- 20,000 μ M) similar to those investigated previously in other cell studies (Famili, *et al.*, 2013). Cell viability

was measured after 5 days of treatment with the neutral red assay and the metabolic activity was measured with the MTT assay. The methodology used in this section is explained in detail in section 2.1.3.4 and section 2.1.3.3 respectively. Cell viability (%) of the cells treated with EP for 5 days is shown in Figure 6.1-a (Neutral Red) and cell metabolic activity (MTT) in Figure 6.1-b.

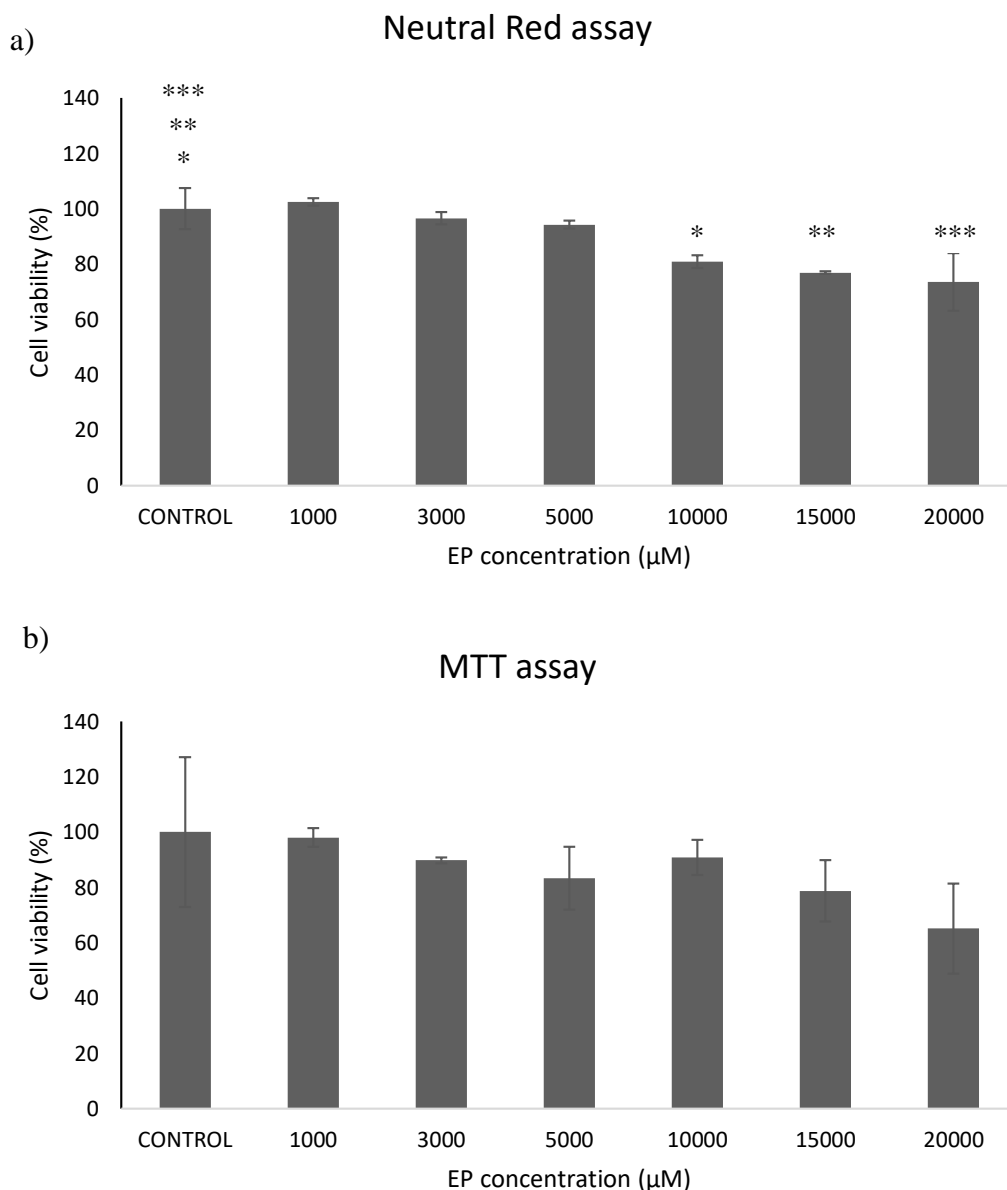


Figure 6.1 Assessment of EP toxicity on cardiac fibroblasts. a) Cell viability measured with Neutral red assay after 5 days of EP exposure in culture. b) Metabolic activity of cardiac fibroblasts measured with MTT assay after 5 days of EP exposure in culture. Cells were seeded at a cell density of 3.5×10^4 cells/ml (700 cells /well). Cells with no EP treatment were used as a Control. Data represent the mean \pm standard deviation from three technical replicates from a single culture * $p < 0.05$.

The metabolic activity of the cells decreased proportionally with the increase in EP concentration, although this reduction was not statistically different from the control (Figure 6.1-b). Cell viability shows a similar pattern, with a decrease of cell viability at higher EP concentrations (10-20 mM) as shown in Figure 6.1-a. In this case, there was a statistical reduction in cell viability at higher EP concentrations, as shown in Figure 6.1-a.

6.2.2 Cell viability – alamarBlue™ assay

AlamarBlue™ (AB) assay was used to measure the cell viability of cardiac fibroblasts treated with EP. AB is well tolerated by the cells and for this reason it is possible to repeat the assay on the same cells over time, thereby providing temporal data that is not possible to obtain using either MTT or Neutral Red assays. Because the aim of this aspect of the study was to examine EP effects on the cells over 5 days, AB was used at day one, day 3 and day 5 of the treatment.

Before using AB assay for the study of EP effects on cells, it was important to investigate for possible interactions between EP and AB. Cell media containing serum has previously been shown to interfere with the measurement of AB *in vitro* (Goegan, *et al.*, 1995). EP standards in the range of 1-20 mM were therefore prepared in serum-free media. Another set of EP standards in the same range were then prepared in 20% serum media. 200 µL of each EP standard was pipetted into single wells of a 96 well plate. 20 µL of AB was added to each well and after 4 hour of incubation in the dark at 37°C, AB was measured at 570 nm using the spectrophotometer. The percentage of AB reduction by EP in serum-free media and from EP in 20% serum media is shown in Figure 6.2.

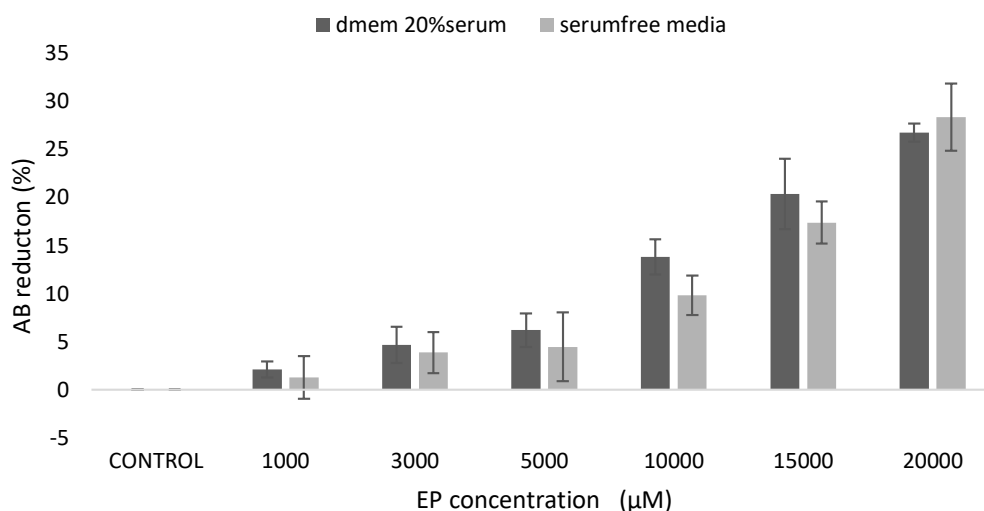


Figure 6.2 Effect of EP on AB reduction. EP standards in 20% serum media and in serum free media were prepared in a sterile environment. 200 µL of each standard was placed in a 24 well plate. 10% AB was added to each well and incubated at 37°C for 4 hours. 20% serum media and serum free media were used as Control respectively. Data represent the mean +/- standard deviation from three replicate measurements from a single experiment. No significant differences were observed between the serum-free and 20% serum media.

The EP standards prepared with 20% serum media showed a moderate but not significant increase in this interaction compared to the standards prepared in serum-free media. This trend stopped only at 20,000 µM EP, where the standard without serum presented a higher interaction with AB, compared to the standards with serum.

The results obtained from this experiment were used in the optimisation of the AB assay for the subsequent cell experiments. Although the effect of serum on AB reduction was not found to be statistically significant, there were still differences and so it was therefore decided to make the following adjustments. In order to avoid the interaction between AB and EP and between AB and FBS, it was necessary to remove EP and 20% serum media before treating the cells with AB. The methodology used in this section is explained in detail in section (2.1.3.1).

Cells were seeded onto 96 well plates at a seeding density of approximately 3.5×10^4 cells/ml (700 cells /well). The cells were then left for 48 hours to settle in the wells. Cell media was removed from the wells at day 1, day 3 and day 5 and substituted with 200 µL/well serum free media with 10% AB. The plate was then incubated in the

dark at 37°C for 4 hours. After this incubation, the media containing AB was removed and transferred to a new 96 well plate for analysis. Fresh media, with replacement of the initial EP concentration, was added to cells for the continuation of the experiment. The cell viability of the cells treated with EP over 5 days, assessed by AB assay, is shown in Figure 6.3.

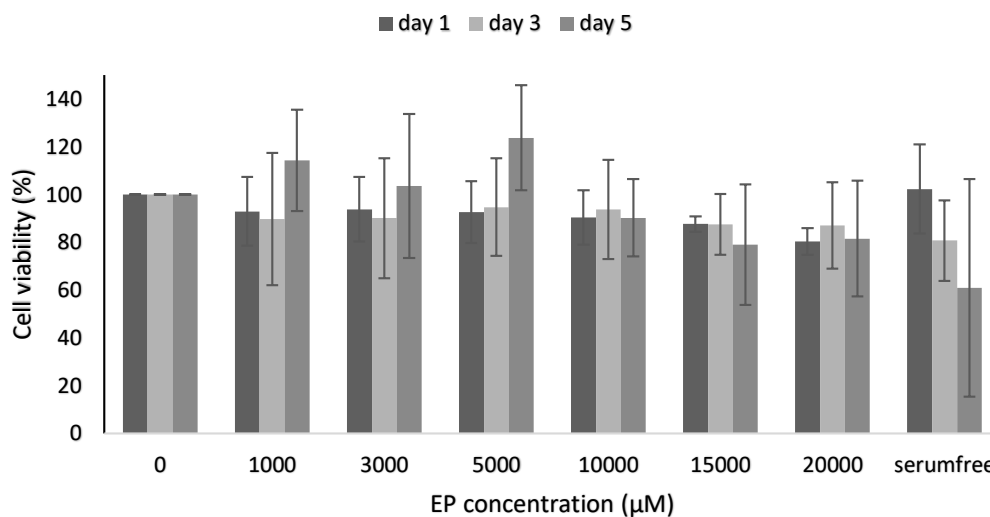


Figure 6.3 Cell viability measurement of cardiac fibroblasts treated with EP (1,000 – 20,000µM) for 5 days. Cell viability was measured with alamarBlue assay after 1 day, 3 days and 5 days of EP exposure in culture. Cells were seeded at a cell density of 3.5×10^4 cells/ml (700 cells /well). Cells with no EP treatment in 20% serum media were used as a negative control, cells with no EP treatment in serum-free media were used as a positive control. Data represent the mean +/- standard deviation from three replicate measurements from three experiments. No Significant differences were observed between the datasets.

Cells treated with EP in the concentration range between 1,000 – 5,000 µM showed an increase in cell viability over the 5 days of the treatment, with a peak of 124 ± 22 % at day 5. After the first day of treatment, cells presented a small reduction in cell viability, possibly because of the presence of EP or simply because in order to treat cells with EP, media was substituted with fresh media containing EP and this change might have stressed the cells. Although there were small differences found between the groups, a one-way ANOVA showed that there was no statistically difference between the different treatment groups.

6.2.3 Cell proliferation – BrdU assay

The effects of EP on cardiac fibroblasts were also assessed with the BrdU cell proliferation assay. The same cell density as the alamarBlue experiment was used in this study. Cells were treated with a range of EP concentration (1,000 – 20,000 μM) and cell proliferation was measured after 1 day and after 5 days of EP treatment. The methodology used in this section is explained in detail in section (2.1.3.1). The cell proliferation (%) of the cells treated with EP at day 1 and 5 days is shown in Figure 6.4.

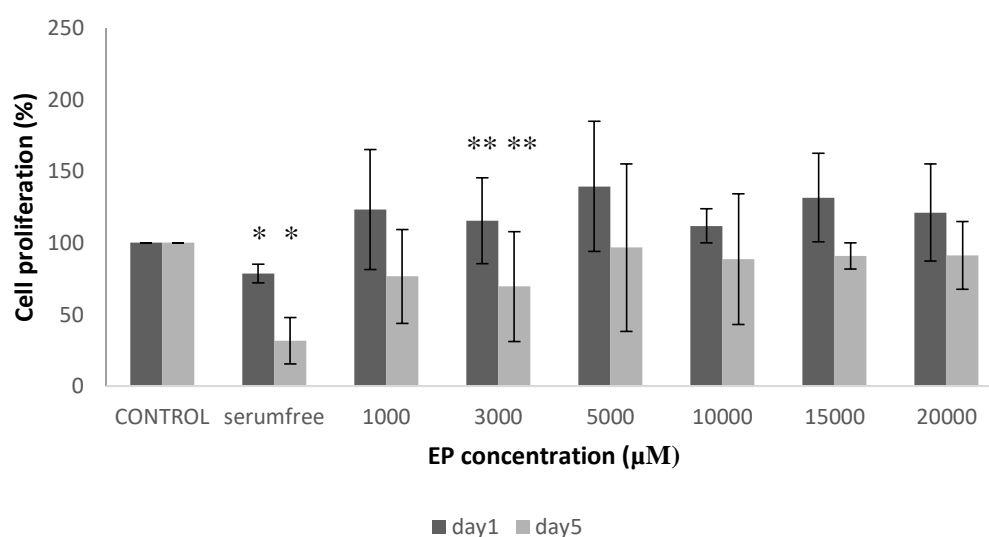


Figure 6.4 Cell proliferation measurement of cardiac fibroblasts treated with EP (1,000–20,000 μM). Cell proliferation was measured with BrdU assay after 1 day and 5 days of EP exposure in culture. Cells were seeded at a cell density of 3.5×10^4 cells/ml (700 cells/well). Cells with no EP treatment in 20% serum media were used as a negative Control, cells with no EP treatment in serum free media were used as a positive Control. Data represent the mean \pm standard deviation from three replicate measurements from three experiments * $p < 0.05$.

The cells treated with EP showed an increase in cell proliferation after 1 day of treatment, with cell proliferation above 100% for cells treated with EP, compared to the control (100%) and the serum-free 78.68 ± 6.51 %. The cells treated with 5,000 μM EP showed the highest cell proliferation of 139.42 ± 45.3 %, although the standard deviation in this case was much higher. Although there were small differences found between the groups, a one-way ANOVA showed that there was no

statistically difference between the cells treated with different EP concentrations at day 1.

After 5 days of treatment, cell proliferation decreased compared to day 1, but a two tailed t-test showed no statistical difference in cell proliferation between day 1 and day 5, excepts for the cells treated with 5,000 μM EP and the serum-free cells. Even in this case, although there appeared to be small differences between the treatment groups, a one-way ANOVA test showed that these were not statistically significant.

6.2.4 Live/dead staining and confocal imaging

Live/dead staining was used to further investigate cell viability with EP treatment. Cardiac fibroblasts were cultured in 35 mm culture Petri dishes. Except for the control, which consisted of cells with no EP treatment in a 20% serum media, one plate was treated with 3,000 μM EP and another one with 10,000 μM EP. In order to investigate the viability of cells exposed to EP, two mid-range EP concentrations were selected to represent a low concentration (3,000 μM) and a medium concentration (10,000 μM) of EP.

After 5 days of cell culture, cells were stained with two fluorescent dyes to detect dead cells and living cells. Propidium Iodide (PI) is a red-fluorescent dye that stains dead cells in a cell population. CFDA produces a green-fluorescence that stains only living cells. The methodology used in this study is described in more detail in section 2.1.5.

The live/dead staining (Figure 6.5a-c) show the live (green) and dead (red) cells in the 3 groups (control, 3,000 μM , 10,000 μM) after 5 days cell culture.

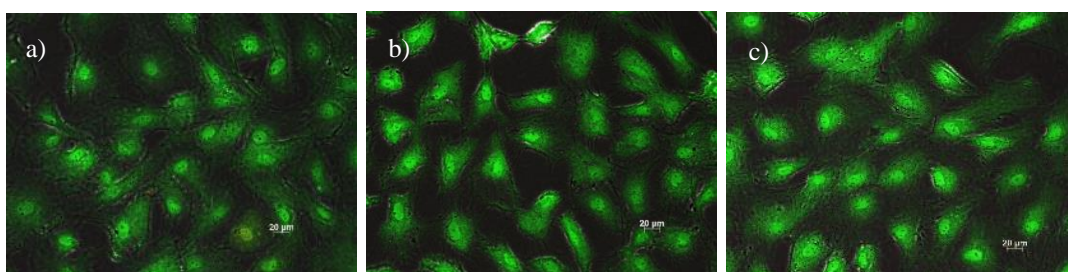


Figure 6.5 Representative images of Live/dead staining of cardiac fibroblasts treated with EP for 5 days. **a)** cardiac fibroblasts with no EP treatment in serum media (Control); **b)** cardiac fibroblasts treated with 3,000 μM EP; **c)** Cardiac fibroblasts treated with 10,000 μM EP. Cells were seeded at a cell density of 3.5×10^4 cells/ml in 35 mm culture Petri dishes (20 μm).

The cells were approximately 80% confluent after 5 days in culture in all three groups. The assay did not detect any obvious dead cells in the three petri dishes. There were no major differences between the control and the cells treated with 3,000 μM or 10,000 μM EP. This result indicates that EP did not induce cell death in the concentration range of 3,000 – 10,000 μM .

6.3 Effect of EP on cardiac fibroblasts treated with hydrogen peroxide

In a previously published study conducted on rat cardiac fibroblasts, an exposure of 100 μM hydrogen peroxide for a period of 24 h lead to a 54% reduction of cardiac fibroblasts survival (Xiaomin Zhang, 2001). This result suggested that the same hydrogen peroxide concentration (100 μM) would be suitable to investigate if EP is able to improve cell viability after H_2O_2 exposure and examine if EP can reduce H_2O_2 induced cell damage. Cardiac fibroblasts were exposed to 100 μM , and after 1 day of H_2O_2 exposure, the media containing H_2O_2 was removed and replaced with media containing EP in the range of 1,000 – 20,000 μM . After 1 day of incubation with EP, the media was removed and cells were analysed using the AlamarBlue assay (2.1.3.1). The methodology used in this section is explained in detail in section (2.1.7).

In a separate experiment, cells were exposed to H_2O_2 (100 μM) alongside EP in the range of 1,000 – 20,000 μM . After 1 day of incubation with both EP and H_2O_2 , the media was removed and cells were incubated with alamerblue in serumfree media and then analysed (2.1.3.1). Cells without hydrogen peroxide were used as a negative control and cells treated with the highest concentration of hydrogen peroxide in absence of EP were used as a positive control. The results are shown in Figure 6.6.

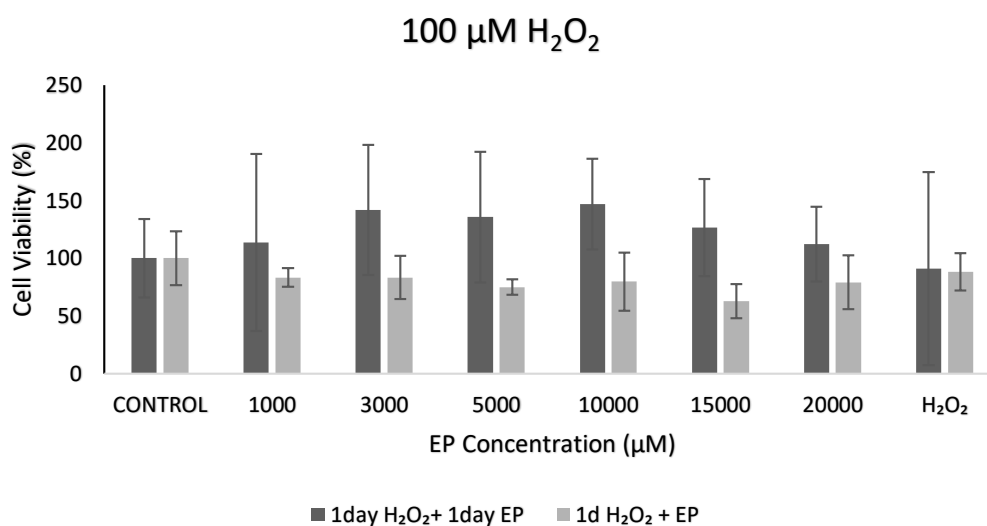


Figure 6.6 Preliminary study of the EP effect on cardiac fibroblasts exposed to 100 μM H_2O_2 for 24 hours. EP was administered after H_2O_2 exposure (blue) or in combination with H_2O_2 (orange). Cell viability was determined with alamarBlue assay. Cells were seeded at a cell density of 3.5×10^4 cells/ml (700 cells /well). Cells in serum media without hydrogen peroxide and EP treatment were used as a negative Control and cells treated with 100 μM H_2O_2 without EP were used as a positive control. Data represent the mean \pm standard deviation from three replicate measurements from one experiment. No Significant differences were observed between the datasets.

The exposure of the cells to 100 μM H_2O_2 did not lead to a substantial cell death, which was expected in the samples treated with H_2O_2 only. In fact, a one-way ANOVA test showed that there was no statistically difference between the groups. Note that this is preliminary data and that more validation is required. For this reason, the experiments were repeated but this time H_2O_2 concentration was increased from 100 to 150 μM . The results obtained are shown in Figure 6.7.

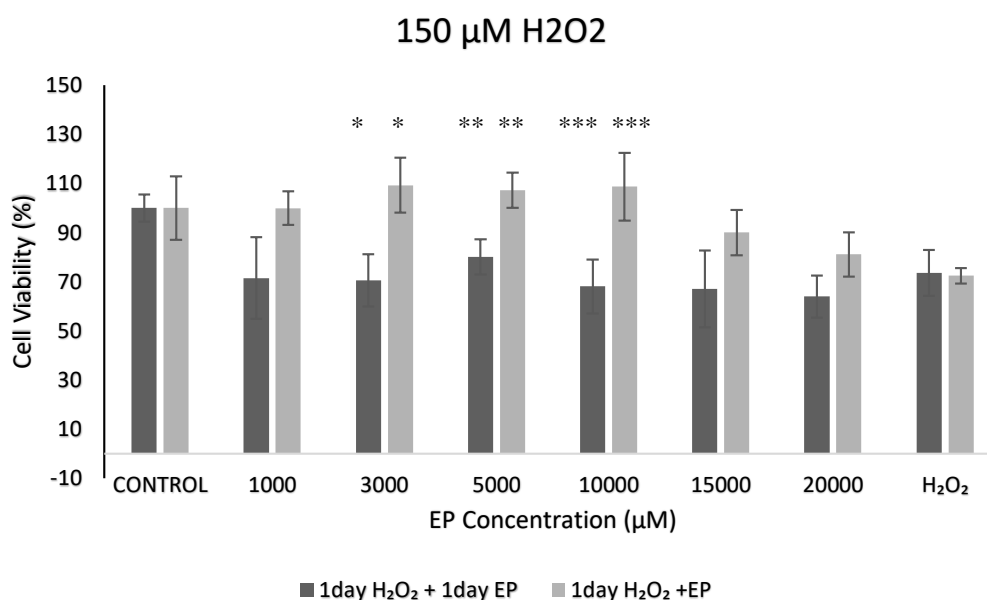


Figure 6.7 Preliminary study of EP effect on cardiac fibroblasts exposed to 150 μ M H₂O₂ for 24 hours. EP was administered after H₂O₂ exposure (dark grey) or in combination with H₂O₂ (light grey). Cell viability was determined with alamarBlue assay. Cells were seeded at a cell density of 3.5×10^4 cells/ml (700 cells/well). Cells without hydrogen peroxide and EP treatment were used as a negative Control and cells treated with the highest concentration of hydrogen peroxide were used as a positive control. Data represent the mean \pm standard deviation from three replicate measurements from one experiment * $p < 0.05$.

Cells treated with 150 μ M H₂O₂ only showed a reduction in cell viability by around 30% compared to the control. This result was similar in both groups (EP post-treatment and co-treatment). The cells co-treated with H₂O₂ and EP at the same time showed a significant increase in cell viability, when exposed to EP with a concentration range of 1,000 to 10,000 μ M compared to the cells treated with H₂O₂ only. This indicates that EP not only reduced the damaging effect of H₂O₂, but in that specific range EP promoted cell viability compared to the positive control. On the other hand, the group of cells treated with EP after the H₂O₂ exposure showed a reduction in cell viability very close to the cells treated with H₂O₂ only. A t-test two tailed distribution analysis ($p < 0.05$) showed that cell viability of the cells treated in the range of 3,000-10,000 EP was statistically higher in the co-treatment study than the post-treatment study, as shown in Figure 6.7. This result suggests that EP was not able to help the cells recover after H₂O₂ exposure, although it was effective to contrast H₂O₂ when added together. Note that this is preliminary data and that more validation is required.

6.4 Preliminary study of alginate scaffold biocompatibility using 3T3 cells

The aim of this aspect of the study was to investigate the biocompatibility of the scaffolds prepared in the previous chapter without EP. It was also important to identify the optimum method to seed the cells onto the scaffolds. Given this, it was decided to use a robust and well characterised 3T3 cell line. Alginate scaffolds were prepared following the methodology explained in section 5.4.2. In this preliminary study, the interaction between the cells and the scaffolds was of primary interest, so no EP was used in this experiment. The cells were seeded at a cell density of 3.5×10^4 cells/ml (700 cells /well) into either 100 μ L dry scaffolds (n=5) or pre-wetted with cell media (n=5) in a 96 well-plate. LDH assay was used to measure viability of the cells that had been seeded onto the scaffolds. LDH assay was preferred to the other methods because it does not interact with the scaffolds and cells directly, but only the cell media is collected and analysed (section 2.1.4.5). 200 μ L of media was collected from each well every day (day 1-5) during the duration of the study. Cell media was always replaced with fresh media, for the continuation of the study. At the end of the incubation period of 5 days, the scaffolds were taken forward for evaluation by fluorescent microscopy (2.1.5).

6.4.1 LDH activity

The viability of the 3T3 cells that had been seeded onto the scaffolds is shown in Figure 6.8.

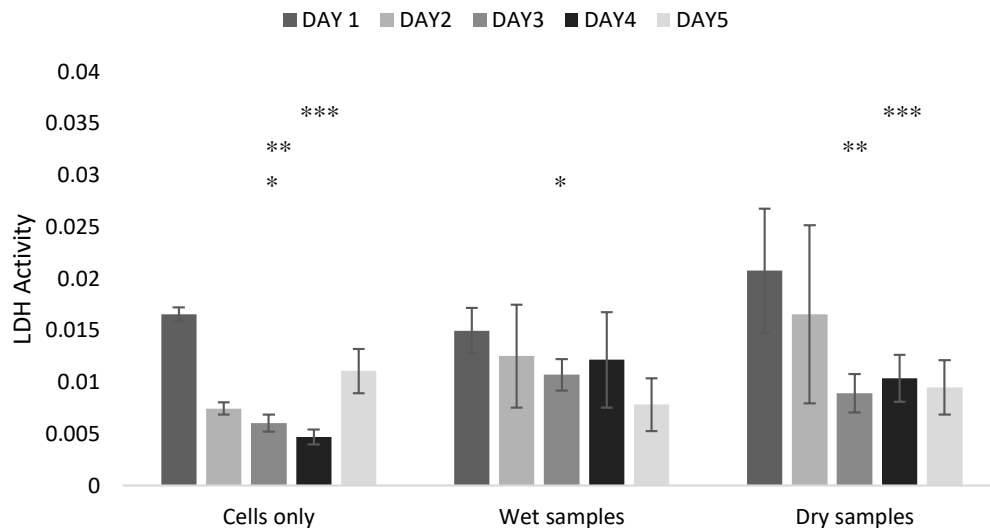


Figure 6.8 LDH assay of 3T3 cells seeded onto alginate scaffolds. The cells were either seeded into dry scaffolds or pre-wetted with cell media ($n=5$). Cells were seeded at a cell density of 3.5×10^4 cells/ml (700 cells /well). Cells with no scaffolds were used as a control. Data represent the mean \pm standard deviation from three replicate measurements from one experiment * $p < 0.05$.

The LDH of the cells decreased over time from day 1 to day 4 and decreased at day 5, while in the samples with alginate scaffolds LDH decreased over time until day 5. In fact, cells with no scaffold showed an increase in LDH activity at day 5, possibly due to the fact that cells were 100% confluent. Cells seeded into dry scaffolds were observed to have a higher LDH at the beginning and at the end of the study compared to the cells seeded onto wetted scaffolds. A t-test, two tailed, showed that there was a statistical difference between the cells only and the scaffolds (both wet and dry) at day 3, while between cells only and dry scaffolds there was statistical difference even at day 4.

6.4.2 Live/dead staining and confocal imaging

After 5 day of cell culture, cells within the two groups of scaffolds were stained with two fluorescent dyes to detect dead cells and living cells, as described in section 2.1.5.

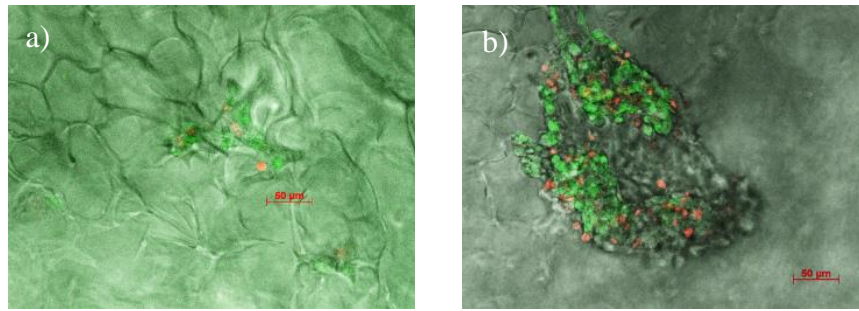


Figure 6.9 Representative images of Live/dead staining of 3T3 cells seeded onto alginate scaffolds after 5 days in culture. a) Live/dead (PI/CFDA) staining of cells seeded onto a dry alginate scaffold; b) Live/dead staining of cells seeded onto a pre-wetted alginate scaffold. The live/dead staining differentiate the live (green) and dead (red) cells. Images representative of 5 separate scaffolds for each group.

The live/dead staining performed on the dry scaffold resulted in the staining not only of the cells, but also of the scaffold. In fact, the Figure 6.9-a shows the scaffold stained green by the CFDA. The purpose of the staining is to highlight the cells (live and dead) present onto the scaffold. The staining of the scaffold limited the detection of the live cells, making the staining unsuitable for this type of scaffold. On the other hand, the pre-wetted scaffolds did not retain the dye, as shown in Figure 6.9-b). This time only the cells were stained and the image obtained clearly shows the live cells (green) and the dead cells (red) on the scaffold. This result demonstrates how the pre-wetting step is very important for the outcomes of the experiment.

In order to understand if the cells were only on the surface of the scaffolds, images of planes were taken at various depths within a pre-wetted sample (z-stacks). Moving through the sequence (from left to right) it is possible to see the cells distributed through the scaffold, from the top surface until a depth of 135µm (Figure 6.10).

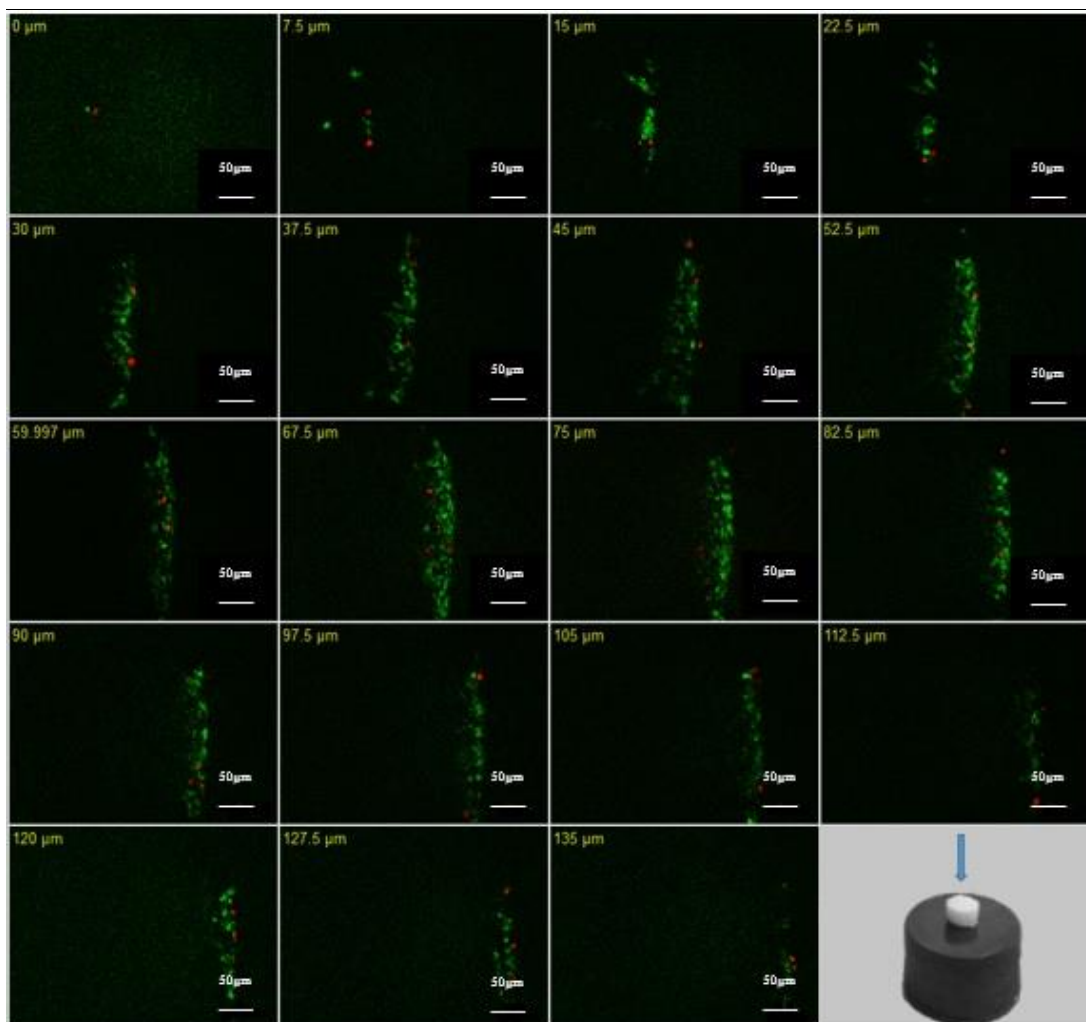


Figure 6.10 Representative images of Live/dead staining of the 3T3 cells seeded onto a pre-wetted sample using z-stacking method. Images of planes were taken at various depths. Cells were seeded at a cell density of 3.5×10^4 cells/ml (700 cells/well). Moving through the sequence (from left to right) it is possible to see the cells distributed through the scaffold, from the top surface until a depth of 135 μ m. Images obtained from a single scaffold.

Cells were found to be present within different layers of the scaffolds over 8 days of culture. The majority of the cells were alive (green) in all the depths, indicating that there was sufficient nutrient flow established through the porous scaffolds. This suggests that the scaffolds were biocompatible and cells were able to migrate and/or proliferate within the scaffolds.

6.5 Effect of double cross-linked alginate scaffold on cardiac fibroblasts

Cardiac fibroblasts were seeded onto four groups of scaffolds (Alginate alone; Alginate:EP; RGD-Alginate alone; RGD-Alginate:EP). The scaffolds produced with double cross-linking (method 6) were shown to have the optimal EP release and porosity suitable for cell infiltration and proliferation (see sections 5.6.2 and 5.8.1). This alginate formulation method was therefore selected to be tested in cell culture. The cells were cultured for 5 days, with medium removed at day 1, 3 and 5 and analysed by LDH assay (section 2.1.3.5). At the end of the incubation period of 5 days, a Neutral Red assay was performed and the patches were then taken forward for evaluation by fluorescent microscopy (section 2.1.4).

6.5.1 Cell viability – Neutral Red assay

In order to select the best method to measure cell viability, MTT and neutral red were used to stain alginate scaffolds. It was observed that MTT assay was retained by the scaffolds, on the other hand, this problem was not found with Neutral red. For this reason, Neutral red assay was used to measure cell viability in this part of the study. The viability of cardiac fibroblasts seeded onto alginate scaffolds was measured after 5 days of incubation. The effect of the alginate scaffolds on cardiac fibroblast viability is shown in figure 6.11.

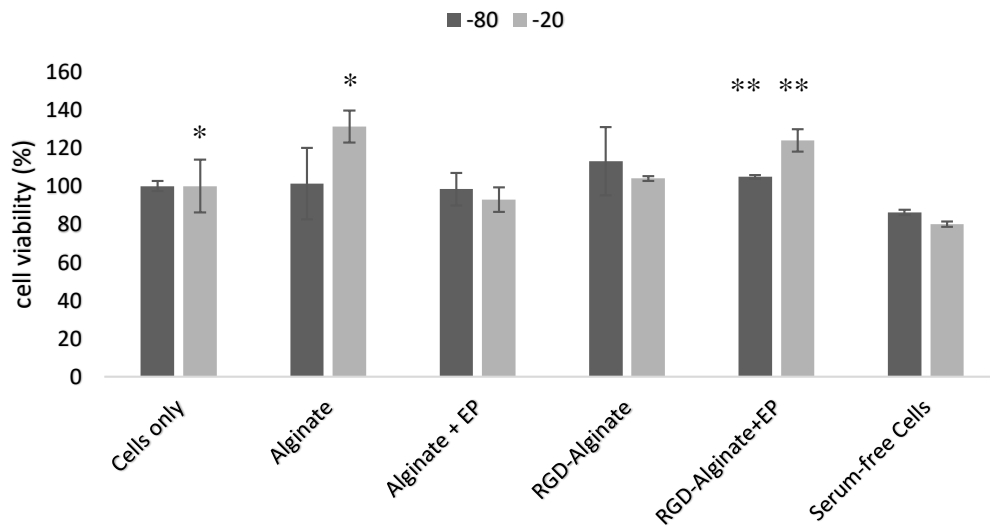


Figure 6.11 Cell viability measurement of cardiac fibroblasts seeded onto four groups of scaffolds; Alginate alone; Alginate:EP; RGD-Alginate alone; RGD-Alginate:EP. The scaffolds were produced with method 6 at -20°C and -80°C . Cells were seeded at a cell density of 3.5×10^4 cells/ml (700 cells /well). After 5 days of incubation, Neutral Red assay was used to measure cell viability ($n=3$) Cells only in 20% serum media were used as a negative Control, cells only in serum-free media were used as a positive Control ($n=3$). Data represent the mean \pm standard deviation from three replicate measurements from one experiment * $p < 0.05$.

The presence of all scaffold types was generally well accepted by the cells, with no clear signs of toxicity. All the scaffolds except Alginate + EP (-20°C / -80°C) showed an increase in cell viability compared to the cells only. Surprisingly, Alginate alone scaffolds (-20°C) showed the highest cell viability over all, even although this type of scaffolds lacks RGD peptide sites. One-way ANOVA showed that the Alginate alone (-20°C) was the only one statistically different from the cells only. Cells seeded onto RGD- Alginate + EP (-20°C) scaffolds presented the second highest cell viability, demonstrating that the cells not only accepted the scaffold, but also the presence of EP. A t-test, two tailed, showed that the scaffolds prepared at -20°C were not statistically different to the scaffolds at -80°C , except for the RGD-Alginate +EP scaffolds, which showed higher cell viability in the scaffolds prepared at -20°C .

6.5.2 LDH assay

LDH assay was used to measure viability of the cells seeded onto the scaffolds. 200 μL of media was collected at day 1, 3 and 5 during the duration of the study. The media was always replaced with fresh media.

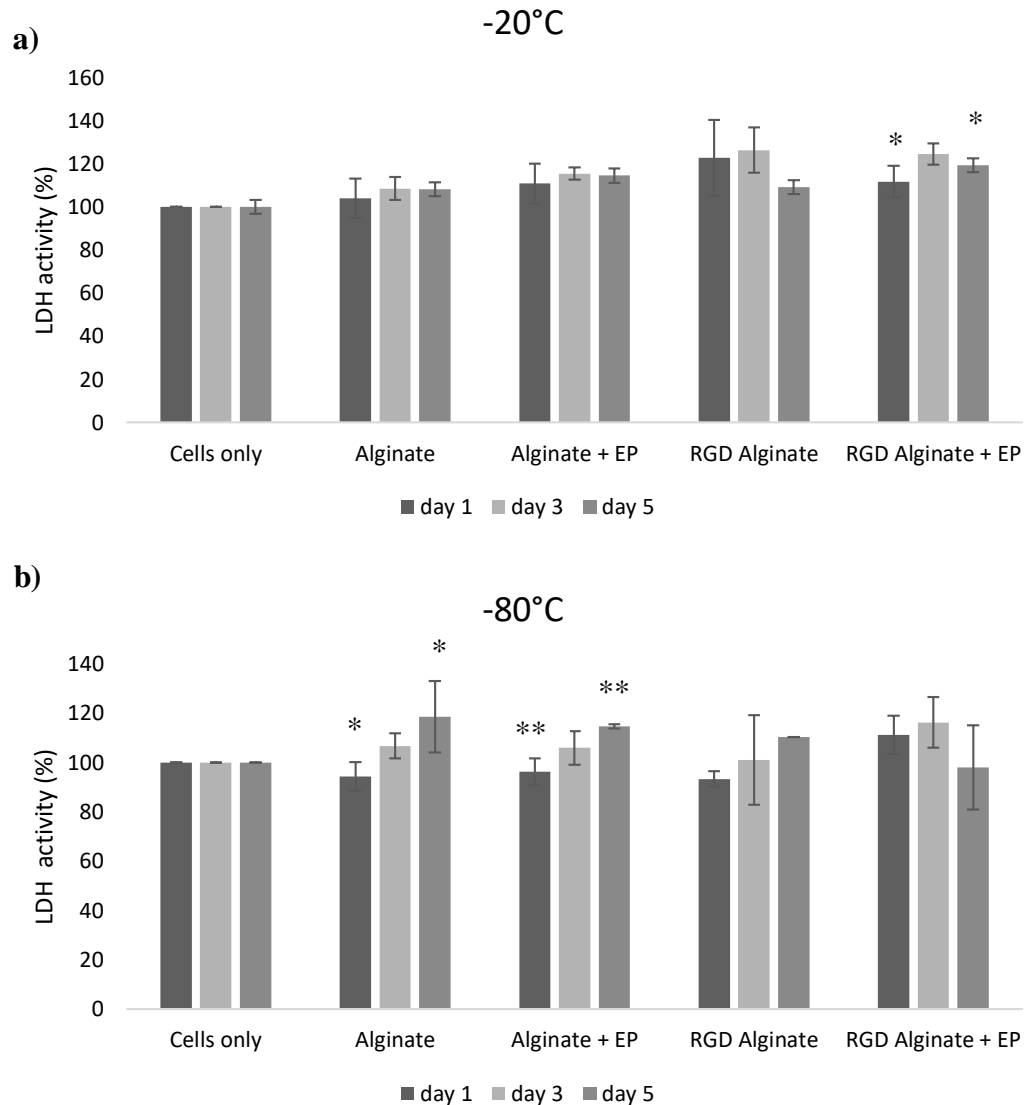


Figure 6.12 LDH activity measurement of cardiac fibroblasts seeded onto four groups of scaffolds; Alginate alone; Alginate:EP; RGD-Alginate alone; RGD- Alginate: EP. Cells were seeded at a cell density of 3.5×10^4 cells/ml (700 cells /well). The scaffolds were produced with method 6 at: **a)** - 20 and **b)** -80°C. At day 1, day3 and day 5 of incubation LDH was measured. Data represent the mean +/- standard deviation from three replicate measurements from one experiment * $p < 0.05$.

The LDH activity of the cells increased at day 3 and decreased at day 5 in the two groups of RGD-scaffolds prepared at -20°C (with and without EP). In fact, the t-test, two tailed, paired analysis showed that only the RGD+EP was statistically different at day 5 compared to day 1.

Cells seeded onto the scaffolds prepared at -80°C showed an increase in LDH activity over time, except for the cells seeded onto the RGD + EP. Alginate scaffolds and alginate scaffolds +EP were found to be statistically different at day 5 compared to day 1 (t-test).

6.5.3 Live/dead staining and confocal imaging

Live/dead staining was used to detect dead cells and living cells, as described in the section 2.1.5.

Alginate scaffolds without RGD (-20 °C) had only a small amount of living cells, especially the scaffold with EP, where the dead cells were higher in number than the living cells (Figure 6.13-c). In contrast, the corresponding scaffolds prepared at -80 °C had a visibly higher amount of live cells compare to the group prepared at -20°C(Figure 6.13-c).

A greater number of live cells was found in those scaffolds prepared with RGD alginate compared to scaffolds prepared without RGD alginate (in both groups -20/-80 °C) (Figure 6.13-a, -b compared to Figure 6.13-c, -d). In particular, cells seeded onto the RGD-alginate scaffolds with and without EP (-20) had mostly viable cells Figure 6.13-c, -d. On the other hand, the corresponding scaffolds prepared at -80°C presented a higher number of dead cells Figure 6.13-c, -d.

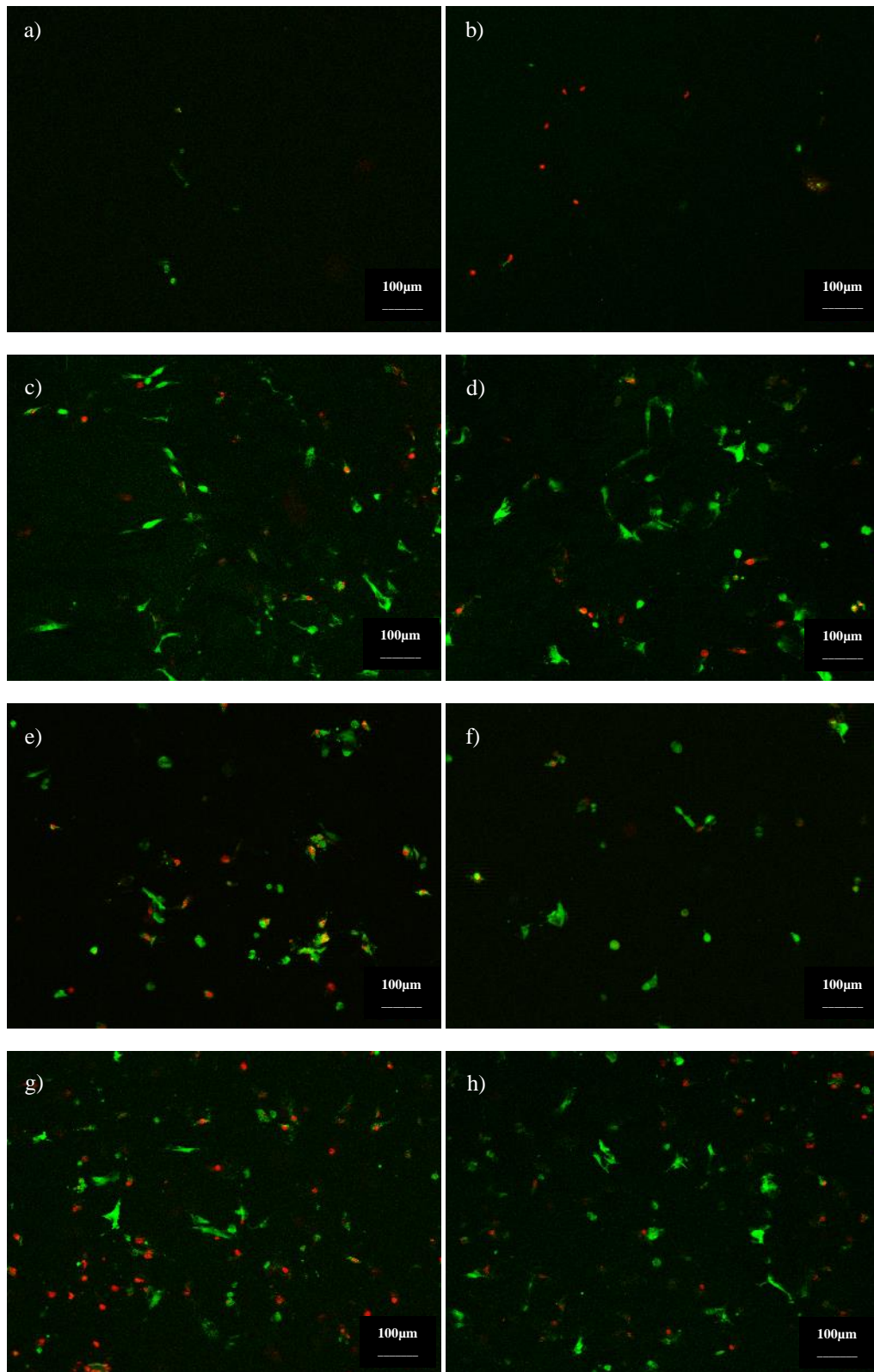


Figure 6.13 Fluorescence microscopy images (10X) following PI (Dead cells, red)/ CFDA (Live cells, green) staining of rat cardiac fibroblasts seeded onto scaffolds produced with method 6 at -20°C: **a)** Alginate alone; **b)** Alginate:EP; **c)** RGD-Alginate alone **d)** RGD-Alginate:EP; and on scaffolds prepared at -80°C: **e)** Alginate alone; **f)** Alginate:EP; **g)** RGD-Alginate alone **h)** RGD-Alginate:EP. Cells were seeded at a cell density of 3.5×10^4 cells/ml (700 cells /well). At the end of the incubation period of 5 days, the patches were taken forward for evaluation by fluorescent microscopy Images are representative of 5 independent images from each sample.

With the aim of understanding if the cells were only on the surface of the scaffolds, images of planes at various depths within the RGD alginate scaffolds with EP (-20/-80 °C) z-stacks were taken at various time points. Moving through the sequence (from left to right) it is possible to see the cells distributed through the scaffold, from the top surface until a distance of 71.62µm for the (-20°C) and 36.05 µm for the -80°C.

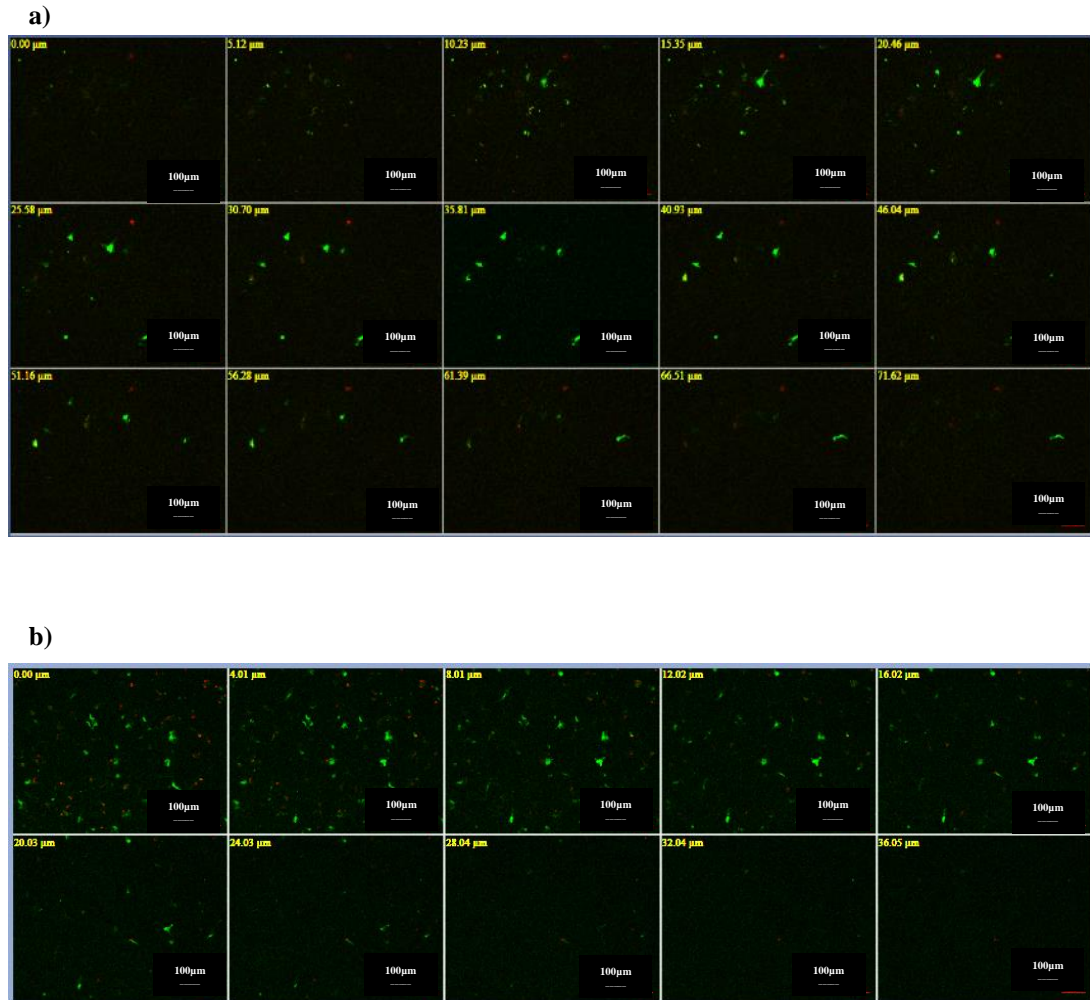


Figure 6.14 Fluorescence microscopy images (10X) following PI (Dead cells, red)/ CFDA (Live cells, green) staining of rat cardiac fibroblasts seeded onto scaffolds produced with method 6 at -20°C: **a)** RGD-Alginate:EP; and on scaffolds prepared at -80°C: **b)** RGD-Alginate:EP. Cells were seeded at a cell density of 3.5×10^4 cells/ml (700 cells /well). At the end of the incubation period of 5 days, the patches were taken forward for evaluation by fluorescent microscopy.

Cells proliferated through the scaffolds over 5 days of culture. The majority of the cells were alive in all the depths, showing that the scaffolds were biocompatible and the nutrients could pass through the porous of the scaffolds. The scaffold prepared at -80°C showed a higher number of dead cells, compared to the scaffold prepared at -20°C. Cells proliferated through the scaffolds reaching different depths, 71.62µm in the scaffold prepared at -20°C and 36.05 µm in the scaffold at -80°C.

6.6 Discussion

6.6.1 Introduction

The ultimate aim of this project was to investigate a novel technology for prevention of damaging cardiac remodelling following ischaemic injury, by reducing the oxidative stress and stimulating the regeneration of functional cardiac tissue. An optimum alginate patch formulation and synthesis method, which provides sustained release of EP over a 28-day period, was identified through the work detailed in chapter 5. However, the potential for this technology to be effective clinically depends to a large extent on its biocompatibility. The overall aim of the work described in this chapter was therefore to investigate the *in vitro* effects of the alginate patches on primary cardiac cells.

6.6.2 EP effects on cardiac fibroblast cell viability and proliferation

Firstly, it was important to characterise the effects of EP alone in the absence of the scaffold. The cytotoxicity of EP has been tested *in vitro* on different cell types, such as human erythrocytes (Birkenmeier, *et al.*, 2016), human blood monocytes (Worku, *et al.*, 2015), human trabecular meshwork cells (Famili, *et al.*, 2013), but not on cardiac fibroblasts. For this reason, it was necessary to investigate the potential cytotoxicity of EP on cardiac fibroblasts. There was no cytotoxicity observed in cells treated with either 3 or 10 mM EP, as evidenced by the absence of red fluorescence in cells stained with PI/CFDA after 5 days in culture (figure 6.5). This finding is in agreement with observations from previous studies, which demonstrated that EP is well tolerated by human erythrocytes (Birkenmeier, *et al.*, 2016), human blood monocytes (Worku, *et al.*, 2015), human trabecular meshwork cells (Famili, *et al.*, 2013).

Various concentrations of EP were administered to cardiac fibroblasts and cell viability measured after 5 day of culture. It was observed that EP had a quite limited dose-dependent effect on cell viability, with viability maintained at around 80% of control at the maximum EP concentration of 20 mM (Figure 6.1-a) and the metabolic activity of 65% (Figure 6.1-b) after 5 days of culture. AB assay was used at day one, day 3 and day 5 of the treatment, to provide more information on the temporal effects of EP on cells. The results confirmed the resistance of cardiac fibroblasts to EP during the whole duration of the study (Figure 6.3). Not only cell viability was maintained at about 80% at high EP concentration of 20 mM, but in the range of 1-5 mM, cells showed a small increase in cell viability compared to the control (Figure 6.3).

The results obtained are in accordance with previous studies that investigated the short term effect of EP exposure on different cell cultures (Birkenmeier, *et al.*, 2016) (Worku, *et al.*, 2015). In the study conducted by Birkenmeier *et al.*, 2016, blood monocytes were treated with EP at increasing concentrations (1-20 mM) for 12 hours at 37°C. The majority of monocytes (approximately 80%) remained viable even at 20 mM EP (Birkenmeier, *et al.*, 2016). The human erythrocytes showed a similar resistance to high concentration of EP as described by Worku *et al.*, 2015. The erythrocytes were exposed to a range of EP concentration of (1–15 mM) for 3 hours and about 80% of the cells remained alive even at 15 mM EP (Worku, *et al.*, 2015). On the other hand, Famili *et al.*, 2013 showed that human trabecular meshwork cells well tolerated EP at the concentration of 1-10 mM but at higher concentration of 20 mM EP reduced cell viability up to 10% after 5 days of incubation (Famili, *et al.*, 2013).

6.6.3 Anti-oxidant effects of EP in cardiac fibroblasts

EP is known to have antioxidant properties, such as being able to scavenge hydrogen peroxide (Yang, *et al.*, 2016). This has been demonstrated in a number of cell types (Famili, *et al.*, 2013)(Yang, *et al.*, 2016)(Zeng, *et al.*, 2007) although it is unclear if it has protective effects on cardiac fibroblasts when exposed to H₂O₂. Given that the alginate patches developed in the current study are intended to be used to help improve regeneration of cardiac tissue following periods of ischaemia that have occurred pre,

during and post-surgery, it was important to examine the temporal effects of EP when cells are exposed to H₂O₂.

Cardiac fibroblasts were treated with H₂O₂ and the effects of EP, delivered in combination with H₂O₂ or after the exposure to H₂O₂, were investigated. In addition, given the intended future potential application of this technology *in vivo*, it was important to determine if EP would be more effective to help cells during Oxidative challenge or after the damage had occurred. It was observed that when cardiac fibroblasts were exposed to a H₂O₂ (150 µM) and EP at the same time, cell viability was maintained above 80% and even increased to 107-109% at EP concentrations of 3,000 and 10,000 µM. On the other hand, cells treated with EP after H₂O₂ exposure did not recover after being stressed, but it appeared that the presence of EP somehow reduced cell viability, compared to the negative control. This result supports previous observations by Famili *et al*, 2013, who showed that the co-treatment of EP and hydrogen peroxide increased the cell viability, compared to the cells without EP treatment or cells with an EP pre-treatment (Famili, *et al.*, 2013). On the other hand, Kim *et al* 2005, obtained completely contrasting results, demonstrating how EP rescued the neuron cells after H₂O₂ exposure (Kim, *et al.*, 2005).

6.6.4 *In vitro* investigation of alginate-EP patches in cell culture

Once the safety of EP on cardiac cells was confirmed and the effectiveness of protecting the cells from H₂O₂ was demonstrated, the next step was to investigate the effects of the scaffolds produced on cells. The effect that this novel scaffold loaded with EP has on cells has not been previously reported and so this study helps to address this gap.

Alginate scaffolds were firstly tested for biocompatibility on a 3T3 cell culture. The results obtained with the LDH assay showed an overall acceptance of the scaffolds by the cells. In particular, it was observed that the cells seeded into dry scaffolds were more stressed at the beginning and at the end of the study compared to the cells seeded onto wetted scaffolds (Figure 6.8). This result suggested that the cells were less stressed when seeded onto wet scaffolds. The results obtained by the live/dead staining confirm the biocompatibility of the scaffolds, with the clear abundance of live cells

(green) on the surface of the wet scaffold (Figure 6.9) and all the way through the scaffold (Figure 6.10).

In order to improve cell attachment and proliferation, alginate scaffolds were prepared using RGD alginate. Several studies have demonstrated how the presence of RGD with alginate scaffolds promoted cell proliferation (Ruvinov & Cohen, 2016). In particular, neonatal rat cardiac cells were seeded into RGD-immobilized or unmodified alginate scaffolds (Shachar, *et al.*, 2011). After 10 days of culture the RGD alginate scaffolds promoted the formation of functional cardiac muscle tissue. In contrast, in the unmodified alginate scaffolds the cells did not form such a structure (Shachar, *et al.*, 2011).

In this study, the effect of the scaffolds on cells was investigated, but perhaps more importantly the effect of the complete EP loaded RGD scaffolds on the cells was also investigated. Alginate scaffolds (-20°C), without RGD and EP, showed the highest cell viability over all (Figure 6.12), although the live/dead staining showed a very small number of cells in the scaffolds (Figure 6.13-a). This result is likely due to the cell proliferation occurring in the well, but not necessarily within the scaffolds. Cells seeded onto RGD-Alginate+EP (-20°C) scaffolds presented the second highest cell viability (Figure 6.12), indicating that the cells benefit from the structure of the scaffold, as well as from the presence of EP. This result was confirmed with the live/dead staining as shown in Figure 6.13-d. Viable cells were found throughout the scaffold, from the top surface until a distance of 71.62µm, demonstrating that the scaffold structure enabled the nutrients to pass through the porous structure (Figure 6.14-a). As expected, the presence of the RGD peptide increased cell attachment and EP increased cell viability compared to the RGD scaffolds without EP. In fact, EP is not only an antioxidant, but it has the ability to enhance ATP levels, crucial for cell viability and proliferation.

6.6.5 Limitations

One of the limitations of this study is the experiment conducted with H₂O₂ was only preliminary. In fact, because of the limited availability of primary cells, it was not possible to produce more replicates of this study.

The effects that the scaffolds have on cardiac fibroblasts were investigated, but it is still unknown the effect that the scaffolds would have on cells if they are exposed to H₂O₂. This experiment was not carried out due to the limited availability of primary cells, making it the main limitation of the study.

Although cardiac fibroblasts represent a useful and relevant cell type for studies of this nature, it is important to recognise that investigating their viability and proliferative response represents just two important functional aspects. However, this study has not considered the impact of EP or indeed the scaffolds on the phenotype of these cells or other important functional aspects. Such studies will need to be completed, alongside investigation of the impact of the scaffolds on cardiac myocytes in culture, before firm conclusions can be drawn on the potential of this technology.

6.6.6 Future work

Several animal studies have shown how EP reduced oxidative stress in myocardial ischemia/reperfusion injury (Guo, *et al.*, 2014)(Jang, *et al.*, 2010)(Woo, *et al.*, 2004). It was also demonstrated that alginate scaffolds are biocompatible and allow cell proliferation *in vivo* (Ruvinov & Cohen, 2016). In addition to studies to address the limitations set out above, the next major step will be the *in vivo* testing of EP loaded scaffolds in small animals. In this way it would be possible to investigate the effectiveness of the EP loaded scaffolds on damaged hearts *in vivo*.

6.6.7 Summary conclusions

In this chapter, it has been shown that EP is not toxic to cardiac fibroblasts in the range of concentrations studied. It was also observed that EP exerted a protective effect on the cells when exposed to H₂O₂ for 24 hours. The patches were tested first in a 3T3 culture demonstrating their biocompatibility over 5 days. The patches with EP were then tested in a cardiac fibroblasts culture. After 5 days of culture, cells proliferated through the scaffolds, preferring the RGD alginate scaffolds with EP.

7 CHAPTER SEVEN

GENERAL DISCUSSION

7.1 Summary

Ischemia/reperfusion leads to high levels of oxidative stress and inflammation, which produce deleterious effects in the myocardium (Hori & Nishida, 2009). In fact, a sustained increase in TNF-beta levels has been recorded in the first 3 weeks after MI (Sia, *et al.*, 2002), while another study showed that in patients treated for acute myocardial infarction, the level of oxidative stress in the blood increased progressively, reaching a peak after 7 days (end point) when the patients were discharged from the hospital (Nikolic-Heitzler, *et al.*, 2006). Anti-inflammatory and antioxidant treatments have been investigated as a possible therapy to limit tissue damage after MI (Hori & Nishida, 2009). Several of these studies have shown promising results in using antioxidants for the inhibition of left ventricular remodelling (Hori & Nishida, 2009).

EP has been demonstrated to reduce oxidative stress and increase myocardial ATP levels and decreased infarct size in rats (Woo, *et al.*, 2004). EP enhanced tissue ATP levels, preserved cardiac function, and attenuated myocardial oxidative injury in a Langendorff perfused heart experiment (Guo, *et al.*, 2014). In rat models of ischaemia/reperfusion, one injection of EP showed to inhibit cytokines production and consequently reduced infarct size (Jang, *et al.*, 2010). Despite the encouraging results obtained in animal models of ischaemia/reperfusion injury, EP failed to reduce the incidence of the post-operative adverse outcomes and it did not decrease the systemic inflammatory markers when administered intravenously in high-risk patients undergoing heart surgery (Bennett-Guerrero, *et al.*, 2009). Although EP was ineffective in the clinical trial, the authors suggested that possibly the dose administered to the patients was not adequate and the length of the treatment might have been insufficient (Bennett-Guerrero, *et al.*, 2009). This suggests that the drug delivery methods used were not effective to reduce oxidative stress after myocardial injury. The delivery of an antioxidant, in this case EP, from an implanted material in

situ would not only minimise any unwanted systemic effects, but also be potentially more effective in the tissue area that needs to be treated (Dikmen, *et al.*, 2011). EP has never been delivered in a sustained manner, so this method of delivery would therefore allow the use of a lower amount of EP and a sustained delivery over several days and potentially weeks.

In order to be able to fully explore the relationship between drug dose and efficacy over time *in vitro*, it is important that there are robust methods in place to allow measurement of EP. There has been little investigation into the methodology to determine the concentration of EP in physiological solution. To our knowledge only one method has been reported for the measurement of EP in physiological solution (Kim, *et al.*, 2011). This method of EP measurement requires several specialist items of equipment, which were not available to this project and indeed are not always readily available in many laboratories. Therefore, there was a need to identify an alternative method that would not only be suitable for the current project, but which could be adopted more widely by other research groups active in this area.

For this reason, 6 different techniques were investigated to assess their suitability for measurement of EP, with the results of this work described in detail in chapter 3. The first method used was the pyruvate assay. Although the assay successfully detected EP in PBS, the range of EP concentrations that could be measured was very limited (40-400 μM). Because EP is well known for its antioxidant effects, it was decided to investigate indirect measurement of EP through the use of antioxidant assays, an approach not previously reported. In this way, the measurement of the antioxidant effect of EP could have been translated into an amount of EP present within the samples tested. Based on this principle, two antioxidant assays, specifically the DPPH assay and the ABTS assay, were used to measure indirectly the amount of EP, by measuring its antioxidant effect. The EP calibration curve obtained with the DPPH assay showed no consistent relationship across the concentration range examined, demonstrating the unsuitability of this method to measure EP. The antioxidant ABTS assay was then investigated as an alternative to the DPPH assay. Although the results obtained showed that EP reduced the formation of the radical cation ABTS^+ , the relationship between EP concentration and ABTS radical formation was not

consistent. This suggested that the ABTS assay, like the DPPH assay discussed before, was not suitable for reliable measurement of EP in solution.

Given that none of the above assays appeared to be suitable for EP measurement, it was decided to investigate UV spectroscopy as a possible alternative method. To our knowledge, this technique has not been investigated for the measurement of EP, so no information on the most appropriate wavelength to select for EP detection was available in the literature. In this study EP was successfully detected in the range of 203-213 nm. The results obtained with the spectrophotometry were confirmed with three different devices, demonstrating the robustness of the data collected. The UV/Vis spec machine was able to detect and measure EP in a range of 78-2,500 μM while the Nanospec device was effective over a greater range of concentrations (78-20,000 μM). HPLC failed to detect EP in physiological solution, although it was found that this method was particularly suitable for measurement of EP in methanol, with an effective calibration range of 70-12,500 μM . Overall, the Nanospec was demonstrated to be a simple, inexpensive and reliable method to measure EP in physiological solution, particularly for the measurement of small volumes (2 μl).

Having optimised the method of EP measurement, the stability of EP in physiological solution during freeze/thaw cycles and during prolonged periods at 37 °C was investigated. Understanding of such stability is crucial if EP is to be delivered from a patch implanted within the body over time, as is the case for the intended application within the present study. The enhanced stability of EP in comparison to standard pyruvate means that it has been the preferred drug in a number of clinical investigations in this area (Flink, 2007). In the present study, the UV absorbance profiles of EP were found to be consistent when measured at different time points during two-weeks incubation in physiological solution at 37 °C. This is an important result because it may suggest a possible application as a sustained release treatment *in-vivo*, although further analysis using HPLC would be required to fully confirm this stability under these conditions. The EP absorbance was also demonstrated to be consistent during repeated freeze/thaw cycles, which is an important observation relevant to interpretation of the results from the subsequent materials development and EP release studies detailed in chapters 4 and 5.

Although alginate hydrogels have been used for different biomedical applications, including as drug delivery vehicles, they have not previously been used to provide sustained delivery of anti-inflammatory/antioxidants onto the myocardium for cardiac regeneration. This challenge provides the overall rationale for the present study and the work detailed in chapters 4 and 5 in particular.

The novelty of the concept being explored in this thesis meant that the optimal release time of EP into the myocardium was unknown. However it is recognised that a sustained increase in TNF-beta levels in the first 3 weeks after MI has been reported in a rat study (Sia, *et al.*, 2002), while in a clinical study patients with acute myocardial infarction presented a progressive increase in oxidative stress levels in the blood, reaching a peak after 7 days (end point) (Nikolic-Heitzler, *et al.*, 2006). It was therefore decided to target the development of alginate materials that would provide EP release for up to 3 weeks. Different approaches were investigated to prepare alginate hydrogel-EP formulations to achieve this. Alginate with high M content was initially used as an inexpensive and convenient material in order to perform some preliminary method development studies. This type of alginate produces a less stable hydrogel, compared to the hydrogels prepared with high G content alginate, due to the fact that the G component of alginate is responsible for the crosslinks with calcium, so higher G content corresponds to higher crosslinking and hence greater stability (Lee & Mooney, 2012). For this reason, high G content alginate was used for the rest of the experiments. EP was successfully loaded into the alginate hydrogels by adding it to the alginate solution before the crosslinking step. Different alginate concentrations (1-2%) and different CaCl₂ concentrations (0.6%, 1% and 1.5%) were used to prepare the gels. In this way it was possible to investigate how those variables can affect the stability of the gels. In order to quantify stability, the gels were immersed in PBS their change in weight measured periodically over 28 days. The change in weight of the gels was relatively small, with little difference between the different formulations tested, suggesting that the alginate and cross-linker concentration do not greatly impact upon the gel stability, at least not at the concentrations and time frame examined in the present study. SEM images of the various gel formulations referred to above suggest that the presence of EP did not interfere with the final morphology of the hydrogel. Ultimately, the results obtained in this aspect of the study demonstrated that the

alginate gels prepared remained stable over 28 days and therefore may be suitable for the delivery of EP over a similar time frame.

Alginate has been used to deliver small drugs in previous work (Lee & Mooney, 2012), but it has never been used to deliver an antioxidant, in particular EP. The various alginate-EP formulations developed are therefore novel, with all of them demonstrating the capacity to provide EP release over time. 1% alginate gels released approximately 2000 μg after 28 days in PBS, which appeared to be independent of the cross-linker concentration. However, increasing the concentration of alginate to 2% lead to an increase in total EP release to approximately 3000 μg . This increase was observed with the 1% and 1.5% formulations but not the 0.6% cross-linker concentration. These results suggest that there may be a relationship between alginate concentration and EP release, meaning that it may be possible to tune the drug dose delivered by varying the concentration of alginate within the formulation. Furthermore, the results with the 2% formulation indicate that the cross-linker concentration may also impact on the EP dose delivered. The scaffolds prepared with 2% alginate and 1%-1.5% CaCl_2 were found to have the highest loading efficiency of 90-97%. This suggests that an increase in density of cross-links within the gel has contributed to increased EP retention. Alginate gels have been used as drug delivery systems to deliver small compounds, such as the anti-inflammatory Flurbiprofen, (Lee & Mooney, 2012), or dobutamine (Lovich, *et al.*, 2011), but with a very limited release of several minutes to hours *in vitro*. In this case, alginate hydrogels released EP over an extended period of time suggesting there might be bonding between the alginate and the EP. This theory is supported by the fact that EP release profiles follow the alginate swelling behaviour, with a reduction in alginate hydrogel weight corresponding to a release of EP in the solution.

It has been suggested that the optimal scaffold for tissue regeneration should have a porous structure with interconnected pores to allow cell infiltration and proliferation, as previously discussed in section 1.5. For this reason, it was important to establish if EP could be incorporated and released from macro-porous alginate scaffolds, thereby providing not only anti-oxidant activity but also an environment to encourage cellular

regeneration. An important initial objective of this aspect of the study was to produce such a scaffold, which would be stable in PBS for at least 3 weeks.

The scaffolds were systematically prepared using a variety of different methods (see Table 2). EP was added to the scaffolds at different stages, depending on the method. EP was added to the dry alginate scaffolds (method 1 and 2), or it was added to the alginate solution (methods 3-6). Alginate was cross-linked in two different ways, either by calcium chloride (method 1-4) or double cross-linked with both calcium gluconate and calcium chloride (method 5-6). Two freezing temperatures (-20/-80°C) were used in order to determine what effect this would have on the stability of the scaffolds. Different methods were investigated not only to find the methodology for the optimal scaffold, but also to understand how the variables, such as freeze-cycles, single or double cross-linking and presence of EP might change the stability of the scaffolds.

Overall, the results showed that the scaffolds displayed similar swelling behaviour in the first weeks followed by a relaxation period with a reduction in swelling. The results suggested that the presence of EP, either added to the alginate solution or after to the scaffolds, interfered somehow with the overall stability of the scaffolds, except for method 1. The results also showed that the different freezing regime used (-20/-80°C) and the number of freeze-drying cycles did not affect the stability of the scaffolds. The scaffolds prepared with method 5 and 6 presented were more complex than the previous methods examined. In fact, method 5 and 6 consisted of double cross-linking of alginate with calcium chloride and calcium gluconate. Two different calcium gluconate concentrations were investigated, 0.4% and 1%. The results showed that the use of lower concentration of calcium gluconate resulted in higher swelling in EP scaffolds compared to the scaffolds prepared at lower calcium gluconate concentration. Although the scaffolds showed signs of degradation (relaxation of the structure), the scaffold structure was still present at the end of the study (28 days). This result suggested that all the scaffolds prepared (method 1-6) are potentially suitable for EP delivery over time.

On investigation of the EP release characteristics from the gels prepared using the same methods referred to above, it was found that the release time and loading

efficiency was different with each formulation method. Scaffolds prepared with method 1 and method 5 were the only ones found to have released all of the EP in the first hour of incubation. The scaffolds prepared with method 3 released EP over 21 days, while the rest of the scaffolds released EP over 28 days. The release profile of the scaffolds prepared with method 2 and method 4 were similar, with an initial burst of EP in the first week with 80-90% of the total EP released by the scaffolds, followed by a slow release of the remaining drug. On the other hand, the scaffolds prepared with method 6 were the only ones with a sustained release of EP over the 28 days, with 50% of the EP released in the first week, followed by a slow release of the remaining EP.

The macro-porous scaffolds preparation methods used in the present study, consisted of different steps which can influence EP retention and release. By investigating the impact of such variables in the formulation process, this study has revealed new insights that may help in the optimisation of drug release from alginates for a range of wider range applications. As an example, it appears that the second freeze-drying step used in methods 1 and 3 has led to a marked reduction in the cumulative mass of EP released, compared to methods 2 and 4. Similarly for the double cross-linked scaffolds (method 5 and 6), this difference in cumulative EP release is enhanced in method 6 compared to method 5. The reason of this EP reduction might be that EP was removed from the patches during the second freeze-drying process. On the other hand, a factor that appears to have a positive effect on the retention of EP within the scaffold structure is the double cross-linking step used in method 6. On the other hand, the double-crosslinking did not have the same positive effect in method 5, although this may be due to the second-freeze-drying step used in method 5. In conclusion, the results suggested that the incorporation of additional cross-linkers and steps and the number of cycles of freeze-drying are the important factors that can be adjusted to achieve optimal drug loading efficiency and release characteristics. Method 6 was demonstrated to have not only the ability to deliver EP in a sustained manner, but also the highest EP loading efficiency of 85-96% compared of the rest of the methods.

In addition to optimising EP release, it was also important to identify the method that produced the most promising macro-porous structure that would permit cell attachment and transport of cells and nutrients through the pores. The porosity of the

scaffolds was therefore calculated and it appeared that all the methods used in the present study led to the production of scaffolds with a porosity being consistently around 90% or above. The presence of EP slightly reduced the porosity of the scaffolds, but it was generally around 90%. Only scaffolds prepared with method 3 (with EP) showed a reduction in porosity, displaying approximately 10% less porosity than the scaffolds without EP. It is possible that the presence of EP lowered the freezing point of the water contained in the alginate solution, resulting in the reduction of the porosity of the structure (Greenslade, 1933).

The scaffolds were frozen before each cycle of freeze-drying and two freezing temperatures were investigated. It appears that the different freezing temperature did not affect the overall porosity of the scaffolds. The use of a double cross-linking did not increase the porosity of the scaffolds compared to the single cross-linking scaffolds (method 1 and 4). On the other hand, it appears that there was a difference in porosity between method 5 and 6, with method 6 showing a higher porosity than method 5. The main difference in methodology between those two methods is the number of freeze-drying cycles used. This result suggests that the second cycle of freeze-drying not only reduced the EP retention, as mentioned previously, but also reduced the porosity of the scaffolds. On the other hand, the different calcium gluconate concentration used in method 5 and 6 appeared to have no impact on the porosity of the scaffolds.

Due to the vast number of alginate scaffolds prepared in this chapter, it was necessary to narrow down the number of samples taken forward for SEM analysis. The SEM study was therefore focussed on the scaffolds prepared using method 6, which showed the highest porosity, the optimal EP release profiles and the highest EP loading efficiency. The SEM images showed a highly porous structure in all the samples, observed at the both the surface and in the internal layers of the scaffolds (horizontal cross-section). The scaffolds prepared at -80°C had a reduced pore size of $97 \pm 11 \mu\text{m}$ (without EP) and $66 \pm 10 \mu\text{m}$ (with EP), compared to the scaffolds prepared at -20°C with pore size of $134 \pm 18 \mu\text{m}$ (without EP) and $164 \pm 11 \mu\text{m}$ (with EP). This is in line with previous studies that have shown that the use of low temperature in the freezing process can lead to smaller pore sizes formation in alginate macro-porous scaffolds cross-linked with calcium gluconate compared to the scaffolds prepared at -20°C

(Shapiro & Cohen, 1997). However, the freezing temperature did not significantly change the porosity of the scaffolds, except in the methods 5 and 6. In fact, even the total EP release was not statistically different between the scaffolds prepared at -20°C or at -80°C . As stated before, the porosity of the scaffolds was always above 90%. When the porosity is compared with the total EP releases by the scaffolds it is clear that a higher porosity corresponded with a higher total EP release, except for the scaffolds prepared with method 4 at -20°C . This suggests that the increase in porosity in the scaffolds leads to a better retention and release of EP.

The work detailed in chapter 5 led to the development of a novel alginate patch that provided sustained release of EP over a potentially therapeutic period, with a pore structure that should permit cell infiltration and regeneration. In chapter 6, the biocompatibility of this scaffold was investigated in order to further evaluate its therapeutic potential. Cardiac fibroblasts are the most abundant cells in the myocardium. They are important not only in the physiological regulation of the myocardium, but also in the remodelling process after ischaemia/reperfusion injury. It is possible to culture them over sustained periods in a way that is more challenging with cardiac myocytes. For these reasons, they were therefore selected as the cell type used in the *in vitro* assessment of the scaffolds.

The cytotoxicity of EP has been previously tested *in vitro* on different cell types, but not on cardiac fibroblasts. It was therefore important to firstly characterise the effects of EP alone in the absence of the scaffold first. There was no cytotoxicity observed in cells treated with either 3 or 10 mM EP, as evidenced by the absence of red fluorescence in cells stained with PI/CFDA after 5 days in culture. EP was found to have a quite limited dose-dependent inhibitory effect on cell viability, with viability maintained at around 75% (NR) of control at the maximum EP concentration of 20 mM and the metabolic activity of 65% (MTT) after 5 days of culture. AB assay was used at day one, day 3 and day 5 of the treatment, to provide more information on the temporal effects of EP on cells. The results confirmed the resistance of cardiac fibroblasts to EP during the whole duration of the study. Not only was cell viability maintained at about 80% at high EP concentration of 20 mM, but in the range of 1- 5 mM, cells showed an increased cell viability compared to the control. The results

obtained were in accordance with previous studies that investigated the short term effect of EP exposure on different cell cultures (Birkenmeier, *et al.*, 2016) (Famili, *et al.*, 2013).

Given that the alginate patches developed in the current study are intended to be used to help improve regeneration of cardiac tissue following periods of ischaemia that have occurred pre-surgery, during and post-surgery, it was important to examine the temporal effects of EP when cells are exposed to oxidative challenge. EP is known to protect against oxidative stress by scavenging hydrogen peroxide in a number of cell types (Famili, *et al.*, 2013) (Yang, *et al.*, 2016) (Zeng, *et al.*, 2007). However, it was unclear if it would exert similar protective effects on cardiac fibroblasts exposed to H₂O₂. Cardiac fibroblasts were treated with H₂O₂ and the effects of EP, delivered either in combination with H₂O₂ or after the exposure to H₂O₂, were examined. In fact, given the potential clinical application of this technology, it was important to determine if EP would be more effective when delivered during reperfusion or following cell damage. It was observed that when cardiac fibroblasts were exposed to a H₂O₂ (150 µM) and EP at the same time, cell viability was maintained above 80% at 20 mM EP and even increased to 107-109% at 3,000 and 10,000 µM EP concentration. On the other hand, cells treated with EP after H₂O₂ exposure did not recover after being stressed. In fact, it appeared that the presence of EP was associated with further reductions in cell viability, compared to the negative control in this case. This result supports previous observations by Famili *et al.*, 2013, who showed that the co-treatment of human trabecular meshwork cells with EP and hydrogen peroxide increased viability, compared to the cells without EP treatment or cells with an EP pre-treatment (Famili, *et al.*, 2013).

Once the safety of EP on cardiac cells was confirmed and the effectiveness of protecting the cells from H₂O₂ was demonstrated, the final part of the study investigated the biocompatibility of the macro-porous scaffolds loaded with EP. In a preliminary study, the alginate scaffolds were firstly screened for biocompatibility on a 3T3 cell culture. The results obtained with the LDH assay showed an overall acceptance of the scaffolds by the cells. In particular, it was observed that the cells seeded into dry scaffolds were more stressed at the beginning and at the end of the

study compared to the cells seeded onto wetted scaffolds. This was also observed with the live/dead staining, showing a clear abundance of live cells on the surface of the wet scaffold.

Several studies have previously demonstrated that the presence of RGD within scaffolds promoted cell proliferation (Ruvinov & Cohen, 2016) (Shachar, *et al.*, 2011). In order to improve cell attachment in the scaffolds prepared in this study, alginate scaffolds were prepared using RGD alginate for the cardiac fibroblast study. Alginate scaffolds (produced using method 6), without RGD and EP, showed the highest cell viability over all, although the live/dead staining showed a small number of cells in the scaffolds. This may be due to the cells adhering to the culture plate surface, thereby proliferating within the well, but not within the scaffolds. Cells seeded onto RGD-Alginate with EP (-20°C) scaffolds presented the second highest cell viability, indicating that the cells may benefit from the structure of the scaffold and/or the presence of EP. This result was confirmed with the live/dead staining. Cells proliferated through the scaffold and remained viable, suggesting that the scaffold structure enabled nutrients to pass through the porous structure. As expected, the presence of the RGD peptide increased cell attachment and EP increased cell viability compared to the RGD scaffolds without EP. In fact, EP is not only an antioxidant, but has the ability of enhancing ATP levels (Taylor, *et al.*, 2005), which is crucial for cell viability and proliferation and so the results observed here are consistent with this.

7.2 Summary of Contribution

The overall aim of the project was to develop an optimal alginate scaffold loaded with EP that could help the regeneration of infarcted myocardium. The gels and the macro-porous scaffolds prepared fulfil successfully the requirements, with alginate gels releasing about 85% of EP in the first week, and the remaining EP over the following weeks, while the optimised macro-porous scaffolds prepared releasing 50% in the first week and gradually releasing the remaining EP for the following weeks. If these technologies were to be applied clinically to aid cardiac recovery following periods of ischaemia/reperfusion injury, such an initial burst of EP may be potentially beneficial to combat the rapid increase of oxidative stress in ischaemic hearts. The following release of the remaining EP by the gels may also provide not only antioxidant

protection, but also the ATP necessary for cell metabolism. In fact, after ischaemia/reperfusion, not only is there a burst of ROS production, but this phase is also characterised by ATP depletion. The recovery of ATP upon reperfusion has been shown to limit cell damage and help cell recovery (Taylor, *et al.*, 2005). Given this, there is significant potential for the technology developed here to be taken forward towards clinical evaluation. However, there are limitations within the current study and other important challenges that would require to be addressed before this can be achieved. These issues will be briefly considered in the following sections.

7.3 Summary of Limitations

EP stability at different temperatures was investigated over a period of 2 weeks, although the following EP release studies were conducted over a prolonged period of time (28 days). Although this represents a limitation of this study, the results provide an indication of the potential EP stability in PBS at body temperature.

In chapter 3, EP stability in solution was measured by using UV spectroscopy. The degradation products of EP might not be detected with a UV spec. Even although HPLC does not have this limitation, it was found not to be unsuitable for EP measurement within PBS solutions, which would have necessitated the use of further processing and separation steps in order to proceed. Although the stability of EP in PBS was investigated, this may be different in plasma, blood, and cell culture media. Despite these limitations, the results obtained in this chapter remain valuable, particularly since they provide the confidence in the analytical methods adopted in subsequent chapters.

The alginate used to prepared the hydrogels had a molecular weight that slightly exceeds the renal clearance threshold and likely will not be completely removed from the body (Al-Shamkhani & Duncan, 1995). The results do however provide an indication of the potential for such gels to provide sustained release of EP.

The stability of alginate gels and alginate scaffolds was studied by measuring the change in weight (swelling ratio) of the two alginate structures over time. The effect of errors in weight measurements due to surface liquid retention upon swelling ratio represents a limitation of these studies. The results do however provide an indication

of the potential stability of alginate gels and alginate scaffolds in PBS at body temperature.

One important limitation of the cell study was the preliminary nature of the cellular experiments conducted with H₂O₂. In fact, given the limited availability of primary cells, it was not possible to produce a greater number of replicates for this aspect of the study.

Finally, although the effects that the scaffolds have on cardiac fibroblasts were investigated, the impact of H₂O₂ on cells within this scaffold environment was not determined due to the limited availability of primary cells. Addressing this limitation should therefore be a priority in future studies. Further information on such future work is provided below.

7.4 Future Research Directions

As a U.S. Food and Drug Administration (FDA)-approved polymer, alginate is biocompatible and biodegradable *in vivo*. It would be expected that the hydrogel will dissolve *in vivo* over time, avoiding any follow-up surgery to remove it after the EP release. In future, alginate gels loaded with EP, based on the work documented in chapter 4, could be delivered by catheter into the heart without the need for open heart surgery. The presence of calcium ions *in vivo* may allow cross-linking to be achieved following such delivery (Landa, *et al.*, 2008). Where open heart surgery is already recommended, then the macro-porous scaffold materials could be optimised to allow them to be placed on the myocardium as part of this procedure. There is, of course, a substantial programme of further *in vitro* development and *in vivo* safety and efficacy assessment, that would be required before any such clinical applications could be considered.

EP has demonstrated beneficial effects in different application areas, not only as a therapeutic for ischaemic hearts, but also to aid recovery from injury to various organs including the brain, kidney, pancreas, liver and lungs (Flink, 2007). It has also been shown to inhibit human leukaemia cells and tumour growth (Birkenmeier, *et al.*, 2016)(Yang, *et al.*, 2016). The technology developed here may therefore have potential for application beyond cardiac injury. The possibility of releasing EP *in situ*

over time may improve the efficacy of EP treatment strategies that rely on more conventional delivery routes, providing more sustained and targeted delivery with a reduction in systemic toxicity.

In this study, it has been shown that EP is not toxic to cardiac fibroblasts in the range of concentrations studied. It was also observed that EP was effective to protect the cells when exposed to H₂O₂ for 24 hours in the preliminary study. Cardiac fibroblasts are responsible for collagen depletion and during the process of scar formation, cardiac fibroblasts undergo a phenotypic modulation to myofibroblasts, which are thought to be responsible for cardiac remodelling that ultimately leads to heart failure (Hori & Nishida, 2009). Collagen depletion by cardiac fibroblasts under oxidative stress could be measured with and without the presence of EP. This would show if EP has any effect on collagen depletion. In fact, it is known that an excess of collagen depletion in the scar is responsible for the cardiomyocytes slippage, which then leads to ventricular remodelling, but it is unknown what effect EP would have on this process. Given the key functional role of cardiomyocytes within the heart, and their response to injury, it would be beneficial to test the same patches developed in this study on these cells. Although in this study, the results indicate that EP may attenuate hydrogen peroxide injury of cardiac fibroblasts, it will be important to replicate these experiments on cardiomyocytes and examine the cell response to EP in the presence of inflammatory cytokines, such as IL-6, IL-10, TNF α , IL-1 α and IL-1 β , which maintain the local inflammatory response to cardiac injury (Baum & Duffy, 2011). Such studies would be an important next step, before future pre-clinical evaluation of the patches in animal model of cardiac injury.

7.5 Summary Conclusions

This study has demonstrated for the first time that alginate represents a suitable delivery system for providing sustained release of ethyl pyruvate. The protective effective of this drug on cardiac fibroblasts shown here, combined with the promising cell viability observed within the delivery scaffold, mean that this approach has significant potential for future development towards clinical evaluation. If these technologies were to be applied clinically to aid cardiac recovery following periods of ischaemia/reperfusion injury, such an initial burst of EP may be potentially beneficial

to combat the rapid increase of oxidative stress in ischaemic hearts. The following release of the remaining EP by the scaffolds may also provide not only antioxidant protection, but also the ATP necessary for cell metabolism. Given this, there is significant potential for the technology developed here to be taken forward for the development of an improved treatment of ischaemia-reperfusion injury and hence heart failure.

9 Bibliography

Adamek, A. *et al.*, 2007. High dose aspirin and left ventricular remodeling after myocardial infarction: Aspirin and myocardial infarction. *Basic Research in Cardiology*, 102(4), p. 334–340.

Al-Shamkhani, A. & Duncan, R., 1995. Radioiodination of alginate via covalently-bound tyrosinamide allows monitoring of its fate in vivo.. *Journal of Bioactive and Compatible Polymers* , Volume 10, p. 4–13.

Andersen, T., Auk-Emblem, P. & Dornish, M., 2015. 3D Cell Culture in Alginate Hydrogels. *Microarrays*, Volume 4, pp. 133-161.

Andersen, T. *et al.*, 2014. In situ gelation for cell immobilization and culture in alginate foam scaffolds.. *Tissue Eng Part A*, Volume (3-4), pp. 600-10.

Annabi, N. *et al.*, 2010. Controlling the Porosity and Microarchitecture of Hydrogels for Tissue Engineering. *Tissue Engineering. Part B, Reviews*, 16(4), p. 371–383..

Assmus, B. *et al.*, 2002. Transplantation of Progenitor Cells and Regeneration Enhancement in Acute Myocardial Infarction (TOPCARE-AMI). *Circulation*, Volume 106, p. 3009 –3017.

Bajpai, S. & Sharma, S., 2004. Investigation of swelling/degradation behaviour of alginate beads crosslinked with Ca²⁺ and Ba²⁺ ions. *Reactive & Functional Polymers*, Volume 59, p. 129–140.

Balakrishnana, B., Lesieur, S., Labarre, D. & Jayakrishnan, A., 2005. Periodate oxidation of sodium alginate in water and in ethanol–water mixture: a comparative study. *Carbohydrate Research*, 340(7), pp. 1425-1429.

Balsam, L. *et al.*, 2004. Hematopoietic stem cells adopt mature haematopoietic fates in ischaemic myocardium.. *Nature* 428, Volume 428, pp. 668 – 673,.

Basili, S. *et al.*, 2010. Intravenous ascorbic acid infusion improves myocardial perfusion grade during elective percutaneous coronary intervention: relationship with oxidative stress markers.. *JACC Cardiovascular Intervention*, Volume 3, pp. 221-229.

Baum, J. & Duffy, H., 2011. Fibroblasts and myofibroblasts: what are we talking about?. *Journal of Cardiovascular Pharmacology*, 57(4), pp. 376-9..

Baum, J. & Duffy, H. S., 2011. Fibroblasts and Myofibroblasts: What are we talking about?. *Cardiovascular Pharmacology*, pp. 376-379.

- Bennett-Guerrero, E. *et al.*, 2009. A Phase II Multicenter Double-Blind Placebo-Controlled Study of Ethyl Pyruvate in High-Risk Patients Undergoing Cardiac Surgery With Cardiopulmonary Bypass. *Cardiothoracic and vascular anesthesia*, 23(3), p. 324–329.
- Betge, S., Lutz, K., Roskos, M. & Figulla, H., 2007. Oral treatment with probucol in a pharmacological dose has no beneficial effects on mortality in chronic ischemic heart failure after large myocardial infarction in rats.. *European Journal of Pharmacology*, 558(1-3), pp. 119-27.
- Birkenmeier, G. *et al.*, 2016. Ethyl Pyruvate Combats Human Leukemia Cells but Spares Normal Blood Cells. *PLoS ONE*, 11(8), p. e0161571.
- Blan, N. & Birla, R., 2008. Design and fabrication of heart muscle using scaffold-based tissue engineering.. *J Biomed Mater Res A*, 86(1), pp. 195-208.
- Bonow, R. *et al.*, 2015. Severity of Remodeling, Myocardial Viability, and Survival in Ischemic LV Dysfunction After Surgical Revascularization.. *JACC Cardiovascular Imaging*, 8(10), pp. 1121-9.
- Bonow, R. *et al.*, 2011. Myocardial viability and survival in ischemic left ventricular dysfunction.. *New England Journal of Medicine*, 364(17), pp. 1617-25.
- Book, W., 2002. Carvedilol: A Nonselective β Blocking Agent With Antioxidant Properties. *Congestive Heart Failure*, 8(3), p. 173–190.
- Bougioukas, I. *et al.*, 2007. Intramyocardial injection of low-dose basic fibroblast growth factor or vascular endothelial growth factor induces angiogenesis in the infarcted rabbit myocardium.. *Cardiovascular Pathology*, 16(2), pp. 63-8..
- Bouhadir, K., Alsberg, E. & Mooney, D., 2001. Hydrogels for combination delivery of antineoplastic agents. *Biomaterials*, 22(19), p. 2625–2633.
- Brunvand, H. *et al.*, 1996. Carvedilol Protects Against Lethal Reperfusion Injury Through Antiadrenergic Mechanisms. *Journal of Cardiovascular Pharmacology*, 28(3), pp. 409-417.
- Calderone, A. *et al.*, 2006. Scar myofibroblasts of the infarcted rat heart express natriuretic peptides.. *Journal of Cell Physiology*, 207(1), pp. 165-73..
- Camelliti, P., Borg, T. K. & Kohl, P., 2005. Structural and functional characterisation of cardiac fibroblasts. *Cardiovascular Research*, pp. 40-51.
- Cao, R. *et al.*, 2004. Comparative evaluation of FGF-2-, VEGF-A-, and VEGF-C-induced angiogenesis, lymphangiogenesis, vascular fenestrations, and permeability.. *Circulation research*, Volume 94, p. 664–670.

- Cargnoni, A. *et al.*, 2000. Reduction of oxidative stress by carvedilol: role in maintenance of ischemic myocardium viability.. *Cardiovascular Research*, Volume 47, p. 556–566..
- Caspi, O. *et al.*, 2007. Transplantation of human embryonic stem cell-derived cardiomyocytes improves myocardial performance in infarcted rat hearts.. *Journal of the American College of Cardiology*, 50(19), pp. J Am Coll Cardiol. 2007 Nov 6;50(19):1884-93.
- Chan, E., Lee, B., Ravindra, P. & Poncelet, D., 2009. Prediction models for shape and size of ca-alginate macrobeads produced through extrusion–dripping method. *Journal of Colloid and Interface Science*, Volume 338, p. 63–72.
- Cheng, B. *et al.*, 2007. Ethyl pyruvate improves survival and ameliorates distant organ injury in rats with severe acute pancreatitis.. *Pancreas*, 35(3), pp. 256-61..
- Chen, Z. *et al.*, 1998. Overexpression of MnSOD protects against myocardial ischemia/reperfusion injury in transgenic mice.. *Journal of Molecular and Cellular Cardiology*, Volume 30, p. 2281–2289..
- Chi, N. *et al.*, 2013. Cardiac repair using chitosan-hyaluronan/silk fibroin patches in a rat heart model with myocardial infarction.. *Carbohydrate Polymers*, 92(1), pp. 591-7.
- Chong, J. *et al.*, 2014. Human embryonic-stem-cell-derived cardiomyocytes regenerate non-human primate hearts.. *Nature*, 510(7504), pp. 273-7.
- Chung, E. *et al.*, 2003. Randomized, double-blind, placebo-controlled, pilot trial of infliximab, a chimeric monoclonal antibody to tumor necrosis factor-alpha, in patients with moderate-to-severe heart failure: results of the anti-TNF Therapy Against Congestive Heart Failure (AT. *Circulation*, 107(25), pp. 3133-40. .
- Cleland, J. *et al.*, 1991. Effect of captopril, an angiotensin-converting enzyme inhibitor, in patients with angina pectoris and heart failure.. *Journal of the American College of Cardiology*, 17(3), pp. 733-9.
- Cowan, C., Atienza, J., Melton, D. & Eggan, K., 2005. Nuclear reprogramming of somatic cells after fusion with human embryonic stem cells.. *Science*, 309(5739), pp. 1369-73..
- Crim, W. *et al.*, 2010. AGI-1067, a novel antioxidant and anti-inflammatory agent, enhances insulin release and protects mouse islets.. *Molecular and Cellular Endocrinology*, 323(2), pp. 246-55.
- Cui, Z., Yang, B. & Li, R.-K., 2016. Application of Biomaterials in Cardiac Repair and Regeneration. *Engineering*, 2(1), pp. 141-148.

Dar, A., Shachar, M., Leor, J. & Cohen, S., 2002. Optimization of cardiac cell seeding and distribution in 3D porous alginate scaffolds. *Biotechnology and Bioengineering*, 80(3), pp. 305-12.

Dasari, T. *et al.*, 2016. Non-eligibility for reperfusion therapy in patients presenting with ST-segment elevation myocardial infarction: contemporary insights from the National Cardiovascular Data Registry (NCDR).. *American Heart Journal*, Volume 172, pp. 1-8.

Deb, S. *et al.*, 2013. Coronary Artery Bypass Graft Surgery vs Percutaneous Interventions in Coronary Revascularization A Systematic Review. *JAMA*, 310(19), pp. 2086-2095.

Deng, C. *et al.*, 2010. A collagen–chitosan hydrogel for endothelial differentiation and angiogenesis.. *Tissue Eng Part A*, 16(10), pp. 3099-109.

Dikmen, G., Genç, L. & Güney, G., 2011. Advantage and Disadvantage in Drug Delivery Systems. *Journal of Materials Science and Engineering*, Volume 5, pp. 468-472.

Dong, J. *et al.*, 2015. Re-evaluation of ABTS*+ Assay for Total Antioxidant Capacity of Natural Products.. *Nat Prod Commun.*, 10(12), pp. 2169-72..

Dufour, G. K. a. J. M., 2012 . Cell lines. Valuable tools or useless artifacts. *Spermatogenesis.*, Issue 2(1), p. 1–5.

Eiselt, P., Lee, K. & Mooney, D., 1999. Rigidity of two-component hydrogels prepared from alginate and poly(ethylene glycol)-diamines.. *Macromolecules*, Volume 32, p. 5561–5566.

Elahi, M., Kong, Y. & Matata, B., 2009. Oxidative stress as a mediator of cardiovascular disease. *Oxidative Medicine and Cellular Longevity*, 2(5), pp. 259-269.

Ellison, G. *et al.*, 2011. Endogenous cardiac stem cell activation by insulin-like growth factor-1/hepatocyte growth factor intracoronary injection fosters survival and regeneration of the infarcted pig heart.. *Journal of the American College of Cardiology*, 58(9), pp. 977-86..

Engberding, N. *et al.*, 2004. Allopurinol Attenuates Left Ventricular Remodeling and Dysfunction After Experimental Myocardial Infarction. A New Action for an Old Drug?. *Circulation*, Volume 110, pp. 2175-2179.

Famili, A., Ammar, D. A. & Kahook, . M. Y., 2013. Ethyl pyruvate treatment mitigates oxidative stress damage in cultured trabecular meshwork cells. *Molecular Vision*, Issue 19, pp. 1304-1309.

- Fan, D., Takawale, A., Lee, J. & Kassiri, Z., 2012. Cardiac fibroblasts, fibrosis and extracellular matrix remodeling in heart disease. *Fibrogenesis & Tissue Repair*, Volume 5, p. 15.
- Fiamingo, A. *et al.*, 2016. Chitosan Hydrogels for the Regeneration of Infarcted Myocardium: Preparation, Physicochemical Characterization, and Biological Evaluation.. *Biomacromolecules*, 17(5), pp. 1662-72..
- Flink, M., 2007. Ethyl pyruvate: a novel anti-inflammatory agent.. *Journal of Internal Medicine*, 26(14), pp. 349-62..
- Formiga, F. *et al.*, 2012. Angiogenic therapy for cardiac repair based on protein delivery systems. *Heart Failure Review*, 17(3), p. 449–473.
- Freyman, T. *et al.*, 2006. A quantitative, randomized study evaluating three methods of mesenchymal stem cell delivery following myocardial infarction.. *European Heart Journal*, 27(9), pp. 1114-22..
- Gajarsa, J. & Kloner, R., 2011. Left ventricular remodeling in the post-infarction heart: a review of cellular, molecular mechanisms, and therapeutic modalities.. *Heart Failures reviews*, 16(1), pp. 13-21.
- Garcia, E. *et al.*, 2012. Antioxidant activity by DPPH assay of potential solutions to be applied on bleached teeth.. *Brazilian Dental Journal*, 23(1), pp. 22-7.
- Ghatak, A. *et al.*, 1996. Oxy free radical system in heart failure and therapeutic role of oral vitamin E. *International Journal of Cardiology*, 57(2), pp. 119-27.
- Gnecchi, M., Zhang, Z., Ni, A. & Dzau, V., 2008. Paracrine mechanisms in adult stem cell signaling and therapy. *Circulation Research*, 103(11), p. 1204–1219.
- Goegan, P., Johnson, G. & Vincent, R., 1995. Effects of serum protein and colloid on the alamarBlue assay in cell cultures. *Toxicology in Vitro*, 9(3), pp. 257-266.
- Greenberg, B. *et al.*, 2015. CUPID 2: A Phase 2b Trial Investigating the Efficacy and Safety of the Intracoronary Administration of AAV1/SERCA2a in Patients with Advanced Heart Failure. *Journal of Cardiac Failure*, 21(11), pp. 939-940.
- Greenslade, T., 1933. Freezing-point lowering. *Journal of Chemical Education*, 10(6), p. 353.
- Guo, J. *et al.*, 2014. Effects of ethyl pyruvate on cardiac function recovery and apoptosis reduction after global cold ischemia and reperfusion.. *Experimental and therapeutic medicine*, 7(5), p. 1197–1202.

- Hamburger, S., Barone, F., Feuerstein, G. & Ruffolo, J. R., 1991. Carvedilol (Kredex®) Reduces Infarct Size in a Canine Model of Acute Myocardial Infarction. *Pharmacology*, 43(3), pp. 113-120.
- Hayashi, M. *et al.*, 2004. Comparison of intramyocardial and intravenous routes of delivering bone marrow cells for the treatment of ischemic heart disease: an experimental study.. *Cell Transplantation*, 13(6), pp. 639-47..
- Heinen, A. *et al.*, 2017. Insulin-Like Growth Factor 1 Preserves Cardiac Function after Myocardial Infarction without Affecting Initial Ischemia and Reperfusion Injury. *The FASEB Journal*, 31(1), pp. 845-6.
- Hori, M. & Nishida, K., 2009. Oxidative stress and left ventricular remodelling. *Cardiovascular Research*, Volume 81, p. 457–464.
- Huangfu, D. *et al.*, 2008. Induction of pluripotent stem cells by defined factors is greatly improved by small molecule compounds. *Nature Biotechnology*, Volume 26, p. 795–797.
- Huangfu, D. *et al.*, 2008. Induction of pluripotent stem cells by defined factors is greatly improved by small molecule compounds. *Nature Biotechnology*, Volume 26, p. 795–797.
- Hwang, H. & Kloner, R., 2011. The combined administration of multiple soluble factors in the repair of chronically infarcted rat myocardium.. *Journal of Cardiovascular Pharmacology*, 57(3), pp. 282-6..
- Jang, I. *et al.*, 2010. Ethyl pyruvate has anti-inflammatory and delayed myocardial protective effects after regional ischemia/reperfusion injury.. *Yonsei Medical Journal*, Volume 51, p. 838–44..
- Jang, I. *et al.*, 2010. Ethyl pyruvate has anti-inflammatory and delayed myocardial protective effects after regional ischemia/reperfusion injury.. *Yonsei Medical journal*, 51(6), pp. 838-844.
- Jaxa-Chamiec, T. *et al.*, 2005. MIVIT Trial Group: Antioxidant effects of combined vitamins C and E in acute myocardial infarction: the randomized, double-blind, placebo controlled, multicenter pilot Myocardial Infarction and VITamins (MIVIT) trial.. *Kardiologia Polska*, Volume 62, pp. 344-350..
- Johansson, A., Johansson-Haque, K., Okret, S. & Palmblad, J., 2008. Ethyl pyruvate modulates acute inflammatory reactions in human endothelial cells in relation to the NF- κ B pathway. *British Journal of Pharmacology*, 154(6), p. 1318–1326.
- Johansson, A. & Palmblad, J., 2009. Ethyl pyruvate modulates adhesive and secretory reactions in human lung epithelial cells.. *Life Science*, Volume 84, p. 805–9.

- Kao, K. & Fink, M., 2010. The biochemical basis for the anti-inflammatory and cytoprotective actions of ethyl pyruvate and related compounds. *Biochemical Pharmacology*, Volume 80, p. 151–159.
- Karantalis, V. *et al.*, 2012. Cell-based therapy for prevention and reversal of myocardial remodeling. *American Journal of Physiology. Heart and Circulatory Physiology*, Volume 33, p. 256–270.
- Keshari, K. & Wilson, D., 2014. Chemistry and biochemistry of ¹³C hyperpolarized magnetic resonance using dynamic nuclear polarization. *Chemical Society review*, 43(5), pp. 1627-59.
- Keyamura, Y. *et al.*, 2014. Add-On Effect of Probucol in Atherosclerotic, Cholesterol-Fed Rabbits Treated with Atorvastatin. *PLoS ONE*, 9(5).
- Kim, H.-J., Kim, S.-W., Lee, J.-K. & Yoon, S.-H., 2011. A Simple and Sensitive High Performance Liquid Chromatography-Electrospray Ionization/Mass Spectrometry Method for the Quantification of Ethyl Pyruvate in Rat Plasma. *Bulletin of the Korean Chemical Society*, 32(4), pp. 1221-1227.
- Kim, J.-B., Yu, Y.-M., Kim, S.-W. & Lee, J.-K., 2005. Anti-inflammatory mechanism is involved in ethyl pyruvate-mediated efficacious neuroprotection in the postischemic brain. *Brain research*, 1060(1–2), p. 188–192.
- Kjekshus, J. *et al.*, 2007. Rosuvastatin in older patients with systolic heart failure. *New England Journal of Medicine*, 357(22), pp. 2248-61.
- Knott, E. *et al.*, 2006. Pyruvate Mitigates Oxidative Stress During Reperfusion of Cardioplegia-Arrested Myocardium. *The Annals of Thoracic Surgery*, 81(3), p. 928–934.
- Kong, P., Christia, P. & Frangogiannis, N., 2014. The pathogenesis of cardiac fibrosis. *Cellular and Molecular Life Sciences*, 71(4), pp. 549-74.
- Laflamme, M. *et al.*, 2007. Cardiomyocytes derived from human embryonic stem cells in pro-survival factors enhance function of infarcted rat hearts. *Nature Biotechnology*, 25(9), pp. 1015-24.
- Laflamme, M. & Murry, C., 2011. Heart regeneration. *Nature*, 473(7347), pp. 326-35.
- Laham, R. *et al.*, 2000. Intrapericardial delivery of fibroblast growth factor-2 induces neovascularization in a porcine model of chronic myocardial ischemia. *Journal of Pharmacology and Experimental Therapeutics*, 292(2), pp. 795-802.
- Landa, N. *et al.*, 2008. Effect of injectable alginate implant on cardiac remodeling and function after recent and old infarcts in rat. *Circulation*, 117(11), pp. 1388-96.

- Lee, C. *et al.*, 2013. Bioinspired, calcium-free alginate hydrogels with tunable physical and mechanical properties and improved biocompatibility.. *Biomacromolecules*, 14(6), pp. 2004-13.
- Lee, K., Kong, H., Larson, R. & Mooney, D., 2003. Hydrogel formation via cell crosslinking. *Advanced materials*, Volume 15, p. 1828–1832.
- Lee, K. & Mooney, D., 2012. Alginate: properties and biomedical applications.. *Progress in Polymer Science*, 37(1), pp. 106-126.
- Lee, K., Peters, M. & Mooney, D., 2003. Comparison of vascular endothelial growth factor and basic fibroblast growth factor on angiogenesis in SCID mice. *Journal of Controlled Release*, 87(1-3), p. 49–56.
- Lee, K. *et al.*, 2000. Controlling mechanical and swelling properties of alginate hydrogels independently by cross-linker type and crosslinking density.. *Macromolecules*, Volume 33, p. 4291–4294..
- Lindenfeld, J., Robertson, A., Lowes, B. & Bristow, M., 2001. Aspirin impairs reverse myocardial remodeling in patients with heart failure treated with beta-blockers. *Journal of the American College of Cardiology*, 38(7), pp. 1950-1956.
- Lin, Y., Chen, L., Li, W. & Fang, J., 2015. Role of high-mobility group box 1 in myocardial ischemia/reperfusion injury and the effect of ethyl pyruvate.. *Experimental and Therapeutic Medicine*, 9(4), p. 1537–41..
- Liu, J. *et al.*, 2011. Metabolomics of Oxidative Stress in Recent Studies of Endogenous and Exogenously Administered Intermediate Metabolites. *International Journal of Molecular Sciences*, 12(10), pp. 6469-6501.
- Li, Z. & Guan, J., 2011. Hydrogels for Cardiac Tissue Engineering. *Polymers*, Volume 3, pp. 740-761.
- Lovich, M. *et al.*, 2011. Local Epicardial Inotropic Drug Delivery Allows Targeted Pharmacologic Intervention with Preservation of Myocardial Loading Conditions. *Journal of pharmaceutical sciences*, 100(11), p. 4993–5006.
- Luan, Z. *et al.*, 2015. Protective effect of ethyl pyruvate on pancreas injury in rats with severe acute pancreatitis.. *Jourlan of Cellular and Molecular Medicine*, 19(11), pp. 2513-20..
- Mackenzie, I. *et al.*, 2016. Multicentre, prospective, randomised, open-label, blinded end point trial of the efficacy of allopurinol therapy in improving cardiovascular outcomes in patients with ischaemic heart disease: protocol of the ALL-HEART study. *British Medical Journal Open*, 6(9).

- Mallet, R. & Bünger, R., 1994. Energetic modulation of cardiac inotropism and sarcoplasmic reticular Ca²⁺ uptake. *Biochimica et Biophysica Acta*, Volume 1224, p. 22–32.
- Mann, D. *et al.*, 2016. One-year follow-up results from AUGMENT-HF: a multicentre randomized controlled clinical trial of the efficacy of left ventricular augmentation with Algisyl in the treatment of heart failure. *European Journal of Heart Failure*, 18(3), pp. 314-25.
- Marchioli, R. *et al.*, 2006. Vitamin E increases the risk of developing heart failure after myocardial infarction: Results from the GISSI-Prevenzione trial. *Journal of Cardiovascular Medicine (Hagerstown)*, Volume 7, p. 347–350.
- Martin, T., McCluskey, C. & Cunningham, M. e. a., 2018. CaMKII δ interacts directly with IKK β and modulates NF- κ B signalling in adult cardiac fibroblasts. *Cellular Signalling*, 51. pp. , Volume 51, pp. 166-175.
- Miyagi, Y. *et al.*, 2011. Biodegradable collagen patch with covalently immobilized VEGF for myocardial repair. *Biomaterials*, 32(5), pp. 1280-90.
- Miyaji, T. *et al.*, 2003. Ethyl pyruvate decreases sepsis-induced acute renal failure and multiple organ damage in aged mice. *Kidney international Journal*, 64(5), pp. 1620-31.
- Mizutani, A. *et al.*, 2010. Inhibition by ethyl pyruvate of the nuclear translocation of nuclear factor- κ B in cultured lung epithelial cell. *Pulmonary Pharmacology and Therapeutics*, 23(4), pp. 308-15.
- Montagnani, S., Rueger, M., Hosoda, T. & Nurzynska, D., 2016. Adult Stem Cells in Tissue Maintenance and Regeneration. *Stem Cells International*, Volume 2016.
- Montgomery, C. & Webb, J., 1956. Metabolic studies on heart mitochondria. II. The inhibitory action of parapyruvate on the tricarboxylic acid cycle. *Biological Chemistry*, Volume 221, p. 359–68.
- Moreyra, A. *et al.*, 2013. Incidence and trends of heart failure admissions after coronary artery bypass grafting surgery. *European Journal of Heart Failure*, 15(1), pp. 46-53.
- Mukherjee, S. *et al.*, 2011. Evaluation of the biocompatibility of PLACL/collagen nanostructured matrices with cardiomyocytes as a model for the regeneration of infarcted myocardium. *Advanced Functional Materials*, 21(12), pp. 2291-2300.
- Murry, C. *et al.*, 2004. Haematopoietic stem cells do not transdifferentiate into cardiac myocytes in myocardial infarcts. *Nature*, Volume 428, p. 664 – 668.

- Murry, C., Wiseman, R., Schwartz, S. & Hauschka, S., 1996. Skeletal myoblast transplantation for repair of myocardial necrosis.. *The Journal of Clinical Investigation*, 98(11), p. 2512–2523..
- Nabel, E. & Braunwald, E., 2012. A Tale of Coronary Artery Disease and Myocardial Infarction. *New England Journal of Medicine*, Volume 366, pp. 54-63.
- Nakagawa, M. *et al.*, 2008. Generation of induced pluripotent stem cells without Myc from mouse and human fibroblasts. *Nature Biotechnology* , Volume 26, p. 101–106.
- Nakamura, R. *et al.*, 2002. Probucol attenuates left ventricular dysfunction and remodeling in tachycardia-induced heart failure: roles of oxidative stress and inflammation.. *Circulation*, 106(3), pp. 362-7..
- Nakamura, T. *et al.*, 2000. Myocardial protection from ischemia/reperfusion injury by endogenous and exogenous HGF. *Journal of Clinical Investigation*, 106(12), pp. 1511-9..
- Nichols, M. *et al.*, 2012. *European Cardiovascular Disease Statistics*, s.l.: European Heart Network, Brussels, European Society of Cardiology, Sophia Antipolis.
- Nikolic-Heitzler, V. *et al.*, 2006. Persistent oxidative stress after myocardial infarction treated by percutaneous coronary intervention. *The Tohoku Journal of Experimental Medicine*, 210(3), pp. 247-55.
- Nussbaum, J. *et al.*, 2007. Transplantation of undifferentiated murine embryonic stem cells in the heart: teratoma formation and immune response.. *FASEB Journal*, 21(7), pp. 1345-57.
- O’Doherty R, G. U. W. W., 2013. Nonviral methods for inducing pluripotency to cells. *Biomed Research International*, 2013(705902), p. 6 pages.
- Olek, R. *et al.*, 2011. Higher Hypochlorous Acid Scavenging Activity of Ethyl Pyruvate Compared to Its Sodium Salt. *Bioscience, Biotechnology and Biochemistry*, 75(3), p. 500–504.
- Olivencia-Yurvati, A., Blair, J., Baig, M. & Mallet, R., 2003. Pyruvate-enhanced cardioprotection during surgery with cardiopulmonary bypass. *Journal of Cardiothoracic and Vascular Anesthesia*, 17(6), p. 715–720.
- Onogi, H. *et al.*, 2006. EDARAVONE REDUCES MYOCARDIAL INFARCT SIZE AND IMPROVES CARDIAC FUNCTION AND REMODELLING IN RABBITS. *Clinical and Experimental Pharmacology and Physiology* , Volume 33, p. 1035–1041.

- Ono, K., Matsumori, A. & Shioi, T., 1998. Cytokine Gene Expression After Myocardial Infarction in Rat Hearts: Possible Implication in Left Ventricular Remodeling. *Circulation*, Volume 98, p. 149–56.
- Orlic, D. *et al.*, 2001. Bone marrow cells regenerate infarcted myocardium.. *Nature*, Volume 410, p. 701–705.
- Oskarsson, H., Coppey, L., Weiss, R. & Li, W., 2000. Antioxidants attenuate myocyte apoptosis in the remote non-infarcted myocardium following large myocardial infarction.. *Cardiovascular Research*, 45(3), pp. 679-87..
- Ostertag, E. *et al.*, 2014. Extension of solid immersion lens technology to super-resolution Raman microscopy. *Nanospectroscopy*, Volume 1, pp. 1-11.
- Pearlman, J. *et al.*, 1995. Magnetic resonance mapping demonstrates benefits of VEGF-induced myocardial angiogenesis.. *nature medicine*, p. 1085–1089.
- Pereira, M., Carvalho, I., Karp, J. & Ferreira, L., 2011. Sensing the cardiac environment: exploiting cues for regeneration.. *Journal of Cardiovascular Translational Research*, 4(5), pp. 616-30.
- Pereira, R. *et al.*, 2013. Development of novel alginate based hydrogel films for wound healing applications. *International journal of biological macromolecules*, 52(1), pp. 221-230.
- Pfeffer, M. *et al.*, 1988. Effect of captopril on progressive ventricular dilatation after anterior myocardial infarction.. *New England Journal of Medicine*, 319(2), pp. 80-6.
- Qian, L. *et al.*, 2012. In vivo reprogramming of murine cardiac fibroblasts into induced cardiomyocytes. *Nature*, 485(7400), p. 593–598..
- Raghuvanshi, R. *et al.*, 2007. Xanthine oxidase as a marker of myocardial infarction. *Indian Journal of Clinical Biochemistry*, 22(2), pp. 90-92.
- Rebouças, J., Santos-Magalhães, N. & Formiga, F., 2016. Cardiac Regeneration using Growth Factors: Advances and Challenges. *Arquivos Brasileiros de Cardiologia*, 170(3), p. 271–275.
- Reinecke, H., Poppa, V. & Murry, C., 2002. Skeletal muscle stem cells do not transdifferentiate into cardiomyocytes after grafting.. *Journal of Molecular and Cellular Cardiology*, Volume 34, p. 241–249.
- Rekhrāj, S. *et al.*, 2013. High-Dose Allopurinol Reduces Left Ventricular Mass in Patients With Ischemic Heart Disease. *Journal of the American College of Cardiology*, 61(9).

Rodrigo, R. *et al.*, 2014. The effectiveness of antioxidant vitamins C and E in reducing myocardial infarct size in patients subjected to percutaneous coronary angioplasty (PREVEC Trial): study protocol for a pilot randomized double-blind controlled trial. *Trials*, 15(192).

Rodrigo, R., Libuy, M., Feliú, F. & Hasson, D., 2013. Review Article: Oxidative Stress-Related Biomarkers in Essential Hypertension and Ischemia-Reperfusion Myocardial Damage. *Disease Markers*, 35(6), p. 773–790.

Ruvinov, E. & Cohen, S., 2016. Alginate biomaterial for the treatment of myocardial infarction: Progress, translational strategies, and clinical outlook ☆: From ocean algae to patient bedside. *Advanced Drug Delivery Reviews*, Volume 96, p. 54–76.

Ruvinov, E., Leor, J. & Cohen, S., 2010. The effects of controlled HGF delivery from an affinity-binding alginate biomaterial on angiogenesis and blood perfusion in a hindlimb ischemia model. *Biomaterials*, 31(16), pp. 4573-82.

Ruvinov, E., Leor, J. & Cohen, S., 2011. The promotion of myocardial repair by the sequential delivery of IGF-1 and HGF from an injectable alginate biomaterial in a model of acute myocardial infarction. *Biomaterials*, 32(2), p. 565–578.

Sabbah, H. *et al.*, 2013. Augmentation of Left Ventricular Wall Thickness With Alginate Hydrogel Implants Improves Left Ventricular Function and Prevents Progressive Remodeling in Dogs With Chronic Heart Failure. *JACC Heart Failure*, 1(3), pp. 252-8..

Sakata, Y. *et al.*, 2004. Activation of Matrix Metalloproteinases Precedes Left Ventricular Remodeling in Hypertensive Heart Failure Rats. Its Inhibition as a Primary Effect of Angiotensin-Converting Enzyme Inhibitor. *Circulation*, Volume 109, pp. 2143-2149.

Sarker, B., Singh, R. & *et al*, 2014. Evaluation of fibroblasts adhesion and proliferation on alginate-gelatin crosslinked hydrogel. *PloS one*, Volume 9.

Schwarz, E. *et al.*, 2000. Evaluation of the effects of intramyocardial injection of DNA expressing vascular endothelial growth factor (VEGF) in a myocardial infarction model in the rat—angiogenesis and angioma formation. *Journal of American College of Cardiology*, Volume 35, p. 1323–1330.

Serpooshan, V. *et al.*, 2013. The effect of bioengineered acellular collagen patch on cardiac remodeling and ventricular function post myocardial infarction. *Biomaterials*, 34(36), pp. 9048-55.

Serpooshan, V. *et al.*, 2013. The effect of bioengineered acellular collagen patch on cardiac remodeling and ventricular function post myocardial infarction. *Biomaterials*, 34(36), pp. 9048-55.

- Seung-Man Han, I.-S. K. N.-K. H., 2006. s.l. Patent No. US20060240080 A1.
- Shachar, M. *et al.*, 2011. The effect of immobilized RGD peptide in alginate scaffolds on cardiac tissue engineering. *Acta Biomaterialia*, 7(1), p. 152–162.
- Shapiro, L. & Cohen, S., 1997. Novel alginate sponges for cell culture and transplantation. *Biomaterials*, 18(8), pp. 583-90.
- Sharpe, N., Murphy, J., Smith, H. & Hannan, S., 1988. Treatment of patients with symptomless left ventricular dysfunction after myocardial infarction. *Lancet*, 1(8580), pp. 255-9.
- Shen, M. *et al.*, 2013. Ethyl pyruvate ameliorates hepatic ischemia-reperfusion injury by inhibiting intrinsic pathway of apoptosis and autophagy. *Mediators of Inflammation*, p. 461536.
- Shoulders, M. & Raines, R., 2009. Collagen structure and stability. *Annual Review in Biochemistry*, Volume 78, p. 929–958.
- Sia, Y. *et al.*, 2002. Improved Post-Myocardial Infarction Survival With Probucol in Rats: Effects on Left Ventricular Function, Morphology, Cardiac Oxidative Stress and Cytokine Expression. *American College of Cardiology*, 39(1), p. 148–56.
- Silva, D. *et al.*, 2016. Chitosan/alginate based multilayers to control drug release from ophthalmic lens. *Colloids and surfaces B: Biointerfaces*, Volume 147, pp. 81-89.
- Simón-Yarza, T. *et al.*, 2012. Vascular Endothelial Growth Factor-Delivery Systems for Cardiac Repair: An Overview. *Theranostics*, 2(6), p. 541–552.
- Sivasubramanian, N. *et al.*, 2001. Left ventricular remodeling in transgenic mice with cardiac restricted overexpression of tumor necrosis factor. *Circulation*, Volume 104, pp. 826-831.
- Smith, J. *et al.*, 2015. Diagnosis and Management of Acute Coronary Syndrome: An Evidence-Based Update. *Journal Of The American Board of Family Medicine*, 28(2), pp. 283-293.
- Song, K. *et al.*, 2012. Heart repair by reprogramming non-myocytes with cardiac transcription factors. *Nature*, 485(7400), pp. 599-604.
- Souders, C., Bowers, S. & Baudino, T., 2009. Cardiac fibroblast: the renaissance cell. *Circulation Research*, 105(12), pp. 1164-76.
- Strauer BE, B. M. Z. T. K. M. H. A. S. R. K. G. W., 2002. Repair of infarcted myocardium by autologous intracoronary mononuclear bone marrow cell transplantation in humans. *Circulation*, 106(15), pp. 1913-8.

- Sun, J. & Tan, H., 2013. Alginate-Based Biomaterials for Regenerative Medicine Applications. *Materials*, Volume 6, pp. 1285-1309.
- Swijnenburg, R. *et al.*, 2005. Embryonic stem cell immunogenicity increases upon differentiation after transplantation into ischemic myocardium.. *Circulation*, 112(9), pp. 166-72..
- Takahashi, K. *et al.*, 2007. Induction of pluripotent stem cells from adult human fibroblasts by defined factors.. *Cell*, Volume 131, p. 861– 872.
- Takahashi, K. & Yamanaka, S., 2006. Induction of pluripotent stem cells from mouse embryonic and adult fibroblast cultures by defined factors.. *Cell*, 126(4), pp. 663-76.
- Takemoto, M. *et al.*, 2001. Statins as antioxidant therapy for preventing cardiac myocyte hypertrophy.. *Journal of Clinical Investigation*, 108(10), pp. 1429-37..
- Tang, X. *et al.*, 2010. Intracoronary administration of cardiac progenitor cells alleviates left ventricular dysfunction in rats with a 30-day-old infarction.. *Circulation*, 121(2), pp. 293-305.
- Tavazzi, L. *et al.*, 2008. Effect of rosuvastatin in patients with chronic heart failure (the GISSI-HF trial): a randomised, double-blind, placebo-controlled trial.. *the Lancet*, 372(9645), pp. 1231-9.
- Taylor, D. *et al.*, 1998. Regenerating functional myocardium: improved performance after skeletal myoblast transplantation.. *Nature Medicine*, 4(8), pp. 929-33..
- Taylor, M. *et al.*, 2005. Ethyl Pyruvate Enhances ATP Levels, Reduces Oxidative Stress and Preserves Cardiac Function in a Rat Model of Off-Pump Coronary Bypass. *Heart Lung Circulation*, 14(1), pp. 25-31.
- Tsujita, K. *et al.*, 2004. Effects of edaravone on reperfusion injury in patients with acute myocardial infarction. *The American Journal of Cardiology*, 94(4), p. 481–484.
- Tsutsui, H., Kinugawa, S. & Matsus, S., 2011. Oxidative stress and heart failure. *American Journal of Physiology - Heart and Circulatory Physiology*, 301(6), pp. 2181-2190.
- Ulloa, L. *et al.*, 2002. Ethyl pyruvate prevents lethality in mice with established lethal sepsis and systemic inflammation.. *Proceedings of the National Academy of Science of the United States of America*, 99(19), pp. 12351-6..
- van Laake, L. *et al.*, 2007. Human embryonic stem cell-derived cardiomyocytes survive and mature in the mouse heart and transiently improve function after myocardial infarction.. *Stem Cell Research*, 1(1), pp. 9-24..

- Vanhoutte, D., Schellings, M., Pinto, Y. & Heymans, S., 2006. Relevance of matrix metalloproteinases and their inhibitors after myocardial infarction: A temporal and spatial window. *Cardiovascular research*, 69(3), pp. 604-613.
- Venugopal, J. *et al.*, 2012. Biomaterial strategies for alleviation of myocardial infarction. *Journal of the Royal Society Interface*, Volume 9, pp. 1-19.
- Vinge, L., Raake, P. & Koch, W., 2008. Gene therapy in heart failure. *Circulation research*, 102(12), pp. 1458-70.
- Von Korff, R., 1964. Pyruvate-C14, purity and stability.. *Analytical Biochem*, Volume 8, p. 171-8..
- Wang, H. *et al.*, 2006. Degradation of RhoA by Smurf1 Ubiquitin Ligase. *Methods in Enzymology*, Volume 406, pp. 437-47..
- Wang, L. *et al.*, 2012. Ethyl pyruvate protects against experimental acute-on-chronic liver failure in rats.. *World Journal of Gastroenterology*, 18(40), pp. 5709-18.
- Wang, P. *et al.*, 1998. Overexpression of human copper, zinc-superoxide dismutase (SOD1) prevents postischemic injury.. *Proceedings of the National Academy of Sciences of the USA*, 95(8), pp. 4556-60..
- Wang, Y. *et al.*, 2009. Degradable PLGA Scaffolds with Basic Fibroblast Growth Factor. *Texas Heart Institute Journal*, 36(2), p. 89-97..
- Watanabe, s. *et al.*, 2017. Protein Phosphatase Inhibitor-1 Gene Therapy in a Swine Model of Nonischemic Heart Failure.. *J Am Coll Cardiol.*, 70(14), pp. 1744-1756..
- Wei, K. *et al.*, 2015. Epicardial FSTL1 reconstitution regenerates the adult mammalian heart.. *Nature*, 525(7570), pp. 479-85.
- Wei, L., Fahey, T., Struthers, A. & MacDonald, T., 2009. Association between allopurinol and mortality in heart failure patients: a long-term follow-up study. *International Journal of Clinical Practice*, 63: , 63(9), p. 1327-1333. .
- Wilkins, E. *et al.*, 2017. *European Cardiovascular Disease Statistics 2017*, Brussels: European Heart Network.
- Willems, J. *et al.*, 1978. Non-enzymatic conversion of pyruvate in aqueous solution to 2,4-dihydroxy-2-methylglutaric acid.. *Federation of European Biochemical Societies Letters*, Volume 86, p. 42-4..
- Woo, J. *et al.*, 2004. Ethyl pyruvate preserves cardiac function and attenuates oxidative injury after prolonged myocardial ischemia.. *Journal of Thoracic Cardiovascular Surgery*, 127(5), pp. 1262-1269.

- Worku, N. *et al.*, 2015. Ethyl Pyruvate Emerges as a Safe and Fast Acting Agent against *Trypanosoma brucei* by Targeting Pyruvate Kinase Activity. *PLoS ONE*, 10(9), p. e0137353.
- Xiaomin Zhang, G. A. K. N. J. Y. W., 2001. Differential vulnerability to oxidative stress in rat cardiac myocytes versus fibroblasts. *Journal of the American College of Cardiology*, 38(7), pp. 2055-2062.
- Yang, R. *et al.*, 2002. Ethyl pyruvate modulates inflammatory gene expression in mice subjected to hemorrhagic shock. *American Journal of Physiology. Gastrointestinal and Liver Physiology*, 283(1), p. G212–22..
- Yang, R., Han, X., Delude, R. & Fink, M., 2003. Ethyl pyruvate ameliorates acute alcohol-induced liver injury and inflammation in mice. *Journal of Laboratory and Clinical Medicine*, 142(5), pp. 322-31..
- Yang, R., Zhu, S. & Tonnessen, T. I., 2016. Ethyl pyruvate is a novel anti-inflammatory agent to treat multiple inflammatory organ injuries. *Journal of Inflammation*, 13(37).
- Yang, Z. *et al.*, 2008. Delayed ethyl pyruvate therapy attenuates experimental severe acute pancreatitis via reduced serum high mobility group box 1 levels in rats. *World Journal of Gastroenterology*, 14(28), pp. 4546-50..
- Yasuda, T. *et al.*, 2005. Quantitative analysis of survival of transplanted smooth muscle cells with real-time polymerase chain reaction. *Journal of Thoracic Cardiovascular Surgery*, 129(4), pp. 904-11..
- Yu, J. *et al.*, 2009. Restoration of left ventricular geometry and improvement of left ventricular function in a rodent model of chronic ischemic cardiomyopathy. *Journal of Thoracic and Cardiovascular Surgery*, 137(1), pp. 180-7.
- Yu, J. *et al.*, 2007. Induced pluripotent stem cell lines derived from human somatic cells. *Science*, Volume 318, p. 1917–1920.
- Zakkar, M., Guida, G., Suleiman, M. & Angelini, G., 2015. Cardiopulmonary Bypass and Oxidative Stress. *Oxidative Medicine and Cellular Longevity*, Volume 2015.
- Zeng, J. *et al.*, 2007. Exogenous ethyl pyruvate versus pyruvate during metabolic recovery after oxidative stress in neonatal rat cerebrocortical slices. *Anesthesiology*, 107(4), pp. 630-40.
- Zhang, Y., Mignone, J. & MacLellan, W., 2015. Cardiac Regeneration and Stem Cells. *Physiological Reviews*, 95(4), pp. 1189-204.

Zhao, X. *et al.*, 2011. Active scaffolds for on-demand drug and cell delivery. *PNAS*, 108(1), pp. 67-72.

Zhao, X. *et al.*, 2011. Active scaffolds for on-demand drug and cell delivery.. *Proceeding of the National Academy of Sciences of the United States of America*, 108(1), pp. 67-72.

Zmora, S., Glicklis, R. & Cohen, S., 2002. Tailoring the pore architecture in 3-D alginate scaffolds by controlling the freezing regime during fabrication. *Biomaterials*, 23(20), pp. 4087-4094.